ACTA POLONIAE PHARMACEUTICA

VOL. 71 No. 3 May/June 2014 ISSN 2353-5288

Drug Research

This Journal is published bimonthly by the Polish Pharmaceutical Society (Issued since 1937)

The electronic version of the journal is a prime and only version. Starting from volume 71, issue no. 2/2014, the journal Acta Poloniae Pharmaceutica - Drug Research is published exclusively in an electronic version. This version can be found in the Internet on page www.actapoloniaepharmaceutica.pl

An access to the journal in its electronic version is free of charge.

Impact factor (2013):	0.665
MNiSW score (2013):	15 points
Index Copernicus (2012):	13.18

Cited in: Chemical Abstracts, International Pharmaceutical Abstracts, EMBASE/Excerpta Medica, Index Medicus, MEDLINE Science Citation Index Expanded Journal Citation Reports/Sci. Ed., Derwent Drug File

Typeset by RADIUS, Warszawa

Acta Poloniae Pharmaceutica – Drug Research

Volume 71, Number 3 May/June 2014

CONTENTS

APPHAX 71 (3) 351 – 522 (2014)

PHARMACOLOGY

GENERAL

SHORT COMMUNICATION

Acta Poloniae Pharmaceutica – Drug Research, Vol. 71 No. 3 pp. 353–361, 2014 ISSN 0001-6837
Polish Pharmaceutical Society

REVIEW

MYCOPHENOLATE MOFETIL – A NEW ATHEROPREVENTIVE DRUG?

WIOLETTA OLEJARZ, DOROTA BRYK and DANUTA ZAPOLSKA-DOWNAR*

Department of Biochemistry and Clinical Chemistry, Warsaw Medical University,
1 Banacha St., 02-097 Warszawa, Poland

Abstract: Atherosclerosis is a form of chronic inflammation in which endothelial cell dysfunction, fibroproliferative process, oxidative stress and inflammatory cell activation are linked to plaque development and destabilization. T-lymphocytes also play a key role in pathogenesis of atherosclerosis. As a consequence, the suggested concept that modulation of an immunological response could be an appropriate target in the prevention of cardiovascular disease, is an important focus of research. Mycophenolate mofetil (MMF) is an inhibitor of inosine monophosphate dehydrogenase (IMPDH), that exerts anti-proliferative and pro-apototic effects, particularly on activated T-lymphocytes. MMF has other anti-atherogenic effects at the level of endothelial cells, monocytes/macrophages, smooth muscle cells and dendritic cells. In addition, MMF exhibits anti-oxidative properties. The present review paper provides an overview about the mechanisms of anti-atherosclerotic properties of MMF.

Keywords: atherosclerosis, mycophenolate mofetil, endothelium, monocyte/macrophage, T-lymphocyte, adhesion molecules, oxidative stress

Atherosclerosis, which causes cardiovascular diseases, is a specific form of chronic inflammation. Atherosclerosis is modified by lipid disorders, oxidative stress and the fibroproliferative process. Endothelium dysfunction plays a key role in the initiation as well as in the progression of atherosclerosis. Moreover, of great importance is that atherosclerosis has both an innate and adaptive defensive mechanism. An innate response depends on macrophages – the main inflammatory cells – playing an important role in the pathogenesis of atherosclerosis. A mechanism of the adaptive response depends on lymphocytes T and B. These cells are able to modulate the atherosclerosis by a secretion of immunoregulatory cytokines and antibodies. Many suggestions present a view that the modulation of the immunological response could be an appropriate target in the prevention of cardiovascular diseases, therefore, mycophenolate mofetil seems to be a reasonable proposal as a drug. The scope of this study is to gather all knowledge about the mechanisms of the anti-atherosclerosis properties of this drug.

Mycophenolate mofetil – structure, metabolism and mechanisms

Mycophenolate mofetil (MMF) is the pro-drug of mycophenolic acid (MPA), which has been isolated from one kind of fungus – Penicillium fungus (1).

Taking a clearly chemical point of view, its structure is expressed as follows: (E)-6-(1,3-dihy-

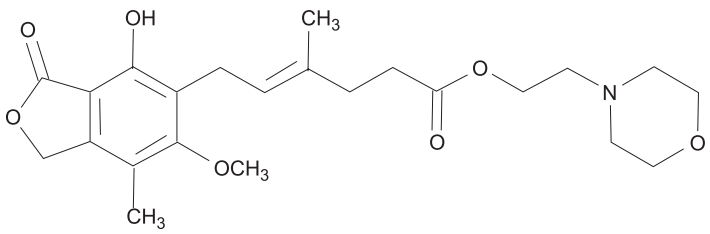

Figure 1. The structure of mycophenolate mofetil

* Corresponding author: e-mail: zapolska@vp.pl

dro-4-hydroxy-6-methoxy-7-methyl-3-oxo-5-isobenzofuranyl)-4-methyl-4-hexenonian 2-morpholinoethyl (Fig. 1). After oral administration and absorption of MMF, the ester linkage is rapidly hydrolyzed by esterases to yield MPA, an active immunosuppressive agent. The bioavailability of oral MPA from MMF is 94% while the maximum plasma concentration occurs about 2 h after administration. MPA undergoes a hepatic glucuronidation through a glucoronozyl transferase to form a mycophenolic acid glucuronide (MPAG), an inactive metabolite, which is secreted into bile. Subsequently, it is converted back to MPA by bacterial glucuronidases and then re-absorbed, and recirculated. At least 90% of MMF is excreted in urine as MPAG (1).

A correct synthesis of purine is necessary to obtain nucleotides, particularly guanosine triphosphate (GTP) and deoxyguanosine triphosphate (dGTP), which are used to synthesize DNA and glycoprotein. The purine synthesis occurs *via* two major pathways: the *de novo* pathway and the salvage pathway (Fig. 2). In the *de novo* pathway, 5-phosphoribosyl-1-pyrophosphate (PRPP) is converted by PPPP synthetase to inosine monophosphate (IMP), which is further modified to guanosine monophosphate (GMP) by the rate limiting enzyme, inosine monophosphate dehydrogenase (IMPDH). IMPDH binds IMP and cofactor NAD, which receives hydrogen from IMP. $NADH_2$ is then released, forming xanthosine monophosphate (XMP), which is subsequently converted to GMP. In the salvage pathway, guanine obtained as a result of nucleotide acid degradation is converted to GMP.

In 1969, Franklin and Cook described the effect of MPA on IMPDH and its ability to inhibit the synthesis of nucleotide acids in eucariotic cells. MPA occupies the catalytic site in IMPDH, which is occupied by NAD and H_2O, thereby inhibiting IMPDH (2). Whereas most human cells types have the capacity to synthesize the guanosine nucleotides by the use of both pathways mentioned above, lymphocytes are almost completely IMPDH-dependent (1, 3). To date, two isoforms of IMPDH have been identified. Stimulated T lymphocytes strongly express isoform II, which has a 5-fold higher affinity to MPA compared to isoform I, of which is constitutively expressed in most cells. Hence, inhibition of IMPDH with MPA is followed by the depletion of the pool of GTP required for DNA synthesis, predominantly in stimulated T-lymphocytes. As a result, MPA inhibits the T-lymphocyte proliferation throughout the blocking cell cycle in the G1 phase. Furthermore, MPA inhibits a production of antibodies stimulated by miogens and antigens, but also induces apoptosis in activated T-lymphocytes. Features of MPA mentioned above are responsible for its immunosuppressive action.

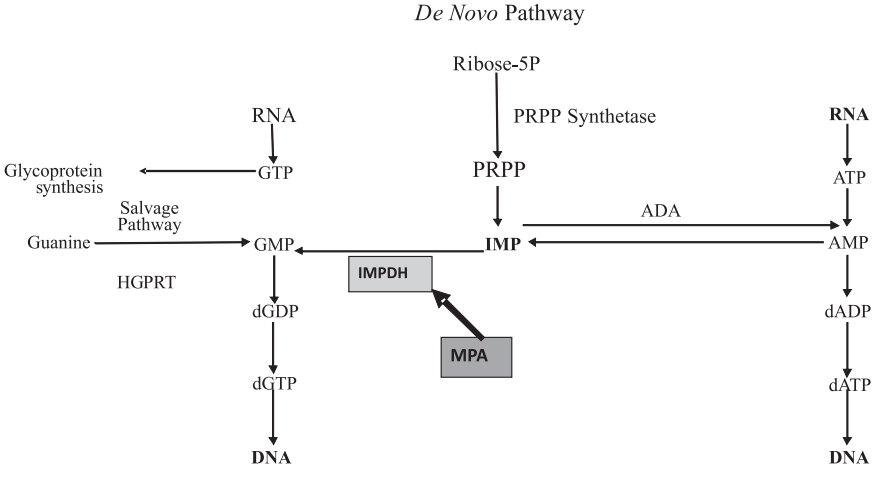

Figure 2. Purine biosynthesis pathways
ADA – adenosine deaminase, dADP – deoxyadenosine diphosphate, dATP – deoxyadenosine triphosphate, dGDP – deoxyguanosine diphosphate, dGTP – deoxyguanosine triphosphate, HGPRT – hypoxanthine-guanine phosphoribosyl transferase, IMP – inosine monophosphate, IMPDH – inosine monophosphate dehydrogenase, MPA – mycophenolic acid, PRPP – 5-phosphoribosyl-1-pyrophosphate

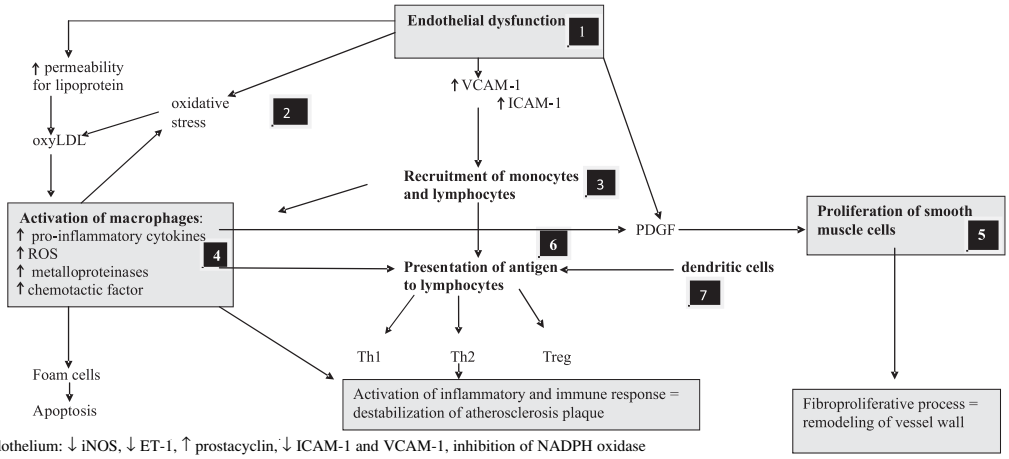

1. Endothelium: ↓ iNOS, ↓ ET-1, ↑ prostacyclin, ↓ ICAM-1 and VCAM-1, inhibition of NADPH oxidase
2. ↓Oxidative stress
3. ↓ Recruitment of monocytes and lymphocytes: decreased affinity of adhesion molecules for their ligands on endothelium
4. Macrophages: ↓ proliferation, ↑ apoptosis, ↓ pro-inflammatory cytokines, ↓ metalloproteinases, ↓ oxidative stress
5. Smooth muscle cells: ↓ proliferation
6. T Lymphocytes: ↓ proliferation, ↑ apoptosis ↓ INFγ, ↑ Treg
7. 6. Dendritic cells: ↓ maturation, ↓ IL-12, ↓ INFγ

Figure 3. Schematic representation of anti-atherogenic properties of MMF
ET-1 – endothelin-1. iNOS – inducible NO synthase, INF – interferon γ, ICAM-1 – intercellular adhesion molecule-1, oxyLDL – oxidized LDL, PDGF – platelet derived growth factor, ROS – reactive oxygen species, Treg.T – regulatory T-lymphocytes, VCAM-1 – vascular cell adhesion molecule-1

Effect of MPA on endothelial cells

Endothelial dysfunction plays a key role in the pathogenesis of atherosclerosis. A hallmark of endothelial dysfunction is the impaired bioavailability of NO, which is caused firstly by diminished synthesis and release, and secondly, by inactivation through increasing local reactive oxygen species (ROS) (4, 5). NO released by endothelial cells is responsible for relaxing smooth muscle cells, and in consequence, controlling intravascular pressure and blood tissue perfusion. Moreover, NO inhibits an aggregation of platelets, adhesion of leukocytes, proliferation of smooth muscles and inflammatory response. NO is synthesized from L-arginine by the constitutive endothelial NO synthase (eNOS; NOS3) in a small amount (6). Another type of NO synthase, so called "inducible NOS" (iNOS; NOS2), synthesizes a higher concentration of NO in activated macrophages or endothelial cells over a longer period.

The activated macrophages also produce ROS, which combine with NO to form peroxynitrites – highly reactive molecules that can react with protein, and in this way, change their function, and therefore, the function of endothelium. It is assumed that iNOS exerts pro-atherogenic activity by protein nitrosylation as well as by downregulation of eNOS activity (7).

It would be therapeutically desirable to inhibit iNOS activity, but not eNOS. Both NOS isoforms require tetrahydrobiopterin (BH_4), which is an essential cofactor for converting L-arginine into NO (6). However, whereas BH_4 is tightly bound to eNOS, the iNOS isoform requires continuous *de novo* synthesis of this co-factor. As it is well known, MPA decreases intracellular content of BH_4 by reducing the intracellular GTP, which is essential for synthesis of this co-factor (8). According to studies by Senda et al. (9), MPA inhibits interferon γ (INFγ) and tumor necrosis α (TNFα)-stimulated iNOS activity, whereas basal NO production, mediated by eNOS, remained unaffected.

Furthermore, endothelial dysfunction, leading to impairment of vasodilatation, is also due to impaired prostacyclin synthesis and up-regulated production of endothelin-1, which is a strong vasoconstrictor. As known from further studies, MPA increased the prostacyclin release and inhibited TNFα-stimulated synthesis of endothelin-1 (10, 11). Based on the data, it might be postulated that MPA exhibits beneficial effects on the vasodilatory function of endothelium.

Endothelial dysfunction is also manifested by shifts from anti-adhesive to pro-adhesive phenotype, which is essential for both progression of atherosclerosis, as well as for the inflammatory process

taking place in the vessel wall (12). This feature of endothelial dysfunction is associated with the appearance of adhesion molecules on their surface as mediators of interactions between cells of the vascular wall and leukocytes, thus, these interactions are essential for the adhesion and trans-endothelial migration of leukocytes. The family of endothelial adhesion molecules includes: selectins E and P, intercellular adhesion molecule-1 (ICAM-1), ICAM-2, vascular cell adhesion molecule-1 (VCAM-1), and platelet-endothelial adhesion molecule-1 (PECAM-1). So far, the best recognized and probably the most important for atherosclerosis are: VCAM-1 and ICAM-1 (13).

Many studies performed *in vitro* on HUVEC (human umbilical vein endothelial cells) stimulated with range of cytokines have shown various effects of MPA on the endothelial adhesion molecules and delivered numerous conflicting results. The study by Hauser et al. (14) reports that MPA did not change the ICAM-1 expression stimulated by TNFα, however, it increased TNFα-induced VCAM-1 and the selectin E expression. Some study results demonstrated that pre-treatment of HUVEC with MPA enhanced the induction of ICAM-1 by interleukin-1β (IL-1β) (15). Other studies demonstrated that MPA revealed to be a strong inhibitor of IL-1β-stimulated of VCAM-1 and the selectin E expression, but its inhibitory effect on the induced expression of ICAM-1 was much weaker (16). Similarly, Rabb et al. (17) demonstrated that MPA inhibited the TNFα-stimulated expression of VCAM-1 and ICAM-1.

An interaction between endothelial adhesion molecules and their ligands on the surface of leukocytes depend on their structure and affinity. As known, mannose and fucose are transferred to glycoproteins through guanosine nucleotides (1). Theoretically, a depletion of GTP by MPA should inhibit the transfer of mannose and fucose to surface receptors, along with the adhesion molecules.

Functional confirmative evidence of this observation was to demonstrate that MPA inhibits adhesion of monocytes to endothelial cells (18) and adhesion and penetration of lymphocytes (16).

The data mentioned above suggest that MMF treatment for medicinal purposes has the capacity to reduce infiltration of circulating monocytes and lymphocytes to the site of inflammation, including atherosclerosis plaque, as has been confirmed in animal studies (19).

MPA impact on monocytes / macrophages

The endothelial dysfunction, simultaneously with a local secretion of chemotactic factors, allows for local recruitment of monocytes inside the intima. Monocytes accumulating in the vascular wall undergo a series of changes typical for macrophages; then scavenger receptors appear on their surface, which participate in the internalization of foreign antigen, for example, modified LDL (20, 21). This leads to their activation and the formation of foam cells. Activated macrophages secrete many factors modulating the course of atherosclerosis. They are the source of many inflammatory cytokines, including IL-1, TNF and IL-6. They secrete many chemotactic factors for monocytes and lymphocytes. They produce an increased number of ROS, which are responsible for oxidative stress in the vascular wall and thus contribute to the formation of oxidized low density lipoprotein (oxyLDL), the main pathogenic factor of atherosclerosis. They are also a source for growth factors, including the platelet derived growth factor (PDGF). The activated macrophages produce metalloproteinases, i.e., enzymes that digest connective tissue matrix, therefore, they might contribute to the destabilization and rupture of atherosclerosis plaque, and by that means leading to acute clinical complications of atherosclerosis. Moreover, macrophages as cells presenting antigen, are able to present it to the lymphocytes $CD4^+$ with the use of major histocompatibility complex (MHC) class II and thus, become a kind of bridge between adaptive and innate responses of the organism.

MPA, by decreasing the level of GTP in monocytes / macrophages, may contribute to a decrease in monocytes recruitment to the intima, and thus to the impairment of inflammatory response of macrophages, which is responsible for atherosclerosis progression. In an earlier study, it was shown that MPA treatment of monocytes decreased a monosylation of glycoproteins and their attachment to endothelial cells and laminin (22). Further studies confirmed this observation showing a reduction of monocyte binding to HUVEC or selectin E after MMF treatment (18). Moreover, these studies demonstrated that MMF attenuated lipopolysacharide (LPS) or INFγ-stimulated expression of ICAM-1 and MHC of class II. Furthermore, MPA also revealed other properties, which may contribute to decreasing the number of monocytes / macrophages in atherosclerotic lesion. Studies performed by Cohn et al. (23) have demonstrated that MPA inhibited a monocyte proliferation as well as arrested their cell cycle in the S phase and increased their apoptosis. Interestingly, exogenous guanosine added before MPA treatment only partially reversed MPA-induced changes in these parameters, which suggests the existence of another type of mechanism, not only the impact of IMPDH itself.

These observations from *in vitro* studies were confirmed in results carried out *in vivo*. It has been demonstrated, by the use of animal experimental model for diabetes, that MMF inhibited glomerular infiltration of macrophages (24). A simultaneous MMF application to mice ApoE ($^{-/-}$), treated with a fat enriched diet, has led to a decrease of the number of monocytes in aorta sections (25). MMF therapy may also lead to attenuation of the inflammatory response. Studies performed by Weimer et al. (26) demonstrated that monocytes received from patients with long-term stable graft functions treated with MMF, secreted a diminished amount of IL-1 and TNF in response to LPS. MMF therapy in patients with a carotid artery stenosis was associated with the decreased expressions of metalloproteinases in sections of these vessels (27).

The above mentioned data suggest that MMF treatment may lead to a decrease in the recruitment of monocytes / macrophages and their activation, and thus to the impairment of inflammation in atherosclerotic plaque.

Effect of MPA on smooth muscle cells

Smooth muscle cells play a key role in the pathogenesis of atherosclerosis (28). Under the influence of locally secreted growth factors (mainly from activated macrophages) mostly PDGF, they migrate from the media to the intima, where they further proliferate and synthesize components of connective tissues. Thanks to the activity of the smooth muscle cells, present in the intima, it first comes forward to form fibrous cap, covering up the atherosclerotic lesion, and then it remodels the vessel wall and narrows it so that it finally leads to the impairment of blood tissues perfusion.

It has been demonstrated that MPA inhibited the PDGF-stimulated proliferation of rat smooth muscle cells and the synthesis of connective tissue components (29). MPA also inhibited a proliferation of the smooth muscle cells induced by endothelin-1 (30) or oleic acid (31). As mentioned earlier, MPA inhibited the secretion of inflammatory cytokines. It is known that IL-1 and TNF stimulate the endothelial and the smooth muscles cells to synthesize PDGF (32). Moreover, IL-6 is a strong stimulator of smooth muscle proliferation. The results of the studies *in vitro* were proven in the animal model for aorta transplantation, in which an application of MMF caused a decrease in appearance of the smooth muscle cells in the intima and an essential reduction of their replication rate (33). Another study, targeted for evaluating MPA impact on the formation of atherosclerosis in a transplanted aorta, showed that the application of this drug inhibited all essential histological features of atherosclerosis in the transplant by reducing smooth muscle cell replication (30).

The above mentioned data suggest that the application of MMF may lead to the impairment of smooth muscle cell proliferation and to the reduction of connective tissue component secretion, thus inhibiting the remodelling of the vessel wall.

MPA impact on lymphocytes

In the chronic inflammatory process, essential for atherosclerosis, there are not only monocytes / macrophages-dependent mechanisms of innate responses involved, but also these adaptive response mechanisms that remain under control of lymphocytes T (34). Lymphocytes T, present on atherosclerosis plaque, include $CD4^+$ (helper lymphocytes) and $CD8^+$ (cytotoxic lymphocytes), wherein $CD4^+$ are more dominative. Active lymphocytes $CD4^+$ support both a humoral and a cellular response. An effective response emerges from the point, in which naive lymphocytes T encounter cells presenting antigen. Here is where bonding of antigens comes forward, cut into small fragments, tied with MHC class II on the surface of cells presenting antigen, by the TCR receptors present on the surface of $CD4^+$.

Macrophages and dendritic cells are the main cells presenting antigen. In order to effectively activate lymphocytes T, except TCR bonding with antigen fragments tied with MHC class II, a co-stimulation is essential, in other words, a simultaneous bonding of proper proteins on lymphocytes and on the cells presenting antigen. As regards to atherosclerosis, the most known are interactions between CD40L on lymphocytes and CD40 on cells presenting antigen. Activation of lymphocytes T may lead to the creation of different types of lymphocytes T. Among $CD4^+$ lymphocytes that dominate in atherosclerotic plaque, the most abundant are lymphocytes Th1, responsible for the cellular response, secreting mainly INFγ and TNFα. Lymphocytes Th2 presence occurs much less, which is responsible for the humoral response and secretion of IL-4, IL-5 and IL-10. It has been suggested that Th1 lymphocytes promote the development and progression of atherosclerosis, whereas Th2 lymphocytes are anti-atherogenic. An essential role of lymphocytes T in the pathogenesis of atherosclerosis was proven in many study results obtained from genetically modified mice, which disclosed an inhibition of the response, dependent from these cells and truly decreased the progression of atherosclerosis, whereas entering $CD4^+$ for mice ApoE ($^{-/-}$) increased the progression of atherosclerosis (35).

In recent years, there were some suggestions that regulatory lymphocytes T (Treg) had a beneficial effect for atherosclerosis (36). This is in regards to a population of lymphocytes T that is responsible for the maintenance of tolerance and control of the immunological response. It has been suggested that the balance between an efector response (Th1 and Th2) and the regulatory immunological one, or lack of one, as refers to atherosclerosis, played an essential role in its development and progression. A transfer of lymphocytes Treg to mice ApoE $(^{-/-})$ led to the inhibition of both the Th1 and the Th2 response with a simultaneous increase of IL-10, the cytokine ranging from a variety spectrum of anti-atherosclerotic activity (37).

As previously mentioned, MPA has a 5-fold higher affinity to IMPDH type II, and the main form is expressed in stimulated lymphocytes (1). An inhibition of this dehydrogenase finally led to the depletion of a pool of GTP required for DNA synthesis, predominantly in activated lymphocytes T. As a consequence, MPA inhibits the lymphocytes T proliferation by blocking them in the G or S phase of the cell cycle. In addition, MPA induced the apoptosis in the activated lymphocytes T from 12 to 82% (23). During the studies performed on mice injected with the superantigen staphylococcal enterotoxin B (SEB), it was proven that MMF accelerated the elimination of SEB-reactive lymphocytes T through an induction of their apoptosis (38).

The depletion of the pool of GTP by MPA also inhibits transfer of mannose and fuctose into glycoproteins, being present on the surface of lymphocytes T, including the glycoproteins responsible for attaching to the endothelial cells (1). Thus, treatment of T-lymphocytes with MPA resulted in attenuation of their adhesion to endothelial cells, as was proven in many studies. The studies performed by Blaheta et. al. (39) revealed a strong inhibition of both the adhesion and the penetration rate of $CD4^+$ and $CD8^+$ T-lymphocytes suggesting that it occurs mainly as a result of reduced binding ability of two essential adhesion molecules for this process: very late antigen (VLA-4 – ligand for VCAM-1) and lymphocyte function-associated antigen (LFA-1 – ligand for ICAM-1).

As seen from the data mentioned above, MPA has the capacity to decrease the number of lymphocytes in the sites of inflammation, including the atherosclerosis plaque, throughout the inhibition of proliferation, an induction of apoptosis and a decreasing attachment to the endothelial cell. This has been confirmed in several *in vivo* studies. The studies performed on rats after cardiac transplantation demonstrated that MMF reduced an accumulation of LFA-1-positive leukocytes in some sections of vessels and the extent of a transplant vasculopathy (40).

Some functions of activated T-lymphocytes might also be impacted by MPA. *In vivo* studies demonstrated that MPA inhibited a phytohemagglutinin or CD3 antibody-stimulated production of INFγ (41). In the earlier cited studies performed on mice injected with superantigen SEB, it was demonstrated that MMF decreased serum levels of TNFα and INFγ was stimulated by this antigen (38). That fact is of much importance taking into consideration that INFγ produced by lymphocytes Th1 was a strong activator of macrophages. Moreover, it inhibited a synthesis of collagen and stimulated macrophages to produce metalloproteinases. Hereby it contributed to the impairment of the fibrous cup covering atherosclerotic plaque, and as a consequence, the formation of plaque prone to rupture. The recently published study results, as regards to patients with a carotid artery stenosis that received MMF for 2 weeks prior to undergoing carotid endarterectomy, were quite interesting (27). In most MMF treated patients, a decreased number of activated lymphocytes T with a simultaneous increase in the number of lymphocytes Treg in sections of carotids was observed.

MPA impact on dendrtic cells

Dendritic cells are major presenters of antigen to the naive T-lymphocytes, thereby initiating their proliferation and differentiation to Th1 or Th2 cells (36). For an efficient antigen presentation, a dentritic cell maturation, as well as up-regulation of MHC molecules and co-stimulatory molecules (CD40 and CD68), are required. As known from *in vitro* results, an oxyLDL, the main pathogenetic factor of atherosclerosis, may be this type of antigen that participates in the maturation and the activation of the dendritic cells (42). The potential role of the dendritic cells in atherosclerosis was underlined by a detection of matured dendritic cells in the plaque co-localized with the activated T lymphocytes (43).

A frequent presence of the dentritic cells, close to the T-lymphocytes in the rupture prone regions, suggests that these cells presenting antigen activate the T-lymphocytes, thereby promoting plaque progression and destabilization. It is widely considered that IL-12, produced by some dendritic cells, played a key role in differentiating lymphocytes T in Th1 as regards to atherosclerosis (36).

As seen from *in vitro* studies performed on murine dendritic cells, MMF impaired their ability

to stimulate allogenic T lymphocytes and reduced the expression of CD40 and CD68 (44). Furthermore, it inhibited the LPS-stimulated production of IL-12. A similar observation was made on human dendritic cells stimulated with LPS or TNFα, which led to evidence that MPA inhibited LPS or TNFα-induced dendritic cells maturation (45). Moreover, MPA inhibited IL-12 and INFγ synthesis induced by both mediators as well as the ability to stimulate allogenic lymphocytes T. An addition of exogenous guanosine reversed the above mentioned MPA impact.

Anti-oxidative properties of MPA

As seen from the basis of knowledge, oxidative stress plays a key role in the pathogenesis of atherosclerosis (46, 47). The increase of oxidative stress is the result of a balance disorder between the production of ROS and the activity of the mechanisms responsible for their removal. An increased ROS formation may, in many ways, contribute to the development and progression of atherosclerosis. First of all, they are responsible for the formation of oxyLDL, the main pathogenic factor of atherosclerosis. ROS may impair the vasoprotective function of the endothelial cells by a rapid inactivation of NO. ROS contribute to the intracellular signalling cascades associated with the inflammatory response. They may function as second messengers by activating some kinases and transcription factors, notably nuclear factor-κB (NF-κB). Moreover, they regulate an expression of many growth factors and pro-oncogenes like c-Myc, c-Fos and c-Jun, hitherto contributing to a migration and a proliferation of smooth muscles, and further to the remodelling of the vessel wall (48). An NADPH oxidase is the principal cause of the increase of oxidative stress in atherosclerosis and is the main source of ROS in endothelial cells (49). The classical NADPH oxidase complex is composed of two cell-membrane subunits: $p22^{phox}$ and $gp91^{phox}$, which form a flavocytochrome B558. The transfer of an electron from NADPH to the molecular oxygen – generating the superoxide radical – is catalyzed by the oxidase, as a result of its activation through a translocation of the cytoplasmic regulatory subunits $p47^{phox}$, $p67^{phox}$, $p40^{phox}$ and Rac, and the binding with cytochrome B558. Some drugs, which maintain the endothelial function and prevent cardiovascular disease progression (statins for example), partly exert their beneficial effects by inactivating endothelial NADPH oxidase (50).

The previous studies showed that MPA exhibits anti-oxidative properties. The studies performed on the endothelial cells showed that MPA inhibited NADPH oxidase activation by reducing the amount of membrane bound Rac1, as well as its activity (51). As it is known, Rac1 is a GTP-dependent protein. Thus, MPA induced inhibition of the endothelial ROS formation may be caused by the depletion of cellular GTP content, which is the likely cause of the subsequent attenuation of Rac1 and NAPH oxidase activity. Another study performed on smooth muscle cells showed that an inhibitory effect of MPA on PDGF-stimulated production of ROS was only partially restored by egzogenous guanosine (29). Going forward, the authors made a further study, which showed that MPA addition into a probe containing H_2O_2 resulted in rapidly reduced hydrogen peroxide concentration. It was assumed that carboxyl, methyl and hydroxyl portions of MPA are expected to react directly with H_2O_2, resulting in a decrease of its amount.

MMF impact on development and progression of atherosclerosis as observed in *in vivo* study

By the use of rabbits fed a high-cholesterol diet, resulting in pathology relevant to the general human population, Greenstein et al. (52) performed studies in order to evaluate the impact of MMF on atherogenesis. These dieted animals simultaneously received MMF (80 mg/kg) for 12 weeks. After a completion of the test, aortic tissue section was immunohistochemically evaluated. In the MMF treated group, plaque area was significantly decreased by 46% and a number of macrophages and smooth muscle cells in this group were reduced to a comparable level of the control group. Also, Romero et al. (53), using the same model of atherogenesis, found that MMF (30 mg/kg, 12 week) reduced atherosclerosis in the aorta by over 50%. Furthermore, the MMF reduced the smooth muscle cell proliferation, and intimal macrophages and foam cell infiltration, as well as the total aortic cholesterol content. Recently, study results were accessible on the other experimental atherosclerosis model by using ApoE $(^{-/-})$ mice, treated simultaneously with 30 mg/kg of MMF and high-fat diet for 3 to 12 weeks (25). In both MMF-treated groups, the macroscopic and the histologic aortic atherosclerosis lesions was significantly reduced in comparison with the control group. Furthermore, the MMF treatment decreased the T-lymphocyte proliferation and cell number, as well as the aortic content of macrophages and their proliferation.

Recent studies have demonstrated that a systemic lupus erythematosus (SLE) was associated

with an increased risk for cardiovascular disease. A study performed on mice LDL ($^{-/-}$) with SLE-susceptible gen, demonstrated that atorvastatin attenuated atherogenesis in mice without the transplanted gen, but failed to reduce the atherosclerotic lesion size in LDL ($^{-/-}$) SLE mice, in spite of a significant reduction in serum cholesterol levels (54). A treatment with MMF or MMF + atorvastatin attenuated atherogenesis in both groups of animals.

It is worth mentioning, although it was not the scope of this publication, that MMF had beneficial effects in cardiac transplant patients beyond the suppression of tissue rejection. MMF treatment resulted in diminished intimal thickening and cardiac allograf vasculopathy compared to those of other immunosupressive drugs. A wide discussion about the results of these studies was available in publication by Gibson et al. (55).

As can be deduced from the presented overview, MMF exerts a plethora of anti-inflammatory effects that could be hypothesized to attenuate pivotal processes in atherosclerosis and it could be a viable preventive agent in people exposed to a significant risk for cardiovascular disease. It seems quite advisable to perform further studies to test this hypothesis.

REFERENCES

1. Allison A.C., Eugui E.M.: Transplantation 80 (2 Suppl.), S181 (2005).
2. Sintchak M.D., Fleming M.A., Futer O., Raybuck S.A., Chambers S.P., Caron P.R., Murcko M.A., Wilson K.P.: Cell 85, 921 (1996).
3. Alison A.C., Eugui E.M.: Immunopharmacology 47, 85 (2000).
4. Landmesser U., Hornig B., Drexler H.: Circulation 109 (21 Suppl. 1), II27 (2004).
5. Cai H., Harrison D.G.: Circ. Res. 87, 840 (2000).
6. Andrew P.J., Mayer B.: Cardiovasc. Res. 43, 52 (1999).
7. Kessler P., Bauersachs J., Busse R., Schini-Kerth V.B.: Arterioscler. Thromb. Vasc. Biol. 17, 1746 (1997).
8. Hatakeyama K., Harada T., Kagamiyama H.: J. Biol. Chem. 267, 20734 (1992).
9. Senda M., DeLustro B., Eugui E., Natsumeda Y.: Transplantation 60, 1143 (1995).
10. Wilasrusmee C., Da Silva M., Singh B., Siddiqui J., Bruch D., Kittur S., Wilasrusmee S., Kittur D.S.: Clin. Transplant. 17 (Suppl. 9), 6 (2003).
11. Yang W.S., Lee J.M., Han N.J., Kim Y.J., Chang J.W., Park S.K.: Atherosclerosis 211, 48 (2010).
12. Zapolska-Downar D.: Czynniki Ryzyka 4, 5 (2000).
13. Galkina E., Ley K.: Arterioscler. Thromb. Vasc. Biol, 27, 2292 (2007).
14. Hauser I.A., Johnson D.R., Thévenod F., Goppelt-Strübe M.: Br. J. Pharmacol. 122, 1315 (1997).
15. Weigel G., Bertalanffy P., Wolner E.: Mol. Pharmacol. 62, 453 (2002).
16. Blaheta R.A., Leckel K., Wittig B., Zenker D., Oppermann E., Harder S., Scholz M., Weber S., Encke A., Markus B.H.: Transplant. Proc. 31, 1250 (1999).
17. Raab M., Daxecker H., Karimi A., Markovic S., Cichna M., Markl P., Müller M.M.: Clin. Chim. Acta 310, 89 (2001).
18. Glomsda B.A., Blaheta R.A., Hailer N.P.: Spinal Cord 41, 610 (2003).
19. Richter M.H., Zahn S., Kraus M., Mohr F.W., Olbrich H.G.: J. Heart Lung Transplant. 22, 1107 (2003).
20. Ross R.: N. Engl. J. Med. 340, 115 (1999).
21. Bobryshev Y.V.: Micron 37, 208 (2006).
22. Laurent A.F., Dumont S., Poindron P., Muller C.D.: Exp. Hematol. 24, 59 (1996).
23. Cohn R.G., Mirkovich A., Dunlap B., Burton P., Chiu S.H., Eugui E., Caulfield J.P.: Transplantation 68, 411 (1999).
24. Utimura R., Fujihara C.K., Mattar A.L., Malheiros D.M., Noronha I.L., Zatz R.: Kidney Int. 63, 209 (2003).
25. Von Vietinghoff S., Koltsova E.K., Mestas J., Diehl C.J., Witztum J.L., Ley K.: J. Am. Coll. Cardiol. 57, 2194 (2011).
26. Weimer R., Mytilineos J., Feustel A., Preiss A., Daniel V., Grimm H., Wiesel M., Opelz G.: Transplantation 75, 2090 (2003).
27. Van Leuven S.I., van Wijk D.F., Volger O.L., de Vries J.P., van der Loos C.M., de Kleijn D.V., Horrevoets A.J. et al.: Atherosclerosis 211, 231 (2010).
28. Schwartz S.M., Virmani R., Rosenfeld M.E.: Curr. Atheroscler. Rep. 2, 422 (2000).
29. Park J., Chang H.K., Ha H., Kim M.S., Ahn H.J., Kim Y.S.: J. Surg. Res. 150, 17 (2008).
30. Shimizu H., Takahashi M., Takeda S., Inoue S., Fujishiro J., Hakamata Y., Kaneko T. et al.: Transplantation 77, 1661 (2004).
31. Ahn H.J., Park J., Song J.S., Ju M.K., Kim M.S., Ha H., Song K.H., Kim Y.S.: Transplantation 84, 634 (2007).

32. Young J.L., Libby P., Schönbeck U.: Thromb. Haemost. 88, 554 (2002).
33. Räisänen-Sokolowski A., Vuoristo P., Myllärniemi M., Yilmaz S., Kallio E., Häyry P.: Transpl. Immunol. 3, 342 (1995).
34. Hansson G.K., Libby P.: Nat. Rev. Immunol. 6, 508 (2006).
35. Hansson G.K., Libby P., Schönbeck U., Yan Z.Q.: Circ. Res. 91, 281 (2002).
36. Mallat Z., Ait-Oufella H., Tedgui A.: Curr. Opin. Lipidol. 16, 518 (2005).
37. Mallat Z., Gojova A., Brun V., Esposito B., Fournier N., Cottrez F., Tedgui A., Groux H.: Circulation 108, 1232 (2003).
38. Izeradjene K., Revillard J.P.: Transplantation 71, 118 (2001).
39. Blaheta R.A., Leckel K., Wittig B., Zenker D., Oppermann E., Harder S., Scholz M. et al.: Transpl. Immunol. 6, 251 (1998).
40. Richter M., Zahn S., Richter H., Mohr F.W., Olbrich H.G.: J. Heart Lung Transplant. 23, 1405 (2004).
41. Izeradjene K., Quemeneur L., Michallet M.C., Bonnefoy-Berard N., Revillard J.P.: Transplant. Proc. 33, 2110 (2001).
42. Perrin-Cocon L., Coutant F., Agaugué S., Deforges S., André P., Lotteau V.: J. Immunol. 167, 3785 (2001).
43. Yilmaz A., Lochno M., Traeg F., Cicha I., Reiss C., Stumpf C., Raaz D. et al.: Atherosclerosis 176, 101 (2004).
44. Mehling A., Grabbe S., Voskort M., Schwarz T., Luger T.A., Beissert S.: J. Immunol. 165, 2374 (2000).
45. Faugaret D., Lemoine R., Baron C., Lebranchu Y., Velge-Roussel F.: Mol. Immunol. 47, 1848 (2010).
46. Madamanchi N.R., Vendrov A., Runge M.S.: Arterioscler. Thromb. Vasc. Biol. 25, 29 (2005).
47. Vogiatzi G., Tousoulis D., Stefanadis C.: Hellenic J. Cardiol. 50, 402 (2009).
48. Ray R., Shah A.M.: Clin. Sci. (Lond) 109, 217 (2005).
49. Frey R.S., Ushio-Fukai M., Malik A.B.: Antioxid. Redox Signal. 11, 791 (2009).
50. Zapolska-Downar D.: Czynniki Ryzyka 56, 29 (2008).
51. Krötz F., Keller M., Derflinger S., Schmid H., Gloe T., Bassermann F., Duyster J. et al.: Hypertension 49, 201 (2007).
52. Greenstein S.M., Sun S., Calderon T.M., Kim D.Y., Schreiber T.C., Schechner R.S.., Tellis V.A., Berman J.W.: J. Surg. Res. 91, 123 (2000).
53. Romero F., Rodríguez-Iturbe B., Pons H., Parra G., Quiroz Y., Rincón J., González L.: Atherosclerosis 152, 127 (2000).
54. Van Leuven S.I., Mendez-Fernandez Y.V., Wilhelm A.J., Wade N.S., Gabriel C.L., Kastelein J.J., Stroes E.S., Tak P.P., Major A.S.: Ann. Rheum. Dis. 71, 408 (2012).
55. Gibson W.T., Hayden M.R.: Ann. N. Y. Acad. Sci. 1110, 209 (2007).

Received: 29. 01. 2013

Acta Poloniae Pharmaceutica – Drug Research, Vol. 71 No. 3 pp. 363–367, 2014 ISSN 0001-6837
Polish Pharmaceutical Society

A REVIEW ON ANTIDIABETIC ACTIVITY OF *CITRULLUS COLOCYNTHIS* SCHRAD.

CHENGHE SHI[1≠], SABIHA KARIM[2], CHUNYONG WANG[1], MINGJING ZHAO[3]* and GHULAM MURTAZA[4]*≠

[1]Department of Traditional Chinese Medicine, Peking University Third Hospital, 100190 Beijing, People's Republic of China
[2]University College of Pharmacy, The University of the Punjab, Lahore, Pakistan
[3]Beijing University of Chinese Medicine, Dongzhimen Hospital, People's Republic of China
[4]Department of Pharmaceutical Sciences, COMSATS Institute of Information Technology, Abbottabad 22060, Pakistan

Abstract: Current studies have elaborated diabetes mellitus as one of the most prevalent endocrine disorder throughout the world. *Citrullus colocynthis* (*C. colocynthis*) is one of the most common traditional plants used as remedy against diabetes mellitus. It is well recognized by its hypoglycemic effect, which is substantiated in current phytotherapy. Its undesired effects include the disturbance of gastrointestinal and urinary tracts. This review article encompasses various blood glucose lowering studies that have been carried out till date. Various parts of plants used in extract preparation were roots, fruits, seeds, rinds and leaves. The nature of these extracts was ethnolic, methanolic, or aqueous and their doses varied from 10 to 500 mg/kg body weight/ day. All these published articles elaborate *C. colocynthis* as a potential antiglycemic medicinal plant.

Keywords: hypoglycemia, *in vitro*, *in vivo*, traditional, extracts

Out of many endocrinal diseases, diabetes mellitus is one of the most commonly prevalent metabolic disorders which distresses over one billion population of world and cause extensive deaths. Various factors causing this disease have been observed including diet and age (1). World Health Organization (WHO) has revealed that three billion diabetic cases would be observed by the year 2025 (2). Due to abnormal metabolism of carbohydrates, diabetic person suffers from abnormally higher blood glucose level than normal, which may cause various complications such as nephrotoxicity and retinopathy as well as untimely, death (3). Chronic diabetic condition disturbs the metabolism of proteins and lipids as well (4) and promotes peroxidation of membrane lipid causing the disturbance in cell function. Hypergycemia also promotes non-enzymatic glycation of proteins leading to increased development of reactive oxygen species (5). There is important role of increased oxidative stress (IOS) in the progress of diabetes as well as its complication due to autocatalytic metabolism, which leads to production of more free radicals and reduction of antioxidants (6). IOS also causes the destruction of red blood cells in diabetic patients (7), this hematological complication disturbs the performance of erythrocytes (8).

Currently, substantial research for safe and efficacious hypoglycemic drugs is in progress, which could also protect diabetic patient from other complications of diabetes (9). In this context, WHO has suggested the utilization of herbal medicines (10).

There is a long history of herbal use as antidiabetic therapy. The validated antidiabetic potential of many plant remedies is available in literature showing controlled analyses in healthy and diseased animals as well as human in last ten years. The mode of antidiabetic effect of these plant remedies involves the modulation of carbohydrate metabolism by restoring integrity and function of the β cells (11, 12).

Citrullus colocynthis (*C. colocynthis*) Schrad. belongs to family Cucurbitaceae. *C. colocynthis*, also known as bitter apple and bitter cucumber, is famous for its medicinal value throughout the world,

* Corresponding authors: G. Murtaza: e-mail: gmdogar356@gmail.com; mobile: 00923142082826; fax: 0092992383441;
M. Zhao: e-mail: Linfengtingchan@foxmail.com

≠ Contributed equally.

especially in Asia and Africa (13). The appearance of *C. colocynthis* resembles that of watermelon, possessing herbaceous stems, triangular and hairy leaves, yellow flowers, and globular bitter fruit. Its fruit consists of an outer hard rind and an inner white spongy pulp. A large number of seeds are embedded in its pulp (14). Pectin, colocynthin, colocynthein, colocynthetin, and gum are main phytochemical constituents found in its pulp, while fixed oil and albuminoids have been isolated from its seeds. These medicinally potential compounds make the fruit pulp and seeds an important medicinal part of this plant. The root and leaf are other medicinal parts of *C. colocynthis* (15).

The objective of this review is to collect and summarize in one place all such data, which involve the study of antidiabetic effect of *C. colocynthis*.

METHODOLOGY

Using English language, various electronic data bases such as Medline (1966 to 2013) and EMBASE (1980 to 2013) were comprehensively used for literature survey using various terms like "*Citrullus colocynthis* Schrad." and "*Citrullus colocynthis* Schrad. and antidiabetic effect" as well as the terms mentioned in title, abstract and keywords were also used for searching. Bibliographies of all concerned publications were also carefully studied for the comprehensive review. Papers were dually checked to avoid duplication.

RESULTS AND DISCUSSION

Current studies have elaborated diabetes mellitus as one of the most prevalent endocrine disorder throughout the world. *C. colocynthis* is one of the most common traditional plants used as remedy against diabetes mellitus. To provide scientific grounds to medicinal use of *C. colocynthis* as antidiabetic remedy, various researchers have carried out scientific studies on its different parts. As far as the preparation of extract of the desired part is concerned, dried plant part (seeds, fruits, roots, rinds or leaves) is chopped to powder and a weighed amount of the powder is subjected to solvent extraction using suitable instrument such as Soxhlet apparatus and appropriate solvent/solvent system at appropriate temperature. The marc was entirely dried and weighed before and after every extraction followed by the concentration of extract to dryness at 40^{o}C under reduced pressure in a rotary vacuum evaporator (16).

We found two such studies in the literature, which involved the use of root extract of *C. colo-*

Table 1. Previous studies showing the animal, part of *Citrullus colocynthis*, and type and dose of extract used.

No.	Part used	Type of extract	Study subject	Dose (mg/kg b.w./ day)	Reference
1	Root	Aqueous extract	Rats	175–300	(16)
2	Root	Aqueous extract	Rats	50 & 100	(17)
3	Fruit pulp	Ethanolic extract	Rats	300	(12)
4	Fruit pulp	Petroleum ether extract	Rats	300 & 500	(18)
5	Fruit pulp and seed	Ethanolic extract	Male rabbits	100 & 200	(19)
6	Fruit pulp	Ethanolic extract	Rats	300	(20)
7	Fruit pulp	Ethanolic extract	Rats	50	(21)
8	Fruit pulp	Suspension	Rats	10 & 90	(22)
9	Fruit pulp	Ethanolic extract	Rats	300	(23)
10	Fruit pulp	Methanolic extract	Rats	250 & 500	(24)
11	Seeds	Ethanolic extract	Rats	250	(26)
12	Seeds	Ethanolic extract	Rats		(25)
13	Leaf	Suspension	Rats	250 & 500	(27)
14	Rind	Aqueous, glycosidic, alkaloidal and saponin extracts	Rabbits	10, 15, 20, 50 & 300	(28)
15	Rind	Aqueous extract	Rats	300	(29)
16	Rind	Ethanolic extract	Rats	300	(30)

cynthis. One of these was conducted by Agarwal et al. (16), who evaluated biochemical parameters of normal and alloxan-induced diabetic (AID) rats after administration of aqueous, chloroform and ethanolic extracts of *C. colocynthis* root to observe its therapeutic effect. The aqueous extract illustrated noteworthy hypoglycemic effect (58.70%) in comparison to chloroform (34.72%) and ethanol (36.60%) extracts. The aqueous extracts exhibited the improved serum levels of urea, protein and lipid as well as retrieved serum level of bilirubin, glutamate oxaloacetate transaminase, glutamate pyruvate transminase and alkaline phosphatase. In another experiment, the researchers distributed rats into three groups keeping one group as control and administered 50 mg and 100 mg of *C. colocynthis* root extract per kilogram of body weight of rat to other two groups for twenty eight days for evaluation of *C. colocynthis* therapeutic efficacy and safety in rats at its antidiabetic dosing amount. Standard kits were used for the study of hematology and biochemistry of rats on 29th day. The hematological, histopathological and biochemical data showed significant antidiabetic effect of *C. colocynthis* as well as were safe in rats at its antidiabetic dosing amount (17).

Similarly, we found eight such studies in literature, which involved the use of fruit pulp extract of *C. colocynthis*. In order to assess the antioxidant effect of *C. colocynthis*, Dallak et al. (12) used extract of its fruit pulp in AID rats. The results exhibited significant reduction ($p < 0.05$) in total erythrocytes count, packed cell volume, thiobarbituric acid reactive substances, and activities of superoxide dismutase (SOD) and catalase (CAT) in the RBC's hemolysate of AID rats, and thus confirmed antioxidant features of *C. colocynthis* pulp extract. Jayaraman et al. (18) reported significant hypoglycemic effect of petroleum ether extract of *C. colocynthis* fruit pulp in STZID albino rats after oral administration of two different doses i.e., 300 and 500 mg of *C. colocynthis* fruit extract per kilogram of rat weight. In another study conducted on 36 white male New Zealand rabbits in Iran, antidiabetic effect of *C. colocynthis* fruit pulp as well as seed extract was determined using enzymatic kit through Elan Auto Analyzer. In comparison to the control group, significant hypoglycemic effect was observed after oral administration of 100 mg of pulp extract of *C. colocythis* per kilogram of rabbit weight, suggesting *C. colocythis* as an excellent antidiabetic drug (19). *C. colocynthis* pulp extract was once again used by Khalil et al., in the year 2010, to study its effect on liver of AID albino rats (20). Compared to the control group, histological study of liver of *C. colocynthis*-treated rats showed significantly lesser changes. Alternatively, AID rats regained normal histology of their liver after treating with *C. colocynthis* pulp extract. These results proved safe hypoglycemic effect of *C. colocynthis* pulp extract in AID rats.

El-Baky and Amin (21) reported that diabetic complications involving microvessels are reflected by nephropathy due to excessive filtration of various compounds like sugars. In this context, the effect of *C. colocynthis* fruits extract on the prevention of diabetic nephropathy was illustrated in STZID male albino rats. According to results, blood glucose¸ urea, creatinine, albumin and uric acid levels were significantly lowered. According to histopathological results, *C. colocynthis* fruit extract has nephroprotective effects concluding that fruit pulp of *C. colocynthis* may exert nephroprotective influences on the functioning of kidney tissues. Salami et al. (22) also observed significant hypoglycemic effects of suspensions of *C. colocynthis* fruit pulp in normal 12 h fasting rats after single dose of 30 mg/kg, while suspensions of *C. colocynthis* fruit pulp in the doses of 10 mg/kg and 90 mg/kg exhibited non-significant hypoglycemic effects. In Sudan, Babiker et al. (23) prepared the ethanolic extract of *C. colocynthis* fruit pulp and observed its influences in the oral dose of 300 mg/kg/mL of extract on fasting blood glucose level and glucose tolerance test. After 4 hours of administration, a swift decrease in blood glucose level of normal fasting rats was observed accompanied by few unwanted effects such as diarrhea, which resulted in death of two out of seven animals showing its toxic nature. Moreover, sub-acute treatment approach has been applied in STZID rats to test blood glucose level using the methanolic extract of *C. colocynthis* fruit pulp in the oral doses of 250 mg/kg and 500 mg/kg (24). There was non-significant ($p > 0.01$) and significant ($p < 0.01$) hypoglycemic effect of 250 mg/kg and 500 mg/kg dose.

We also found two such studies in the literature, which involved the use of seed extract of *C. colocynthis*. Sebbagh et al. (25) compared the antidiabetic potential of *C. colocynthis*, sunflower or olive oils in streptozotocin (STZ)-induced diabetes (STZID) in rats and found that diet rich with *C. colocynthis* oil exerted significantly higher hypoglycemic effect in rats administered with or without insulin as compared to foods containing other oils. Conclusively, the results reported that antidiabetic effect of *C. colocynthis* oil occurs through the preservation or restoration of pancreatic β cells in STZIT rats. Lakshmi et al. (26) tested the ethanolic

extract (in the oral doses of 250 mg/kg body weight) of *C. colocynthis* seeds for its hypoglycemic feature in AID rats, which had elevated levels of biochemical parameters. After administration of extracts, the values of these biochemical parameters significantly reverted back to their approximately normal levels along with the improvement in their glycogen level. As a conclusion, *C. colocynthis* seeds extract has hypoglycemic activity similar to standard oral hypoglycemic drug, gliclazide.

We also found one such study in the literature, which involved the use of leaf extract of *C. colocynthis*. Gurudeeban and Ramanathan (27) investigated the hypoglycemic influence of *C. colocynthis* on hepatic hexokinase and gluconeogenic enzymes like glucose-6-phosphatase and fructose 1,6-bisphosphatase of control and AID rats after oral intake of its leaf suspension in the doses of 250 mg/kg and 500 mg/kg of body weight for sixty days and found a significant fall in blood glucose level from 381 ± 34 to 105 ± 35 mg/dL. There was a reduction in the activities of glucose-6 phosphatase and fructose 1,6-bisphosphatase, and an enhancement in liver hexokinase activity supporting the hypoglycemic importance of this medicinal plant.

Abdel-Hassan et al. (28) investigated the hypoglycemic potential of the aqueous, glycosidic, alkaloidal and saponin extracts of *C. colocynthis* rind in normal rabbits, while fasting AID rabbits were used also for the elaboration of the hypoglycemic effects of saponin extract. Orally administered aqueous extract in the dose of 300 mg/kg in normal rabbits provoked significant hypoglycemic effect after one hour and intensively significant during 1–6 hours, possibly due to the tertiary and quaternary alkaloids, glycoside and saponin components present in the aqueous extract of the rind of *C. colocynthis* at a dose of 50 mg/kg of body weight in normoglycemic rabbits. The same extent of hypoglycemic effect was observed from the glycosidic extract that significantly reduced the fasting glucose levels after two hours and highly significant ($p < 0.001$) after six hours. Orally administered alkaloidal extract in the dose of 300 mg/kg in normal rabbits provoked non-significant hypoglycemic effect even after 6 hours. The saponin extract, in the oral doses of 10, 15 and 20 mg/kg of AID rabbits, exerted more prominent hypoglycemic effect after one hour and strongly significant ($p < 0.001$) after 3 hours. Conclusively, the aqueous extract of the rind of *C. colocynthis* exhibited glucose lowering effect, possibly due to the presence of saponin and glycosides.

Jeyanthi et al. (29) measured the biochemical parameters in normal and AID rats to investigate the hypoglycemic influence of aqueous extract of *C. colocynthis* in the dose of 300 mg/kg body weight for twenty two days. According to observations, the activity of enzymes involved in carbohydrate metabolism as well as the increased blood glucose, insulin, hemoglobin, HbA1C and glycogen levels in AID rats reverted back to normal level after treating with extract, which indicates the hypoglycemic activity of this medicinal plant.

Aghanouri et al. (30) investigated the possible antihyperglycemic influence of *C. colocynthis* in STZID Wistar rats. According to results, there was a significant ($p < 0.05$) antihyperglycemic influence of this medicinal plant in the STZID rats after 10 days of drug administration, which elaborate *C. Colocynthis* as a suitable herbal medicine against diabetic condition.

CONCLUSION

This review article encompasses various blood glucose lowering studies that have been carried out till date. Various parts of the plant used in extract preparation were roots, fruits, seeds, rinds, and leaves. The nature of these extracts was ethanolic, methanolic, or aqueous and their doses varied from 10 to 500 mg/kg body weight/ day. All these published articles elaborate *C. colocynthis* as a potential antiglycemic medicinal plant, however, in depth toxicity studies of this plant are still to be done.

REFERENCES

1. Zimmet P.Z.: Diabetologia 42, 499 (1999).
2. Pradeepa R., Mohan V.: Indian J. Med. Res. 116, 121 (2002).
3. Aravind K., Pradeepa R., Deepa R.: Indian J. Med. Res. 116, 163 (2002).
4. Rao B.K., Kesavulu M.M., Giri R., AppaRao C.H.: J. Ethnopharmacol. 67, 103 (1999).
5. Nishikawa T., Edelstien D., Du X.L.: Nature 404, 787 (2000).
6. Baynes J.W.: Diabetes 40, 406 (1991).
7. Rice-Evans C., Omorphos S.C., Baysal E.: J. Biochem. 237, 265 (1986).
8. Comazzi S., Spagnolo V., Bonfanti U.: J. Comp. Clin. Pathol. 12, 199 (2004).
9. Krishna B., Nammi S., Kota M.K., Krishna Rao R.V., Koteswara Rao N., Annapurna A.: J. Ethnopharmacol. 91, 95 (2004).
10. WHO. Expert Committee on Diabetes mellitus, Second Report. World Health Organ Tech. Rep. Ser. 646, 1–80 (1980).
11. Mansi K., Lahham J.: J. Basic Appl. Sci. 4, 57 (2008).

12. Dallak M., Bin-Jaliah I.: Pak. J. Physiol. 6, 1 (2010).
13. Rahimi R., Amin G., Ardekani M.R.S.: J. Altern. Complement. Med. 18, 551 (2012).
14. Shahabi S., Hassan Z.M., Mahdavi M.: J. Altern. Complement. Med. 14, 147 (2008).
15. Ardekani M.R.S., Rahimi R., Javadi B.: J. Trad. Chin. Med. 31, 27 (2011).
16. Agarwal V., Sharma A.K., Upadhyay A., Singh G., Gupta R.: Acta Pol. Pharm. Drug Res. 69, 75 (2012).
17. Atole S.K., Jangde C.R., Philip P., Rekhe D.S., Aghav D.V., Waghode H.J.: Veterinary World 2, 423 (2009).
18. Jayaraman R., Shivakumar A., Anitha T., Joshi V.D., Palei N.N.: Rom. J. Biol. Plant Biol. 54, 127 (2009).
19. Dashti N., Zamani M., Mahdavi R., Rahimi O.: J. Jahrom Univ. Med. Sci. 9, 13 (2012).
20. Khalil M., Mohamed G., Dallak M., Al-Hashem F., Sakr H, et al.: Am. J. Biochem. Biotechnol. 6, 155 (2010).
21. El-Baky A.E.A., Amin H.K.: Int. J. Pharm. Stud. Res. 2, 1 (2011).
22. Salami M., Aqanouri Z., Karimian M., Enshai M.: Ethnopharmacology 3, 50 (2004).
23. Babiker H.A., Eldin I.M.T., Abd-Elwahab H.M.: Gezira J. Health Sci. 8, 1 (2012).
24. Jayaraman R., Kumar G.A.S., Raj P.V., Nitesh K., Naryanan K.: Biomed. 4, 269 (2009).
25. Sebbagh N., Cruciani-Guglielmacci C., Ouali F., Berthault M.F., Rouch C. et al.: Diabetes Metab. 35, 178 (2009).
26. Lakshmi B., Sendrayaperumal V., Subramanian S.: Int. J. Pharm. Sci. Rev. Res. 19, 47 (2013).
27. Gurudeeban S., Ramanathan T.: Ethnopharmacology 11, 10 (2010).
28. Abdel-Hassan I.A., Abdel-Barry J.A., Mohammeda S.T.: J. Ethnopharmacol. 71, 325 (2000).
29. Jeyanthi K.A., Mary C.A.: IUP J. Biotechnol. 3, 30 (2009).
30. Aghanouri Z., Noureddini M., Salami M.: Feyz J. Kashan Univ. Med. Sci. 12, 1 (2009).

Received: 24. 06. 2013

Acta Poloniae Pharmaceutica – Drug Research, Vol. 71 No. 3 pp. 369–377, 2014 ISSN 0001-6837
Polish Pharmaceutical Society

THE ROLE OF ZINC IN THE PATHOGENESIS AND TREATMENT OF CENTRAL NERVOUS SYSTEM (CNS) DISEASES. IMPLICATIONS OF ZINC HOMEOSTASIS FOR PROPER CNS FUNCTION

MAŁGORZATA TYSZKA-CZOCHARA[1*], AGATA GRZYWACZ[2], JOANNA GDULA-ARGASIŃSKA[1], TADEUSZ LIBROWSKI[1], BOGDAN WILIŃSKI[3] and WŁODZIMIERZ OPOKA[2]

[1]Department of Radioligands, [2]Department of Inorganic Chemistry, Faculty of Pharmacy, Jagiellonian University Medical College, Medyczna 9, 30-688 Kraków, Poland
[3]Department of Human Developmental Biology, Jagiellonian University Medical College, Kopernika 7, 31-034 Kraków, Poland

Abstract: Zinc, the essential trace element, is known to play multiple biological functions in human organism. This metal is a component of many structural as well as regulatory and catalytic proteins. The precise regulation of zinc homeostasis is essential for central nervous system and for the whole organism. Zinc plays a significant role in the brain development and in the proper brain function at every stage of life. This article is a review of knowledge about the role of zinc in central nervous system (CNS) function. The influence of this biometal on etiopathogenesis, prevention and treatment of selected brain diseases and disorders was discussed. Zinc imbalance can result not only from insufficient dietary intake, but also from impaired activity of zinc transport proteins and zinc dependent regulation of metabolic pathways. It is known that some neurodegenerative processes are connected with zinc dyshomeostasis and it may influence the state of Alzheimer's disease, depression and ageing-connected loss of cognitive function. The exact role of zinc and zinc-binding proteins in CNS pathogenesis processes is being under intensive investigation. The appropriate zinc supplementation in brain diseases may help in the prevention as well as in the proper treatment of several brain dysfunctions.

Keywords: zinc, central nervous system, Alzheimer's disease, depression, brain ischemia

Abbreviations: 5-HT – 5-hydroxytryptamine, AD – Alzheimer's disease, ADHD – attention deficit-hyperactivity disorder, AMPA – 2-amino-3-(5-methyl-3-oxo-1,2-oxazol-4-yl)-propanoic acid, ASD – autism spectrum disorder, BDNF – brain-derived neurotrophic factor, CMS – chronic mild stress, CNS – central nervous system, CTR1 – copper transporter (SLC31A1 member 1), DMT1 – divalent metal-ion transporter 1 (DMT1/DCT1/SLC11A2), ERK – extracellular-signal-regulated kinase, FST – forced swim test, GABA – γ-aminobutyric acid, IFN – interferon, IL – interleukin, LTD – long term depression, LTP – long term potentiation, MAPK – mitogen-activated protein kinases, MT – metallothionein, MTF1 – metal-regulatory transcription factor 1, NF-κB – nuclear factor of κ-light-polypeptide gene enhancer in B-cells, NGF – nerve growth factor, NK cells – natural killer cells, NMDA – *N*-methyl-D-aspartic acid, PD – Parkinson's disease, ROS – reactive oxygen species, SOD – superoxide dismutase, TGFB1 – transforming growth factor β1, TNF – tumor necrosis factor, TrkB – tyrosine-related kinase B, TST – tail suspension test, ZIP – Zrt- and Irt-like proteins (SLC39 – solute-linked carrier 39), ZnT/CDF – zinc transporter (SLC30 – solute-linked carrier 30)

Zinc plays an essential role in the number of biochemical processes crucial for cell survival (Fig. 1). Evidently, unbalanced homeostasis of this biometal affects cell function. This bivalent metal constitutes a prostetic group of a number of enzymes like carbonic anhydrase, alcohol dehydrogenase, alkaline phosphatase, phospholipase C, carboxypeptidase, Zn-Cu superoxide dismutase (SOD) and others regulatory proteins (1, 2). It is also a critical component of DNA and RNA polymerases and has a fundamental role for nucleic acid metabolism and gene activation and repression. At the transcriptional level of protein expression, zinc fingers structure enables transcription factors to anchor to DNA helix (3). This biometal regulates cell cycle by the influence on cyclines and cyclin-dependent kinases (4). The activities of many growth factors are zinc dependent, hence cell proliferation is regulated by the concentration of zinc ions (5). Zinc regulates microtubule polymerization process in the division

* Corresponding author: e-mail: mtyszka@poczta.fm; phone: +48504053552

of cells, providing the correct cell cytoskeletal formation and cell mitosis (4).

One of the most important functions of zinc in organism is an antioxidative protection (6, 7). Zinc decreases ROS generation by several mechanisms. Firstly, the zinc antioxidative effect occurs through activity of zinc dependent enzyme, superoxide dismutase (1). Secondly, zinc metallothioneins (MT) can bind and neutralize ROS due to their sulfhydryl groups (7). Additionally, zinc ions have influence on signal transduction pathway *via* inhibition of NF-κB, TGFB1 and MAPK (8, 9).

Zinc activity occurs through inhibition of caspases and protection from ROS-related release of cytochrome C from mitochondria and this way suppresses apoptosis induction process (9). It was established that zinc in hippocampus could inhibit cell apoptosis and prevent mitochondrial dysfunction through the activation of BDNF and the regulation of TrkB pathway (9). The proper zinc balance and the expression of zinc transporters in organism is crucial for anticancerogenic protection (7, 10), because optimal zinc levels have an impact on growth factors and cytokines, which enables to remove malicious cells in apoptosis process. Other mechanism of cell protection by zinc ions is according to expression and folding regulation of tumor suppressor genes products. Notably, this metal ion is crucial for immunoregulation due to decreasing the synthesis of TNF-α, and other interleukin proinflammatory cytokines (7). Zinc is also indispensable for proliferation and proper function of T lymphocyte subpopulations (11). Additionally, zinc ions are necessary for proper hormonal balance and in this way exert the effect on the whole organism (5, 12). Zinc ions are components of hormones (i.e., thymus hormones) or regulate hormones synthesis and ensure the appropriate hormone trails (i.e., insulin). The disturbances in zinc homeostasis are important causative factors of unbalanced organism functioning, which may lead to inflammation process and the development of diseases like arthritis, ulcers, cancer, and brain disorders (10).

Zinc absorption and transport

The total content of zinc in the adult human body is approximately 2 grams (10, 13). The requirement for this element for adult women is about 8 mg and for adult men about 11 mg per day and the similar amount is excreted daily (14). There is no mechanism enabling to store zinc in the body so it should be ingested regularly. In physiological conditions, zinc homeostasis strictly depends on maintaining its amounts on stable level in the organism. The importance of keeping zinc homeostasis is reflected by the complexity of zinc transport into and inside the cells (15, 16). There are two families of mammalian specific zinc transporters identified: ZIP/SLC39 family transporter, which transports zinc into the cytoplasm and ZnT/CDF/SLC30 family transporter, which acts in efflux zinc ions from the cell. Zinc transporters expression is regulated by zinc level in cytoplasm and outside the cells, according to the cell type and function, by zinc dependent transcription factors, especially metal regulatory transcription factor 1 (MTF1) (1, 16).

In human, the dietary zinc is mostly absorbed in duodenum, ileum and jejunum by active transport trough ZIP4/SLC39A4 zinc transporter, localized on the apical surfaces of the enterocytes (16). However, there are other zinc uptake possibilities in the intestinal tract i.e., ZIP1/SLC39A1 transporter expressed in small intestine, divalent metal-ion transporter 1 (DMT1/DCT1/SLC11A2) as well as copper transporter 1 (CTR1/SLC31A1) (16, 17). Zinc absorption can be affected by cations like copper, chromium, calcium, manganese and cadmium ions that can compete for zinc transporters (15, 17). The process of absorbance, transport and bioavailability may be affected by diet composition. The influence of diet components on zinc absorption and reabsorption was a subject of interest (18).

It is known that zinc ions in cell cytoplasm are accumulated bound to metallothionein proteins (1, 15). Further zinc transport from enterocytes into the bloodstream occurs through the ZnT1 transporter. Zinc ions in the blood are transported as complexes with albumins (52%), macroglobulins (40%), and amino acids (8%). In human serum there is about 15 μM/L of zinc and this concentration is similar to that in other mammals (10, 16). Zinc is absorbed to tissues and cells from blood mostly by ZIP1 and ZIP4 zinc transporters, and then, inside the cells, with both, ZIP and ZnT family (ZnT2/SLC30A2, ZnT4/SLC30A4, ZnT5/SLC30A5, ZnT6/SLC30A6, ZnT7/SLC30A7, ZIP7/SLC39A7, ZIP8/SLC39A8) to nucleus or other cell compartments, where it plays catalytic roles or is stored in Golgi apparatus vesicles (15–17). Zinc is excreted from cells by the zinc efflux transporter ZnT1/SLC30A1 and is eliminated from the organism with feces (over 10 mg/day) and urine (0.4 mg/day) (10).

The role of zinc in brain function

Zinc is transported from blood trough blood brain barrier system, mostly in the form of complexes with amino acids, especially L-histidine and cysteine (15, 19). Zinc transport in nervous cells is

shown in Figure 1. The average zinc concentration in brain is between 10 and 15 μg/g wet tissue (13), however, it may vary in different brain parts. The highest zinc level in the brain was found in hippocampus, amygdala and cerebellum (13, 19). There are three pools of zinc considered in the brain (15, 21). First, about 90% of total zinc, is the metal tightly bound to proteins. Second pool includes about 10% of brain zinc, which is present in a form of ions; this pool is stored in presynaptic vesicles of glutamatergic neurons where it is transported by specific transporter ZnT3/SLC30A3. Third pool, free zinc ions in non-precised compartments, is less than 1%. The measured zinc contents, especially in last two (labile, chelatable) pools vary depending on sample preparation method and measurement techniques (13, 19).

This element is reported to have a second messenger activity in the brain (22). Accordingly, in mammals zinc containing vesicles were found mostly in the glutamatergic neurons in brain cortex, hippocampus and amygdala, brain compartments responsible for learning, memory, cognition and mood regulation (10, 23, 24). During the neuronal activity, when zinc with glutamate is released from synaptic vesicles into synaptic cleft, zinc interactions with postsynaptic receptors may occur. The well known process of zinc inhibition of NMDA receptors in synapses occurs through two mechanisms, voltage independent allosteric inhibition, which reduce ion cannel opening frequency, and voltage dependent inhibition by blocking open channels (21, 25). Another interaction mechanism consists of inhibition of GABA receptor-mediated response, which leads to reduction of neuronal excitability. Furthermore, zinc can enhance AMPA receptors in postsynaptic cells and in that way zinc may regulate cell excitation (22, 25). Extracellular zinc in synaptic cleft may be reuptaken by both pre- and postsynaptic neurons and also glial cells (22).

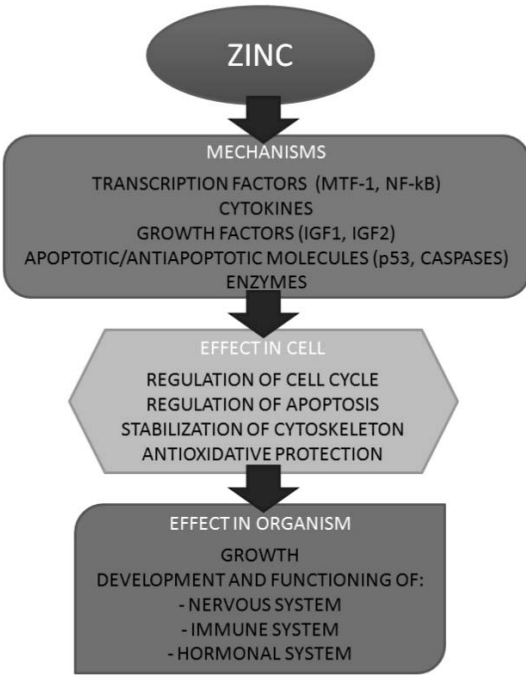

Figure 1. The mechanisms of zinc action in the organism. The scheme presents zinc action including the level of the particular cells and the whole organism as an integral system (1, 2)

The adequate zinc level is critical for CNS development and the differentiation of nervous stem cells in mammals (9, 26). The sustainable zinc homeostasis is necessary for the proper development of brain, especially for cerebellum, stellate, basket and also for Purkinje and granule cells. It was observed, that in the developing rat brain zinc accumulates in those cells, which should be eliminated for proper development (26). On the other hand, inadequate zinc status affects growth and maturation of neurons by disturbing zinc-dependent receptor functions. The rat model experiments showed decreased proliferation of neural precursor cells in adults as a result of the postnatal zinc deficiency (9). Studies with primary cultures of rat cortical neurons and human neuroblastoma IMR-32 cells proved that low zinc level reduced cell viability, decreased cell proliferation and increased neuronal apoptotic cell death (8). Zinc regulative role in the cortical plasticity is important for brain development and functioning of processes like learning and memory (25, 26). The experiments with cultured rat cortical neurons and hippocampal slices showed that zinc ions can transactivate TrkB through pathway independent on neurotrophins. Zinc can modulate long-term potentiation (LTP), long term depression (LTD) and synaptic plasticity in this process (25). Additionally, zinc may increase postsynaptic density of excitatory synapses in BDNF activation pathway (9).

The elevated zinc level, about 300 μM extracellular and over 400 nM intracellular (10, 27), is toxic to neurons. The experiments with cultured cortical neurons demonstrated that elevated zinc concentrations result in lower ATP synthesis caused by inhibition of glycolytic pathway enzymes such as glyceric aldehyde 3-phosphate dehydrogenase and phosphofructokinase and that way affects cells survival (27). The synaptically released extracellular zinc can reach the toxic amounts during pathological states like seizure, cerebral ischemia and trau-

matic brain injury (21, 27). Moreover, other observations indicate that glucose starvation may increase zinc ions toxicity for rat cerebellar granule neurons (29). In proposed mechanism, a lack of glucose induces activation of NMDA-channels and growing accumulation of calcium and zinc ions in mitochondria, which lead to severe neuronal damage. However, in neuroblastoma IMR-32 cell *in vitro* model, it was shown that high concentrations of zinc ions may reduce toxic effect of other toxic metals (8, 17).

Disturbances of zinc homeostasis are considered as important factors in neurodegenerative brain disorders. Adequate zinc intake is crucial for proper cognitive functions, especially in children and elderly human (19, 23, 24, 26, 30, 31). The alterations in zinc level have been reported in such diseases as depression and ADHD, Alzheimer's disease (AD), Parkinson's disease (PD) as well as in brain ischemia and traumatic brain injury.

The role of zinc in ischemic brain injury

In the conditions of brain ischemia, which can be caused by stroke and traumatic brain injury, zinc ions seem to play an important role in the neuronal damage process (27, 28). The synaptically released zinc ions are proposed as a critical component of the excitotoxicity cascade occurring in the course of ischemia (27). During ischemia, oxygen deficit results in increasing acidosis (21). In turn, acidosis can trigger more zinc release from MT proteins, which was demonstrated *in vitro* in rat-cultured neurons (21, 27, 28). Therefore in the conditions of growing oxidative stress typical for ischemia, additional MTs release of zinc ions can finally lead to apoptosis of neurons and glial cells (27). In addition, *in vitro* studies demonstrated that zinc insults affect cellular respiration and ATP depletion (27). Moreover, when ATP deficits cause progressive depolarization and affect ionic homeostasis of the cells, the repetitive waves of zinc release from synaptic vesicles into extracellular space were observed (27). The spreading depolarization and intensive zinc efflux can increase intracellular calcium flow (21) and that way calcium and zinc ions may work synergistically causing neurotoxicity (21). This results in alterations of plasma membranes permeability, mitochondrial damage and release of glutamate from neuronal vesicles (27, 28). In ischemic conditions large amounts of zinc may enter postsynaptic neurons through routes that are normally used by calcium. The studies with rat cortical neurons primary cultures showed, that zinc ions were influxed to postsynaptic neurons and glial cells after depolarization through voltage dependent calcium channels (21, 25). Additionally, this process

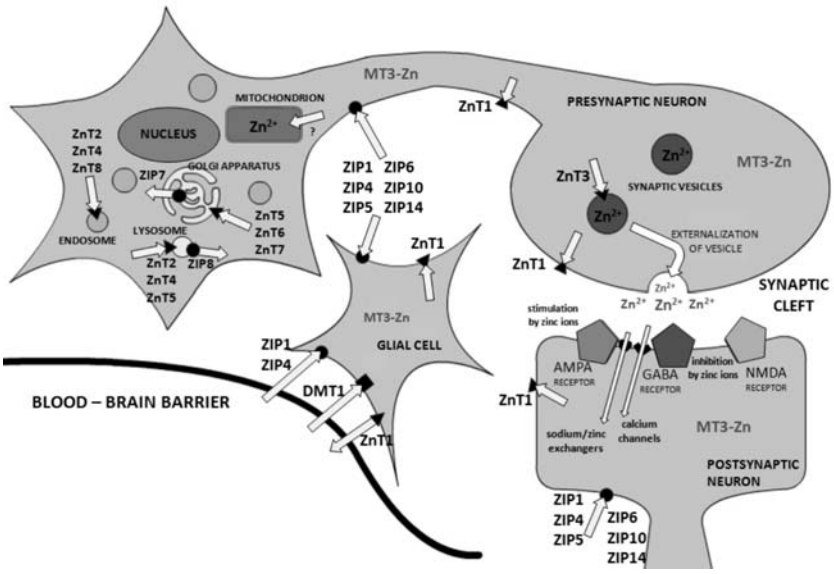

Figure 2. The mechanisms of zinc transport in nervous system. The direction of zinc ions flux presented with arrows; black circles – ZnT family of zinc transporters, black triangles – ZIP family of zinc transporters , black square – DMT1 transporter, MT3 – metallothionein 3 (neuron specific protein) (10, 15, 16, 24, 32)

may be enhanced by activity of glutamate, which, as mentioned, is released altogether with zinc (32). The rising glutamate amounts in extracellular space may cause additional opening of calcium channels leading to increased excitotoxicity (21). The studies on animal ischemic models confirmed extracellular accumulation of high zinc amounts in neurons and in extracellular space (27, 32).

On the other hand, it was demonstrated in ischemic state models that zinc chelation can decrease zinc accumulation and therefore degradation of nervous cells (27). However, there is also evidence that in ischemic conditions high zinc ions level may exert a neuroprotective effect (19). It is presumed that zinc downregulates the NMDA receptors and in that way may decrease toxicity of calcium ions (21, 25). Also the effectiveness of zinc bondage to metallothioneins may play a protective role in the brain injury (32). Zinc-dependent antioxidative enzymes may also have beneficial effect in conditions of ion dyshomeostasis caused by ischemia. *In vitro* studies with hippocampal rat neurons confirmed important role of proper zinc transport during ischemia (27, 28), because very high zinc concentrations (150 mM/L) were shown to increase (transiently) ZnT1 mRNA level in cells. These findings suggest that increased ZnT1 expression could be a defense mechanism from delayed, zinc-related neuronal damage caused by elevated zinc efflux (27, 32).

In reperfusion process, which follows ischemia, changes of zinc concentration in particular compartments can be continuously injuring for neurons (27, 28) but exact mechanism of action is under investigation. However, the effect of regulation is not clear, because inflammation process occurs in parallel, where zinc is ascribed to play beneficial role.

All presented findings and mixed data indicate that proper zinc level in specific neuronal compartments is essential for brain function and need to be precisely controlled in narrow concentration range, since even slightly disturbance may lead to neuronal damage during pathological ischemic conditions.

The role of zinc in depression

Despite of intensive clinical studies on depressive disorders, it is difficult to elucidate its pathophysiology. The most probable causes are connected with the loss of homeostasis of the stress hormones, neurotransmitters, neurotrophic factors, and additionally, disturbed trace elements levels (33, 34). Moreover, all those factors apply to only some types of depressed patients but not for others. Regardless of exact cause of this disease, the increased neuronal death by ROS formation and inflammation was postulated in most cases (35). The excessive inflammation process in depressed patients is manifested by elevated levels of pro inflammatory mediators (IL-1, IL-2, IL-6, TNF-α, IFN-γ) (35). As it was mentioned before, disregulation of inflammatory pathways may be correlated with decreased zinc level. In zinc deficiency conditions the proper function of immune system, differentiation of the immune cells and response of T helper lymphocytes is usually inappropriate. Schmidt considered that early life stress is a major risk factor for development of later depression due to affected neurogenesis in brain, especially in hippocampus (33, 34). On the molecular level, these processes may be zinc-dependent *via* antioxidative activity changes and its influence on proper course of brain development process. Additionally, Takeda hypothesized that corticosterone-mediated increase in postsynaptic zinc signal may decrease synaptic plasticity LPT and in that way affects hippocampal functions and in consequence induces depression in chronic stress conditions (36). Animal models of depression are commonly based on measuring acute or chronic stress, i.e., in FST and TST or chronic mild stress (CMS). It was observed that administration of zinc as well as antidepressants could reduce the durance of depressed behavior of animals in these models (33, 37). The other rodent models of depression are based on diet zinc-deprived, which can also generate depression-like behavior. These findings were consistent with clinical evidences, especially obtained in the treatment resistant cases when patients with depression had significantly lower serum zinc level compared to non-depressed. On the other hand, it has been reported that successful depression therapy can lead to zinc level normalization (33).

The important zinc dependent mechanism, which disturbances may exert influence on depression in patients is neuromodulation of NMDA receptors (25). The altered regulation of these receptors may lead to the development of depression symptoms. As previously mentioned, zinc ions released in synaptic cleft causes effective inhibition of NMDA receptors. The antidepressant mechanism, proposed by Duman and Violets, is based on rapid induction of synaptogenesis by NMDA receptor inhibition agents (34). Additionally, important role in the synaptogenesis is also played by NGF, BDNF and neurotrophins, which concentrations can be reduced by stress in rodents and in depressed human patients (37, 38). Moreover, it was demon-

strated that zinc supplementation could increase BDNF protein level in rodents (38).

In a view of these findings, it seems obvious that there is a relationship between zinc homeostasis and depression progress in humans. Unfortunately, there is no exact *in vitro* cell culture model of depression, which could help study the exact mechanisms in physiologically active nervous cells.

The role of zinc in Alzheimer's disease

Alzheimer's disease is an age-related neurodegenerative disorder manifested by the progressive dementia. It is well documented that brains of AD patients typically exhibit intracellular neurofibrillary tangles deposits of τ protein and extracellular β-amyloid plaques (39). However, the exact mechanism of neurodegeneration in AD is unclear and still there is no effective therapy of this disease. Clinical examinations data revealed the noticeable disturbances in zinc concentration in serum, brain cells and compartments and in synaptic vesicles of AD patients compared with control subjects (19, 23). It was considered that etiology of AD might involve abnormal concentration and disturbed compartmentalization of zinc ions. Indeed, increased concentration of extracellular zinc ions in the brain can be of importance in AD pathogenesis (40, 41). It has been demonstrated that β-amyloid plaques contain high concentrations of metal ions, especially iron, copper and zinc. In addition, results of *in vitro* studies demonstrated that zinc binding could accelerate the β-amyloid peptide formation (42). In consistence with these findings, it was observed that the formation of amyloid plaques in APP transgenic mice (AD model with mutations of amyloid precursor protein) was effectively inhibited due to the application of metal chelating agents. The maintenance of proper zinc concentration is crucial, because the enzymes, which restrain abnormal folding and aggregation of the β-amyloid such as neprilysin and insulysin, are zinc dependent proteins (39).

The changes in zinc levels can be caused by the altered expression of zinc transporters, especially ZnT1, ZnT3, ZnT4, ZnT6 and MT proteins (24, 40–42, 44). The extracellular concentration of zinc in hippocampus and cerebral cortex depends on the activity of zinc transporter ZnT3. The abnormally increased activity of ZnT3 may additionally elevate the extracellular zinc and in that way it induces the formation of β-amyloid plaques. This process is thought to be the first step in zinc homeostasis disruption in course of that pathological state. The inhibition of β-amyloid concentration was observed in brains of ZnT3 gene knock-out animals (Tg2576 mice) (44). However, excessively reduced activity of ZnT3 transporter may affect signal transduction in neurons, which can result in memory difficulties. Beyer et al. (42) demonstrated that the AD severity is connected with the significant loss of ZnT3 expression in the cortical regions of human brain. It was concluded that ZnT3-derived extracellular zinc pool is important for the proper regulation of normal cognitive function by modulation of the synaptic neurotransmission. The observations of ZnT3 gene knock-out mice behavior confirmed that animals exhibit deficits in learning and memory. What is more, the loss of memory functions were age-dependent and it is presumed that the adverse effects could be similar to those observed in AD patients, which underline the importance of proper expression of ZnT3 protein in specific regions for maintaining the brain function (41, 45).

Thus, once disturbed zinc concentration and distribution can influence zinc transporters expression. The altered zinc homeostasis manifested in the elevated extracellular zinc state may in consequence lead to up-regulation of expression of ZnT1 protein, which in turn exports zinc ions outside cells (24, 44). The raised concentration of extracellular zinc can be interpreted as a signal for the enhanced synthesis of this zinc exporter. Finally, it results in the enormous zinc export outside cells and the augmented zinc imbalance. The recent results demonstrated the increased expression patterns of zinc transporting proteins ZnT1, ZnT3, ZnT4, ZnT6, and ZnT7 in brain vessels of mice model APPswe/PS1dE9 (44).

The additional zinc activity connected with AD development is revealed in the hyperphosphorylation of τ protein. This phenomenon promotes polymerization of this protein and generation of neurofibrillary tangles in AD neurons (46). Kim et al. (46) showed that zinc regulates phosphorylation of τ protein through extracellular signal-regulated kinase pathway (MAPK/ERK); τ protein deposits affect microtubule function in neurons and probably may be the important cause of neuronal death in AD.

The regulation tissue-distant metabolic transitions by zinc, such as insulin synthesis and secretion pathways, may influence AD development. The recent experimental reports suggest the dependence between regulation of cells insulin sensitivity and AD pathogenesis, which ultimately qualify to name this disease as "diabetes type 3" (47).

The progressive loss of synaptic connections and the neuronal degeneration lead to the advancement of dementia in AD pathogenesis (21). The

influence of elevated ROS activity on the disease development is consistent with the frequently reported increased ROS formation observed in AD patient neurons. The explanation may be the failure in mitochondria functioning, which lead to the depolarization of mitochondrial membranes and in consequence to the increased ROS activity (48, 49). It is obvious that ROS are especially harmful in CNS because of pro-oxidation of lipids, which are essential for proper nerve membranes function and also for the conductivity and signal transduction pathways. Summarizing, the role of zinc in the pathogenesis of AD may be miscellaneous. Further studies are necessary to understand the complex role of zinc in the AD severity and treatment.

Other CNS disorders connected with zinc imbalance

There are recent clinical evidences that other CNS diseases may be correlated with zinc dyshomeostasis. The main symptoms of Parkinson's disease in human are motoric dysfunctions and a decrease in kinetic abilities. This neurodegenerative disorder is the consequence of dopaminergic neurons damage resulted from the progressive deficiency of neurotransmitter dopamine (23, 47). The biochemical processes affected in PD may be correlated with disruptions of zinc homeostasis. Clinical studies with PD patients suggested significantly decreased zinc status in patient blood serum compared with healthy elders control group. Another meaningful observation concerned protein deposits connected with metal ions disturbances in patient brain compartments, which showed some similarities to those observed in Alzheimer's disease (23). Experiments *in vitro* on clonal CHO cell line with overexpressed D2 receptors showed that zinc ions may have influence on dopamine receptors modulation and in that way low zinc status could be another factor reducing dopamine activity (50). Additionally, lowered zinc concentration may have influence on pathophysiology of PD by increased inflammation processes, generation of ROS and affected neurotropic factors levels, resulted in the proceeding neuronal degeneration.

As it was mentioned before, in the developing human brain, disrupted trace metal homeostasis may disturb the proper conduct of the process and in consequence affect hippocampus functioning. This, in turn, may lead to the following: affected attention, memory and activity levels in human but especially can correlate with children affected behavior. The epidemiological and clinical studies showed that children with ADHD disorder had decreased level of zinc in blood, hair and urine compared with control groups of children without attention problems (30). Additionally, the relation between effectiveness of methylphenidate and amphetamine derivatives used in ADHD treatment altogether with zinc supplementation was observed (51). Zinc role in ADHD disorder may be correlated with the activity of this biometal as a second messenger in brain cells. In turn, positive zinc action on attention processes may be connected with zinc regulation of dopamine metabolism and transport (47, 51). However, double blind placebo controlled study by Bilici et al. (53) showed that beneficial effects of 150 mg/day zinc sulfate supplementation for 12 weeks on ADHD symptoms were limited and rather comparable with placebo. All these findings indicate necessity of further studies on zinc role in ADHD disorder.

In autism spectrum disorder (ASD) the progress of disease may interfere with adequate supply of trace elements. ASD is a neural development disorder characterized by occurrence of repetitive behaviors and affected social interaction (31). Pathogenesis of this disorder is unknown but genetic, life-style and environmental factors are being under consideration now. It was hypothesized that one of important factors may be early zinc deficiency combined with accumulation of other toxic metals. Preliminary studies showed that most of children exhibiting ASD symptoms had significantly lowered zinc levels in hair (31). Also Faber et. al. suggested the importance of zinc deficiency and the probability of metallothionein detoxification system disturbances in ASD pathogenesis (54). They hypothesized that plasma zinc/copper ratio may be considered as a one of biomarkers of autism susceptibility in children. It was also reported that supplementation of nutrients, including zinc, during infancy development, can reduce severity of ASD symptoms (31). However, the exact mechanisms of beneficial effects of Zn in etiology of this disorder are not proved enough.

On the basis of presented studies, disturbances of zinc balance during human life span seem to be an important factor correlated with development of CNS diseases.

CONCLUSIONS

Zinc plays an essential role in the number of processes crucial for proper cells and organism function. The most important, regulated by this biometal, are gene expression, antioxidation defense and apoptosis. During human growth zinc can influence development and proper function of nervous system and neuronal plasticity. Specific zinc trans-

porters strictly regulate the uptake of this ion into the organism. However, zinc concentration in the diet is important, due to the lack of mechanisms which allow to store this biometal for a long time. The zinc imbalance can result not only from insufficient dietary intake, but also from impaired activity of zinc transport proteins and zinc dependent regulation of metabolic pathways. The crucial role of zinc homeostasis in CNS exhibits influence on proper function of learning, cognition and mood regulation. The adequate zinc levels in specific brain compartments seem to be critical for the proper brain functioning because even slight disturbances in zinc homeostasis may lead to or participate in the development of several disorders.

The exact role of zinc and zinc-binding proteins in CNS pathogenesis processes is being under intensive investigation. Therefore, the pressing issue is to dispel the doubts on the adequate zinc level in specific pools and find out how the concentration changes may be involved in the pathogenesis of diseases and brain dysfunctions. Notably, there is a need to develop reliable methods of determination zinc disturbances in the brain with the potential to use them in diagnosis of neurodegenerative diseases. The crucial issue is also to determinate appropriate zinc supplementation in brain diseases prevention as well as in proper treatment. Many detailed mechanisms of zinc activity in living cells are known to date but further research warrants understanding of complex influence of zinc on human organism.

REFERENCES

1. McCall K.A., Huang C., Fierke C.A.: J. Nutr. 130, 1437S (2000).
2. Solé Pascual A., Tyszka-Czochara M., Gdula-Argasińska J., Librowski T., Grzywacz A., Opoka W.: Med. Inter. Rev. 98, 55 (2012).
3. Ali A.A., Timinszky G., Arribas-Bosacoma R., Kozlowski M., Hassa P.O., Hassler M. et al.: Nat. Struct. Mol. Biol. 19, 685 (2012).
4. Chesters J.K., Petrie L.: J. Nutr. Biochem. 10, 279 (1999).
5. Hamza R.T., Hamed A.I., Sallam M.T.: Ital. J. Pediatr. 38, 21 (2012).
6. Gdula-Argasińska J., Tyszka-Czochara M., Paśko P., Opoka W.: Med. Inter. Rev. 99, 41 (2012).
7. Bao B., Prasad A.S., Beck F.W., Fitzgerald J.T., Snell D., Bao G.W. et al.: Am. J. Clin. Nutr. 91, 1634 (2010).
8. Mackenzie G.G., Zago M.P., Keen C.L., Oteiza P.I.: J. Biol. Chem. 277, 34610 (2002).
9. Xu H., Gao H.L., Zheng W., Xin N., Chi Z.H., Bai S.L. et al.: Hippocampus 21, 495 (2011).
10. Plum L.M., Rink L., Haase H.: Int. J. Environ. Res. Public Health 7, 1342 (2010).
11. Hönscheid A., Rink L., Haase H.: Endocr. Metab. Immune Disord. Drug Targets 9, 132 (2009).
12. Ertek S., Cicero A.F., Caglar O., Erdogan G.: Hormones (Athens) 9, 263 (2010).
13. Opoka W., Jakubowska M., Baś B., Sowa-Kućma M.: Biol. Trace Elem. Res. 142, 671 (2011).
14. Wojtasik A., Jarosz M., Stoś K.: in Nutrition Standards for Polish Population – amendment (Polish), Jarosz M. Ed., p. 123, Instytut Żywności i Żywienia, Warszawa 2012.
15. Costello L.C., Fenselau C.C., Franklin R.B.: J. Inorg. Biochem. 105, 589 (2011).
16. Wang X., Zhou B.: IUBMB Life 62, 176 (2010).
17. Espinoza A., Le Blanc S., Olivares M., Pizarro F., Ruz M., Arredondo M.: Biol. Trace Elem. Res. 146, 281 (2012).
18. Foster M., Karra M., Picone T., Chu A., Hancock D.P., Petocz P. et al.: Biol. Trace Elem. Res. 149, 135 (2012).
19. Pavlica S., Gebhardt R.: Neurochem. Int. 56, 84 (2010).
20. Bjorklund N.L., Sadagoparamanujam V.M., Taglialatela G.: J. Neurosci. Methods. 203, 146 (2012).
21. Morris D.R., Levenson C.W.: J. Toxicol., 2012, 785647; DOI: 10.1155/2012/785647 (2012).
22. Yamasaki S., Sakata-Sogawa K., Hasegawa A., Suzuki T., Kabu K., Sato E. et al.: J. Cell Biol. 177, 637 (2007).
23. Brewer G.J., Kanzer S.H., Zimmerman E.A., Molho E.S., Celmins D.F., Heckman S.M. et. al.: Am. J. Alzheimers Dis. Other Demen. 25, 572 (2010).
24. Lovell M.A., Smith J.L., Markesbery W.R.: J. Neuropathol. Exp. Neurol. 65, 489 (2006).
25. Izumi Y., Auberson Y.P., Zorumski C.F.: J. Neurosci. 26, 7181 (2006).
26. Levenson C.W., Morris D.: Adv. Nutr. 2, 96 (2011).
27. Stork C.J., Li Y.V. J. Cereb. Blood Flow Metab. 29, 1399 (2009).
28. Carter R.E., Aiba I., Dietz R.M., Sheline C.T., Shuttleworth C.W.: J. Cereb. Blood Flow Metab. 31, 1073 (2011).
29. Isaev N.K., Lozier E.R., Novikova S.V., Silachev D.N., Zorov D.B., Stelmashook E.V.: Brain Res. Bull. 87, 80 (2012).

30. Toren P., Eldar S., Sela B.A., Wolmer L., Weitz R., Inbar D. et. al.: Biol. Psychiatry 40, 1308 (1996).
31. Yasuda H., Yoshida K., Yasuda Y., Tsutsui T.: Sci. Rep. 1, 129 (2011).
32. Malaiyandi L.M., Dineley K.E., Reynolds I.J.: Glia 45, 346 (2004).
33. Schmidt M.V.: Psychoneuroendocrinology 36, 330 (2011).
34. Duman R.S., Voleti B.: Trends Neurosci. 35, 47 (2012).
35. Penninx B.W., Kritchevsky S.B., Yaffe K., Newman A.B., Simonsick E.M., Rubin S. et. al.: Biol. Psychiatry 54, 566 (2003).
36. Takeda A., Tamano H., Ogawa T., Takada S., Ando M., Oku N. et al.: Behav. Brain Res. 226, 259 (2012).
37. First M., Gil-Ad I., Taler M., Tarasenko I., Novak N., Weizman A.: J. Mol. Neurosci. 50, 88 (2012).
38. Koike H., Fukumoto K., Iijima M., Chaki S.: Behav. Brain Res. 238, 48 (2013).
39. Miners J.S., Barua N., Kehoe P.G., Gill S., Love S.: J. Neuropathol. Exp. Neurol., 70, 944 (2011).
40. Lyubartseva G., Lovell M.A.: Biofactors 38, 98 (2012).
41. Adlard P.A., Parncutt J.M., Finkelstein D.I., Bush A.I.: J. Neurosci. 30, 1631 (2010).
42. Nair N.G., Perry G., Smith M.A., Reddy V.P.: J. Alzheimers Dis. 20, 57 (2010).
43. Beyer N., Coulson D., Heggarty S. Ravid R., Irvine G.B., Hellemans J. et al.: Mol. Neurodegener. 4, 53 (2009).
44. Smith J.L., Xiong S., Markesbery W.R., Lovell M.A.: Neuroscience 140, 879 (2006).
45. Martel G., Hevi C., Kane-Goldsmith N., Shumyatsky G.P.: Behav. Brain Res. 223, 233 (2011).
46. Kim I., Park E.J., Seo J., Ko S.J., Lee J., Kim C.H.: Neuroreport 22, 839 (2011).
47. Myers S.A., Nield A., Myers M.: J. Nutr. Metab. 2012, 173712. DOI:10.1155/2012/173712 (2012).
48. Axelsen P.H., Komatsu H., Murray I.V.: Physiology (Bethesda) 26, 54 (2011).
49. Bhamra M.S., Ashton N.J.: Electrophoresis 33, 3598 (2012).
50. Schetz J.A., Chu A., Sibley D.R.: J. Pharmacol. Exp. Ther. 289, 956 (1999).
51. Arnold L.E., Disilvestro R.A., Bozzolo D., Bozzolo H., Crowl L., Fernandez S. et al.: J. Child Adolesc. Psychopharmacol. 21, 1 (2011).
52. Lepping P., Huber M.: CNS Drugs 24, 721 (2010).
53. Bilici M., Yıldırım F., Kandil S., Bekaroğlu M., Yıldırmış S., Değer O. et. al.: Prog. Neuropsychopharmacol. Biol. Psychiatry 28, 181 (2004).
54. Faber S., Zinn G.M., Kern J.C., Kingston H.M.: Biomarkers 14, 171 (2009).

Received: 12. 07. 2013

Acta Poloniae Pharmaceutica – Drug Research, Vol. 71 No. 3 pp. 379–383, 2014 ISSN 0001-6837
Polish Pharmaceutical Society

ANALYSIS

REVERSED-PHASE TLC STUDY OF SOME LONG CHAIN ARYLPIPERAZINE OF IMIDAZOLIDINE-2,4-DIONE AND IMIDAZO[2,1-*f*]PURINE-2,4-DIONE DERIVATIVES

AGNIESZKA ZAGÓRSKA[1], ANNA CZOPEK[1], KAROLINA PEŁKA[1], KRYSTYNA STANISZ-WALLIS[2] and MACIEJ PAWŁOWSKI[1]

[1]Department of Pharmaceutical Chemistry, [2]Department of Pharmacokinetics and Physical Pharmacy, Pharmaceutical Faculty, Jagiellonian University Medical College, 9 Medyczna St., 30-688 Kraków, Poland

Abstract: The chromatographic parameters of arylpiperazinylpropyl derivatives of imidazolidine-2,4-dione and imidazo[2,1-*f*]purine-2,4-dione were investigated using reversed-phase thin layer chromatography method. The results revealed that R_{M0} of investigated compounds depended on substituent in arylpiperazinyl fragment as well as on a nature of (cycloalkyl)aromatic ring at 5 position of imidazolidine-2,4-dione and at 7 position of imidazo[2,1-*f*]theophylline. The R_{M0} parameters were compared with computationally calculated partition coefficients values by principal component analysis (PCA). To verify the influence of lipophilic parameter of investigated compounds on their biological activity the statistical analysis of Mann-Whitney was performed.

Keywords: imidazolidine-2,4-diones, imidazo[2,1-*f*]purine-2,4-diones, lipophilicity

The monoamine hypothesis of depression postulates that a functional deficiency of 5-hydroxytryptamine (5-HT, serotonin) or noradrenaline and/or dopamine in the brain is a key to the pathology and/or behavioral manifestations associated with depression. An arylpiperazine moiety is one of the most universal templates used for designing agents active on serotonin (5-HT) receptors. Simple arylpiperazines are classified as non-selective 5-HT and other receptor ligands but long chain arylpiperazines (LCAPs) have been found as serotonin receptor ligands in particular 5-HT_{1A} and 5-HT_{2A} ones. Their general chemical structure contains: an alkyl chain (2–4 methylene units) attached to the N4 atom of the piperazine moiety, and a terminal fragment: amide or imide. The significance of the terminal part in ligand-receptor interaction has been the subject of many structure-activity relationships studies (1–3).

Lipophilicity is one of the most important physicochemical properties frequently used in QSAR (quantitative structure–activity relationship) analysis. This parameter, expressed as a partition coefficient or its decimal logarithm (log*P*), can be determined experimentally by various analytical methods (RP-HPLC, spectrophotometry, MEEKC, cyclic voltametry, titrimetry); however, the reversed-phase thin-layer chromatography (RP-TLC) is often used technique in recent years in this case (4–8). In this report, we describe the use of RP-TLC to determine the lipophilicity of some LCAPs derivatives of imidazolidine-2,4-dione (**1**-**10**) and imidazo[2,1-*f*]purine-2,4-dione (**11**-**22**). The investigated compounds have interesting biological properties and have been tested as a potential antidepressant or antipsychotic agents (9, 10). The relationship between the concentration of the organic modifier in the mobile phase and the chromatographic properties of the investigated compounds, as well as the influence of substituent on the lipophilicity of compounds **1**–**22**, was also studied. The lipophilicity values determined chromatographically were compared with the theoretically calculated partition coefficients values obtained by the use of computational methods. To verify the influence of lipophilic parameters of investigated compounds on their biological activity, the statistical analysis was performed.

* Corresponding author: e-mail: azagorsk@cm-uj.krakow.pl; phone: + 4812 6205456, fax: +4812 6205405

EXPERIMENTAL

The investigated LCAPs derivatives of imidazolidine-2,4-dione and imidazo[2,1-*f*]purine-2,4-dione were synthesized according to the methods described in the literature (9, 10). The chemical structures of these compounds are presented in Table 1. Methanol used was HPLC grade from E. Merck (Darmstadt, Germany). Water was deionized by use of a Millipore system. TLC was performed on precoated C18 F_{254} plates (10 × 20 cm, E. Merck) in horizontal DSII chambers (Chromdes, Lublin, Poland) under unsaturated (sandwich) conditions at room temperature. Mixtures of methanol content ranging between 50 and 80% (v/v) in 5% increments and water were used as seven mobile phases. The investigated compounds were separately dissolved in methanol (1 mg/mL) and applied on the plates (10 μL) as spots. The starting points were 10 mm from the bottom edge of the plates and development was carried out over 9.0 cm. After the development (30–60 min), the plates were air-dried at room temperature (22°C) and examined under a 254-nm UV lamp (CM-10, Spectroline, New York, USA). Each experiment was run in triplicate.

All graphs and statistical procedures were performed using the computer program Statistica for Windows (v.10.0, Statsoft Inc., 2011).

Table 1. The structures of compounds **1**–**22**.

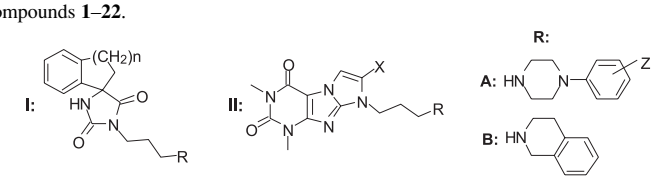

Comp.	Core	X/n	R	Z	Comp.	Core	X/n	R	Z
1	I	1	A	H	**12**	II	H	A	2-OCH_3
2	I	1	A	2-OCH_3	**13**	II	H	A	3-Cl
3	I	1	A	3-Cl	**14**	II	H	B	–
4	I	1	A	3-CF_3	**15**	II	CH_3	A	H
5	I	1	B	–	**16**	II	CH_3	A	2-OCH_3
6	I	2	A	H	**17**	II	CH_3	A	3-Cl
7	I	2	A	2-OCH_3	**18**	II	CH_3	B	–
8	I	2	A	3-Cl	**19**	II	C_6H_5	A	H
9	I	2	A	3-CF_3	**20**	II	C_6H_5	A	2-OCH_3
10	I	2	B	–	**21**	II	C_6H_5	A	3-Cl
11	II	H	A	H	**22**	II	C_6H_5	B	–

Table 2. R_{M0} (intercept), and r (correlation coefficient) values for linear relationship $R_M = R_{M0} + bC$.

Compound	R_{M0}	r	Compound	R_{M0}	r
1	3.261	0.9919	**12**	3.194	0.9970
2	2.943	0.9912	**13**	3.315	0.9965
3	3.354	0.9835	**14**	3.096	0.9990
4	3.702	0.9931	**15**	3.946	0.9874
5	3.541	0.9895	**16**	3.185	0.9925
6	3.020	0.9654	**17**	3.944	0.9950
7	3.516	0.9960	**18**	2.799	0.9874
8	3.665	0.9857	**19**	3.468	0.9915
9	3.947	0.9970	**20**	3.867	0.9925
10	2.678	0.9745	**21**	3.002	0.9931
11	3.729	0.9874	**22**	3.391	0.9825

Table 3. Log*P* values obtained by the use of computational methods.

Compound	*A*log*P*$_s$	milog*P*	logP$_{KOWIN}$	*X*log*P*2	logP$_{PALLAS}$	logP$_{CAChe}$
1	2.79	2.98	3.58	2.63	2.40	3.09
2	2.96	2.98	3.5	2.63	2.34	2.84
3	3.56	3.63	4.14	3.34	3.04	3.61
4	3.81	3.85	4.46	3.64	3.28	3.98
5	2.75	2.78	3.70	2.46	2.86	2.90
6	3.34	3.50	3.99	3.08	2.73	3.49
7	2.99	3.51	4.07	3.20	2.68	3.24
8	3.92	4.15	4.63	3.91	3.36	4.01
9	4.23	4.37	4.95	4.21	3.62	4.37
10	3.24	3.30	4.19	3.03	3.40	3.29
11	2.36	2.32	2.65	2.02	1.50	1.96
12	2.43	2.33	2.73	1.93	1.57	1.70
13	2.95	2.97	3.29	2.64	2.24	2.48
14	2.03	2.12	2.85	1.76	0.77	1.76
15	2.73	2.54	3.20	2.48	0.99	1.52
16	2.80	2.55	3.28	2.39	1.05	1.27
17	3.26	3.19	3.84	3.10	1.73	2.04
18	2.41	2.34	2.40	2.22	1.28	1.33
19	3.65	3.99	4.41	3.83	2.93	2.96
20	3.65	4.00	4.49	3.75	3.00	2.71
21	4.13	4.64	5.06	4.45	3.67	3.48
22	3.42	3.72	-	3.70	2.71	2.76

RESULTS

The relative lipophilicity (R_{M0}) of the investigated compounds was determined with the use of nonpolar RP-C18 plates. On the basis of literature data (11, 12), methanol was selected as the organic modifier of the mobile phases. For all the compounds and each seven mobile phase, the R_M values were calculated by the use of the well known formula $R_M = \log ([1 - R_F]/R_F)$. The calculated R_M values were then used for the calculation of R_{M0} values extrapolated to zero percent of methanol concentration with the equation $R_M = R_{M0} + bC$, where C is the concentration in volume percent of methanol in the mobile phase and b is the change in R_M caused by unit methanol concentration in the mobile phase. The obtained R_{M0} values for investigated compounds were also compared with the theoretical values of partition coefficients. The coefficients *A*log*Ps*, milog*P*, logP_{KOWIN} and *X*log*P*2 were calculated from the Virtual Computational Laboratory website (13), logP_{Pallas} by Pallas 3.1 and Xlog*P* by CAChe 7.75. To verify the influence of parameter R_{M0} of investigated compounds on their biological activity, the statistical analysis was performed.

DISCUSSION AND CONCLUSION

It was found that the R_M values decreased linearly with increasing concentration of organic modifier in the eluent. The relationships between the relative lipophilicity expressed as R_{M0} values and the concentration of methanol in the mobile phase showed good linearity for all seven mobile phase systems ($r > 0.97$), as shown in Table 2. For investigated compounds, the relationship between the structure and values of R_{M0} was observed. The extension of the ring in position 5 of hydantoin and the introduction of phenyl moiety at position 7 of imidazo[2,1-*f*]theophylline caused a significant increase of R_{M0} values. The introduction of electron withdrawing substituents (Cl, CF_3) into the phenylpiperazine system resulted in a significant increase of R_{M0} values for imidazolidine-2,4-dione derivatives. The

Table 4. The eigenvalues and the ratios of the variance explained by the seven components using covariance matrix.

Component	Eingenvalue	Variance explained (%)	Total variance explained (%)
1	5.556159	79.37370	79.3737
2	0.994110	14.20157	93.5753
3	0.312365	4.46236	98.0376
4	0.057631	0.82330	98.8609
5	0.048352	0.69075	99.5517
6	0.027833	0.39761	99.9493
7	0.003550	0.05072	100.0000

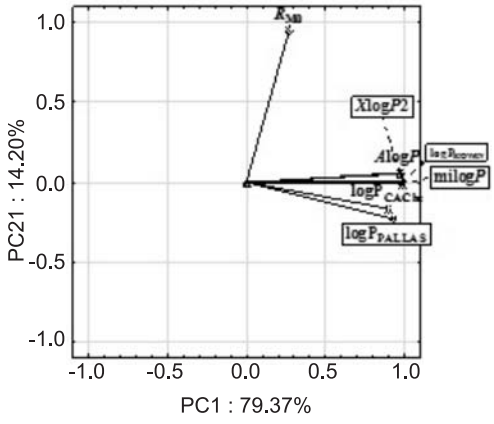

Figure 1. Comparison of the obtained R_{M0} values with the calculated coefficients by PCA

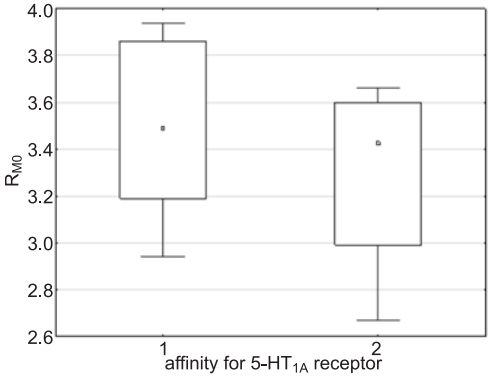

Figure 2. R_{M0} ranges and mean lipophilicity for all compounds, except **14**, **18**, **21** and **22** ($K_{i\ 5\text{-}HT1A}$: 1 < 100 nM, 2 > 100 nM)

substituents at position 2 or 3 of aromatic ring can be arranged in series, according to obtained R_{M0} values, namely: CF_3 > Cl > OCH_3. Furthermore, replacement of the arylpiperazine fragment with

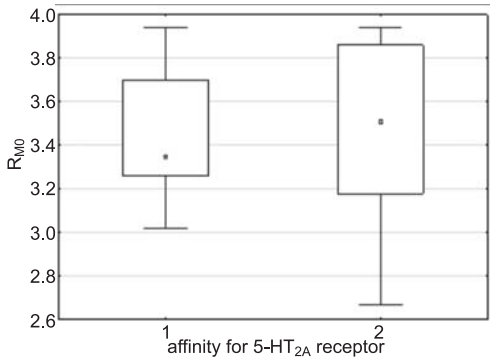

Figure 3. R_{M0} ranges and mean lipophilicity for all compounds, except **14**, **18, 21** and **22** ($K_{i\ 5\text{-}HT2A}$: 1 < 100 nM, 2 > 100 nM)

tetrahydroisoquinoline moiety caused a decrease of adjusted relative lipophilicity parameter. Surprisingly, in the 7-phenyl-imidazo[2,1-*f*]purine-2,4-dione group, the exchange of tetrahydroisoquinoline moiety into phenylpiperazine derivatives as well as the introduction of methoxy group caused an increase of experimental R_{M0} values, most likely due to electron interactions of individual fragments. The obtained results revealed that substituent in arylpiperazinyl fragment as well as a nature of (cycloalkyl)aromatic ring at 5 position of imidazolidine-2,4-dione and at 7 position of imidazo[2,1-*f*]theophylline had an impact on R_{M0} values. Moreover, the experimental coefficients differ from the computationally calculated partition coefficients (Table 3); only the *A*log*P*s coefficient can be slightly compared with the obtained R_{M0} values.

The multivariate comparison of the experimentally obtained values and the coefficients calculated by the computational methods was made by principal component analysis (PCA). This technique decorrelates the variables and converts them into the linear combinations called "principal components." The graphical interpretation of the multidimension-

al space of the data set used by the PCA transformation is obtained with a smaller number of new dimensions of space. The second column of Table 4 explained the percent of observed variance. The first component (PC1) of the index explains 79.4% of the total variance. The second component (PC2) explains 14.2%, while the third component (PC3) explains only 4.46% of the total variance. Together, the first two principal components contain 93.58% of the total variance. The first component is determined by the theoretical variables computationally calculated and are closely related, therefore, constitute a homogeneous group. The second component represents the empirical variable R_{M0}. Both components are mutually orthogonal, that is not depend on each other (Fig. 1).

The differences between the computationally calculated partition coefficients confirm the legitimacy of the determination of lipophilicity for the investigated compounds by the use of the experimental (RP-TLC) method. It can be anticipated that the experimental results would give a better correlation with the biological activity than the theoretical ones. For investigated compounds, the impact of lipophilicity on the affinity for 5-HT receptors in the Mann-Whitney test was statistically not significant (Figs. 2 and 3). It suggested that lipophilicity is one of the many factors, which could influence and modify the activity of the investigated compounds for 5-HT receptors.

Acknowledgment

We are pleased to acknowledge the generous financial support of this work by the Medical College of Jagiellonian University (grant No. K/ZDS/001909).

REFERENCES

1. Badarau E., Suzenet F., Bojarski A. J., Finaru A-L., Guillaumet G.: Bioorg. Med. Chem. 19, 1600 (2009).
2. Volk B., Gacsalyi I., Pallagi K., Poszavacz L., Gyonos I., Szabo E., Bako T., Spedding M., Simig G., Szenasi G.: J. Med. Chem. 54, 6657 (2011).
3. Chłoń-Rzepa G., Żmudzki P., Zajdel P., Bojarski A.J., Duszyńska B., Nikiforuk A., Tatarczyńska E., Pawłowski M.: Bioorg. Med. Chem. 15, 5239 (2007).
4. Morak-Młodawska B., Pluta K.: J. Liq. Chromatogr. Relat. Technol. 31, 611 (2008).
5. Waksmundzka-Hajnos M., Matosiuk D., Petruczynik A., Kijkowska-Murak U.: Acta Chromatogr. 20, 563 (2008).
6. Inglot T., Gumieniczek A., Komsta Ł., Kasińska A.: Chromatographia 68, 977 (2008).
7. Pękala E., Marona H.: Biomed. Chromatogr. 23, 543 (2009).
8. Kulig K., Malawska B.: J. Planar Chromatogr. 22, 141 (2009).
9. Czopek A., Byrtus H., Kołaczkowski M., Pawłowski M., Dybała M., Nowak G., Tatarczyńska E., Wesołowska A., Chojnacka-Wójcik E.: Eur. J. Med. Chem. 45, 1295 (2010).
10. Zagórska A., Jurczyk S., Pawłowski M., Dybała M., Nowak G., Tatarczyńska E., Nikiforuk A., Chojnacka-Wójcik E.: Eur. J. Med. Chem. 44, 4288 (2009).
11. Komsta Ł., Skibiński R., Berecka A., Gumieniczek A., Radkiewicz B., Radoń M.: J. Pharm. Biomed. Anal. 53, 911 (2010).
12. Rutkowska E., Pająk K., Jóźwiak K.: Acta Pol. Pharm. Drug Res. 70, 3 (2013).
13. Tetko I.V., Tanchuk V.J.: VCC-Lab 2002, www.vcclab.org/lab/alogps\

Received: 30. 07. 2013

Acta Poloniae Pharmaceutica – Drug Research, Vol. 71 No. 3 pp. 385–391, 2014 ISSN 0001-6837
Polish Pharmaceutical Society

LEVELS OF SOME MICROELEMENTS AND ESSENTIAL HEAVY METALS IN HERBAL TEAS IN SERBIA

ŽELJKO MIHALJEV[1] , MILICA ŽIVKOV-BALOŠ[1*], ŽELJKO ĆUPIĆ[2] and SANDRA JAKŠIĆ[1]

[1] Scientific Veterinary Institute „Novi Sad“, Rumenački put 20, 21000 Novi Sad, Serbia
[2]Research Institute for Reproduction, Artificial Insemination and Embryotransfer “Temerin”, Industrijska zona bb, 21235 Temerin, Serbia

Abstract: Levels of Fe, Mn, Cu, Zn, Mo, Co, Ni, Se, Sn and Al were determined in 14 medicinal plants from Serbia, which are widely used in phytopharmacy as herbal teas. The following plants were investigated: yarrow (*Achillea millefolium* L.*)*, basil (*Ocimum basilicum* L.*),* St. John’s wort (*Hypericum perforatum* L.*),* peppermint (*Mentha x piperita* L.), field horsetail (*Equisetum arvense* L.), stinging nettle (*Urtica dioica* L.), thyme (*Thymus serpyllum* L.), maize silk (*Zea mays* L. – *Maydis stigma*), hibiscus (*Hibiscus sabdariffa* L.), marshmallow (*Althaea officinalis* L.), chamomile (*Matricaria chamomilla* L.), rosehip/dog rose (*Rosa canina* L.), winter savory (*Satureja montana* L.) and spearmint (*Mentha spicata* L.). A total of 16 samples of different parts of medicinal plants (root, leaf, flower, herba) were examined, whereby 13 samples were delivered in original package and three samples were loose leaf herbs. Samples were prepared using the microwave digestion technique, and measurements were performed applying the atomic absorption spectrometry and mass spectrometry with inductively coupled plasma. Contents of microelements in the examined samples were in the range: Mn (23.86 – 453.71 mg/kg); Fe (61.87 – 673.0 mg/kg); Cu (6.68 – 24.46 mg/kg); Zn (16.11 – 113.81 mg/kg); Mo (0.576 – 4.265 mg/kg); Co (0.039 – 0.532 mg/kg); Se (0.036 – 0.146 mg/kg); Ni (0.738 – 6.034 mg/kg); Al (154.0 – 3015.0 mg/kg) and Sn (2.68 – 10.22 mg/kg). According to determined amounts of microelements, the investigated samples of herbal teas are considered safe for human consumption.

Keywords: herbal teas, microelements, AAS, ICP- MS

Mineral elements are of a unique and manifold importance for both the plant world and human beings. Minerals are found in plants as ions, inorganic and organic salts or are incorporated into diverse organic compounds (1). Mineral elements are involved in a range of chemical reactions in plants. According to their proportional representation in the plant composition, they are grouped into macro, micro and ultra microelements. The content of mineral elements in plants may vary significantly. Variations in mineral matter content in plants are due to a variety of factors, including plant species, plant age, pedological features of soil, climate and implementation of agrotechnical measures (2–5). The same plant species differ in microelement content under different ecological conditions, while diverse species in the same biotope accumulate different amounts of microelements (6).

Human body needs appropriate concentrations of various minerals to maintain the normal function and sustain life. Deficiency or excess of essential heavy metals in the diet can induce various health disorders. Medicinal plants are either direct or indirect source of minerals in human diet and regular consumption of tea can contribute to the dietary requirements of these elements (5). Species used for obtaining a range of phytopreparations in pharmaceutical industry, supplied as monocomponent teas or tea blends that are widely applied in traditional medicine in Serbia and thus are of particular importance. Sources for obtaining medicinal raw material are wild crafted plants (over 200 species) or cultivated plants (ca. 30 species) (7). Chemical composition of teas is very complex, encompassing flavonoids, alkaloids, enzymes, minerals and trace elements (8). In Serbia, herbal teas are mainly prepared from aromatic herbal species that contain etheric oils, which are not only remedial but also have a very pleasant scent and aroma. Phytotherapy has a very long tradition and became popular in modern medicine, since medicinal herbs are not aggressive and do not have severe side effects.

* Corresponding author: e-mail: milica@niv.ns.ac.rs; phone: +381214895360; fax: +38121518544

Intensive agrotechnical measures in modern agriculture, vicinity of industrial plants, mines, traffic roads inevitably lead to contamination of the soil and plants with pesticides and heavy metals (9). Plants are a link for the transfer of trace elements from soil to man. Thus, the content of heavy metals is an important criterion when using plant material in the production of traditional remedies and herbal infusions (10). In that respect, continuous and planned monitoring of hygienic safety of plants used as raw material in pharmaceutical industry is important. The determination of microelements content is important in view of plant, animal and human health and environmental aspect as well (4). However, there are no standards for medicinal raw plant materials, which establish a permissible level of microelements except for heavy metals: lead, cadmium (11) and mercury (12). Content and bioavailability of potentially harmful microelements as well as their interaction with the plant constituents need to be established prior to potential toxicity assessment.

Owing to the importance of minerals present in teas, in the present study, some microelements (Mo, Co, Ni, Se, Sn, Al) including essential heavy metals (Fe, Cu, Zn, Mn), were determined in order to update and evaluate the knowledge on the presence and to determine the correlation between the selected elements in different Serbian tea plant samples. The aim was also to establish the health-safety of these phyto products, having in mind their wide application in folk medicine.

EXPERIMENTAL

Materials

All samples used in this research are herbal teas (Table 1), widely applied and popular among Serbian population and in folk medicine practices. Cultivated herbal tea samples in original package (samples No. 1–13) were collected from the retail shops in the territory of Novi Sad (Vojvodina, North Serbia region, locality I), whereas three samples of wild growing medicinal plants (samples No. 14, 15 and 16) were collected directly from the natural habitat (East Serbia region, locality II).

The following reagents were used: standard solutions of Mn, Fe, Cu, Zn, Mo, Co, Ni, Se, Sn and Al at a concentration of 1 mg/kg (Accu Trace™ Reference Standard, USA), nitric acid and H_2O_2 (Merck, Germany), deionized water with conductivity < 0.2 μS/cm.

Apparatus

The mineralization was carried out in a microwave digestion system (Ethos Microwave Labstation, Milestone, Italy).

Table 1. Herbal teas and plant parts used in research.

No	Plant	Latin name (family)	Parts with medicinal properties
1	Yarrow	*Achillea millefolium L.* (Asteraceae)	herba
2	Basil	*Ocimum basilicum L* (Lamiaceae)	herba
3	St. John's wort	*Hypericum perforatum L.* (Hypericaceae)	herba
4	Peppermint	*Mentha x piperita L.* (Lamiaceae)	leaf
5	Field horsetail	*Equisetum arvense L.* (Equisetaceae)	herba
6	Stinging nettle	*Urtica dioica L.* (Urticaceae)	root
7	Stinging nettle	*Urtica dioica L.* (Urticaceae)	leaf
8	Thyme	*Thymus serpyllum L.* (Lamiaceae)	herba
9	Maize	*Zea mays, Maydis stigma* (Poaceae)	silk
10	Hibiscus	*Hibiscus sabdariffa L.* (Malvaceae)	flower
11	Marshmallow	*Althaea officinalis L.* (Malvaceae)	root
12	Chamomile	*Matricaria chamomilla L.* (Asteraceae)	flower
13	Rosehip, dog rose	*Rosa canina L.* (Rosaceae)	fruit
14	Winter savory	*Satureja montana L.* (Lamiaceae)	herba
15	St. John's wort	*Hypericum perforatum L.* (Hypericaceae)	herba
16	Spearmint	*Mentha spicata L.* (Lamiaceae)	herba

The measurements were performed using atomic absorption spectrophotometer SpectrAA-10 (Varian, USA) and inductively coupled plasma mass spectrometer Agilent ICP-MS 7700x.

Procedures

The measurement of the content of elements in herbal tea samples was performed subsequent to determining the loss of mass after drying according to the procedure given in the European Pharmacopoeia 6.0 (13).

The samples were prepared applying the microwave digestion method (14) with the use of the mixture H_2O_2/HNO_3 (1 : 4, v/v). After this process, the samples were transferred to 50 mL volumetric flasks and diluted with deionized water.

Determination of Mn, Fe, Cu, Zn by AAS method

The concentrations of manganese (λ = 279.5 nm), iron (λ = 248.3 nm), copper (λ = 324.7 nm) and zinc (λ = 213.9 nm) were determined by atomic absorption spectrophotometry applying Varian SpectrAA-10 apparatus. The measurements were performed in triplicates for each particular sample.

Determination of Mo, Co, Ni, Se, Al, Sn by ICP-MS method

Determination of cobalt (He-M, IT 0.1 s/P), nickel (He-M, IT 1 s/P), selenium (He-M, IT 5 s/P), molybdenum (He-M, IT 0.1 s/P), tin (NoG-M, IT 0.1 s/P) and aluminium (He-M, IT 0.3 s/P) was performed using Agilent ICP-MS 7700 mass spectrometer under common operating conditions with an excitation power of plasma of 1550 w, flow-rate of carrier gas 1.01–1.11 L/min, flow rate of He gas 3.2–4.0 mL/min. Peristaltic pump program: uptake speed 0.50 rps; uptake time 25 s and stabilization time 20 s in spectrum multi tune mode. Determination was done using isotopes: ^{59}Co, ^{60}Ni, ^{78}Se, ^{95}Mo, ^{118}Sn and ^{27}Al.

Statistical analysis:

The results were expressed as the means and standard deviations. Pearson correlation coefficient was used for comparing the results between microelements. Significance level was determined as $p < 0.01$. The analysis was performed using a software package IBM SPSS Statistics 20.

Table 2. Content of microelements determined by AAS in the herbal tea samples, mg/kg dry weight, n = 3.

Sample no.	**Mn** [mg/kg]	**Fe** [mg/kg]	**Cu** [mg/kg]	**Zn** [mg/kg]
1.	77.90	67.24	15.56	28.48
2.	71.98	539.87	24.46	38.09
3.	80.86	63.71	10.93	22.18
4.	111.97	443.90	17.15	26.86
5.	254.70	617.46	7.76	27.9
6.	28.18	673.00	12.71	22.75
7.	57.84	303.00	13.23	29.14
8.	127.06	445.78	8.94	44.26
9.	31.60	193.21	8.10	59.80
10.	453.71	219.82	7.80	46.24
11.	23.86	114.16	15.69	23.59
12.	76.14	130.26	14.25	34.67
13.	70.99	61.87	6.68	16.11
14.	54.22	155.83	10.76	51.11
15.	170.78	217.32	19.86	113.81
16.	37.24	150.85	15.87	31.43
Mean	108.06	274.83	13.11	38.53
min	23.86	61.87	6.68	16.11
max	453.71	673	24.46	113.81
CV [%]	101	74	38	60

RESULTS AND DISCUSSION

In Table 2, the results of contents of Mn, Fe, Cu and Zn determined by AAS in examined tea samples are displayed.

The contents of Mn in herbal teas ranged from 23.86 ± 0.43 mg/kg (marshmallow root) to 453.71 ± 14.07 mg/kg (hibiscus flower), with an average value of 108.06 mg/kg and CV 101.48%. Mn contents in herbal teas: peppermint, chamomile, stinging nettle (leaf), stinging nettle (root), St. John's wort, yarrow and basil correspond with the results of other authors, including low content in the marshmallow (15–17). Concentration of Mn in the peppermint and chamomile was also in accordance with recent data from the literature (111.97 in relation to 120.4 mg/kg and 76.14 in relation to 69.3 mg/kg), but Mn content obtained in rosehip tea was multifold lower (70.99 in relation to 1585.9 mg/kg) (8). The cited authors themselves pointed out the high manganese levels in herbal teas obtained in their research. It should be emphasized that content of Mn in hibiscus tea (453.71 ± 14.07 mg/kg) was elevated as compared to other samples. Similar results revealing high Mn content in hibiscus (717 ± 15 mg/kg), but also in chamomile (137 ± 5 mg/kg) as compared to other plants are pointed out in the researches from Bulgaria and Macedonia (18). Manganese content in stinging nettle leaf sample is in correlation with the result obtained for nettle (herba) collected from natural habitats from Transylvania: 52.73 ± 0.21 mg/kg (4). The obtained levels of Mn in chamomile, St. John's wort, stinging nettle, peppermint, rosehip, yarrow and thyme were somewhat higher than levels measured in Romanian plants, especially for field horsetail: 254.70 in relation to 18 mg/kg (19).

The levels of Fe established in herbal teas ranged from 61.87 ± 1.11 mg/kg (rosehip) to 673 ± 18.18 mg/kg (stinging nettle – root). High Fe content in the following herbal teas should be pointed out: basil, peppermint, field horsetail, stinging nettle – root and thyme. Higher Fe concentration was observed in the peppermint leaf as compared to the samples of spearmint (herba). This could be explained by its function in chlorophyll synthesis in the leaf. Wild growing St. John's wort obtained from locality II revealed higher content of Fe as compared to the cultivated St. John's wort (locality I). Fe levels established in the following herbal teas: peppermint, stinging nettle, St. John's wort, marshmallow, yarrow and basil compare well with some minor differences with previous results for Serbian samples (15).

Maximum Cu level was established in basil, being 24.46 ± 0.19 mg/kg, while minimum Cu content (6.68 ± 0.06 mg/kg) was determined in rosehip fruit. Copper concentrations in chamomile, stinging nettle, St. John's wort and marshmallow are in accordance with the results of other authors (15), whereas Cu levels obtained in peppermint, yarrow and basil were somewhat higher than those reported by aforementioned authors. Content of Cu measured in stinging nettle is the same as recorded in Transylvanian nettle herba (4). On the other hand, this content is lower than in Romanian sample (20). Obtained levels in samples of peppermint, chamomile, and thyme are higher than in Romanian plants (20).

The concentrations of zinc were fairly consistent among the tea samples, with the exception of St. John's wort from the locality II that revealed maximum content of Zn of 113.81 ± 4.89 mg/kg. This value was five times higher than that measured in St. John's wort sample originating from the locality I (22.18 ± 1.10 mg/kg). Potential reason for such difference is most probably the soil type. Results on Zn content in peppermint, chamomile, stinging nettle, St. John's wort, marshmallow, yarrow and basil correspond with the results of other authors (15). Furthermore, measured Zn concentrations in peppermint and rosehip well correspond with recent result, but levels obtained for chamomile were higher (8). The obtained Zn content in samples of chamomile and hibiscus were similar as determined in Bulgarian and Macedonian plants, being 45 ± 2 and 33 ± 2 mg/kg, respectively (18).

As it can be seen from Table 3, Mo content in tea samples was low. Maximum Mo content was measured in a sample of nettle leaf: 4.265 ± 0.034 mg/kg and the minimum content was determined in rosehip 0.576 ± 0.011 mg/kg. Mo content in nettle root (0.733 ± 0.011 mg/kg) was somewhat lower than in Hungarian research for nettle (herba): 1.14 ± 0.77 mg/kg (4). In nettle leaf, Mo content was significantly higher: 4.265 ± 0.034 mg/kg, which probably can be explained by its increased presence in the composition of nitrate reductase in the nettle leaf.

Maximum Co level was established in field horsetail being 0.532 ± 0.002 mg/kg, while minimum Co content (0.039 ± 0.001 mg/kg) was determined in rosehip fruit. In nettle sample from Transylvania, Co was not detected (4). Co content was below the detection limit in samples of peppermint, chamomile, nettle and thyme from Romania (20). Contrary to this, higher Co content was determined in chamomile and hibiscus samples in

Table 3. Content of microelements determined by ICP-MS in the herbal tea samples, mg/kg dry weight, n = 3.

Sample No.	**Mo** [mg/kg]	**Co** [mg/kg]	**Ni** [mg/kg]	**Se** [mg/kg]	**Al** [mg/kg]	**Sn** [mg/kg]
1.	2.267	0.130	2.401	0.055	3015	3.01
2.	2.720	0.310	1.037	0.084	808	6.09
3.	2.212	0.102	2.567	0.085	1340	5.87
4.	2.695	0.161	1.882	0.107	554	3.66
5.	0.972	0.532	2.763	0.063	1702	2.77
6.	0.733	0.485	6.034	0.047	585	2.77
7.	4.265	0.084	0.738	0.074	222	10.22
8.	0.747	0.199	1.938	0.086	903	3.85
9.	2.369	0.079	1.012	0.047	438	3.89
10.	1.123	0.314	3.481	0.104	1185	2.68
11.	0.680	0.100	1.362	0.102	1383	2.79
12.	1.940	0.104	2.518	0.146	1354	3.99
13.	0.576	0.039	1.262	0.080	351	3.01
14.	0.778	0.074	0.892	0.036	225	6.05
15.	1.707	0.350	2.645	0.078	154	5.37
16.	1.507	0.060	0.816	0.062	622	6.91
Mean	1.706	0.195	2.084	0.078	928	4.56
min	0.576	0.039	0.738	0.036	154	2.68
max	4.265	0.532	6.034	0.146	3015	10.22
CV [%]	60	80	65	35	79	45

Bulgaria: 0.30 ± 0.01 and 1.00 ± 0.03 mg/kg, respectively (18).

Maximum Ni content was measured in a sample of nettle root and the minimum content was recorded in nettle leaf. Similar results were obtained for Co content suggesting similar mechanisms of its uptake from the soil. Ni content in St. John's wort samples originating from two different locations was almost the same. In rosehip, peppermint, chamomile, St. Jon's wort and nettle leaf, Ni contents were similar to Romanian results: 0.9; 1.8; 3.9; 2.1; and 0.6 ppm, respectively (19). When comparing the results with Romanian ones and taking into consideration the type of mint and plant part, peppermint and nettle leaf samples were comparable, while results for nettle root indicated 10 times higher content of Ni. Results for chamomile and yarrow were similar to those obtained in previous investigations for these plants in Serbia (3.14 and 3.27 mg Ni/kg) (17).

Maximum Se content was measured in a sample of chamomile flower 0.146 ± 0.004 mg/kg, while the minimum content was determined in winter savory: 0.036 ± 0.001 mg/kg. Similar to Ni, Se content in samples of St. John's wort from two localities were comparable. Contents of Se in St. Jon's wort and nettle were higher than those obtained in Romanian samples (21). This can be explained by the soil type and fertilizer application in cultivated conditions.

In the analyzed herbal teas, unexpectedly high values for Al were obtained, especially in yarrow. The lowest content of Al was determined in St. John's wort from the locality II – natural habitat, while cultivated St. John's wort from locality I revealed 10 times higher Al content. On the other hand, Al content in cultivated peppermint leaf was similar to those in spearmint from locality II. Analogous conclusions about the effects of plant species and locality on the mineral composition are confirmed in the literature (6). Content of Al in root nettle sample (585 ± 11 mg/kg) is similar to the results obtained in Transylvanian samples of nettle (herba): 476.8 ± 6.38 mg/kg (4). Result 222 ± 22 mg/kg in leaf nettle sample corresponds to previous Serbian result, while Al content in other tea samples is different (15).

Maximum Sn level was established in nettle leaf, being 10.22 ± 0.09 mg/kg, while minimum Sn content (2.68 ± 0.02 mg/kg) was determined in

hibiscus flower. As visible from Table 3, Sn content in St. John's wort from locality I is equal to that at locality II. Concentration of Sn determined in peppermint and chamomile sample was similar to previous results (8), while content measured in rosehip was lower.

Results of microelements determination in some Polish herbs showed lower mean concentrations of Cu, higher levels of Zn and Ni and similar content of Fe in comparison to Serbian tea herbs (22); while another research demonstrated similar content of Ni and lower of Fe and Cu (23). Results on Mn, Fe, Cu and Zn levels in Spanish peppermint and chamomile are very similar to our results, while Al content was different (24).

In order to estimate possible correlation between microelements, the obtained results are analyzed using statistical software. Results demonstrated significant Pearson correlations (at the 0.01 level) between Fe-Co, Co-Ni, Mo-Sn and Ni-Sn: 0.78; 0.70; 0.66 and –0.50, respectively. Contrary to the literature data (25), our results did not show any significant correlation between Zn-Cu and Mn-Zn, but the investigated herbal teas were different. Correlations are comparable to those reported for Romanian herbal teas with respect to significant Fe-Co correlation and without correlations between Zn-Cu-Mn (19).

CONCLUSION

Sixteen samples of 14 different herbal teas widely consumed among Serbian population were analyzed for concentration of microelements, with an aim of establishing the mineral status and hence the health safety of medicinal plants used for very popular herbal teas. The contents of the examined elements were within the ranges reported in the literature, with some variations associated with plant species, applied agricultural measures and pedological features of soil. Large scale variability in the concentration of microelements was observed according to the species of medicinal plants and the availability of microelements in the soil. The highest contents of essential heavy metals were established for Fe (61.87–673.0 mg/kg). Maximum Fe level was observed in stinging nettle root (673 ± 18.18 mg/kg). The research revealed that basil, peppermint, stinging nettle (root), field horsetail and thyme are rich in iron. Thus, these plants are beneficial Fe source for humans. The highest variations are established for Mn content (CV = 101.48%) and the lowest for selenium (CV = 35.67%). The examined plant species may be considered as non-toxic natural source of essential microelements.

This paper is one of the rare comprehensive examinations of mineral composition of plants from different geographical regions of Serbia and represents a basis for further research on availability and interactions with other tea constituents. However, continuous monitoring of products for human consumption conducted by relevant institutions is indispensible. Thus, there is an increasing demand for even more reliable and rapid methods of quality control of medicinal plants. Cultivation of medicinal plants and good agricultural practice are the first step in quality and health safety assurance of plant-based medicinal products.

Acknowledgment

Research was financed by the Ministry of Educations, Science and Technology, Republic of Serbia, projects No. TR 31084 and TR 31071.

REFERENCES

1. Kastori R., Maksimović I.: in Ishrana biljaka, Vojvođanska akademija nauka i umetnosti, Novi Sad, 2008.
2. Živkov-Baloš M., Mihaljev Ž., Mašić Z.: Savremena poljop. 48, 285 (1999).
3. Radanović D., Antić-Mladenović S., Nastovski T.: in Proceedings from the Third Conference on Medicinal and Aromatic Plants of Southeast European Countries, p. 10, Belgrade, Serbia (2006).
4. Szentmihályi K., Marczal G., Then M.: Thaiszia – J. Bot., Košice, 16, 99 (2006).
5. Saletovic M., Hodzic Z., Banjanin B, Kesic A: HealthMED 5, 1358 (2011).
6. Kashin V.K.: Chem. Sus. Dev. 19, 237 (2011).
7. Kovačević N.: *Osnovi farmakognozije*, Srpska školska knjiga, Farmaceutski fakultet, Beograd 2002.
8. Ražić S., Kuntić V.: Int. J. Food Prop. 16, 1 (2013).
9. Seenivasan S., Manikandan N., Muraleedharan N.N., Selvasundaram R.: Food Control 19, 746 (2008).
10. Kostić D., Mitić S., Zarubica A., Mitić M., Veličković J., Ranđelović S.: Hem. Ind. 65, 165 (2011).
11. World Health Organization WHO: guidelines for assessing quality of herbal medicines with reference to contaminants and residues, Geneva 2007.
12. European Pharmacopoeia 7.0. Council of Europe, Strasbourg 2010.

13. European Pharmacopoeia 6.0. Council of Europe, Strasbourg 2008.
14. Milestone's Tips & Techniques Book and Aplication – An Operations Overview & Practical Guide by Keneth Borowsky, Method: Tea Leaves – Application Note 003, 2000.
15. Ražić S., Onjia A., Dogo S., Slavković L., Popović A.: Talanta 67, 233 (2005).
16. Ražić S., Dogo S., Slavković L.: J. Serb. Chem. Soc. 71, 1095 (2006).
17. Ražić S., Dogo S., Slavković L.: J. Nat. Med. 62, 340 (2008).
18. Gentscheva D.G., Stafilov T., Ivanova H.E.: Eurasian J. Anal. Chem. 5, 104 (2010).
19. Stef S.D., Gergen I., Traşcă I.T., Hărmăneşcu M., Stef L., Drugă M., Biron R., Hegheduş – Mîndru G.: Anim. Sci. Biotechnol., 43, 127 (2010).
20. Kékedy-Nagy L., Ionescu A.: Acta Universitatis Sapientiae, Agriculture and Environment 1, 11, (2009).
21. Antal, S.D., Canciu, M.C., Dehelean, A.C., Anke, M.: in Analele Universităţii din Oradea-Fascicula Biologie, Vol. XVII/1, p. 23, (2010).
22. Kalny P., Fijałek Z., Daszczuk A., Ostapczuk P.: Sci. Total Environ. 381, 99 (2007).
23. Kalny P., Wyderska S., Fijałek Z., Wroczyński P.: Acta Pol. Pharm. Drug Res. 69, 279 (2012).
24. Queralt I., Ovejero M., Carvalho M.L., Marques A.F., Llabres J.M.: X-Ray Spectrom. 34, 213 (2005).
25. Konieczynski P., Wesolowski M.: Food Chem. 103, 210 (2007).

Received: 13. 08. 2013

Acta Poloniae Pharmaceutica – Drug Research, Vol. 71 No. 3 pp. 393–400, 2014 ISSN 0001-6837
Polish Pharmaceutical Society

STABILITY INDICATING HPLC-UV METHOD FOR DETERMINATION OF DAPOXETINE HCl IN PHARMACEUTICAL PRODUCT

KAI BIN LIEW and KOK KHIANG PEH*

School of Pharmaceutical Sciences, Universiti Sains Malaysia, 11800 Minden, Penang, Malaysia

Abstract: A stability-indicating HPLC-UV method for the determination of dapoxetine hydrochloride in solution and pharmaceutical product was developed. The mobile phase was composed of acetonitrile and 0.2 M ammonium acetate buffer at 50 : 50 ratio. The chromatographic parameters, theoretical plates (N), tailing factor (T), capacity factor (k') and peak asymmetry factor (As) were calculated. Stress degradation studies, namely, acid, alkali, oxidation, heat and UV light, were performed. The analyte was eluted at 5.8 min using gradient system at a flow rate of 1.5 mL/min. The theoretical plates count was > 2000, tailing factor < 1.54, capacity factor > 5.38 and peak asymmetry factor was < 1.10. The method was linear from 1 to 40 µg/mL with a correlation coefficient of 0.9994. The intraday precision and accuracy values were 0.14–1.54% and 0.63–1.83%, respectively. On the other hand, the interday precision and accuracy results were 0.49–1.83% and 1.15–1.85%, respectively. The drug solution was stable at ambient room temperature (26°C) for 48 h. Dapoxetine HCl was found susceptible to oxidation and degraded slightly under acid and alkali conditions but was stable under UV light and heat. No interference from tablet excipients and degradation products was found. Hence, the method can be employed as a stability-indicating method for the determination of dapoxetine HCl in pharmaceutical products.

Keywords: dapoxetine HCl, stress degradation study, stability indicating HPLC-UV method

Dapoxetine hydrochloride (dapoxetine HCl), (1S)-N,N-dimethyl-3-naphthalen-1-yloxy-1-phenylpropan-1-amine hydrochloride, belongs to a pharmacological group called selective serotonin reuptake inhibitors (1). The chemical structure of dapoxetine HCl is shown in Figure 1. Dapoxetine HCl is used in the treatment of anxiety disorder and depression. It was also reported to delay ejaculation in men during sexual relationship and patented for premature ejaculation (2).

Up-to-date, there are only a few publications on quantification of dapoxetine HCl. Giri et al. (1) reported a HPLC-UV method for simultaneous quantification of tadalafil and dapoxetine in drug solution. The linearity of dapoxetine HCl only covered the range of 0.75–12 µg/mL, which might not be sufficiently sensitive to detect dapoxetine HCl in dissolution study. Chandran et al. (3) reported a RP-HPLC method to simultaneously quantify tadalafil and dapoxetine HCl but dapoxetine HCl was eluted at 11.4 min, which was too long. The UV spectrophotometric method reported by Amin et al. (4) and thin layer high performance liquid chromatography reported by Pandya et al. (5) were not selective and specific.

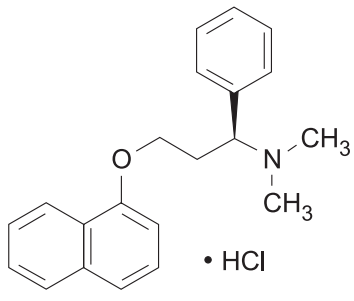

Figure 1. Chemical structure of dapoxetine HCl

Hitherto, the reported methods did not carry out suitability tests and stress degradation study on dapoxetine HCl solution and tablets. The environmental factors such as temperature, humidity, and light can be detrimental to active pharmaceutical ingredient (6) and its quality might be greatly compromised by the changes in the environmental factors (7). International Conference on Harmonization (ICH) guideline on Stability Testing of New Drug Substances and Products requires stress tests to elucidate the inherent stability characteristics of the

* Corresponding author: e-mail: kkpeh@usm.my; kkpehken@gmail.com; phone: 604-6532257; fax: 604-6570017

active pharmaceutical ingredient. Stability-indicating methods have received considerable attention for the determination of drugs (8).

The aim of this study was to develop and validate a simple, rapid and reproducible stability-indicating RP-HPLC-UV method to quantify dapoxetine HCl in drug solution and a pharmaceutical product, Priligy® tablets.

EXPERIMENTAL

Materials

Dapoxetine hydrochloride was a free sample from Rakshit Drugs PVT LTD. (India). Ammonium acetate, potassium dihydrogen phosphate, HPLC-grade acetronitrile, analytical grade hydrochloric acid, sodium hydroxide and analytical grade hydrogen peroxide solution were purchased from Merck (USA). Priligy® tablets (Janssen-Cilag, Italy) were purchased from a local pharmacy.

Instrumentation

The HPLC system comprised of a Shimadzu (VP series, Kyoto, Japan) pump (LC-20AT vp) with solvent cabinet, a degasser (DGU-20A_3), a column oven (CTO-10S VP), an auto-injector (SIL-20A HT VP), a UV/VIS detector (SPD-20A vp), and a computer software (LC-Solution VP).

Chromatographic condition

The separation was carried out using a Synchronize (Thermo Scientific, USA) C-18 column (150 × 4.6 mm ID, 5 µm). The column temperature was set at 30°C. The detection wavelength was 240 nm. Sample of 25 µL was injected onto the column.

Mobile phase optimization and elution system

Different compositions of mobile phase were studied to determine the optimum mobile phase for good resolution and short elution time. Two elution methods were studied, namely, isocratic and gradient systems.

For isocratic elution system, various compositions of mobile phase studied are shown in Table 1. The 0.2 M buffer solution was prepared by weighing 15.42 g of ammonium acetate and dissolving in 1 L of distilled water. The buffer solution was mixed with acetonitrile, accordingly. The mobile phase was filtered through 0.45 µm nylon membrane filter (Whatman, UK) under vaccum using a filtration set.

Table 1. Various compositions of mobile phase used for isocratic system.

Acetonitrile : 0.2 M ammonium acetate buffer (v/v)	pH	Flow rate (mL/min)
30 : 70	7.20	1.2
30 : 70	6.00	1.2
30 : 70	5.00	1.2
50 : 50	7.40	1.2
70 : 30	7.70	1.5
90 : 10	7.90	1.5

Table 2. Various composition of mobile phase and time programme for gradient system.

Time (min)	Acetonitrile : 0.2 M ammonium acetate buffer (v/v)		
	Trial 1	Trial 2	Trial 3
0.00	50 : 50	50 : 50	50 : 50
0.50	50 : 50	50 : 50	50 : 50
2.50	60 : 40	75 : 25	90 : 10
6.50	60 : 40	75 : 25	90 : 10
6.51	50 : 50	50 : 50	50 : 50
8.00	50 : 50	50 : 50	50 : 50

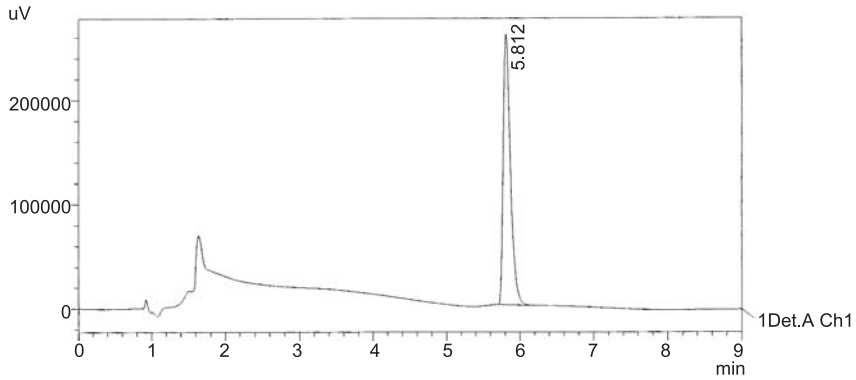

Figure 2. Chromatogram of 40 μg/mL dapoxetine HCl solution (RT = 5.812 min)

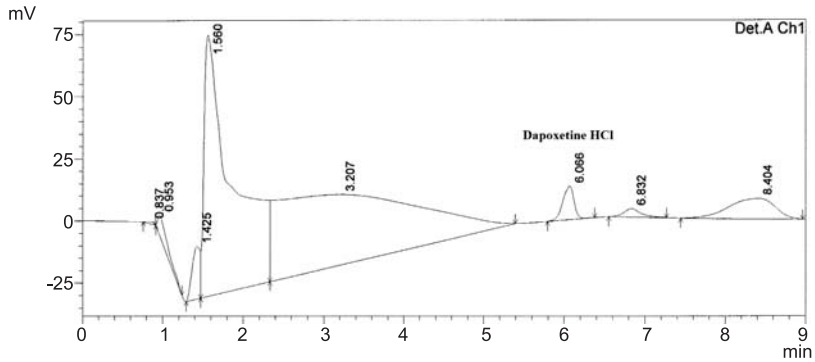

Figure 3a. Chromatogram of drug solution (zero hour) in oxidative degradation

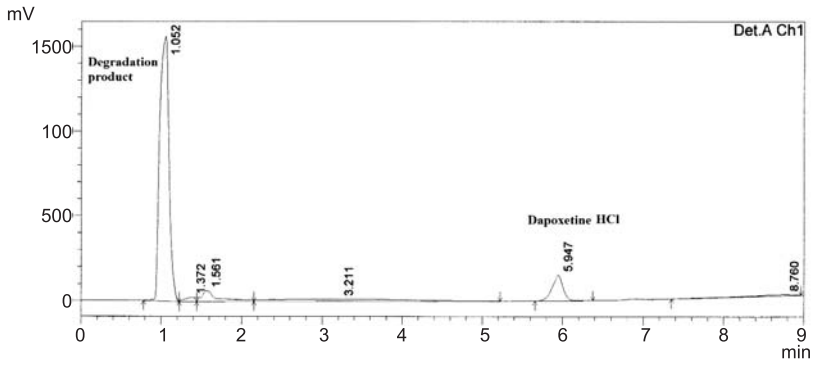

Figure 3b. Chromatogram of drug solution (after 3 h) in oxidative degradation study

The filtered mixture was degassed using a ultrasonicator for 15 min.

On the other hand, for gradient elution system, acetonitrile and 0.2 M buffer solution was run according to the time program presented in Table 2.

Preparation of stock standard solution

Forty milligrams of dapoxetine HCl working standard was weighed and transferred to a 100 mL volumetric flask and dissolved in 50 mL of mobile phase. The volumetric flask was shaken using ultra-

sonicator for 5 min. The solution was diluted to volume with mobile phase. The stock standard solution had a concentration of 400 µg/mL of dapoxetine hydrochloride.

Preparation of working standard solution

Two and a half milliliters of stock standard solution (400 µg/mL) was pipetted into 10 mL volumetric flasks and diluted to final volume with mobile phase and mixed well. This working standard solution had a concentration of 100 µg/mL of dapoxetine HCl.

Preparation of standard drug solutions for standard calibration curve

Samples of 0.1, 0.2, 0.4, 0.8, 1.6, 3.2 and 4.0 mL of the working standard solution were pipetted into seven separate 10 mL volumetric flasks and diluted to the final volume with mobile phase and mixed well. These seven standard solutions had concentrations of 1, 2, 4, 8, 16, 32 and 40 µg/mL of dapoxetine HCl.

Preparation of quality control standard solutions

Three quality control standard solutions at 3 (low), 20 (medium) and 30 (high) µg/mL were prepared and used in method validation. Samples of 0.3, 2.0 and 3.0 mL of the working standard solution were pipetted into three separate 10 mL volumetric flasks and diluted to the final volume with mobile phase and mixed well. These three quality control standard solutions had concentrations of 3, 20 and 30 µg/mL of dapoxetine HCl.

System suitability study

The chromatographic parameters, such as: theoretical plates (N), tailing factor (T), capacity factor (k') and peak asymmetry factor (As), were calculated. The value of tailing factor should be not more than 2.0 (9). Peak asymmetry factor (As) is the simplest way of measuring the degree of peak distortion (skew). The peak asymmetry was determined at 10% peak height. For a tailed peak, As > 1. For a fronted peak, As < 1. For a symmetric peak, As = 1. Recommended acceptance criteria for asymmetry factor is between 0.9 to 1.1 (10, 11). Capacity factor (k') is an indicator of efficiency of a column to retain sample molecule during an isocratic separation. The literature proposed the acceptable k' value ranges 2–10 (11).

Linearity

Few concentrations of calibration standard namely: 1, 2, 4, 8, 16, 32 and 40 µg/mL were prepared using the stock solution described above. The standard calibration curve was constructed using peak area *versus* known concentrations of dapoxetine HCl. The linear regression line was used to determine the linearity and concentration of the samples. The linearity of dapoxetine HCl was conducted using six sets of the calibration standards.

Precision and accuracy

Three quality control standard solutions at 1 (LOQ), 3, 20 and 30 µg/mL, were prepared to determine the method precision and accuracy. For intra-day precision and accuracy, six sets of standard solutions were assayed on the same day. For inter-day precision and accuracy, six sets of standard solutions were injected over six consecutive days, with one standard calibration curve injected on each day. The coefficient of variation (% CV) was calculated for the precision of the assay, using the following equation:

$$CV\ (\%) = \frac{Standard\ deviation}{Mean\ volume} \times 100\%$$

Table 3. Results of system suitability at LOQ and three quality control samples. The mean ± SD, n = 6.

Parameter	Dapoxetine HCl (µg/mL)			
	1.0	**3.0**	**20.0**	**30.0**
Theorectical plates	18706.10 ± 662.89	16880.03 ± 1019.93	16721.05 ± 1650.51	16877.40 ± 1399.83
Tailing factor	1.33 ± 0.04	1.52 ± 0.10	1.54 ± 0.16	1.51 ± 0.14
Peak asymmetry factor	1.08 ± 0.13	1.09 ± 0.03	1.10 ± 0.05	1.08 ± 0.04
Capacity factor	5.43 ± 0.01	5.40 ± 0.03	5.39 ± 0.03	5.38 ± 0.03
Resolution	25.88 ± 1.65	24.34 ± 1.02	25.37 ± 0.79	25.55 ± 0.67
Height equivalent to the theoretical plate (HETP)	8.03 ± 0.29	8.91 ± 0.52	9.04 ± 0.83	8.94 ± 0.72

Table 4. Results of six standard calibration curves.

Set	Slope	Intercept	R^2
1	45502.03	5079.47	0.9995
2	44652.70	4475.19	0.9995
3	44889.85	4752.52	0.9994
4	44982.31	5550.40	0.9992
5	45053.13	1792.50	0.9992
6	45056.47	3381.20	0.9997
Mean	45022.75	4171.88	0.9994
SD	278.57	1374.03	0.0002

The accuracy was presented as the relative percentage error (% bias) of calculated concentration of the samples. The accuracy was computed using the following equation:

$$\text{Accuracy} = \frac{(\text{Calculated concentration} - C_{std})}{C_{std}} \times 100\%$$

where C_{std} = the concentration of standard solution.

Limit of quantification (LOQ)

The LOQ was the lowest point of concentration in the calibration curve. Acceptance criteria were RSD of 2% for precision and accuracy of 2%.

Limit of detection (LOD)

The LOD value was determined by injecting samples successively until a concentration at a signal to noise ratio of 3:1 was obtained.

Stock solution stability

The stock standard solution of dapoxetine hydrochloride (400 µg/mL) was kept at ambient room temperature (26°C, 65% RH). Sample was injected and collected at 6 and 48 h. The instrumental responses at 6 and 48 h were compared with fresh samples.

Stress degradation studies

Dapoxetine HCL solution of 0.35 mg/mL was prepared by weighing 35 mg of dapoxetine HCl powder (equivalent to 30 mg of dapoxetine) and dissolving it in a 100 mL volumetric flask. On the other hand, ten tablets of Priligy® were crushed with mortar and pestle. Powder with weight equivalent to the mean weight of ten tablets (containing 35 mg of dapoxetine HCl equivalent to 30 mg of dapoxetine) was taken and dissolved in a 100 mL volumetric flask. The mixture of 0.2 M phosphate buffer and acetonitrile (50 : 50, v/v) was used as solvent.

Acid degradation study

One milliliter of the sample solution was transferred into a 10 mL volumetric flask. Two sets of flasks for each study were prepared. Three milliliters of 3 M HCl was added into each of the flask. For the first set, 3 mL of 3 M NaOH was added immediately to neutralize the solution and adjusted to volume. It served as the zero hour sample. Twenty five microliters of the solution was injected into HPLC apparatus. Another set of flasks was left on the bench under room temperature (28°C, 60% RH) and the same neutralization procedure was performed after 3 h.

Alkali degradation study

One milliliter of the sample solution was transferred into a 10 mL volumetric flask. Two sets of flasks for each study were prepared. Three milliliters of 3 M NaOH was added into each of the flask. For the first set, 3 mL of 3 M HCl was added immediately to neutralize the solution and adjusted to volume. It served as the zero hour sample. Twenty five microliters of the solution was injected into HPLC apparatus. Another set of flasks was left on the bench under room temperature (28°C, 60% RH) and the same neutralization procedure was performed after 3 h.

Oxidative (H_2O_2) degradation

One milliliter of the sample solution was transferred into a 10 mL volumetric flask. Two sets of flasks for each study were prepared. Three milliliters of 35% H_2O_2 was added into each flask. For the first set, the solution was adjusted to volume and 25 µL of the solution was injected into HPLC column immediately. It served as zero hour sample. Another set of flasks was left on the bench under room temperature (28°C, 65% RH) and the same procedure was performed after 3 h.

Heat degradation study

One milliliter of the sample solution was transferred into a 10 mL volumetric flask. Two sets of flasks were prepared. For the first set, the solution was adjusted to volume and 25 µL of the solution was injected into HPLC column immediately. It served as the zero hour sample. Another set of flasks was heated in water bath at 80°C and the samples were injected after heating for 2 h.

UV light degradation

One milliliter of the sample solution was transferred into a 10 mL volumetric flask. Two sets of flasks were prepared. For the first set, the solution was adjusted to volume and 25 µL of the solution was injected into HPLC column immediately. It served as the zero hour sample. Another set of flasks was stored in UV cabinet (254 nm) and the samples were injected after 24 h.

Assay of dapoxetine HCl in pharmaceutical tablet

The HPLC-UV method was applied to determine dapoxetine HCl content of Priligy®, a commercial immediate release dapoxetine HCl tablets. Ten tablets were weighed and crushed using mortar and pestle. The powder was mixed well. Powder with weight equivalent to the mean weight of ten tablets (containing 30 mg of dapoxetine) was taken and dissolved in a 10 mL volumetric flask with mobile phase. The solution was subjected to sonication for 15 min. The sample of 0.1 mL was drawn and diluted with mobile phase to 10 mL in a volumetric flask to give a drug concentration of 30 µg/mL. The sample of 25 µL was injected into the HPLC system.

RESULTS

System suitability

The result of theoretical plates number (N), tailing factor (T), peak asymmetry factor (As), capacity factor (k'), resolution and height equivalent to theoretical plate (HETP) at three QC concentrations and LOQ are shown in Table 3. The average theoretical plate was > 2000. Both tailing factor (< 2) and peak asymmetry factor (0.9–1.1) met the requirement stated in USP 34. The capacity factor was in the ideal range between 2 and 10 (11).

Linearity

The standard calibration curve exhibited an excellent linearity and a good correlation coefficient over the given range of 1–40 µg/mL of dapoxetine HCl. The mean linear regression equation from six calibration curves was, $y = 45022.75 (\pm 278.57) x + 4171.88 (\pm 1374.03)$, (x = dapoxetine concentration, y = average peak area), with a correlation coefficient of 0.9994 (0.0002) as given in Figure 4. The six standard calibration curves were injected over six days to test the reproducibility of the method. The results are presented in Table 4.

Precision and accuracy

The results of precision and accuracy are shown in Table 5. Precision and accuracy were tested at four concentrations, namely, LOQ, 3, 20 and 30 µg/mL. Intra-day precision was in the range of 0.14–1.54% whereas intra-day accuracy was in the range of 0.63–1.83%. Inter-day precision and accuracy were in the range of 0.49–1.83% and 1.15–1.85%, respectively. The results were within the ± 2% range recommended by USP guidelines. Hence, the method indicates good precision and accuracy.

Specificity

There was no peak found at the retention time of the analyte in the blank solution. The results from the stress testing studies indicated that the method was highly specific for dapoxetine HCl. The degradation products were completely resolved from the parent compound.

Table 5. Result of intra-day and inter-day precision and accuracy. The result is presented as the mean, n = 6.

Conc. (µg/mL)	Intra-day		Inter-day	
	Precision (% CV)	Accuracy (% bias)	Precision (% CV)	Accuracy (% bias)
1	1.38	1.83	1.83	1.63
3	1.54	0.63	0.89	1.15
20	0.14	1.55	0.49	1.51
30	0.20	1.81	0.98	1.85

Table 6. Results of stress degradation studies. The mean ± SD, n = 3.

Parameters		Exposure time (h)	
		Assay at 0 h (%)	Assay after 3 h (%)
Acid hydrolysis	In drug solution	99.87 ± 0.15	95.18 ± 1.34
	In tablet formulation	101.00 ± 0.03	93.51 ± 0.05
Alkali hydrolysis	In drug solution	99.25 ± 1.28	97.57 ± 0.75
	in tablet formulation	100.48 ± 0.05	98.40 ± 0.75
H_2O_2 Oxidation	In drug solution	83.58 ± 2.47	5.88 ± 3.59
	In tablet formulation	81.05 ± 1.45	1.56 ± 0.96
Heat degradation	In drug solution	100.45 ± 0.29	101.53 ± 0.52
	In tablet formulation	99.38 ± 0.05	101.85 ± 3.50
UV degradation	In drug solution	100.08 ± 1.34	101.94 ± 0.88
	In tablet formulation	101.97 ± 3.67	105.28 ± 5.24

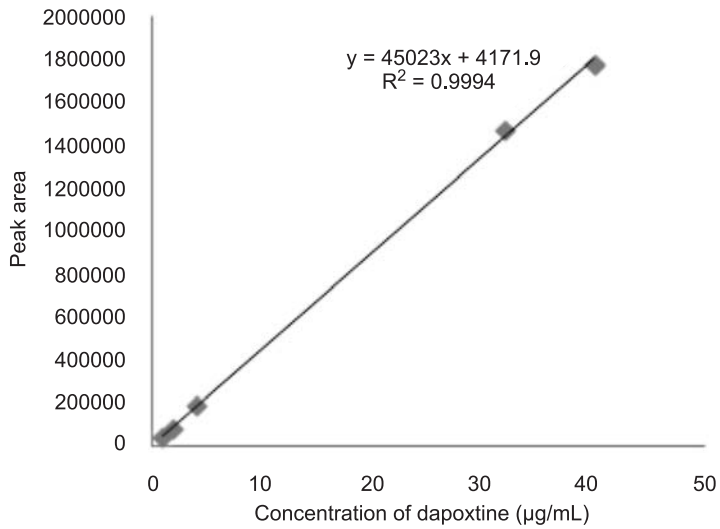

Figure 4. Mean standard calibration curve. The mean ± SD (n = 6)

LOQ and LOD

The LOQ was 1 µg/mL with inter-day precision and accuracy of 1.83 and 1.63%, respectively. The LOD was 0.01 µg/mL.

Stock solution stability

The percentage of dapoxetine HCl remained after 6 and 48 h storage at ambient room temperature was 99.70 and 99.32%, respectively. The results suggest that the stock solution was stable for 48 h when kept at ambient room temperature.

Assay of dapoxetine content in tablet

The result of assay content of Prilligy tablets calculated in this study was within 98–102%.

DISCUSSION

Initially, Synchronize C-18 analytical column with 250 mm length was used. However, the elution time of the analyte was too long for all the compositions of acetonitrile and 0.2 M ammonium acetate buffer studied, ranging from 20 to 30 min. At ace-

tonitrile content of 90%, an elution time of 20 min was obtained, which was too long. Although a shorter Synchronize C-18 column with 150 mm length was used, the elution time could only be shortened to 16 min. The elution time was considered too long and unsuitable for analysis of large quantity of samples. As such, gradient elution system was studied.

It was found that gradient elution is able to produce a relatively higher peak height in a shorter operation cycle when compared with isocratic elution (12). Figure 2 shows the chromatogram of 40 µg/mL dapoxetine HCl in drug solution separated using gradient elution system. The composition of mobile phase of trial 3 was selected based on the shortest elution time. The retention time was 5.8 min. This method was used for method validation procedure and subsequent tests. The method was validated and reproducible.

Susceptibility to oxidation, hydrolytic, and photolytic stability are required by the ICH guideline (8). An ideal stability-indicating method is one that can quantify the standard drug alone and also resolve its degradation products (13). The chromatograms of oxidative degradation study in drug solution at zero hour and 3 hours are presented in Figures 3a and 3b, respectively. The method was able to separate both analyte and degradation product peak that was eluted at 1.05 min. The results of acid, alkali, oxidation, heat and UV degradation are shown in Table 6, respectively. Dapoxetine HCl was found easily oxidized by hydrogen peroxide even just exposed to it for 5 min (from preparation to injection). The assay of drug dropped slightly in acid and alkali condition. Dapoxetine HCl was found stable in UV light and heat.

CONCLUSION

It can be concluded that a stability indicating HPLC-UV method for determination of dapoxetine HCl in tablets was successfully developed. The method was rapid, simple, precise, sensitive and reproducible. The method can also be used to assay dapoxetine HCl in other pharmaceutical dosage forms such as capsules.

REFERENCES

1. Giri A.D., Bhusari V.K., Dhaneshwar S.R.: IJPPS. 4, 654 (2012).
2. Reddy B.P., Reddy K.A., Reddy M.S.: Academic Journals 2, 001 (2010).
3. Chandran M., Kannan K.: J. Sci. Res. Pharm. 1, 36 (2012).
4. Amin G., Chapla B., Pandya A., Kakadiya J., Baria D.: IJPRBS. 1, 247 (2012).
5. Pandya A., Amin G., Chapla B., Patel N., Kakadiya J.: IJPRBS. 1, 236 (2012).
6. Ahuja S., Alsante K.M.: Handbook of Isolation and Characterization of Impurities in Pharmaceuticals. p. 133, Academic Press, San Diego 2003.
7. Khan H., Ali M., Ahuja A., Ali J.: Curr. Pharm. Anal. 6, 142 (2010).
8. ICH, Q1A Stability Testing of New Drug Substances and Products. International Conference on Harmonization, Geneva 1993.
9. United States Pharmacopoeia 34. The National Formulary USP Convention, Inc., Rockville, Maryland 2011.
10. Paul S.C.: Fundamental Terminology, Parameters, Variables and Theory, in Troubleshooting HPLC Systems, A Bench Manual. Paul C.S. Ed., p. 49, John Wiley & Sons, New York 2000.
11. Snyder L.R., Kirkland J.J., Glajch J.L.: Practical HPLC Method Developement, p. 1, Wiley Interscience, New York 1997.
12. Shrivastava A., Gupta V.B.. J. Adv. Sci. Res. 3, 12 (2012).
13. Kadi A.A., Mohamed M.S., Kassem M.G., Darwish I.A.: *C*hem. Cent. J. 5, 30 doi:10.1186/1752-153X-5-30 (2011).

Received: 14. 08. 2013

Acta Poloniae Pharmaceutica – Drug Research, Vol. 71 No. 3 pp. 401–407, 2014 ISSN 0001-6837
Polish Pharmaceutical Society

DRUG SYNTHESIS

DESIGN AND SYNTHESIS OF NOVEL THIOPHENES BEARING BIOLOGICALLY ACTIVE ANILINE, AMINOPYRIDINE, BENZYLAMINE, NICOTINAMIDE, PYRIMIDINE AND TRIAZOLOPYRIMIDINE MOIETIES SEARCHING FOR CYTOTOXIC AGENTS

MOSTAFA M. GHORAB[1,2]*, MARWA G. El-GAZZAR[2] and MANSOUR S. ALSAID[1]

[1] Department of Pharmacognosy, College of Pharmacy, King Saud University, P.O. Box 2457, Riyadh 11451, Saudi Arabia
[2]Department of Drug Radiation Research, National Center for Radiation Research and Technology, Atomic Energy Authority, P.O. Box 29, Nasr City, Cairo, Egypt

Abstract: To discover new bioactive lead compounds for medicinal purposes, herein, (E)-3-(substituted amino)-1-thiophen-2-yl-prop-2-en-1-ones **3–8**, aminopyridines **9–11**, benzylamine **12**, nicotinamide **13**, pyrimidines **14**, **15**, hexanoic acid **16** and triazolopyrimidine **19** were prepared and tested for cytotoxic activity. Results showed that the tested compounds exhibited a remarkable activity, especially compounds **3** and **19** with IC_{50} values (55.2 and 50.49 μM, respectively) compared to doxorubicin (IC_{50} = 71.8 μM) as a reference drug.

Keywords: thiophene, aniline, aminopyridine, nicotinamide, pyrimidine, triazolo-pyrimidine, cytotoxic activity

Thiophenes have been reported to possess interesting biological and pharmacological activities and several derivatives with this ring are used as antibacterial (1–4), anti-inflammatory (5), anticancer (6–12), and antiviral (13) agents. Moreover, from the literature survey it was found that aniline, pyridine, nicotinamide, pyrimidine, triazolopyrimidine derivatives showed wide spectrum of biological activities, especially anticancer activities (14–19). As a part of our ongoing research program directed towards developing new approaches to a variety of heterocyclic ring systems for anticancer activity, especially those containing sulfur compounds (20–27), we report herein the utility of (*E*)-3-(dimethylamino)-1-(thiophen-2-yl)prop-2-en-1-one **2** (28) for the synthesis of target compounds.

EXPERIMENTAL

Chemistry

Melting points are uncorrected and were determined on BUCHI melting point apparatus B-545 (BUCHI Labortechnik AG CH-9230 Flawil, Switzerland). Elemental analyses (C, H, N) were performed on Carlo Erba 1108 Elemental Analyzer. All these data were within ±0.4% of the theoretical values. The IR spectra (KBr) were measured on Shimadzu IR 110 spectrophotometer (Shimadzu, Koyoto, Japan), ^{1}HNMR and ^{13}CNMR spectra were obtained by a Bruker proton NMR-Avance 500 instrument (500 MHz) (Bruker, Germany), in dimethyl sulfoxide-d_6 as a solvent, using tetramethylsilane (TMS) as an internal standard. All reactions were monitored by thin layer chromatograph using precoated aluminium sheets (Silica gel Merck 60 F_{254}) and were visualized by UV lamp (Merck, Germany). All chemicals were commercially supplied from Sigma-Aldrich, USA.

(*E*)-3-(dimethylamino)-1-thiophen-2-yl-prop-2-en-1-one (2)

Compound **2** was prepared according to previously described method (28).

(*E*)-3-(3-substituted phenylamino)-1-thiophen-2-yl-prop-2-en-1-ones (3–8)

General procedure

A mixture of **2** (28) (1.81 g, 0.01 mol) and the appropriate amine, namely: 3-ethylaniline, 4-

* Corresponding author: e-mail: mmsghorab@gmail.com

ethoxyaniline, 3,4,5-trimethoxyaniline, 2-chloro-5-nitroaniline, 2-methyl-4-nitroaniline and 2,4-dibromoaniline (0.01 mol) in ethanol (20 mL) containing acetic acid (5 mL) was refluxed for 2 h. The precipitated product was collected by filteration, washed with ethanol and crystallized from dioxane to give **3**–**8**, respectively.

(*E*)-3-(3-ethylphenylamino)-1-thiophen-2-yl-prop-2-en-1-one (3)

Yield 88%; m.p. 110.5°C; IR (KBr, cm^{-1}): 3464 (NH), 2960, 2836 (CH aliph.), 1624 (C=O), ^{1}H-NMR (DMSO-d_6, δ, ppm): 1.19 (t, 3H, CH_3), 2.6 (q, 2H, CH_2), 6.0, 6.3 (2d, 2H, CH=CH, *J* = 7.3 Hz), 7.0–8.1 (m, 7H, Ar-H), 11.7 (d, 1H, NH, *J* = 7.1 Hz). ^{13}C-NMR (DMSO-d_6, δ, ppm): 15.4, 28.1, 93.0, 113.1, 114.9, 115.5, 128.4, 129.6, 132.5, 139.9, 140.8, 143.7, 145.4, 146.8, 182.7. Analysis: calcd. for $C_{15}H_{15}NOS$ (257.35): C 70.01, H 5.87, N 5.44%; found: C 70.32, H 6.20, N 5.60%.

(*E*)-3-(4-ethoxyphenylamino)-1-thiophen-2-yl-prop-2-en-1-one (4)

Yield 78%; m.p. 135.6°C; IR (KBr, cm^{-1}): 3430 (NH), 3070 (CH arom.), 2970, 2866 (CH aliph.), 1632 (C=O). ^{1}H-NMR (DMSO-d_6, δ, ppm): 1.3 (t, 3H, CH_3), 3.9 (q, 2H, CH_2), 5.9, 6.9. (2d, 2H, CH=CH, *J* = 7.3, 7.4 Hz), 7.4–7.9 (m, 7H, Ar-H), 11.7 (d, 1H, NH, *J* = 8.1 Hz). ^{13}C-NMR (DMSO-d_6, δ, ppm): 14.8, 63.2, 96.0, 115.3, 115.4, 116.9, 117.6, 129.2, 133.2, 134.0, 144.4, 146.2, 147.1, 154.9, 180.4. Analysis: calcd. for $C_{15}H_{15}NO_2S$ (273.35): C 65.91, H 5.53, N 5.12%; found: C 65.68, H 5.22, N 5.40%.

(*E*) 3-(3,4,5-trimethoxyphenylamino)-1-thiophen-2-yl-prop-2-en-1-one (5)

Yield 82%; m.p. 99.5°C; IR (KBr, cm^{-1}): 3406 (NH), 3089 (CH arom.), 2939, 2870 (CH aliph.), 1636 (C=O). ^{1}H-NMR (DMSO-d_6, δ, ppm): 3.6, 3.7 (2s, 9H, $3OCH_3$), 6.3, 6.8 (2d, 2H, CH=CH; *J* = 8.3 Hz), 7.2–7.9 (m, 5H, Ar-H), 10.9 (d, 1H, NH, *J* = 8.1 Hz). Analysis: calcd. for $C_{16}H_{17}NO_4S$ (319.38): C 60.17, H 5.37, N 4.39%; found: C 59.88, H 5.09, N 4.72%.

(*E*)-3-(2-chloro-5-nitrophenylamino)-1-thiophen-2-yl-prop-2-en-1-one (6)

Yield 69%; m.p. 177.7°C; IR (KBr, cm^{-1}): 3429 (NH), 3082 (CH arom.), 2940, 2860 (CH aliph.), 1628 (C=O), 1562, 1346 (NO_2), 732 (C-Cl). ^{1}H-NMR (DMSO-d_6, δ, ppm): 6.2, 6.8 (2d, 2H, CH=CH, *J* = 7.0, 7.1 Hz], 7.3–8.0 (m, 6H, Ar-H), 10.6 (d, 1H, NH, *J* = 7.7 Hz). Analysis: calcd. for $C_{13}H_9ClN_2O_3S$ (308.74): C 50.57, H 2.94, N 9.07%; found: C 50.20, H 3.30, N 9.38%.

(*E*)-3-(2-methyl-4-nitrophenylamino)-1-thiophen-2-yl-prop-2-en-1-one (7)

Yield 69%; m.p. 217.2°C; IR (KBr, cm^{-1}): 3468 (NH), 3100 (CH arom.) 2970, 2840 (CH aliph.), 1636 (C=O), 1581, 1373 (NO_2), ^{1}H-NMR (DMSO-d_6, δ, ppm): 2.1 (s, 3H, CH_3), 6.4, 6.9 (2d, 2H, CH=CH, *J* = 7.0, 7.1 Hz), 7.0–7.9 (m, 6H, Ar-H), 10.8 (d, 1H, NH, *J* = 7.4 Hz). Analysis: calcd. for $C_{14}H_{12}N_2O_3S$ (288.32): C 58.32, H 4.20, N 9.72%; found: C 58.08, H 4.12, N 9.41%.

(*E*)-3-(2,4-dibromophenylamino)-1-thiophen-2-yl-prop-2-en-1-one (8)

Yield 82%; m.p. 143.5°C; IR (KBr, cm^{-1}): 3448 (NH), 3048 (CH arom.), 2940, 2870 (CH aliph.), 1628 (C=O), 771 (C–Br). ^{1}H-NMR (DMSO-d_6, δ, ppm): 6.1, 6.8 (2d, 2H, CH=CH, *J* = 7.4, 7.5 Hz), 7.1–7.9 (m, 6H, Ar-H), 12.0 [d, 1H, NH, *J* = 8.1 Hz]. ^{13}C-NMR (DMSO-d_6, δ, ppm): 95.5, 114.8, 116.6, 120.0, 128.6, 132.6, 134.8, 137.5, 138.6, 143.7, 145.5, 146.5, 183.4. Analysis: calcd. for $C_{13}H_9Br_2NOS$ (387.09): C 40.34, H 2.34, N 3.62%; found: C 40.10, H 2.62, N 3.33%.

(*E*)-3-(substituted amino)-1-thiophen-2-yl-prop-2-en-1-ones (9–11)

A mixture of **2** (1.81 g, 0.01 mol) and 4-aminopyridine or 3-amino-2-chloropyridine and/or 2-amino-4-chloropyridine (0.01 mol) in ethanol (20 mL) containing acetic acid (5 mL) was refluxed for 8 h. The reaction mixture was filtered while hot and crystallized from dimethylformamide/ethanol to give **9**–**11**, respectively.

(*E*)-3-(pyridin-4-ylamino)-1-thiophen-2-yl-prop-2-en-1-one (9)

Yield 90%, m.p. 213.4°C; IR (KBr, cm^{-1}): 3433 (NH), 3093 (CH arom.), 2970, 2860 (CH aliph.), 1639 (C=O), 1620 (C=N). ^{1}H-NMR (DMSO-d_6, δ, ppm): 6.4, 6.8 (2d, 2H, CH=CH, *J* = 7.6 Hz), 7.1–8.3 [m, 7H, Ar-H], 10.8 (d, 1H, NH, *J* = 7.2 Hz). Analysis: calcd. for $C_{12}H_{10}N_2OS$ (230.29): C 62.59, H 4.38, N 12.16%; found: C 62.24, H 4.56, N 12.39%.

(*E*)-3-(2-chloropyridin-3-ylamino)-1-thiophen-2-yl-prop-2-en-1-one (10)

Yield 69%; m.p. 153.2°C; IR (KBr, cm^{-1}): 3383 (NH), 3055 (CH arom.) 2940, 2863 (CH aliph.), 1701 (C=O), 1639 (C=N), 856 (C-Cl). ^{1}H-NMR (DMSO-d_6, δ, ppm): 6.2, 7.2 (2d, 2H, CH=CH, *J* =

6.8, 6.9 Hz), 7.3–8.0 (m, 6H, Ar-H], 12.0 (d, 1H, NH, *J* = 7.4 Hz) ^{13}C-NMR (DMSO-d_6, δ, ppm): 96.3, 123.6, 124.1, 128.6, 136.0, 138.0, 141.4, 142.4, 143.5, 145.4, 146.3, 183.7. Analysis: calcd. for $C_{12}H_9ClN_2OS$ (264.73): C 54.44, H 3.43, N 10.58%. found: C 54.63, H 3.81, N 10.21%.

(*E*)-3-(4-chloropyridin-2-ylamino)-1-thiophen-2-yl-prop-2-en-1-one (11)

Yield 76%; m.p. 200.8°C; IR (KBr, cm^{-1}): 3448 (NH), 3060 (CH arom.), 2980, 2872 (CH aliph.), 1632 (C=O), 1592 (C=N), 775 (C-Cl). ^{1}H-NMR (DMSO-d_6, δ, ppm): 6.4, 6.9 (2d, 2H, CH=CH, *J* = 7.6, 7.7 Hz), 7.2–8.0 (m, 5H, Ar-H), 8.3 (s, 1H, N=CH), 10.6 (d, 1H, NH, *J* = 8.2 Hz). ^{13}C-NMR (DMSO-d_6, δ, ppm): 97.3, 115.6, 123.4, 131.3, 133.1, 134.2, 148.8, 151.3, 152.8, 153.8, 163.4, 190.2. Analysis: calcd. for $C_{12}H_9ClN_2OS$ (264.01): C 54.44, H 3.43, N 10.58%; found: C 54.71, H 3.72, N 10.30%.

(*E*)-3-(4-chlorobenzylamino)-1-thiophen-2-yl-prop-2-en-1-one (12), (*E*)-*N*-(3-oxo-3-thiophen-2-yl-prop-1-en-yl nicotinamide (13) and (*E*)-3-(pyrimidin-2-yl-amino)-1-thiophen-2-yl-prop-2-en-1-one (14)

A mixture of **2** (1.81 g, 0.01 mol) and 4-chlorobenzylamine or nicotinamide and/or 2-aminopyrimidine (0.01 mol) in ethanol (20 mL) and acetic acid (20 mL) was heated under reflux for 12 h. The obtained solid was crystallized from dioxane to give **12**–**14**, respectively.

12: Yield 67%; m.p. 131.7°C; IR (KBr, cm^{-1}): 3300 (NH), 3076 (CH arom.), 2940, 2834 (CH aliph.) 1642 (C=O), 831 (C–Cl). ^{1}H-NMR (DMSO-d_6, δ, ppm): 3.8 (s, 2H, CH_2), 6.7, 7.4 (2d, 2H, CH=CH, *J* = 6.8, 6.9 Hz), 7.3–7.9 (m, 7H, Ar-H), 8.2 (d, 1H, NH, *J* = 8.3 Hz). Analysis: calcd. for $C_{12}H_{12}ClN_2OS$ (277.03): C 60.54, H 4.35, N 5.04%; found: C 60.83, H 3.95, N 5.28%.

13: Yield 56%; m.p. 204.7°C; IR (KBr, cm^{-1}): 3448 (NH), 3078 (CH arom.), 2970, 2846 (CH aliph.), 1640, 1635 (2C=O), 1610 (C=N). ^{1}H-NMR (DMSO-d_6, δ, ppm): 7.2, 8.2 (2d, 2H, CH=CH; *J* = 7.1, 7.6 Hz], 7.3–9.1 (m, 7H, Ar-H + NH). 8.4 (s, 1H, N = CH). ^{13}C-NMR (DMSO-d_6, δ, ppm): 99.6, 125.6, 128.8, 132.1, 135.1, 136.9, 138.1, 140.2, 142.6, 148.6, 151.8, 166.7, 186.3. Analysis: calcd. for $C_{13}H_{10}N_2O_2S$ (258.05): C 60.45, H 3.90, N 10.85%; found: C 60.59, H 3.56, N 10.31%.

14: Yield 70%; m.p. 192.9°C; IR (KBr, cm^{-1}): 3290 (NH), 3074 (CH arom.), 2960, 2836 (CH aliph.), 1628 (C=O), 1573 (C=N). ^{1}H-NMR (DMSO-d_6, δ, ppm): 6.0, 7.4 (2d, 2H, CH=CH, *J* = 6.6; 6.7 Hz), 7.5–8.5) (m, 6H, Ar-H), 10.6 (d, 1H, NH, *J* = 6.9 Hz). Analysis: calcd. for $C_{11}H_9N_3OS$ (231.05): C 57.13, H 3.92, N 18.17%; found: C 57.27, H 3.46, N 18.49).

(*E*)-5-(3-oxo-3-thiophen-2-yl-prop-1-enyl-amino)pyrimidin-2,4-(1*H*,3*H*)-dione, (15), 6-(*E*)-3-oxo-3-thiophen-2-yl-prop-1-enylamino)hexanoic acid (16) and 7-thiophen-2-yl-[1,2,4]triazolo[1,5-a]pyrimidine (19)

To a solution of **2** (1.81 g, 0.01 mol) in acetic acid (20 mL) was added appropriate amine, namely: 5-aminouracil or 6-aminocaproic acid and/or 2*H*-1,2,4-triazol-3-amine **17** (0.012 mol). The reaction mixture was refluxed for 10 h, then cooled. The solid that deposited after cooling was filtered off and crystallized from dioxane-ethanol mixture to give **15**, **16** and **19**, respectively.

15: Yield 59%; m.p. 332.0°C; IR (KBr, cm^{-1}): 3433, 3275, 3232 (3NH), 3089 (CH arom.), 2980, 2816 (CH aliph.), 1720, 1660, 1643 (3C=O), ^{1}H-NMR (DMSO-d_6, δ, ppm): 6.3, 7.2 (2d, 2H, CH=CH, *J* = 7.8 Hz], 7.3–8.1 (m, 6H, Ar-H + 2NH + CH pyrimidine), 10.6 (d, 1H, NH, *J* = 7.0, Hz). Analysis: calcd. for $C_{11}H_9N_3O_3S$ (263.27): C 50.18, H 3.45, N 15.96; found: C 50.55, H 3.12, N 15.69%.

16: Yield 61%; m.p. 219.8°C; IR (KBr, cm^{-1}) 3490 (OH), 3160 (NH), 2931, 2858 (CH aliph.), 1683, 1628 (2C=O). ^{1}H-NMR (DMSO-d_6, δ, ppm): 1.3- 2.7 (m, 10H, 5CH_2], 6.1, 7.2 [2d, 2H, CH=CH, *J* = 7.6, 7.7 Hz], 7.6-7.9 [m, 3H, Ar-H], 9.4 (s, 1H, NH, D_2O-exchangeable), 10.9 [s, 1H, OH, D_2O-exchangeable]. Analysis: calcd. for $C_{13}H_{17}NO_3S$: C, 58.40; H, 6.41; N, 5.24%; found: C, 58.62; H, 6.72; N, 5.39%.

19: Yield 66%; m.p. 180.8°C; IR (KBr, cm^{-1}): 3105 (CH arom.), 2924, 2860 (CH aliph.), 1620 (C=N). ^{1}H-NMR (DMSO-d_6, δ, ppm): 7.0–8.0 (m, 4H, Ar-H), 8.3 (s, 1H, CH-pyrazole), 7.5, 7.9 (2d, 2H, 2CH pyrimidine, *J* = 7.8 Hz). Analysis: calcd. for $C_9H_6N_4S$ (202.24): C 53.45, H 2.99, N 27.70%; found: C 53.75, H 3.22, N 27.90%.

***In vitro* cytotoxic activity**

The human tumor breast cancer cell line (MCF7) was obtained from the National Cancer Institute, Cairo, Egypt. The cytotoxic activity of some newly synthesized compounds was measured by the Sulforhodamine-B stain (SRB) assay as reported by Skehan et al. (29). Cells were plated in 96-multiwell plate (10^4 cells per well) for 24 h before treatment with the compounds to allow attachment of cell to the wall of the plate. Tested compounds were dissolved in DMSO and diluted

with saline to the appropriate volume. Different concentrations of the compounds under test (5, 12.5, 25 and 40 µmol/L) were added to the cell monolayer. Triplicate wells were prepared for each individual dose. Monolayer cells were incubated with the compounds for 48 h at 37°C and in atmosphere of air and 5% CO_2. After 48 h, cells were fixed, washed and stained for 30 min. with 0.4% (w/v) SRB dissolved in 1% acetic acid. Unbound dye was removed by four washes with 1% acetic acid, and attached stain was recovered with Tris-EDTA buffer. Color intensity was measured in an ELISA reader (Sunostick Medical Technology, SPR-960B, U.K.). Negative control was added by using the cell lines with the

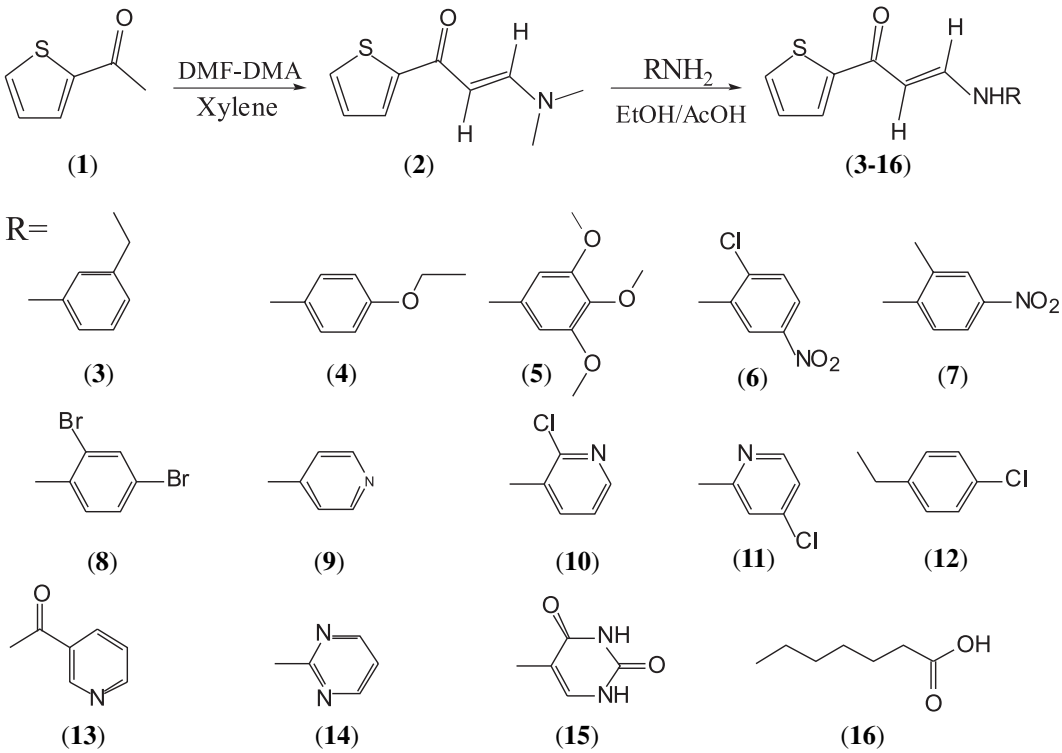

Scheme 1. Synthetic pathways for compounds **2–16**

Table 1. *In vitro* cytotoxic activity of some newly synthesized compounds against human breast cancer cell line (MCF7).

Compd. no.	Control	Compound concentration (µmol/L)				IC_{50} µM
		5	12.5	25	40	
		Surviving fraction (mean ± SE) [a]				
DOX	1.00	0.721 ± 0.020	0.546 ± 0.020	0.461 ± 0.010	0.494 ± 0.030	71.8
3	1.00	0.614 ± 0.002	0.519 ± 0.009	0.365 ± 0.028	0.279 ± 0.047	55.2
6	1.00	0.810 ± 0.058	0.647 ± 0.026	0.471 ± 0.030	0.311 ± 0.022	72.7
9	1.00	0.887 ± 0.032	0.672 ± 0.024	0.479 ± 0.023	0.393 ± 0.015	100
12	1.00	0.683 ± 0.085	0.680 ± 0.016	0.534 ± 0.022	0.348 ± 0.043	112.1
13	1.00	0.806 ± 0.008	0.631 ± 0.033	0.418 ± 0.032	0.332 ± 0.081	79.06
15	1.00	0.829 ± 0.017	0.636 ± 0.015	0.490 ± 0.003	0.460 ± 0.027	83.3
19	1.00	0.577 ± 0.044	0.421 ± 0.012	0.369 ± 0.014	0.211 ± 0.065	50.49

[a] n = 3. DOX = doxorubicin.

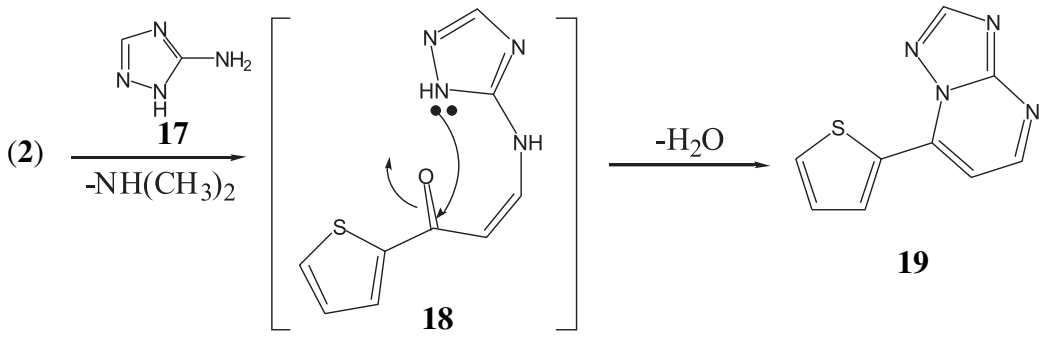

Scheme 2. Synthetic pathway for compound **19**

solvent without drug. The relation between surviving fraction and drug concentration was plotted to get the survival curve of each tumor cell line after the specified time. The concentration required for 50% inhibition of cell viability (IC_{50}) was calculated and compared with the reference drug doxorubicin and the results are given in Table 1.

RESULTS AND DISCUSSION

Chemistry

Schemes 1 and 2 outline the synthetic pathway used to obtain compounds **3-16**, **19**. The starting material (*E*)-3-(dimethylamino)-1-thiophen-2-yl-prop-2-en-1-one **2** was prepared *via* reaction of acetylthiophene **1** with dimethylformamide-dimethylacetal (DMF-DMA) (28). Treatment of compound **2** with aniline derivatives gave the corresponding secondary amine derivatives **3–8**, respectively (Scheme 1). The structure of the later products were assigned on the basis of their analytical and spectral data. IR spectra of compounds **3–8** exhibited, in each case, NH absorption bands in the region 3408–3468 cm^{-1}. Also, the enaminone **2** reacted with 4-aminopyridine or 3-amino-2-chloropyridine and/or 2-amino-4-chloropyridine in ethanol/acetic acid to give the corresponding pyridine derivatives **9–11**, respectively (Scheme 1). When compound **2** was reacted with 4-chlorobenzylamine in refluxing ethanol/acetic acid, it furnished the corresponding (*E*)-3-(4-chlorobenzylamine)-1-thiophene-2-yl-prop-2-en-1-one **12**. On the other hand, nicotinamide **13**, pyrimidine **14** and **15** derivatives were obtained in good yield *via* reaction of compound **2** with nicotinamide or 2-aminopyrimidine or aminouracil. (*E*)-4-(3-oxo-3-thiophen-2-yl-prop-1-enylamino)butanoic acid **16** was obtained *via* reaction of **2** with 6-aminocapproic acid (Scheme 1). The reactivity of enaminone **2** towards some heterocyclic amines was also examined. Thus, reaction of **2** with 5-amino-1,2,4-triazole in ethanol/acetic acid yielded the respective 1,2,4-triazolo[1,5-a]pyrimidine derivative **19** through the formation of intermediate **18**. (Scheme 2). To account for the formation of the product **19** it is suggested that the studied reaction started with Michael-type addition of the exocyclic amino group of the amine used to the activated double bond of **2** followed by in-situ tandem elimination of dimethylamine to give the intermediate **18**, then, dehydrative cyclization to give **19** (Scheme 2). The ^{1}H-NMR spectrum of **19** revealed two doublets signals at 7.5, 7.9 ppm with J = 7.8 Hz assignable to two vicinal protons of the pyrimidine ring residue.

In vitro cytotoxic activity

Some newly synthesized compounds were evaluated for their *in vitro* cytotoxic activity against human breast cancer cell line (MCF7). Doxorubicin, which is one of the most effective anticancer agents, was used as the reference drug in this study. The relationship between surviving fraction and drug concentration was plotted to obtain the survival curve of breast cancer cell line (MCF7). The response parameter calculated was the IC_{50} value, which corresponds to the concentration required for 50% inhibition of cell viability. Table 1 shows the *in vitro* cytotoxic activity of the tested compounds compared to the reference drug. It was found that, in the negative control, solvent has no effect on the

cells as the surviving fraction is 1.00, the most potent compounds were the aniline derivative **3** having ethyl group at 3-position (IC_{50} = 55.2 µM) and the triazolopyrimidine derivative **19** (IC_{50} = 50.49 µM), which were found to be more potent than the reference drug doxorubicin (IC_{50} = 71.8 µM). Also, the aniline derivative **6** (IC_{50} = 72.7 µM) was found to be nearly as potent as the reference drug. Isosteric replacement of the benzene ring with pyridine led to a drop in the activity as in compound **9** (IC_{50} = 100 µM) and also a drop in the activity was shown by replacing the aniline ring with benzyl amine moiety as in compound **12** (IC_{50} = 112.1 µM), an improvement in the activity was observed upon incorporation of nicotinamide moiety in compound **13** (IC_{50} = 79.06 µM), while the pyrimidine derivative **15** (IC_{50} = 83.3 µM) showed less activity.

CONCLUSION

From the above results, we can conclude that administration of the tested compounds on human breast (MCF7) cell lines showed promising cytotoxic activity. The most potent compounds are (*E*)-3-(3-ethylphenylamino)-1-thiophen-2-yl-prop-2-enone **3** (IC_{50} = 55.20 µM) and 7-thiophen-2-yl-[1,2,4]triazolo[1,5-a]pyrimidine **19** (IC_{50} =50.49 µM), which were found to be more potent than doxorubicin (IC_{50} = 71.8 µM), and aniline **6** carrying chloro moiety at 2-position, nitro group at 5-position (IC_{50} = 72.7 µM), which is as potent as the reference drug.

Acknowledgment

The authors would like to extend their sincere appreciation to the Deanship of Scientific Research at King Saud University for its funding of this research through the Research Group Project no. RGP-VPP-302.

REFERENCES

1. Pardeshi S., Bobade V.D.: Bioorg. Med. Chem. Lett. 21, 6559 (2011).
2. Khera M.K., Cliffe I.A., Prakash O.: Bioorg. Med. Chem. Lett. 21, 5266 (2011).
3. Bondock S., Fadaly W., Metwally M.A: Eur. J. Med. Chem. 45, 3692 (2010).
4. Lu X., Wan B., Franzblau S.G., You Q.: Eur. J. Med. Chem. 46, 3551 (2011).
5. Hu Y., Yang S., Shilliday F.B., Heyde B.R., Mandrell K.M., Robins R.H., Xie J. et al.: Drug. Metab. Dispos. 38, 1522 (2010).
6. Lin H.L., Zhang H., Medower C., Hollenberg P.F., Johnson W.W.: Drug. Metab. Dispos. 39, 345 (2011).
7. Romagnoli R., Baraldi P.G., Cara C.L., Hamel E., Basso G., Bortolozzi R., Viola G.: Eur. J. Med. Chem. 45, 5781 (2010).
8. Romagnoli R., Baraldi P.G., Carrion M.D., Cruz-Lopez O., Tolomeo M., Grimaudo S., Di Cristina A. et al.: Bioorg. Med. Chem. 18, 5114 (2010).
9. Medower C., Wen L., Johnson W.W.: Chem. Res. Toxicol. 21, 1570 (2008).
10. Dallemagne P., Khanh L.P, Alsaïdi A., Varlet I., Collot V., Paillet M., Bureau R., Rault S.: Bioorg. Med. Chem. 11, 1161 (2003).
11. Dallemagne P., Khanh L.P., Alsaïdi A., Renault O., Varlet I., Collot V., Bureau R., Rault S.: Bioorg. Med. Chem. 10, 2185 (2002).
12. Simoni D., Romagnoli R., Baruchello R., Rondanin R., Rizzi M., Pavani M.G., Alloatti D. et al.: J. Med. Chem. 49, 3143 (2006).
13. Rashad A.E., Shamroukh A.H., Abdel-Megeid R.E., Mostafa A., El-Shesheny R., Kandeil A., Ali M.A., Banert K.: Eur. J. Med. Chem. 45, 5251 (2010).
14. Fedeles B.I., Zhu A.Y., Young K.S., Hillier S.M., Proffitt K.D., Essigmann J.M., Croy R.G.: J. Biol. Chem. 286, 33910 (2011).
15. Abdel-Megeed M.F., Badr B.E., Azaam M.M., El-Hiti G.A.: Bioorg. Med. Chem., 20, 2252 (2012).
16. Zhang H., Lu X., Zhang L.R., Liu J.J., Yang X.H., Wang X.M., Zhu H.L.: Bioorg. Med. Chem. 20, 1411 (2012).
17. Liu H.Y., Ding L., Yu Y., Chu Y., Zhu H.: J. Chromatogr. B Analyt. Technol. Biomed. Life Sci. 893, 49 (2012).
18. Huang L.H., Zheng Y.F., Lu Y.Z., Song C.J., Wang Y.G., Yu B., Liu H.M.: Steroids 77, 710 (2012).
19. Zhang N., Ayral-Kaloustian S., Nguyen T., Afragola J., Hernandez R., Lucas J., Gibbons J., Beyer C.: J. Med. Chem. 50, 319 (2007).
20. Ghorab M.M., Ragab F.A., Heiba H.I., Arafa R.K., El-Hossary E.M.: Eur. J. Med. Chem. 459, 3677 (2010).
21. Ghorab M.M., Ragab F.A., Hamed M.M.: Eur. J. Med. Chem. 44, 4211 (2009).
22. Ghorab M.M., Ragab F.A., Alquasoumi S.I., Alafeefy A.M., Aboulmagd S.A.: Eur. J. Med. Chem. 45, 171 (2010).
23. Ghorab M.M., Ragab F.A., Heiba H.I., Youssef H.A., El-Gazzar M.G.: Bioorg. Med. Chem. Lett. 20, 6316 (2010).

24. Ghorab M.M., Ragab F.A., Heiba H.I., El-Gazzar Marwa G., El-Gazzar Mostafa G: Acta Pharm. 61, 415 (2011).
25. Ghorab M.M., Ragab F.A., Heiba H., El-Gazzar Marwa G., El-Gazzar Mostafa G.: Arzneimittelforschung 62, 46 (2012).
26. El-Said M.S., El-Gazzar M.G., Al-Dossari M.S., Ghorab M.M: Arzneimittelforschung 62, 149 (2012).
27. Al-Said M.S., El-Gazzar M.G., Ghorab M.M: Eur. J. Chem. 3, 228 (2012).
28. Greenhill J.V: Adv. Heterocycl. Chem. 67, 207 (1997).
29. Skehan P., Storeng R., Scudiero D., Monks A., McMahon J., Vistica D., Warren J.T. et al.: J. Natl. Cancer Inst. 82, 1107 (1990).

Received: 10. 09. 2013

Acta Poloniae Pharmaceutica – Drug Research, Vol. 71 No. 3 pp. 409–413, 2014 ISSN 0001-6837
Polish Pharmaceutical Society

NATURAL DRUGS

WATER-SOLUBLE COMPOUNDS OF LETTUCE INHIBIT DNA DAMAGE AND LIPID PEROXIDATION INDUCED BY GLUCOSE/SERUM DEPRIVATION IN N2A CELLS

ELHAM ASADPOUR[1], AHMAD GHORBANI[2] AND HAMID R. SADEGHNIA[1,2,3]*

[1] Department of Pharmacology, School of Medicine, Mashhad University of Medical Sciences, Mashhad, Iran
[2] Pharmacological Research Center of Medicinal Plants, School of Medicine, Mashhad University of Medical Sciences, Mashhad, Iran
[3] Neurocognitive Research Center, School of Medicine, Mashhad University of Medical Sciences, Mashhad, Iran

Abstract: Oxidative stress, increase of lipid peroxidation and resultant DNA damage are associated with pathophysiology of many human diseases such as acute and chronic CNS injuries and diseases, cancer, and also aging. This work was done to investigate whether water fraction from the hydroalcoholic extract of green leaf lettuce (*Lactuca sativa* L.) can protect N2a cells against glucose/serum deprivation (GSD)-induced lipid peroxidation and DNA fragmentation. The cells were cultivated for 12 h in GSD condition in the absence or presence of the lettuce fraction. The total antioxidant ability of the lettuce water fraction was determined using ferric reducing antioxidant power (FRAP) assay. The intracellular lipid peroxidation was evaluated by malondialdehyde (MDA) level. DNA damage was determined using single cell gel electrophoresis. Using FRAP assay, the antioxidant activity of lettuce water fraction was found to be 574 µmol/g, which is equivalent to 64.1 mg of pure ascorbic acid. Exposure of the cells to GSD condition led to a significant increase of MDA level and DNA fragmentation. Lettuce extract at 400 µg/mL could decrease the elevated intracellular lipid peroxidation and DNA damage. The present study demonstrates that lettuce exerts genoprotective effect through inhibition of oxidative stress.

Keywords: lettuce, water fraction, DNA damage, lipid peroxidation, antioxidant activity

It is well documented that oxidative stress, increase of lipid peroxidation and resultant DNA damage are major contributors to the pathophysiology of a variety of neurodegenerative disorders including ischemic stroke (1). By disruption of normal structure and function of cell and organelle membrane lipid bilayers, lipid peroxidation may alter membrane permeability, transport processes and ?uid plasticity and also result in the generation of several toxic aldehydes including malondialdehyde (MDA) and acrolein (2). These highly reactive electrophilic aldehydes react directly with DNA and proteins and these types of protein or DNA adducts, if not efficiently removed, deregulate cell homeostasis, which may finally lead to apoptosis (3, 4). It has been well documented that DNA damage is associated with many human diseases such as cancer, diabetes, neurological degeneration, and also aging (5–7). Therefore, to protect body cells against DNA damage, a balance must be preserved between reactive oxygen production and the antioxidant defense system (8). Consumption of natural antioxidants like vitamin A, ascorbic acid, vitamin E and plants flavonoids has positive effect in combating the oxidative stress (7).

Lettuce (*Lactuca sativa* L.), a vegetable of Compositae (Asteraceae) family, is an important leafy vegetable mainly consumed fresh in salad and a rich source of phytochemicals with antioxidant activity such as phenolic compounds, vitamins A, C and E, as well as minerals, which are essential for promoting health and preventing diseases (9–11). It has been reported to have some medicinal values including anti-inflammatory, analgesic and sedative-

* Corresponding author: e-mail: SadeghniaHR@mums.ac.ir; phone: +985118828566, fax: +985118828567

hypnotic activity (11–13). Deshmukh and co-workers showed that lettuce protect neurons against D-galactose-induced oxidative stress (14). Also, a recent study demonstrated that phenolic extract of romaine lettuce can inhibit H_2O_2-induced cytotoxicity *via* antioxidant activity (15). We previously found that ethyl acetate and water fractions of lettuce hydroalcoholic extract have cytoprotective properties against cell death induced by glucose and serum deprivation (16). The present work was carried out to investigate whether water fraction of lettuce hydroalcoholic extract has inhibitory effect on GSD-induced lipid peroxidation and DNA damage in N2a cells.

EXPERIMENTAL

Cell lines and chemicals

High glucose (4.5 g/L) Dulbecco's modified Eagles medium (DMEM), glucose-free DMEM and fetal bovine serum (FBS) were purchased from Gibco (Carlsbad, CA, USA). Low melting point (LMP) and normal melting point (NMP) agarose were obtained from Fermentas (Glen Burnie, MD, USA). Ethylene diaminetetraacetic acid disodium salt (Na_2EDTA), Tris(hydroxymethyl)aminomethane, t-octylphenoxypolyethoxyethanol (Triton X-100), ethidium bromide, trichloroacetic acid, butylated hydroxytoluene, 2,4,6-tris(2-pyridyl)-1,3,5-triazine (TPTZ) and thiobarbituric acid (TBA) were obtained from Merck (Darmstadt, Germany). Bicinchoninic acid (BCA) protein assay kit was purchased from Sigma (St. Louis, MO, USA).

Preparation of water fraction from the hydroalcoholic extract

The fresh green leaf lettuce (*Lactuca sativa* L.) collected from Neyshabure (North-East area of Iran) was identified by the herbarium of School of Pharmacy (Mashhad University of Medical Sciences, Iran) and a voucher specimen (12596) has been deposited in this institute. Fifty grams of the aerial parts were dried, powdered and subjected to the extraction for 24 h with 70% ethanol using Soxhlet apparatus. The extract was then dried on a water bath and the residue was suspended in 400 mL of distilled water. Then, it was partitioned with ethyl acetate (6 × 300 mL). The ethyl acetate-soluble fraction was separated and the remained solution further partitioned with *n*-butanol (6 × 300 mL). The superior *n*-butanol layer was also removed and the lower water-soluble layer was considered as water fraction (WF) (17–19). The resulting fraction was dried on a water bath (the yield was 19.9%) and working solutions were made up in culture media.

Cell culture and treatment

The N2a (mouse neuroblastoma cell line) cells were cultivated in high-glucose DMEM supplemented with 10% FBS. The cells at sub-confluent stage were harvested using trypsin and seeded in 96-well plate. Twenty four hours later, the standard medium was replaced by glucose- and serum-free DMEM (GSD) to induce DNA damage. The cells were further incubated in this condition for 12 h at 37°C and 5% CO_2. In treatment groups, the cells were preincubated with WF (50 and 400 µg/mL) for 2 h and then incubated simultaneously for another 12 h in GSD condition. These doses were chosen based on IC_{50} (concentration of 50% inhibition) calculated from earlier experiments (16). Blank and solvent controls were treated identically.

Ferric/reducing antioxidant power (FRAP) assay

The total antioxidant ability of the WF was determined using ferric reducing antioxidant power (FRAP) assay based on the method of Benzie and Strain (20) with some modifications (21). Briefly, to 1 mL WF in 0.1 M phosphate buffer (pH 7.3), 3 mL of freshly prepared and prewarmed (37°C) FRAP reagent (consisting of 300 mM acetate buffer pH = 3.6, 10 mM TPTZ in 40 mM HCl and 20 mM $FeCl_3 \times 6H_2O$ in the ratio of 10 : 1 : 1, v/v/v) was added and the reaction mixture was incubated at 37°C for 10 min. The ferric reducing ability of WF (the absorbance of the blue colored complex of Fe^{II}-TPTZ) was read against the blank (3 mL FRAP reagent + 1 mL phosphate buffer 0.1 M, pH 7.3) at 593 nm. Standard solutions of Fe^{II} in the range of 100 to 1000 µM were prepared from ferrous sulfate ($FeSO_4 \times 7H_2O$) in distilled water. The data were expressed as µmol ferric ions reduced to ferrous form per gram of the extract (FRAP value). Ascorbic acid was used as a reference. The antioxidant assay was repeated three times (22).

Lipid peroxidation assay

The end product of lipid peroxidation is malondialdehyde (MDA), which reacts with TBA to form a pink-colored complex with a peak absorbance at 530 nm (23). To perform the assay, the treated cells were scraped into trichloroacetic acid (2.5%, 1 mL) and centrifuged at 13000 × g at 4°C for 2 min. The lysate supernatant (500 µL) was removed and added to trichloroacetic acid (15%, 400 µL) and TBA 0.67%/butylated hydroxytoluene 0.01% (800 µL). BHT was added to prevent sample oxidation during processing. This mixture was vortexed, boiled for 20 min and then the reaction was stopped by cooling in an ice water bath. After cen-

trifugation at 2500 rpm for 10 min at 4°C, the fluorescence intensity of supernatant was read in excitation/emission of 530/550 nm (24). The MDA amounts were expressed as nmol/mg protein. Protein content was determined using BCA kit.

Single cell gel electrophoresis (comet) assay

The alkaline SCGE (comet) assay was conducted based on the method described previously (25, 26). After 12 h incubation in glucose- and FBS-free medium, the cells were harvested for alkaline single cell gel electrophoresis (comet) assay. In brief, 10 µL of cell suspension was mixed with 90 µL LMP agarose and the mixture was layered over a microscope slide precoated with a layer of 100 µL NMP agarose. The slides were then covered with a cover slip and placed on ice to allow agarose to cool down and solidify. Finally, another layer of LMP agarose was added on top. The slides were then immersed in cold lysis solution (2.5 M NaCl, 100 mM Na_2EDTA, 10 mM Trizma, 1% sarkosyl, 10% DMSO, 1% Triton X-100, pH 10) and kept at 0°C overnight. After that, the slides were placed on a horizontal gel electrophoresis platform containing a prechilled alkaline solution (300 mM NaOH, 1 mM Na_2EDTA, pH > 13) for 40 min. They were then electrophoresed (25 V, 300 mA) at 0°C for 30 min. Finally, the slides were rinsed gently three times with 400 mM trizma solution (adjusted to pH 7.5 by HCl) to neutralize the excess alkali, stained with 50 µL of 20 µg/mL ethidium bromide, and covered with a cover slip. While undamaged cells resemble an intact nucleus without a tail, damaged cells have the appearance of a comet. For analysis, 150 nuclei

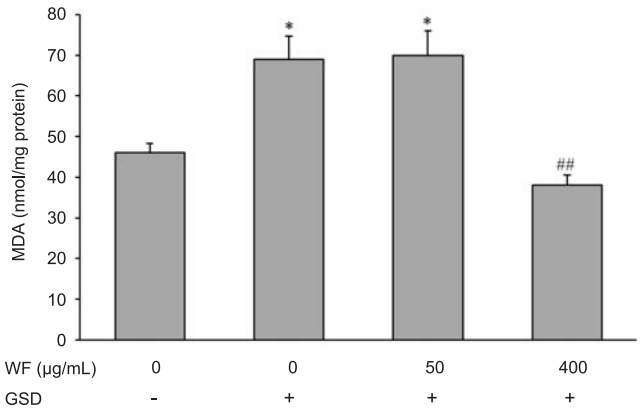

Figure 1. Effect of water fraction (WF) of lettuce on lipid peroxidation induced by glucose/serum deprivation (GSD) in N2a cells. The lipid peroxidation level was evaluated by measuring the concentration of malondialdehyde (MDA). Data are the mean ± SEM of two independent experiments performed in triplicate; *$p < 0.05$ *vs.* untreated cells cultured in normal condition; ##$p < 0.01$ *vs.* untreated cells cultured in GSD condition

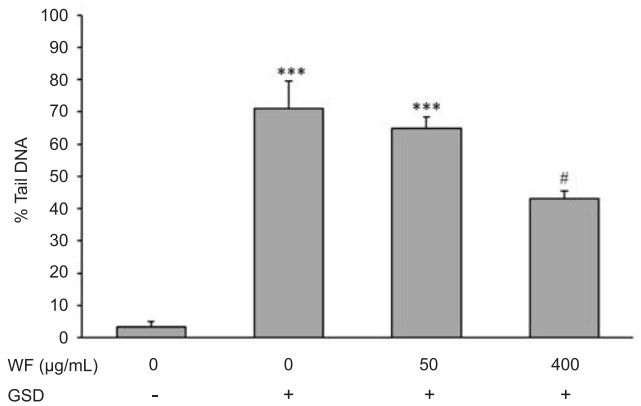

Figure 2. Effect of water fraction (WF) of lettuce on DNA damage in N2a cells cultured in the glucose/serum deprivation (GSD) condition. The percent of DNA in the comet tail (% tail DNA), which is an estimation of DNA damage, was determined using comet assay. Data are mean ± SEM of two independent experiments performed in triplicate; ***$p < 0.001$ *vs.* untreated cells cultured in GSD condition; #$p < 0.05$ *vs.* untreated cells cultured in GSD condition

were randomly selected from three replicated slides and examined using fluorescence microscope equipped with an excitation filter of 520–550 nm and a barrier filter of 580 nm. The percent of DNA in the comet tail (% tail DNA), which is an estimation of DNA damage, was analyzed using the computerized image analysis software (CASP software).

Statistical analysis

The results were presented as the mean ± SEM. Comparison between groups was made by one way analysis of variance (ANOVA) followed by Tukey's *post hoc* test. Differences were considered significant when p values were less than 0.05.

RESULTS

Total antioxidant activity

Using the FRAP assay, the antioxidant activity of lettuce water fraction was found to be 574 µmol/g of dry water fraction of lettuce leaves, while the antioxidant potential of pure vitamin C was 8960 µmol/g.

Effect of lettuce on lipid peroxidation

Exposure of N2a cells to glucose- and serum-free condition resulted in a significant ($p < 0.05$) increase of MDA level (69.0 ± 5.7 nmol/mg protein) as compared to control cells cultured in standard condition (46.0 ± 2.4 nmol/mg protein). The content of MDA was significantly ($p < 0.01$) decreased in the cells treated with 400 µg/mL (38.0 ± 2.5 nmol/mg protein) of the WF (Fig. 1). The lettuce in low concentration (50 µg/mL) failed to change MDA concentration (70.0 ± 6.0 nmol/mg protein).

Effect of lettuce on oxidative DNA damage

The cells cultured in standard condition showed only minor DNA fragmentation (3.4 ± 1.5%) as estimated by measurement of percent of DNA in the comet tail (% tail DNA). However, as shown in Figure 2, glucose and serum deprivation significantly increased the percent of DNA fragmentation (71.0 ± 8.5%, $p < 0.001$). A significant decrease in DNA damage was seen following treatment with 400 µg/mL (43 ± 2.5%, $p < 0.05$) of the WF. Again, the lettuce fraction was ineffective on DNA damage at concentration of 50 µg/mL.

DISCUSSION AND CONCLUSION

In the present study, we showed that lettuce has an overall protective effect against glucose/serum deprivation-induced lipid peroxidation and DNA fragmentation. Deprivation of cells from glucose and serum is a reliable *in vitro* model for induction of cytotoxicity and evaluation of cytoprotective activity of natural materials (27). It is well documented that lipid peroxidation induced by oxidative stress plays an important role in DNA damage (6). Since the GSD-induced overproduction of MDA was markedly inhibited by WF of lettuce, it is reasonable to assume that protective effect of this fraction is mediated, at least partially, thorough its antioxidant properties. This is in agreement with previous studies, which revealed that lettuce is a good source of antioxidants such as quercetin, caffeic acid, tocopherol, ascorbic acid, carotenoids and phenolic compounds (3, 8). Using FRAP assay, it is estimated that 1 g WF contains an amount of antioxidant power similar to that found in 64.1 mg of pure ascorbic acid (vitamin C), highlighting the enormous antioxidant potential of lettuce. Due to several reasons, one may consider the FRAP assay as suitable method for assessment of total antioxidants in plants. In the FRAP assay, pretreatment is not required, stoichiometric factors are constant and linearity is maintained over a wide range. Moreover, the FRAP assay, unlike other assays, directly measures antioxidants or reductants in a sample. The other assays indirectly measure the inhibition of reactive species (or free radicals) generated in the reaction mixture and therefore, the results also strongly depend on the type of reactive species used (28). Our result is in agreement with that of Tiveron et al. (29) who showed lettuce present high antioxidant activity not only in the FRAP assay (447.1 µmol Fe^{II}/g), but also in the DPPH (2,2-diphenyl-1-picrylhydrazyl radical) (77.2 µmol Trolox/g) and the α-carotene bleaching (90%) methods. The antioxidant activity of lettuce correlated very well to the total phenolic contents, mainly flavonoids (quercetin glycosides, luteolin) and phenolic acids (caffeoyl and p-coumaroyl esters) (29, 30). Heimler et al. (31) also found the considerable polyphenol content and antiradical activity in *Lactuca sativa*.

Antioxidant agents have differing solubilities: water-soluble ascorbic acid, phenolic compounds, glutathione and urate, lipid-soluble tocopherols and carotenoids and intermediate-soluble hydroxycinnamic acids and flavonoids (32, 33). Since we used water-soluble fraction of lettuce, it seems that water-soluble antioxidants such as ascorbic acid and phenolic compounds are mainly involved in the cytoprotective activity of lettuce. Beside, in our preliminary works, it was found that ethyl acetate fraction (intermediary water-soluble antioxidants) of lettuce can also induce cytoprotective activity (unpublished data). Therefore, the exact nature of compounds

responsible for the protective action of lettuce still remained to be elucidated.

Recently, Okada and Okada (34) reported that aqueous extract of lettuce seeds offer protection against amyloid α (Aα)-mediated oxidative stress and cell death using hippocampus neurons, probably through high phenolic content and radical scavenging activity. Neuroprotective effects of phenolic extract of romaine lettuce and its pure caffeic acid derivatives against oxidative stress caused by hydrogen peroxide were also reported in PC12 cells (15).

In summary, our study revealed that water-soluble fraction of lettuce exerts protective effect against glucose/serum deprivation-induced DNA damage. This effect is mediated through inhibition of oxidative stress.

Acknowledgment

This work was supported by a grant from Research Council of Mashhad University of Medical Sciences, Mashhad, Iran. The authors declare that they have no conflict of interest.

REFERENCES

1. Smith J.A., Park S., Krause J.S., Banik N.L.: Neurochem. Int. 62, 764 (2013).
2. Catalá A.: Biochimie 94, 101 (2011).
3. Sancar A., Lindsey-Boltz L.A., Unsal-Kacmaz K., Linn S.: Annual Rev. Biochem. 73, 39 (2004).
4. Sultana R., Perluigi M., Allan Butterfield D.: Free Radic. Biol. Med. 62, 157 (2013).
5. Hoeijmakers J.H.: New Eng. J. Med. 361, 1475 (2009).
6. Nair U., Bartsch H., Nair J.: Free Rad. Biol. Med. 43, 1109 (2007).
7. Shukla V., Mishra S.K., Pant H.C.: Adv. Pharmacol. Sci. 2011, 572634 (2011).
8. Yu B.P.: Physiol. Rev. 74, 139 (1994).
9. Kang H.M., Saltveit M.E.: J. Agric. Food Chem. 50, 7536 (2002).
10. Serafini M., Bugianesi R., Salucci M., Azzini E., Raguzzini A., Maiani G.: Br. J. Nutr. 88, 615 (2002).
11. Altunkaya A., Becker E.M., Gokmen V., Skibsted L.H.: Food Chem. 115, 163 (2009).
12. Barnes J.: Drug Saf. 26, 829 (2003).
13. Sayyah M., Hadidi N., Kamalinejad M.: J. Ethnopharmacol. 92, 325 (2004).
14. Deshmukh A.A., Gajare K.A., Pillai M.M.: J. Herbal Med. Toxicol. 1, 43 (2007).
15. Im S.E., Yoon H., Nam T.G., Heo H.J., Lee C.Y., Kim D.O.: J. Med. Food 13, 779 (2010).
16. Sadeghnia H.R., Farahmand S.K., Asadpur E., Rakhshandeh H., Ghorbani A.: African J. Pharm. Pharmacol. 6, 2464 (2012).
17. Rakhshandeh H., Sadeghnia H.R., Ghorbani A.: Nat. Prod. Res. (2011).
18. Mortazavian S.M., Ghorbani A., Hesari T.G.: Iran. J. Obstet. Gynecol. Infert. 15, 9-16 (2012).
19. Ghorbani A., Rakhshandeh H., Sadeghnia H.R.: Iran. J. Pharm. Res. 12, 401 (2013).
20. Benzie I.F.F., Strain J.J.: Methods Enzymol. 299, 15 (1999).
21. Sadeghnia H.R., Kamkar M., Assadpour E., Boroushaki M.T., Ghorbani A.: Iran. J. Basic Med. Sci. 16, 73 (2013).
22. Benzie I.F.F., Szeto Y.T.: J. Agric. Food Chem. 47, 633 (1999).
23. Siddiqui M.A., Kashyap M.P., Kumar V., Al-Khedhairy A.A., Musarrat J., Pant A.B.: Toxicol. Invitro. 24, 1592 (2010).
24. Wang X., Dykens J.A., Perez E., Liu R., Yang S., Covey D.F., Simpkins J.W.: Mol. Pharmacol. 70, 395-404 (2006).
25. Hosseinzadeh H., Sadeghnia H.R.: DNA Cell Biol. 26, 841 (2007).
26. Forouzanfar F., Goli A.A., Assadpour E., Ghorbani A., Sadeghnia H.R.: Evid. Based Complement. Alternat. Med. 2013, 7167730 (2013).
27. Mousavi S.H., Tayarani-Najaran Z., Asghari M., Sadeghnia H.R.: Cell Mol. Neurobiol. 30, 591 (2010).
28. Halvorsen B.L., Holte K., Myhrstad M.C.W., Barikmo I., Hvattum E., Remberg S.F., Wold A.B., et al.: J. Nutr. 461 (2001).
29. Tiveron A.P., Melo P.S., Bergamaschi K.B., Vieira T.M.S.F., Regitano-d'Arce M.A.B., Alencar S.M.: Int. J. Mol. Sci. 13, 8943 (2012).
30. Ribas-Agustí A., Gratacós-Cubarsí M., Sárraga C., García-Regueiro J.A., Castellari M.: Phytochem. Anal. 22, 555 (2011).
31. Heimler D., Isolani L., Vignolini P., Tombelli S., Romani A.: J. Agric. Food Chem. 55, 1724 (2007).
32. Eastwood M.A.: QJM 92, 527 (1999).
33. Podsędek A.: LWT-Food Sci. Technol. 40, 1 (2007).
34. Okada Y., Okada M.: J. Pharm. Bioallied Sci. 5, 141 (2013).

Received: 24. 09. 2012

Acta Poloniae Pharmaceutica – Drug Research, Vol. 71 No. 3 pp. 415–421, 2014 ISSN 0001-6837
Polish Pharmaceutical Society

ANTIMICROBIAL ACTIVITY OF FRUITS OF *SOLANUM NIGRUM* AND *SOLANUM XANTHOCARPUM*

KHIZAR ABBAS[1,2], UZMA NIAZ[1], TALIB HUSSAIN[1], M. ASIF SAEED[1], ZEESHAN JAVAID[3]*, ARFAT IDREES[4] and SHAHID RASOOL[5]

[1]University College of Pharmacy, University of the Punjab, Lahore, Pakistan
[2]College of Pharmacy, GC University, Faisalabad, Pakistan
[3]Akson College of Health Sciences, Mirpur University of Science & Technology, Mirpur, A.J. & Kashmir, Pakistan
[4]Faculty of Pharmacy and Alternative Medicine, The Islamia University of Bahawalpur, Pakistan
[5]Faculty of Pharmacy, University of Sargodha, Sargodha, Pakistan

Abstract: Current study was conducted to investigate antimicrobial activity of fruit extracts of two Solanaceous plants (*Solanum nigrum* and *Solanum xanthocarpum*) found in Pakistan. Petroleum ether, chloroform, dichloromethane, ethyl acetate, acetone, methanol and water were utilized for extraction. The highest percentages of polar components of both the species were extracted by water; little amount of non-polar components by petroleum ether while very low quantities by other solvents. Antimicrobial activities were estimated by measuring zones of inhibition through hole-plate diffusion method, against three species of Gram positive bacteria, five species of Gram negative bacteria and three species of fungi selected for this study. Doses of 5, 10 and 15 mg/mL prepared through methanolic extracts of each plant's powdered fruit material displayed significant zones of inhibition against all three Gram positive bacteria, three of the Gram negative bacteria out of five and against all three fungi. Although these doses exhibited significant zones of inhibition but they are not as potent as standards: ampicillin or amphotericin B. The present study assures the possible potential of antimicrobial as well as antifungal activity of fruit extracts of these plants.

Keywords: antimicrobial activity, *Solanum nigrum*, *Solanum xanthocarpum*, zones of inhibition, antifungal activity, solvent extraction

Pakistan is among the reasonably diverse countries in biological resources. Here people trust on natural sources, have invaluable and uninterrupted practice of the use of medicinal plants and other natural resources for healthcare necessities (1). The knowledge of naturally occurring medicinal plants (drugs) was slowly acquired by humans on the basis of experience (2). Plants play important function in developing modern medicines as they contain active phytochemical components. They have beneficial effects on the community by improving the health of human beings by treating many diseases for many years (3, 4). For such activity, the source of phytochemicals have commonly found in leaves, barks, roots, flowers, fruits and seeds of the plants (5). Sandhu and Heinrich (6) and Gupta et al. (7) has pointed out that many rural communities in developing countries depend on plant sources for their nutrient and scrounge, making household utilities as well as utilized them for fire, shadow and as herbal drugs.

The plants usually possess antimicrobial substances for their own protection from microbial infection and deterioration; that's why they are being used for the conservation and safety of food products (8–10). Ushimaru et al. (11) assessed the antimicrobial activity of aqueous and ethanol extracts of nine Nigerian species against four nutrient borne bacteria for checking their pharmacological activity in the direction of formulating new anti-abscessed agents. Many analytical reports showed that *Solanum* plants are important source of large number of phytochemical compounds with substantial curative application against human pathogens (12). So they could be assessed as an alternate way to fight against bacterial diseases (13).

* Corresponding author: e-mail: drmianjavaid@hotmail.com; phone: 0092-300-7311771

Black nightshade *(Solanum nigrum* L.) is a weed of amentaceous land, gardens, and soils rich in nitrogen and is broadly distributed in Pakistan (14). The fruit of *S. nigrum* contains many ingredients including fatty acid, tannins, cellulose, resins, dextrin, ash and moisture. Methanolic root extracts of *S. nigrum* showed antimicrobial and antifungal properties (15). It was also demonstrated that the *S. nigrum* extract acts as a larvicidal agent against five laboratory colonized strains of mosquito species (16). Fruits also contain tropeine, an alkaloid having mydriatic action, along with solanine (17). Four anti-cancer steroidal glycosides; solasonine, solamargine, diosgenin and solasodine were isolated from the immature *S. nigrum* fruits (18). Recent phytochemical analysis of *S. nigrum* fruit has resulted in the isolation of two novel disaccharides along with protein, fibre, carbohydrate, minerals like magnesium, phosphorus and vitamin C, B and folic acid (19).

Solanum xanthocarpum is also recognized as Indian night-shade or yellow berried nightshade plant. It is well versed in India and Pakistan; often in wastage places, on roadsides and in open spaces as well. Its fruit contains carpesterol, glucose, galactose, potassium chloride, a number of steroidal compounds and alkaloids mainly in the form of glycoalkaloids. The flavanoids quercitrin and apigenin glycosides were the major chemical constituents present in the fruits of *S. xanthocarpum* (20, 21). Many therapeutic activities of the fruits of this plant have been reported. Its' being used for itching and fever, reduces adipose tissues as well as seminal ejaculation (22, 23). The aqueous and organic solvent extracts of different parts of the plant demonstrated that all the extracts had very strong biological inhibition effects (24). Methanolic extracts of *S. xanthocarpum* and *Datura metel* exhibited highly significant antifungal activity against different species of pathogenic Aspergilli (25). Okram et al. (26) also investigated the strong inhibitory effects on the radiated growth of *Aspergillus niger* and *Trichoderma viride*.

The main objective of this study was to take into account the important aspect of antibacterial potential of fruits of *Solanum nigrum* L. and *Solanum xanthocarpum* Schrad & Wendl. along with antifungal activity and the main reason for choosing the fruits of these plants among the diversity is the reality that local people often employ these two important fruits as folk medicines for various infections. It is thus essential to assess the medicinal plants scientifically for various complaints that were made against the traditional medicine in the past.

EXPERIMENTAL

Chemicals and reagents

Ampicillin pure powder (Glaxo-Smith-Kline, Pakistan), Amphotericin B pure powder (Fada Pharma, Argentina), Nutrient agar medium (Merck lot no. NA806), Sabouraud dextrose agar media (Merck lot no. 111674/249), double distilled deionized water. Petroleum ether, chloroform, methanol, $DMSO_4$, ethyl acetate, acetone, dichloromethane. All the solvents were of analytical grade.

Plant collection

Fruits of *Solanum nigrum* L. and *Solanum xanthocarpum* Schrad & Wendl. were collected from the rural areas of district Muzaffargarh, South Punjab-Pakistan. After authentication by Herbarium staff of Bahauddin Zakariya University Multan, Pakistan, the voucher specimens were submitted in the Herbarium of Pharmacognosy Department, University College of Pharmacy, University of the Punjab, Lahore, Pakistan, for further reference. The fruits were dried under shade for a period of one month to achieve complete dryness and then pulverized to obtain coarse and fine powders.

Solvent extraction

The weighed quantities of dried powdered materials collected from fruits of both the plants were extracted with various solvents successively such as petroleum ether, chloroform, dichloromethane, ethyl acetate, acetone and water. The maceration was carried out for seven days at room temperature for individual solvent and successively repeated for each solvent with a sequence as mentioned above. The extracts for each solvent were collected separately, then filtered and dried under vacuum in a rotary evaporator at $40 \pm 5^{o}C$. These dried extracts were weighed to calculate the total percentage yield for individual solvent and were redissolved in dimethyl sulfate ($DMSO_4$) for antimicrobial activity analysis and stored in labelled sterile screw capped bottles.

Preparation of methanolic extract

The weighed quantities of dried powdered materials of fruits of both the plants were extracted individually thrice with each time using 1 liter of methanol by maceration for seven days at room temperature. The methanolic extracts obtained from both the plants were filtered, dried and stored according to the procedure as mentioned above.

Test microorganisms

Antibacterial and antifungal studies were conducted upon three species of Gram positive bacteria; *Micrococcus varians* (ATCC No. 9341), *Micrococcus luteus* (ATCC No. 9342), *Staphylococcus aureus* (ATCC NO. 25923), five species of Gram negative bacteria; *Salmonella typhi* (ATCC No. 19430), *Pasteurella maltocida* (ATCC No. 51687), *Escherichia coli* (ATCC No. 25922), *Klebsiella pneumoniae* (ATCC NO. 700721), *Vibrio cholerae* (ATCC No. 39541) and three species of fungi; *Aspergillus niger* (ATCC No. 16404), *Aspergillus flavus* (ATCC No. 204304), *Aspergillus fumigatus* (ATCC No. 204305). Pure cultures of these microorganisms were collected from Department of Microbiology, University of Veterinary and Animal Sciences (UVAS), Lahore, Pakistan.

Assay methodology

Hole-plate diffusion method was employed to test the antibacterial and antifungal activity of fruit extracts of both the plants. A suitable suspension (inoculum) of each microorganism was prepared by incorporating one loop full of fresh microorganism in 10 mL of sterilized water for injection near flame. Ten milliliters of prepared inoculum of each Gram positive and Gram negative microorganism was then separately poured in each of 500 mL of sterile liquefied nutrient agar medium for determination of antibacterial activity. Similarly, 10 mL of prepared inoculum of fungal species was separately poured in each of 500 mL of sterile liquefied Sabouraud dextrose agar medium for determination of antifungal activity. These media were properly labelled for each microorganism and then gently shaken to allow uniform mixing of the inoculum with the medium. After mixing, they were poured in labelled sterile Petri dishes in a specified quantity to maintain a depth of media up to 8 mm, while it was being spread with the help of spreader. Each prepared Petri dish was gently rotated for proper and uniform spreading of medium and allowed to solidify at room temperature.

For different solvent extracts of *S. nigrum*, eight holes were made in the solidified medium at uniform distance from each other with stainless steel borer and numbered as 1 to 8. Hole no. 1 was filled with positive control reference solution while hole 8 with negative control $DMSO_4$ solvent. Holes from 2 to 7 were filled with sample solutions of different solvents extract of *S. nigrum* including methanolic extract at a dose of 20 mg/mL.

For comparative antibacterial and antifungal activities of both the plants, three doses i.e., 5, 10 and 15 mg/mL of methanolic extracts of fruits of both the plants were used. For methanolic extract five holes were made in the solidified medium. The holes were numbered as 1, 2, 3, 4, and 5 and filled aseptically with reference and sample solutions. Reference or positive controlled antibacterial/antifungal solution were filled in hole no. 1, while hole no. 2, 3 and 4 were filled with methanolic extract of fruit of *S. nigrum* with 5, 10 and 15 mg/mL concentrations, respectively. The solvent extracts were diluted to solutions of different concentrations with $DMSO_4$ solvent. Hole no. 5 was filled aseptically with the negative controlled reference solvent sample i.e., $DMSO_4$. The different solvents and methanolic extracts of fruit of *S. xanthocarpum* were also treated in a similar manner.

For antibacterial activity, the Petri dishes were kept in an incubator at 32 ± 2.5^oC for 48 h, whereas for antifungal activity; the incubation temperature was 22 ± 2.5^oC for 72 h. In each case, zones of inhibition were observed and measured with the help of vernier calliper. The experiments were performed in three replicates. Results were expressed as the mean zones of inhibition.

Statistical analysis

The mean zones of inhibitions caused by the solvent extracts of the plant's fruit materials and standard drugs were calculated and reliability of the samples was assessed by calculating standard deviation.

RESULTS AND DISCUSSIONS

Fruits of *S. nigrum* and *S. xanthocarpum* collected from dissimilar localities in different seasons showed that the local mesophytic soil and climatic conditions affected the advent of both the plant fruits. A great variation in the appearance of fruits of both the plants was found in the size and shape arrangements and also in the number and color of the berries and seeds etc. On the basis of such ecological variations, different chemical identification tests were performed to determine the naturally occurring as well as secondary metabolites (alkaloids, flavonoids, sapogenins, steroids, sterols etc.). Positive results indicated the presence of these metabolities, which caused the fruits to adjust themselves according to different conditions (27).

The extracts obtained by extraction of dried powder of fruits of both the plants by using different types of solvents, were compared for efficiency of eluting solvents by calculating the percentage yield of extracted materials. It was found that maximum

Table 1. Percentage yield of the extracted materials of dried powdered fruits of *S. nigrum* and *S. xanthocarpum* plants by different solvents.

Solvents	Percentage yields	
	Solanum nigrum	*Solanum xanthocarpum*
Petroleum ether	5.79	6.68
Chloroform	8.47	9.42
Dichloromethane	10.26	11.73
Ethyl acetate	12.87	13.27
Acetone	14.89	16.29
Water	41.63	42.47
Total yield	94.07	99.86
Methanol	36.52	39.56

Table 2. Antimicrobial activity of various solvent extracted materials of dried powdered fruit of *Solanum nigrum* (dose level = 20 mg/mL).

Microorganisms	**Zones of inhibition (mm) ± SE**						
	P-ether	**Chlo.**	**Dimet.**	**Et-act.**	**Acet.**	**Meth.**	**Water**
Gram positive bacteria							
Micrococcus luteus	3.2 ± 3.1	9.2 ± 1.25	8.5 ± 2.0	6.5 ± 3.2	7.6 ± 1.3	3.4 ± 2.1	13.5 ± 3.4
Staphylococcus aureus	3.4 ± 2.2	8.5 ± 2.12	7.5 ± 1.8	7.2 ± 2.0	8.3 ± 2.0	15.2 ± 3.5	14.7 ± 2.4
Gram negative bacteria							
Salmonella typhi	4.5 ± 2.4	7.6 ±1.8	7.6 ± 1.5	6.7 ± 2.5	6.5 ± 2.0	15.2 ± 3.3	15.3 ± 3.2
Escherichia coli	6.2 ± 1.3	6.7±1.4	8.5 ± 2.0	7.5 ± 2.3	7.9 ± 2.1	14.3 ± 2.6	16.4 ± 3.0
Fungi							
Candida albicans	3.7 ± 2.0	5.8 ± 2.6	6.4 ± 3.3	6.7 ± 1.3	5.3 ± 1.0	7.6 ± 1.0	4.8 ± 2.10

P-ether = Petroleum ether; Chlo. = Chloroform; Dimet. = Dichloromethane; Et-act. = Ethyl acetate; Acet. = Acetone; Meth. = Methanol

Table 3. Antimicrobial activity of various solvent extracted materials of dried powdered fruit of *Solanum xanthocarpum* (dose level = 20 mg/mL).

Microorganisms	**Zones of inhibition (mm) ± SE**						
	P-ether	**Chlo.**	**Dimet.**	**Et-act.**	**Acet.**	**Meth.**	**Water**
Gram positive bacteria							
Micrococcus luteus	3.6 ± 2.5	7.5 ± 2.2	9.7 ± 1.2	9.8 ± 2.1	6.2 ± 2.3	13.7 ± 0.4	12.7 ± 2.0
Staphylococcus aureus	3.9 ± 3.2	8.3 ± 3.1	8.8 ± 2.4	7.4 ± 3.2	8.0 ± 2.1	14.1 ± 2.4	14.0 ± 2.2
Gram negative bacteria							
Salmonella typhi	6.5 ± 2.2	6.6 ± 2.4	8.9 ± 2.6	5.7 ± 3.1	6.0 ± 1.1	14.1 ± 1.3	15.7 ± 1.2
Escherichia coli	8.6 ± 1.	4 7.6 ± 1.5	9.7 ± 2.3	8.1 ± 2.5	8.9 ± 0.7	14.2 ± 2.4	17.8 ± 2.4
Fungi							
Candida albicans	5.6 ± 2.3	7.7 ± 1.8	7.3 ± 3.7	6.0 ± 1.0	4.3 ± 1.2	7.0 ± 0.5	7.9 ± 2.6

P-ether = Petroleum ether; Chlo. = Chloroform; Dimet. = Dichloromethane; Et-act. = Ethyl acetate; Acet. = Acetone; Meth. = Methanol

Table 4. Comparative antimicrobial activities of the methanolic extract of the dried powdered fruit of *S. nigrum*, *S. xanthocarpum* and standard drugs.

Microorganisms	**Zones of inhibition (mm) ± SE**						
	***S. nigrum* (Dose = mg/mL)**			***S. xanthocarpum* (Dose = mg/mL)**			**Stand. drug***
	5	**10**	**15**	**5**	**10**	**15**	**(1 or 2)**
Gram positive bacteria							
Micrococcus varians	10.2 ± 1.3	12.2 ± 1.0	13.3 ± 1.0	7.4 ± 2.3	9.6 ± 2.1	10 ± 3.2	14 ± 5.2
Micrococcus luteus	10.1 ± 2.0	11.8 ± 1.0	12.5 ± 2.3	8.6 ± 3.2	9.2 ± 2.3	11 ± 2.1	31 ± 4.3
Staphylococcus aureus	9.1 ± 3.1	10.3 ± 2.1	11.3 ± 3.2	07 ± 4.2	9.6 ± 3.4	11.3 ± 2.0	9 ± 2.5
Gram negative bacteria							
Salmonella typhi	11.3 ± 3.1	12.4 ± 4.0	14.6 ± 2.0	10.6 ± 1.2	12.3 ± 1.2	13 ± 2.3	25 ± 2.4
Pasteurella maltocida	8.2 ± 1.4	10.6 ± 2.1	10.7 ± 1.3	12.5 ± 1.3	14.2 ± 1.0	14.9 ± 3.3	20 ± 2.2
Escherichia coli	9.0 ± 2.1	11.0 ± 1.1	11.6 ± 2.1	12.0 ± 1.0	13.0 ± 1.0	14.0 ± 1.1	15 ± 2.3
Klebsiella pneumoniae	0.0 ± 0.0	0.0 ± 0.0	0.0 ± 0.0	0.0 ± 0.0	0.0 ± 0.0	0.0 ± 0.0	23 ± 3.6
Vibrio cholerae	0.0 ± 0.0	0.0 ± 0.0	0.0 ± 0.0	0.0 ± 0.0	0.0 ± 0.0	0.0 ± 0.0	34 ± 3.2
Fungi							
Aspergillus niger	4.6 ± 1.5	6.7 ± 2.1	9.3 ± 3.1	5.9 ± 1.0	6.4 ± 2.3	6.5 ± 2.4	11 ± 3.1
Aspergillus flavus	5.5 ± 1.3	6.6 ± 3.2	6.9 ± 2.0	7.5 ± 2.7	8.5 ± 2.5	9.3 ± 1.5	12 ± 2.5
Aspergillus fumigatus	6.6 ± 3.2	7.1 ± 1.0	7.6 ± 3.2	7.4 ± 1.4	7.8 ± 2.4	8.3 ± 2.3	13 ± 3.4

*Stand. drug – ampicillin in dose 125 mg/mL (**1**) and amphotericin B in dose 5 mg/mL (**2**).

efficiency was shown by water for both the fruits i.e., 41.63 and 42.47%, and methanol 36.52 and 39.56% for *S. nigrum* and *S. xanthocarpum*, respectively, whereas the least amount was extracted by petroleum ether as shown in Table 1. The results elaborate that polar solvents like methanol and water yielded a higher percentage of extracted materials mainly of polar components as compared to other solvent extracts (28). Among these two solvent extracted materials, water was found to be the most potential candidate, which extracted the highest percentage of highly polar components present in the powders of both the species (29). On the other hand, petroleum ether is non-polar in nature and it extracted the non-polar materials but yielded in least quantity, which is one of the evidence that these plants contain very small amount of non-polar compounds. Chloroform, dichloromethane, ethyl acetate and acetone possess intermediate polarities, so they extracted the components from fruits that possess intermediate polarities but extracted in minute quantities that is also indicative of very low percentage of these components in the extracts (30).

The results of preliminary antimicrobial activities of various solvent extracts of fruits of both the plants against three types of microorganisms (Gram positive bacteria, Gram negative bacteria and fungi) have been demonstrated in Tables 2 and 3. When these results were critically evaluated, it was found that the extracts, which have been extracted by using more polar solvents have greater potential for antimicrobial activity as compared to those extracted with less polar solvents. The antimicrobial substances generally possess intermediate polarity and smaller molecular weight antimicrobial substances are generally miscible with polar solvents, so can be easily concentrated in the polar solvent extracts. Also the antimicrobial activity is always dependent on the concentration of extracted antimicrobial metabolites, which can be enhanced with the increased polarity of solvents (31).

The observation that the compounds having activity against microorganisms are more soluble in polar solvents provides the basis for comparative study of extracts of fruits of plants to find the minimum inhibitory concentration against these organisms when these were extracted with a polar solvent – methanol. Findings of comparative antimicrobial activities of three doses i.e., 5, 10 and 15 mg/mL of methanolic extracts of fruits of *Solanum nigrum* and

Solanum xanthocarpum, along with the standard drugs (positive controlled reference drugs i.e., ampicillin or amphotericin B) against three species of Gram positive bacteria, five species of Gram negative bacteria and three species of fungi depict significant zones of inhibition against three Gram positive bacteria (*Micrococcus varians*, *Micrococcus luteus* and *Staphylococcus aureus*), three Gram negative bacteria (*Salmonella typhi*, *Pasteurella maltocida* and *Escherichia coli*) out of five and three species of fungi (*Aspergillus niger*, *Aspergillus flavus* and *Aspergillus fumigatus*). Although three doses of both the extracts displayed well marked inhibitory effects and exhibited significant zones of inhibition against nine microorganisms, yet it appeared to possess lesser activities than the standard ampicillin (with standard dose = 125 mg/mL), and amphotericin B (with standard dose = 5 mg/mL). So it is clear here that these extracts do possess antimicrobial and antifungal activity but not as potent as the standard antibacterials and antifungals (32). Therefore, we would like to state that the constituents of fruit extracts may serve as a beneficial source of industrial drugs useful in treatment of some bacterial infections (33). Since both the plants contain alkaloids, glycosides, lignins, tannins, and terpenoid compounds like monoterpenes, sesquiterpenes, diterpenes or triterpenes, probably these compounds get through the bacterial and fungal cell wall/membrane and supress their growth or if these compounds deeply penetrated, might kill them completely. These results are more or less similar to the previous findings by other workers, who explored the antibacterial and antifungal potential of natural products, against wide ranges of microorganisms, particularly from various members of family Solanaceae (34, 35).

From comparative study, it was found that the fruit extract of *S. xanthocarpum* has more antimicrobial activity against Gram negative bacteria as well as showed greater antifungal activity as compared to *S. nigrum,* whereas *S. nigrum* was found to be more potent against Gram positive bacteria as compred to *S. xanthocarpum*. The reason for being *S. xanthocarpum* more potent is that it contains specifically carpesterol and similar other steroidal glycoside, which are absent or not present in appreciable or distinguishable quantities in *S. nigrum* (36). These results have been shown in Table 4.

CONCLUSION

Above mentioned results revealed that by increasing the polarity of various solvents, concentration of extracted compounds and their antibacterial as well as antifungal activity increases. That's why the rural community mostly use it as a folk medicine. This investigation has created the possibility of use of these plants in drug development for human consumption. However, the effects of these plants on more pathogenic organisms and toxicological investigations need to be carried out.

REFERENCES

1. Oudhia P.: Planta Med. 15, 175 (2003).
2. Balandrin M.F., Klocke J.A., Wurtele E.S., Bollinger W.H.: Science 228, 1154 (1985).
3. Mata A.T., Proenca C., Ferreira A.R., Serralheiro M.L.M., Nogueira J.M.F., Araujo M.E.M.: Food Chem. 103, 778 (2007).
4. Sokovic M., Van-Griensven L.J.L.D.: Eur. J. Plant Pathol. 116, 211 (2006).
5. Zafar M., Khan M.A., Ahmad M., Sultana S., Qureshi R., Tareen R.B.: J. Med. Plants Res. 4, 1584 (2010).
6. Sandhu D.S., Heinrich M.: Phytother. Res. 19, 633 (2005).
7. Gupta M.P., Solis P.N., Calderon A.I., Guionneau-Sinclair F., Correa M. et al.: J. Ethnopharmacol. 96, 389 (2005).
8. Chandarana H., Baluja S., Chand S.V.: Turk. J. Biol. 29, 83 (2005).
9. Wannissorn B., Jarikasem S., Siriwangchai T., Thubthimthed S.: Fitoterapia 76, 233 (2005).
10. Smid E.J., Gorris L.G.M.: Natural Antimicrobials for Food Preservation, Handbook of Food Preservation, pp. 285–308, Marcel Dekker, New York 1999.
11. Ushimaru P.I., Da Silva M.T.N., Di Stasi L.C., Barbosa L., Junior A.F.: Braz. J. Microbiol. 38, 717 (2007).
12. Udayakumar R., Velmurugan K., Srinivasan D., Krishna R.R.: Anc. Sci. Life 23, 90 (2003).
13. Meera P., Dora P.A., Samvat J.K.: Geobios 26, 17 (1999).
14. Edmonds J.M., James A.C.: Black nightshades. *Solanum nigrum* L. and related species, p. 8, International Plant Genetic Resources Institute, Rome, Italy, 1997.
15. Ravi V., Saleem T.S.M., Maiti P.P., Gauthaman K., Ramamurthy J.: Afr. J. Pharm. Pharmacol. 3, 454 (2009).
16. Raghavendra K., Singh S.P., Subbarao S.K., Dash A.P.: Indian J. Med. Res. 130, 74 (2009).
17. Ghosh A., Das B.K., Roy A., Mandal B., Chandra G.: Nat. Med. 62, 259 (2007).

18. Saijo R., Murakami K., Nohara T., Tomimatsa A., Saito A., Matsuoka K.: Yakugaku Zasshi 102, 300 (1982).
19. Chen R., Feng L., Li H.D., Zhang H., Yang F.: Carbohydr. Res. 344, 1775 (2009).
20. Li Z., Cheng X., Wang C.J., Li G.L., Xia S.Z., Wei F.H.: Zhongguo Ji Sheng Chong Xue Yu Ji Sheng Chong Bing Za Zhi 30, 206 (2005).
21. Gunaselvi G., Kulasekaren V., Gopal V.: Int. J. Pharmtech. Res. 2, 1772 (2000).
22. Zaman M.B., Khan M.S.: Hundred Drug Plants of West Pakistan, pp. 63–64, Medicinal Plant Branch, Pakistan Forest Institute, Peshawar, Pakistan 1970.
23. Singh V.K., Ali Z.A., Zaide S.T.H., Siddiqui M.K.: Fitoterpia 16, 137 (1996).
24. Salar R.K., Suchitra: Afr. J. Microbiol. Res. 3, 97 (2009).
25. Dabur R., Singh H., Chhillar A.K., Ali M., Sharma G.L.: Fitoterapia 75, 389 (2004).
26. Okram M.S., Subharani K., Singh N.I., Devi N.B., Nevidita L.: Nat. Prod. Res. 21, 585 (2007).
27. Sarin R.: Biotechnology 4, 79 (2005).
28. Gupta A.K., Ganguly P., Majumder U.K., Ghosal S.: Pharmacology online 1, 757 (2009).
29. Weissenberg M.M.: Phytochemistry 58, 501 (2001).
30. Wang L., Weller C.L.: Trends Food Sci. Technol. 17, 300 (2006).
31. Visht S., Chaturvedi S.: Current Pharma Research 2, 584 (2012).
32. Tambekar D.H., Dahikar S.B.: IJPSR 2, 311 (2011).
33. Malik F., Hussain S., Mirza T., Hameed A., Ahmad S., Riaz H., Shah P.A., Usmanghani K.: J. Med. Plants Res. 5, 3052 (2011).
34. Priya P., Pal J.A., Aditya G., Gopal R.: Phcog. J. 2, 400 (2010).
35. Palombo E.A., Semple S.J.: J. Ethnopharmacol. 77, 151 (2001).
36. Singh O.M., Subharani K., Singh N.I., Devi N.B., Nevidita L.: Nat. Prod. Res. 21, 585 (2007).

Received: 26. 03. 2013

Acta Poloniae Pharmaceutica – Drug Research, Vol. 71 No. 3 pp. 423–430, 2014 ISSN 0001-6837
Polish Pharmaceutical Society

NEW WITHANOLIDE, ACYL AND MENTHYL GLUCOSIDES FROM FRUITS OF *WITHANIA COAGULANS* DUNAL

ABUZER ALI, MOHD. JAMEEL and MOHAMMED ALI*

Phytochemistry Research Laboratory, Department of Pharmacognosy and Phytochemistry, Faculty of Pharmacy, Jamia Hamdard, New Delhi-110062, India

Abstract: The fruits of *Withania coagulans* Dunal (family: Solanaceae) are sweet, sedative, emetic, alterative and diuretic; used to treat asthma, biliousness, strangury, wounds, dyspepsia, flatulent colic, liver complaints and intestinal infections. Phytochemical investigation of the fruits yielded a withanolide tetraglucoside identified as (20S, 22R)-5α, 20α-diacetoxy-6β-hydroxy-1-oxowitha-2,24-dienolide-6-β-*D*-glucopyranosyl-(6'→1'')-β-*D*-glucopyranosyl-(6''→1''')-β-*D*-glucopyranosyl-(6'''→1'''')-β-*D*-glucopyranoside), a capryloyl hexaglucoside formulated as *n*-octanoyl-β-*D*-glucopyranosyl-(6a→1b)-β-*D*-glucopyranosyl-(6b→1c)-β-*D*-glucopyranosyl-(6c→1d)-β-*D*-glucopyranosyl-(6d→1e)-glucopyranosyl-(6e→1f)-glucopyranoside and a menthyl tetraglucoside characterized as menthol-*O*-α-L-glucopyranosyl-(2a→1b)-*O*-α-L-glucopyranosyl-(2b→1c)-*O*-α-L-glucopyranosyl-(2c→1d)-*O*-α-L-glucopyranoside along with three fatty acid esters, *n*-nonacosanyl linolenate, *n*-octacosanyl linolenate and *n*-heptacosanyl linolenate. The structures of the isolated phytoconstituents have been established on the basis of spectral data analysis and chemical means.

Keywords: *Withania coagulans*, Solanaceae, fruits, menthyl tetraglucoside, withacoagulinyl tetraglucoside, capryloyl hexaglucoside

Withania coagulans Dunal (family: Solanaceae), commonly known as cheese maker or vegetable rennet is a rigid, gray-white undershrub, 60–120 cm high, popularly known as Indian rennet. It is distributed from east of the Mediterranean region extending to southern Asia; found in northern India (1), paleotropical regions of Pakistan (2), Afghanistan and Iran (3). The fruits are globose, red or brownish, smooth berries, enclosed in leathery calyx; pulp is brown having nauseous and fruity odor (1). The fruits and leaves of this plant are used as a coagulant. The milk coagulating property of the fruits is attributed to the pulp and husk of the berries, which contain an enzyme called withanin, having milk-coagulating activity (4, 5). The fruits of the plant are sweet, sedative, emetic, alterative and diuretic. A composite Ayurvedic medicine 'Liv 52' is a hepatoprotective herbal preparation and contains extracts from *W. coagulans* and *W. somnifera*. The fruits are used for the treatment of asthma, biliousness, strangury, wounds, dyspepsia, flatulent colic, chronic liver complaints and intestinal infections in the Indian traditional system of medicine (6). In addition, *W. coagulans* is used to cure nervous exhaustion, disability, insomnia, wasting diseases, failure to thrive in children and impotence. In some parts of Pak-Indian sub-continent, the berries are used as a blood purifier. The fruits contain esterases, free amino acids, fatty oil, essential oil, alkaloids (7), withanolide F (8), 17β-hydroxywithanolide K; 14,15β-epoxywithanolide I (9), coagulin A-S and U (10-13), withacoagulin (7, 14), withacoagulin A-I (15, 16), coagulanolide (17) sitosterol-β-*D*-glucoside (18), coagulansins A and B (19) and bispicropodophyllin glucoside (20). This article describes the isolation and characterization of glycosides and fatty acids from the fruits of *W. coagulans* procured from Delhi.

EXPERIMENTAL

General

Melting points were determined on a Perfit apparatus without correction. The IR spectra were measured in KBr pellets on a Bio-Red FT-IR spectrometer. Ultraviolet (UV) spectra were obtained in methanol with a Lambda Bio 20 spectrometer. ^{1}H (400 MHz), ^{13}C (100 MHz), COSY and HMBC

* Corresponding author: e-mail: maliphyto@gmail.com

NMR spectra were recorded on Bruker spectrospin spectrometer. $CDCl_3$, DMSO-d_6 and MeOD (Sigma-Aldrich, Bangalore, India) were used as solvents and TMS as an internal standard. ESI MS analyses were performed on a Waters Q-TOF Premier (Micromass MS Technologies, Manchester, UK) Mass Spectrometer. Column chromatography separations were carried out on silica gel (Merck, 60–120 mesh, Mumbai, India). Precoated silica gel plates (Merck, Silica gel 60 F_{254}) were used for analytical thin layer chromatography visualized by exposure to iodine vapors and UV radiations.

Plant material

The fruits of *W. coagulans* were procured from the local market of Delhi, and identified by Dr. H.B. Singh, Scientist F and Head, Raw Materials Herbarium and Museum, National Institute of Science Communication and Information Resources (NISCAIR), New Delhi. A voucher specimen of drug was deposited in the herbarium of NISCAIR with a reference number NISCAIR/RHMD/Consult/-2010-11/1665/263.

Extraction and isolation

The fruits of *W. coagulans* (500 g) were coarsely powdered and extracted exhaustively with methanol using a Soxhlet apparatus for 18 h. The extract was concentrated under reduced pressure to get dark brown mass (163 g). Small portion of the extract was analyzed chemically to determine the presence of different chemical constituents. The extract (50 g) was suspended in distilled water (250 mL) and partitioned with petroleum ether (250 mL × 5), successively, to give petroleum ether and water soluble fractions. The petroleum ether fraction was subjected to silica gel column chromatography eluting with petroleum ether, petroleum ether-chloroform (1 : 1, v/v) and chloroform to obtained compound **1**, **2** and **3**. The aqueous fraction was dried and dissolved in minimum amount of methanol and adsorbed on silica gel for preparation of slurry. The slurry was dried and subjected to silica gel column loaded in chloroform. The column was eluted with chloroform-methanol (17 : 3, 3:1 and 1:1, v/v) mixtures to obtained compound **4**, **5** and **6**.

***n*-Nonacosanyl linolenate (1)**

Elution of the column of the petroleum ether fraction with petroleum ether gave pale yellow sticky mass of **1**, purified by preparative TLC (petroleum ether), 394 mg (0.788% yield): R_f 0.86 (petroleum ether-chloroform, 1 : 1, v/v); $UV_{\lambda max}$ (MeOH): 213, 274 nm; IR ν_{max} (KBr, cm^{-1}): 2926, 2827, 1721, 1640, 1439, 1345, 1241, 1157, 1071, 1007, 789, 710; ^{1}H NMR ($CDCl_3$, δ, ppm): 5.37 (1H, m, H-10), 5.33 (1H, m, H-12), 5.01 (1H, m, H-13), 4.96 (1H, m, H-15), 4.93 (1H, m, H-16), 4.90 (1H, m, H-9), 3.66 (2H, brs, H-1'), 2.29 (2H, t, J = 7.6 Hz, H-2), 2.07 (2H, m, H-11), 2.04 (2H, m, H_2-14), 2.01 (2H, m, H-8), 1.98 (2H, m, H_2-17), 1.63 (4H, m, 2 × CH_2), 1.58 (4H, m, 2 × CH_2), 1.33 (2H, m, CH_2), 1.30 (6H, m, 3 × CH_2), 1.28 (8H, m, 4 × CH_2), 1.25 (42H, brs, 21 × CH_2), 0.88 (3H, t, J = 6.8 Hz, Me-18), 0.83 (3H, t, J = 7.2 Hz, Me-27'); ^{13}C NMR ($CDCl_3$, δ, ppm): 173.11 (C-1), 139.25 (C-12), 137.36 (C-13), 130.03 (C-15), 128.57 (C-10), 121.28 (C-16), 114.08 (C-9), 63.21 (C-1'), 51.44 (C-11), 34.11 (C-14), 31.95 (C-2), 31.63 (CH_2), 31.44 (CH_2), 30.19 (CH_2), 29.72 (23 × CH_2), 29.54 (CH_2), 29.39 (CH_2), 29.28 (CH_2), 29.18 (CH_2), 28.97 (CH_2), 27.22 (CH_2), 24.96 (CH_2), 22.71 (CH_2), 14.13 (C-18, C-29'); ESI-MS m/z (rel. int.): 684 $[M]^+$ ($C_{47}H_{88}O_2$) (49.9), 407 (4.1), 261 (32.5).

***n*-Octacosanyl linolenate (2)**

Elution of the column with petroleum ether-chloroform (1 : 1, v/v) yielded colorless mass of **2**, recrystallized from acetone-methanol (1 : 1, v/v), 556 mg (1.12% yield); R_f 0.32 (petroleum ether-chloroform, 1 : 1, v/v); m.p. 92–93°C; $UV_{\lambda max}$ (MeOH): 222, 274 nm; IR ν_{max} (KBr, cm^{-1}): 2908, 2841, 1727, 1642, 1449, 1305, 1237, 1158, 720; ^{1}H NMR ($CDCl_3$, δ, ppm): 5.37 (1H, m, H-10), 5.31 (1H, m, H-12), 5.27 (1H, m, H-9), 5.25 (1H, m, H-13), 4.30 (1H, dd, J = 4.4, 7.6 Hz, H_2-1'a), 4.20 (1H, dd, J = 6.0, 4.4 Hz, H_2-1'b), 2.76 (2H, m, H_2-11), 2.30 (2H, t, J = 7.2 Hz, H_2-2), 2.05 (2H, m, H_2-8), 2.01 (2H, m, H_2-14), 1.61 (4H, m, 2 × CH_2), 1.33 (2H, m, CH_2), 1.31 (2H, m, CH_2), 1.29 (34H, brs, 17 × CH_2), 1.27 (26H, brs, 13 × CH_2), 0.87 (3H, t, J = 6.8 Hz, Me-18), 0.84 (3H, t, J = 6.4 Hz, Me-28'); ^{13}C NMR ($CDCl_3$, δ, ppm): 171.64 (C-1), 130.24 (C-10), 130.03 (C-12), 128.06 (C-9), 127.71 (C-13), 66.85 (C-1'), 34.21 (C-11), 34.01 (C-8, C-14), 31.85 (CH_2), 31.55 (CH_2), 29.71 (25 × CH_2), 29.37 (2 × CH_2), 29.14 (CH_2), 27.20 (CH_2), 25.68 (CH_2), 24.88 (CH_2), 24.53 (CH_2), 22.19 (CH_2), 14.09 (C-18, C-28'); ESI-MS m/z (rel. int.): 672 $[M]^+$ ($C_{46}H_{88}O_2$) (3.6), 279 (83.5), 263 (1.5).

***n*-Heptacosanyl linolenate (3)**

Elution of the column with chloroform furnished pale yellow mass of **3**, recrystallized from chloroform-methanol (1 : 1, v/v), 431 mg (0.862% yield); R_f 0.58 (chloroform-methanol, 9.5 : 0.5, v/v); m.p. 115–117°C; $UV_{\lambda max}$ (MeOH): 207, 273 nm; IR ν_{max} (KBr, cm^{-1}): 2905, 2835, 1721, 1645, 1492,

1419, 1242, 923, 721; ^{1}H NMR ($CDCl_3$, δ, ppm): 5.38 (1H, m, H-12), 5.35 (1H, m, H-10), 5.32 (1H, m, H-9), 5.30 (1H, m, H-13), 4.28 (2H, t, *J* = 6.4 Hz, H_2-1'), 2.81 (2H, m, H_2-11), 2.34 (2H, t, *J* = 7.2 Hz, H_2-2), 2.28 (2H, m, H_2-8), 2.01 (2H, m, H-14), 1.64 (2H, m, CH_2), 1.57 (2H, m, CH_2), 1.30 (24H, brs, 12 × CH_2), 1.25 (36H, brs, 18 × CH_2), 0.89 (3H, t, *J* = 6.8 Hz, Me-18), 0.84 (3H, t, *J* = 6.5 Hz, Me-15); ^{13}C NMR ($CDCl_3$, δ, ppm): 167.65 (C-1), 132.39 (C-10), 130.99 (C-12), 128.69 (C-9), 118.41 (C-13), 71.18 (C-1'), 35.61 (C-2), 33.43 (CH_2), 31.38 (CH_2), 29.72 (27 × CH_2), 29.72 (CH_2), 29.56 (CH_2), 29.41 (CH_2), 29.27 (CH_2), 26.13 (CH_2), 21.15 (CH_2), 14.26 (Me-18, Me-15'); ESI-MS *m*/*z* (rel. int.): 658 $[M]^+$ ($C_{45}H_{86}O_2$) (4.8), 279 (100).

Withacoagulinyl tetraglucoside (4)

Elution of column of the water soluble fraction with chloroform-methanol (17 : 3, v/v) gave colorless solid mass of **4**, recrystallized from methanol, 312 mg (0.624% yield); R_f 0.78 (chloroform-methanol-acetic acid, 2 : 9 : 0.02, v/v/v); m.p. 208–209°C; UV λ_{max} (MeOH): 225 nm (log ε 4.7); IR ν_{max} (KBr, cm^{-1}): 3480, 3365, 3260, 2977, 2842, 1722, 1704, 1684, 1382, 1214, 1073; ^{1}H NMR (DMSO-d_6, δ, ppm): 6.77 (1H, m, H-3), 5.73 (1H, d, *J* = 15.6 Hz, H-2), 4.87 (1H, dd, *J* = 13.7, 4.8 Hz, H-22), 4.56 (1H, d, *J* = 7.8 Hz, H-1'), 4.41 (1H, d, *J* = 7.2 Hz, H-1''), 4.29 (1H, d, *J* = 7.1 Hz, H-1'''), 4.27 (1H, d, *J* = 7.2 Hz, H-1''''), 4.10 (1H, m, H-5'), 4.08 (1H, m, H-5''), 4.05 (1H, m, H-5'''), 4.02 (1H, m, H-5''''), 3.87 (1H, dd, *J* = 7.8, 5.2 Hz, H-2'), 3.84 (1H, dd, *J* = 7.2, 6.4 Hz, H-2''), 3.81 (1H, dd, *J* = 8.4, 7.1 Hz, H-2'''), 3.79 (1H, dd, *J* = 7.2, 6.4 Hz, H-2''''), 3.73 (1H, m, H-3'), 3.71 (1H, m, H-3''), 3.67 (1H, m, H-3'''), 3.64 (1H, m, H-3''''), 3.62 (1H, m, H-4'), 3.60 (1H, m, H-4''), 3.57 (1H, m, H-4'''), 3.56 (1H, m, H-4''''), 3.53 (1H, dd, *J* = 4.8, 4.0 Hz, H-6), 3.49 (2H, d, *J* = 9.2 Hz, H-6'), 3.43 (2H, d, *J* = 6.8 Hz, H-6''), 3.39 (2H, d, *J* = 10.8 Hz, H-6'''), 3.19 (2H, d, *J* = 8.2 Hz, H-6''''), 2.94 (1H, d, *J* = 7.0 Hz, H-4a), 2.79 (1H, d, *J* = 13.7 Hz, H-23a), 2.76 (1H, d, *J* = 4.8 Hz, H-4b), 2.75 (3H, brs, $COCH_3$), 2.72 (3H, brs, $COCH_3$), 2.51 (1H, d, *J* = 4.8 Hz, H-23b), 2.41 (1H, m, H-14), 2.14 (1H, m, H-15a), 1.17 (1H, m, H-15b), 2.36 (1H, dd, *J* = 4.8, 8.0 Hz, H-7a), 2.20 (1H, dd, *J* = 4.0, 5.6 Hz, H-7b), 1.97 (1H, m, H-9), 1.97 (3H, brs, CH_3-28), 1.86 (3H, brs, CH_3-27), 1.62 (1H, dd, *J* = 4.0, 7.2 Hz, H-8), 1.73 (1H, m, H-12a), 1.59 (1H, m, H-12b), 1.57 (1H, m, H-11a), 1.53 (1H, m, H-11b), 1.55 (1H, m, H-17), 1.37 (1H, m, H-16a), 1.32 (1H, m, H-16b), 1.40 (3H, brs, H-21), 1.29 (3H, brs, CH_3-19), 1.12 (3H, brs, CH_3-18); ^{13}C NMR (DMSO-d_6, δ, ppm): 203.61 (C-1), 174.22, 172.10, 167.85 (C-26), 152.23 (C-24), 134.99 (C-3), 125.50 (C-2), 120.54 (C-25), 101.78 (C-1'), 101.58 (C-1''), 101.51 (C-1'''), 97.86 (C-1''''), 87.44 (C-5'), 82.65 (C-5''), 81.81 (C-5'''), 81.60 (C-22), 78.51 (C-20), 76.56 (C-5''''), 76.43 (C-2'), 76.12 (C-2''), 75.54 (C-2'''), 75.35 (C-6), 174.22, 172.10, (2 × $\underline{C}OCH_3$), 73.61 (C-2''''), 73.23 (C-5), 72.47 (C-3'), 70.14 (C-3'''), 69.84 (C-3''''), 69.80 (C-4'''), 68.02 (C-4''''), 68.02 (C-4'), 64.51 (C-4''), 63.17 (C-6'), 63.12 (C-6''), 63.01 (C-6'''), 61.32 (C-6'''') 55.76 (C-17), 54.34 (C-10), 52.92 (C-14), 51.86 (C-9), 42.91 (C-13), 37.41 (C-12), 36.12 (C-4), 34.30 (C-8), 31.78 (C-7), 29.12 (C-23), 25.53 (C-16), 24.74 (C-11), 24.70 (C-15), 21.77, 19.69 (2 × CO$\underline{C}H_3$), 19.32 (C-28), 18.19 (C-21), 17.34 (C-19), 16.54 (C-27), 11.08 (C-18); ESI MS *m*/*z* (rel. int.): 1204 $[M]^+$ ($C_{56}H_{84}O_{28}$) (1.6), 507 (22.8), 490 (4.1), 211 (3.3), 169 (5.6), 125 (4.3).

Hydrolysis of **4**: Compound **4** (30 mg) was dissolved in ethanol (5 mL), dil. HCl (2 mL) was added and the reaction mixture was heated on a steam bath for 1 h. The solvent was evaporated under reduced pressure and the residue was dissolved in chloroform to separate aglycone units. The residue was dissolved in water and chromatographed on silica gel TLC plate along with the standard samples of sugars using *n*-butanol-acetic acid-water (4 : 1 : 5, v/v/v) as developing solvent system. The sugar was identified as *D*-glucose, R_f 0.12; $[\alpha]_D^{20}$ +52.7, H_2O.

Capryloyl hexaglucoside (5)

Elution of the column with chloroform-methanol (3 : 1, v/v) afforded colorless crystalline mass of **5**; recrystallized from chloroform-methanol (1 : 1, v/v), 248 mg (0.496% yield); R_f 0.67 (chloroform-methanol, 1 : 9, v/v); m.p. 131–132°C; UV λ_{max} (MeOH): 211 nm (log ε 4.7): IR ν_{max} (KBr, cm^{-1}): 3445, 3328, 3278, 2916, 2838, 1723, 1641,1356, 1226, 1053, 811; ^{1}H NMR (MeOD, δ, ppm): 5.41 (1H, d, *J* = 8.0 Hz, H-1a), 5.16 (1H, d, *J* = 7.5 Hz, H-1b), 5.12 (1H, d, *J* = 7.3 Hz, H-1c), 4.81 (1H, d, *J* = 7.0 Hz, H-1d), 4.52 (1H, d, *J* = 7.5 Hz, H-1e), 4.49 (1H, d, *J* = 8.3 Hz, H-1f), 4.08 (1H, m, H-5d), 4.06 (1H, m, H-5a), 4.04 (1H, m, H-5b), 4.02 (1H, m, H-5c), 3.99 (1H, m, H-5e), 3.89 (1H, m, H-5f), 3.88 (1H, m, H-2b), 3.86 (1H, m, H-2c), 3.85 (1H, m, H-2d), 3.83 (1H, m, H-2e), 3.82 (1H, m, H-2f), 3.76 (1H, m, H-3b), 3.75 (1H, m, H-3c), 3.74 (1H, m, H-3d), 3.71 (1H, m, H-3e), 3.69 (1H, m, H-3f), 3.67 (1H, m, H-4a), 3.66 (1H, m, H-4b), 3.64 (1H, m, H-4c), 3.61 (1H, m, H-4d), 3.55 (1H, m, H-4e), 3.53 (1H, m, H-4f), 3.40 (1H, d, *J* = 7.2 Hz, H-6a), 3.39 (1H, d, *J* = 6.8 Hz, H-6a), 3.33 (1H, d, *J* = 8.0 Hz, H-6b), 3.33 (1H, d, *J* = 8.0 Hz, H-6c), 3.30 (1H, d, *J*

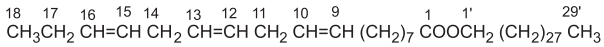

1

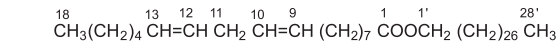

2

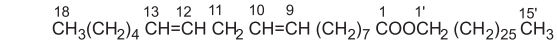

3

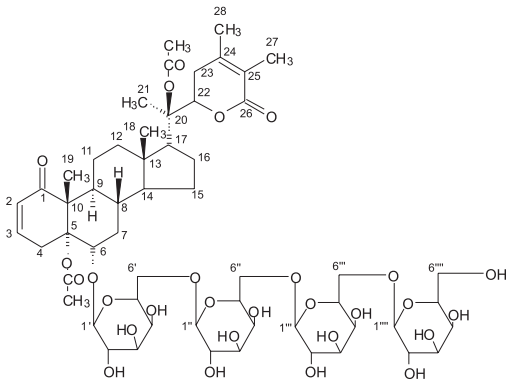

4

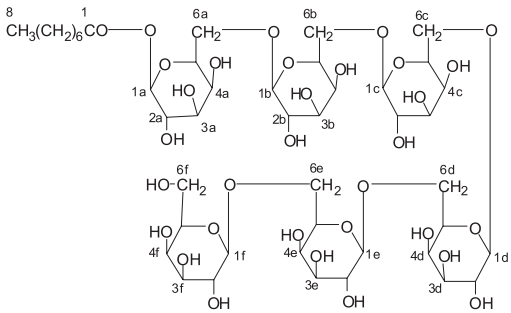

5

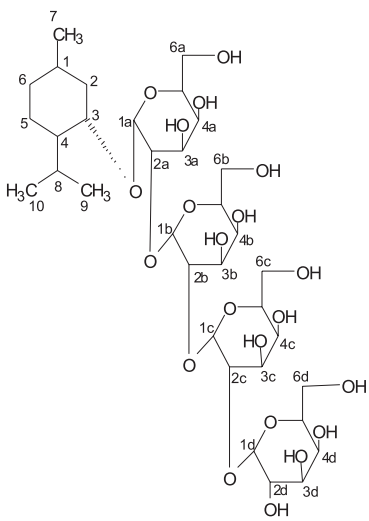

6

Figure 1. Structure of compounds **1**–**6** isolated from the methanolic extract of fruits of *W. coagulans*

= 9.0 Hz, H-6d), 3.32 (1H, d, *J* = 9.2 Hz, H-6e), 3.18 (1H, d, *J* = 6.4 Hz, H-6f), 3.16 (1H, d, *J* = 7.2 Hz, H-6f), 2.83 (2H, t, *J* = 7.2 Hz, H-2), 2.77 (2H, m, H-3), 1.87 (2H, m, H-4), 1.29 (2H, m, H-5), 1.27 (2H, brs, H-6), 1.27 (2H, brs, H-7), 0.85 (3H, t, *J* = 6.3 Hz, H-8); ^{13}C NMR (MeOD, δ, ppm): 172.08 (C-1), 104.51 (C-1a), 103.85 (C-1b), 101.74 (C-1c), 97.92 (C-1d), 96.68 (C-1e),92.50 (C-1f), 82.70 (C-5a), 82.18 (C-5b), 81.75 (C-5c), 81.69 (C-5d), 77.82 (C-5f), 77.39 (C-5e), 76.56 (C-2a), 76.51 (C-2b), 75.72 (C-2c), 75.24 (C-2d), 74.81 (C-2e), 74.26 (C-2f), 73.63 (C-3a), 73.41 (C-3c), 73.32 (C-3b), 73.29 (C-3d), 73.14 (C-3e), 72.92 (C-3f), 72.31 (C-4a), 71.69 (C-4b), 70.38 (C-4c), 70.38 (C-4d), 69.78 (C-4e), 67.22 (C-4f), 64.36 (C-6a), 63.64 (C-6b), 63.15 (C-6c), 62.51 (C-6d), 61.36 (C-6e), 61.19 (C-6f), 51.09 (C-2), 43.12 (C-3), 29.34 (C-4), 29.34 (C-5), 22.36 (C-6), 22.36 (C-7), 13.18 (C-8); ESI MS *m*/*z* (rel. int.) 972 $[M]^+$ ($C_{32}H_{76}O_3$) (1.3), 793 (4.7), 341 (4.3), 179 (4.2), 143 (18.8).

Hydrolysis of **5**: Compound **5** (35 mg) was dissolved in ethanol (5 mL), dil. HCl (2 mL) was added and the reaction mixture was heated on a steam bath for 1 h. The solvent was evaporated under reduced pressure and the residue was dissolved in chloroform to separate caprylic acid as an aglycone unit. The residue was dissolved in water and chromatographed on silica gel TLC plate along with the standard samples of sugars using *n*-butanol-acetic acid-water (4 : 1 : 5, v/v/v) as developing solvent system. The sugar was identified as *D*-glucose, R_f 0.12; $[\alpha]_D^{20}$ +52.7, H_2O.

Menthyl tetraglucoside (6)

Elution of the column with chloroform-methanol (1 : 1, v/v) afforded yellow crystals of **6**, recrystallized from chloroform-methanol (1 :1, v/v), 194 mg (0.38% yield); R_f 0.62 (methanol : water, 9.8 : 0.2, v/v); m.p. 187–188°C; UV λ_{max} (MeOH): 209 nm (log ε 4.3); IR ν_{max} (KBr, cm^{-1}): 3445, 3318, 3255, 2908, 2823, 1610, 1386, 1036 and 917; ^{1}H NMR (DMSO d_6, δ, ppm): 5.16 (1H, d, *J* = 2.8 Hz, H-1a), 4.90 (1H, d, *J* = 3.6 Hz, H-1b), 4.66 (1H, d, *J* = 5.3 Hz, H-1c), 4.27 (1H, d, *J* = 5.9 Hz, H-1d), 3.88 (1H, m, H-5a), 3.76 (1H, m, H-5b), 3.75 (1H, m, H-5c), 3.65 (1H, m, H-5d), 3.57 (1H, m, H-2d), 3.55 (1H, m, H-2c), 3.52 (1H, m, H-2b), 3.51 (1H, m, H-2a), 3.50 (1H, m, H-3a), 3.49 (1H, dd, *J* = 5.2, 3.6, 7.2 Hz, H-3), 3.45 (1H, m, H-3d), 3.45 (1H, m, H-3c), 3.42 (1H, m, H-3b), 3.40 (1H, m, H-4d), 3.37 (1H, m, H-4c), 3.35 (1H, m, H-4b), 3.33 (1H, m, H-4a), 3.19 (1H, d, *J* = 7.1 Hz, H-6a), 3.17 (1H, d, *J* = 8.0 Hz, H-6a), 3.15 (1H, d, *J* = 7.6 Hz, H-6b), 3.11 (1H, d, *J* = 7.6 Hz, H-6b), 3.11 (1H, d, *J* = 7.6 Hz, H-6c), 3.09 (1H, d, *J* = 7.6 Hz, H-6c), 3.06 (1H, d, *J* = 9.2 Hz, H-6d), 3.02 (1H, d, *J* = 6.8 Hz, H-6d), 1.89 (1H, m, H-4), 1.74 (1H, m, H-1), 1.72 (1H, m, H-2), 1.66 (1H, m, H-8), 1.61 (1H, m, H-2), 1.31 (1H, m, H-6), 1.27 (1H, m, H-6), 1.23 (1H, m, H-5), 1.20 (1H, m, H-5), 0.92 (3H, d, *J* = 6.6 Hz, H-10), 0.88 (3H, d, *J* = 6.1 Hz, H-9), 0.83 (3H, d, *J* = 6.5 Hz, H-7); ^{13}C NMR (DMSO d_6, δ, ppm): 104.35 (C-1b), 102.32 (C-1a), 97.15 (C-1c), 92.16 (C-1d), 83.23 (C-2a), 82.81 (C-2b), 82.13 (C-2c), 77.42 (C-5a), 77.02 (C-5b),76.08 (C-5c), 75.61 (C-5d), 75.52 (C-2d), 74.64 (C-3), 73.01 (C-3a), 72.67 (C-3b), 72.28 (C-3c), 72.18 (C-3d), 71.97 (C-4d), 70.63 (C-4c), 70.28 (C-4b), 70.17 (C-4a), 62.54 (C-6d), 62.44 (C-6c), 61.11 (C-6b), 60.84 (C-6a), 55.71 (C-4), 53.71 (C-2), 51.66 (C-1), 45.76 (C-8), 43.41 (C-5), 29.27 (C-6), 24.14 (C-7), 17.67 (C-9), 17.19 (C-10); ESI MS *m*/*z* (rel. Int.) 804 $[M]^+$ ($C_{34}H_{60}O_{21}$) (2.1), 641(5.3), 479(4.6), 179 (18.3).

Hydrolysis of **6:** Compound **6** (25 mg) was dissolved in ethanol (5 mL), dil. HCl (2 mL) was added and the reaction mixture was heated on a steam bath for 1 h. The solvent was evaporated under reduced pressure and the residue was dissolved in chloroform to separate aglycone units. The residue was dissolved in water and chromatographed on silica gel TLC plate along with the standard samples of sugars using *n*-butanol-acetic acid-water (4 : 1 : 5, v/v/v) as developing solvent system. The sugar was identified as L-glucose, R_f 0.12; $[\alpha]_D^{20}$ –51° (H_2O, 10%).

RESULTS AND DISCUSSION

Compounds **1**, **2** and **3** are the fatty esters characterized as *n*-nonacosanyl linolenate, *n*-octacosanyl linolenate and *n*-heptacosanyl linolenate, respectively.

Compound **4**, named withacoagulinyl tetraglucoside, was a colorless solid mass from chloroform-methanol (17 : 3, v/v) and had UV λ_{max} maximum at 225 nm characteristic of summation of absorptions of conjugated enone and the conjugated δ-lactone chromophores, which are commonly present in withanolides. The IR spectrum showed absorption bands for hydroxyl groups (3480, 3365, 3260 cm^{-1}), acetyl function (1722 cm^{-1}), α, β- and δ- lactones (1704 cm^{-1}) and cyclohexanone (1684 cm^{-1}). It gave positive test of glycosides and its molecular ion peak was determined at *m*/*z* 1204 on the basis of mass and ^{13}C NMR spectra consistent with the molecular formula of a diacetoxy withanolide tetraglycoside, $C_{56}H_{84}O_{28}$. The fragment ion peaks at *m*/*z* 125 [C_{20}-C_{22} fission, $C_7H_9O_2]^+$, 211 [C_{17}-C_{20} fission,

$C_{11}H_{15}O_4]^+$ and 169 [211-$COCH_3]^+$ suggested that **4** was a C-20 acetoxy withanolide. Expulsion of the tetraglycoside from the molecular ion peak produced an ion peak at *m*/*z* 507 $[C_{28}H_{43}O_8]^+$ supporting the presence of two acetoxy groups in the withanolide nucleus. The ^{1}H NMR spectrum of **4** showed a one-proton doublet at δ 5.73 ppm (*J* = 15.6 Hz) and a one-proton multiplet at δ 6.77 ppm assigned to vinylic H-2 and H-3 protons, respectively, nearby to the carbonyl function. Five three-proton singlets at δ 1.12, 1.29, 1.40, 1.86 and 1.97 ppm were ascribed to five tertiary methyl protons. The appearance of the C-21 methyl as a singlet in the downfield region (δ 1.40 ppm) suggested the location of the methyl function to tertiary oxygenated carbon C-20. The downfield chemical shift of the C-27 and C-28 methyl singlet (δ 1.86 and 1.97 ppm, respectively) indicated that these methyl functionalities were present on vinylic carbons. A one-proton double doublet at δ 4.87 ppm (*J* = 13.7, 4.8 Hz) was accounted to C-22 methine proton of the lactone moiety. A one-proton double doublet at δ 3.53 with coupling interactions of 4.8 and 4.0 Hz was attributed to β-oriented oxygenated H-6 proton. Four-one proton doublets at δ, ppm 4.56 (*J* = 7.8 Hz), 4.41 (*J* = 7.2 Hz), 4.29 (*J* = 7.1 Hz) and 4.27 (*J* = 7.2 Hz) were associated with the anomeric H-1', H-1'', H-1''' and H-1'''' protons, respectively. The other sugar protons appear between δ 4.10–3.19 ppm. Two acetoxy protons resonated as broad singlets at δ 2.75 and 2.72 ppm. The ^{13}C NMR spectrum of **4** showed 28 carbon signals for withanolide skeleton and 24 signals for glycosidic linkage and signals for two acetoxy carbons consistent with the 5,6,20-trioxygenated withanolide structure. The presence of ^{1}H NMR signals for oxygenated methylene protons as doublet at δ 3.49 (H_2-6'), 3.43 (H_2-6''), 3.39 (H_2-6''') ppm and the corresponding carbon signals in the ^{13}C NMR spectrum in the deshielded region at δ 63.17 (C-6'), 63.12 (C-6'') and 63.01 (C-6''') ppm suggested (1→6) linkage of the sugar units. The ^{1}H–^{1}H COSY spectrum of **4** showed correlations of H-3 with H-2 and H_2-4; H-6 with H_2-7, H-8 and H-1'; H-22 with H_2-23, H_2-6' with H-5' and H-1''; H_2-6'' with H-5'' and H-1''' and H-1'''' with H_2-6''', H-2'''' and H-3''''. The HMBC spectrum exhibited interactions of H-2, H-3 with C-1; $COCH_3$, H_2-22, H-17 with C-20; H-6 and H-2' with C-1'; H_2-6' and H-2'' with C-1'' and H_2-6''' and H-2'''' with C-1''''. In the HSQC spectrum of **4** H-6 at δ 3.53 ppm was coupled with C-6 at δ 75.35 ppm; H-22 at δ 4.87 ppm was coupled with C-22 at δ 81.60 ppm; H-1' at δ 4.56 ppm was coupled with C-1' at 101.78 ppm and H-1'''' at δ 4.27 ppm interacted with C-1'''' at δ 97.86 ppm. The ^{1}H and ^{13}C NMR spectral data of the withanolide unit were compared with the reported data of withanolides (17, 21, 22). Acid hydrolysis of **4** yielded *D*-glucose (co-TLC comparable $[\alpha]_D^{20}$ + 52.7, H_2O). On the basis of these evidences the structure of **4** was elucidated as (20S,22R)-5α,20β-diacetoxy-6α-hydroxy-1-oxowitha-2,24-dienolide-6-β-*D*-glucopyranosyl-(6'→1'')-β-*D*-glucopyranosyl-(6''→1''')-β-*D*-glucopyranosyl-(6'''→1'''')-β-*D*-glucopyranoside. This is new withanolide glucoside.

Compound **5**, named capryloyl hexaglucoside, was obtained as a colorless crystalline mass from chloroform-methanol (3 : 1, v/v) eluants. It gave positive tests for glycosides and had IR absorption bands for hydroxyl groups (3445, 3328, 3278 cm^{-1}) and ester function (1723 cm^{-1}). Its molecular ion peak was established at *m*/*z* 972 on the basis of mass and ^{13}C NMR spectra consistent with the molecular formula of a fatty acid hexaglycoside $C_{32}H_{76}O_3$. The ion peak arising at *m*/*z* 143 $[CH_3(CH_2)_6CO]^+$ suggested the presence of an octadecanoyl group as an aglycone. The ion generating at *m*/*z* 179 $[C_6H_{11}O_6]^+$, 341 $[C_6H_{11}O_6$-$C_6H_9O_5]^+$ and 793 $[M-179]^+$ suggested the presence of hexose units in the terminal site of the sugar chain. The ^{1}H NMR spectrum of **5** showed a three-proton triplet at δ 0.85 ppm (*J* = 6.3 Hz) assigned to primary C-8 methyl protons. The methylene proton appeared from δ 2.83 to 1.27 ppm. Six one-proton doublets at δ ppm 5.41 (*J* = 8.0 Hz), 5.16 (*J* = 7.5 Hz), 5.12 (*J* = 7.3 Hz), 4.81 (*J* = 7.0 Hz), 4.52 (*J* = 7.5 Hz) and 4.49 (*J* = 8.3 Hz) were ascribed to anomeric C-1a to C-1f protons, respectively. The other sugar protons appeared from δ 4.06 to 3.16 ppm. The ^{13}C NMR spectrum of **5** displayed signals for ester carbon at δ 172.08 ppm (C-1), methyl carbon at δ 13.18 ppm (C-8), anomeric carbons from δ 104.51 to 92.50 ppm and other sugar carbons between δ 82.70–61.19 ppm. The presence of ^{1}H NMR signals of the oxygenated methylene protons in the deshielded region from δ 3.40 to 3.30 ppm and the corresponding carbon signals at δ ppm 64.36 (C-6a), 63.64 (C-6b), 63.15 (C-6c), 62.51 (C-6d) and 61.36 (C-6e) suggested (1→6) linkage of the sugar units. The absence of any proton signal beyond δ 5.41 ppm and carbon signal in the downfield region after δ 104.51 ppm suggested saturated nature of the molecule. The ^{1}H–^{1}H COSY spectrum of **5** showed correlations of Me-8 with H_2-6; H-1a with H-2a and H-5a; H-1b with H_2-6a and H-2b; H-1e with H_2-6d and H-2e; and H-1f with H_2-6e and H-2f. The HMBC spectrum of **5** exhibited interactions of H_2-2 and H-1a with C-1; H_2-6a, H-2b and H-3b with C-1b; H_2-6b and H-2c with C-1c; H-1e, H-4d

and H-5d with C-6d; and H-1f, H-4e and H-5e with C-6f. Acid hydrolysis of **5** yielded caprylic acid and *D*-glucose, co-TLC comparable. On the basis of these observations the structure of **5** has been characterized as *n*-octanoyl-β-*D*-glucopyranosyl-(6a→1b)-β-*D*-glucopyranosyl-(6b→1c)-β-*D*-glucopyranosyl-(6c→1d)-β-*D*-glucopyranosyl-(6d→1e)-glucopyranosyl-(6e→1f)-glucopyranoside. The is a new acyl glucoside.

Compound **6**, named menthyl tetraglucoside, was obtained as yellow crystalline mass from chloroform-methanol (1 : 1, v/v) eluants. It gave positive test for glycosides and showed IR absorption bands for hydroxyl groups (3445, 3318, 3255 cm^{-1}). On the basis of mass and ^{13}C NMR spectra, its molecular ion peak was determined at *m*/*z* 804 consistent with the molecular formula of a monoterpenic tetraglycoside $C_{34}H_{60}O_{21}$. The ion peaks generated at *m*/*z* 179 $[C_6H_{11}O_6]^+$, 641 $[M\text{-}C_6H_{11}O_5]^+$ and 479 $[M\text{-}C_6H_{11}O_5\text{-}C_6H_{11}O_5]^+$ indicated that hexose units were present in the sugar chain. The ^1H NMR spectrum of **6** exhibited four one-proton doublets at δ ppm 5.16 (*J* = 2.8 Hz), 4.90 (*J* = 3.6 Hz), 4.66 (*J* = 5.3 Hz) and 4.27 (*J* = 5.9 Hz) assigned to anomeric H-1a, H-1b, H-1c and H-1d, respectively, and their low coupling interactions suggested α-orientation of the sugars units. The other sugar protons appeared from δ 3.88 to 3.02 ppm. A one-proton triplet at δ 3.49 ppm (*J* = 5.2, 3.6, 7.2 Hz) was ascribed to β-oriented oxygenated methine H-3 proton. Three doublets at δ ppm 0.83 (*J* = 6.5 Hz), 0.88 (*J* = 6.1 Hz) and 0.92 (*J* = 6.6 Hz) integrating for three protons each were attributed to secondary C-7, C-9 and C-10 methyl protons of menthol-type molecule. The other methine and methylene protons resonated from δ 1.89 to 1.20 ppm. The ^{13}C NMR spectrum of **6** displayed signals for anomeric carbons at δ ppm 102.32 (C-1α) and 104.35 (C-1b), 97.15 (C-1c) and 92.16 (C-1d) and methyl carbons at δ ppm 24.14 (C-7), 17.67 (C-9) and 17.19 (C-10). The absence of ^1H NMR signal beyond δ 5.16 ppm and ^{13}C NMR signal after δ 104.35 ppm supported saturated nature of the compound. The presence of H-2a, H-2b, H-3c and H-3d in δ 3.57–3.51 ppm in the deshielded region and the respective carbon signals in the range of δ 83.23–82.13 ppm indicated (1→2) attachment of the sugar units. The ^1H–^1H COSY spectrum of **6** showed correlations of H-3 with H_2-2, H-4 and H-1a; H-1b with H-2a and H-2b; H-1c with H-2b, H-2c and H-3c; and H-1d with H-2c and H-2d. The HMBC spectrum of **6**, exhibited interactions of H-3 and H-1b with C-1a; H-2a and H-2b with C-1b; H-2b and H-2c with C-1c; and H-2c and H-2d with C-1d. The acid hydrolysis of **6** yielded α-menthol and α-glucose, co-TLC comparable, $[\alpha]_D^{20}$ –51° (H_2O, 10%). On the basis of these evidences the structure of **6** has been elucidated as menthol-*O*-α-L-glucopyranosyl-(2a→1b)-*O*-α-L-glucopyranosyl-(2b→1c)-*O*-α-L-glucopyranosyl-(2c→1d)-*O*-α-L-glucopyranoside. This is new menthol tetraglucoside.

CONCLUSION

The present work characterized fatty esters and glucosides of withanolide, fatty acid and menthol from the fruits of *Withania coagulans* Dunal. The existing knowledge regarding its phytoconstituents may be increased by the present phytochemical investigation, which may be responsible for medicinal property of the plant and may be used as chromatographic marker of the drug and for quality control of the drug.

Acknowledgments

The authors would like to express their gratitude to Jamia Hamdard, New Delhi for providing infrastructures and other facilities. The author (Abuzer Ali) is thankful to Department of Science and Technology, New Delhi for financial assistance.

REFERENCES

1. Anonymous: The Wealth of India: A Dictionary of Indian Raw Materials and Industrial Products (Sp-W). CSIR, New Delhi 2005.
2. Ali N., Ahmad B., Bashir S., Shah J., Azam S., Ahmad M.: Afr. J. Pharm. Pharmacol. 3, 439 (2009).
3. Hoda. Q, Ahmad S., Akhtar M., Najmi A.K., Pillai K.K., Ahmad S.J.: Hum. Exp. Toxicol. 29, 653 (2010).
4. Jaiswal D., Rai P.K., Watal G.: Indian J. Clin. Biochem. 24, 88 (2009).
5. Hemalatha S., Kumar R., Kumar M.: Pharmacog. Rev. 2, 351 (2008).
6. Kirtikar K.R., Basu B.D.: Indian Medicinal Plants, p. 1777, International Book Distributors, Dehradun, India 1999.
7. Rahman A.U., Shahwar D.E., Naz A., Choudhary M.I.: Phytochemistry 63, 387 (2003).
8. Glotter E., Abraham A., Gunzberg G., Kirson I.: J. Chem. Soc. Perkin Trans. 1, 341 (1977).
9. Choudhary M.I., Shahwar D.E., Zeba P., Jabbar A., Ali I., Rahman A.U.: Phytochemistry 40, 1243 (1995).

10. Khodaei M., Jafari M., Noori M.: Adv. Life Sci. 2, 6 (2012).
11. Rahman A.U., Choudhary M.I., Qureshi S., Gul W., Yousaf M.: J. Nat. Prod. 61, 812 (1998).
12. Rahman A.U., Shabbir M., Yousaf M., Qureshi S., Shahwar D.E., Naz A., Choudhary M.I.: Phytochemistry 52, 1361 (1999).
13. Rahman A.U., Choudhary M.I., Yousaf M., Gul W., Qureshi S.: Chem. Pharm. 46, 1853 (1998).
14. Singh A., Duggal S., Singh H., Singh J., Katekhaye S.: Int. J. Green Pharm. 229 (2010).
15. Haq I.U., Youn U.J., Chai X., Park E.J., Kondratyuk T.P., Simmons C.J., Borris R.P., Mirza B., Pezzuto J.M., Chang L.C.: J. Nat. Prod. 76, 22 (2013).
16. Huang C.F., Ma L., Sun L.J., Ali M., Arfan M., Liu J.W., Hu L.H.: Chem. Biodiver. 6, 1415 (2009).
17. Maurya R., Akansha, Jayendra, Singh, A.B., Shrivastava, A.K.: Bioorg. Med. Chem. Lett. 18, 6534 (2008).
18. Ramaiah P.A.: Phytochemistry 23, 143 (1984).
19. Jahan E., Perveen S., Fatima I., Malik A.: Helv. Chim. Acta 93, 530 (2010).
20. Alam M.N., Yousaf M., Qureshi S., Baig I., Nasim S., Rahman A.U., Choudhary M.I.: Helv. Chim. Acta 86, 607 (2003).
21. Zhao J., Nakamura N., Hattori M., Kuboyama T., Tohda C., Komatsu K.: Chem. Pharm. Bull. 50, 760 (2002).
22. Lal P., Misra L., Sangwan R.S., Tulib R.: Z. Naturforsch. 61b, 1143 (2006).

Received: 30. 07. 2013

Acta Poloniae Pharmaceutica – Drug Research, Vol. 71 No. 3 pp. 431–438, 2014 ISSN 0001-6837
Polish Pharmaceutical Society

PHARMACEUTICAL TECHNOLOGY

STABILITY OF [(*N*-PIPERIDINE)METHYLENE]DAUNORUBICIN HYDROCHLORIDE AND [(*N*-PYRROLIDINE)METHYLENE]DAUNORUBICIN HYDROCHLORIDE IN SOLID STATE

BEATA MEDENECKA[1], PRZEMYSŁAW ZALEWSKI[1]*, WITOLD KYCLER[2]
MIKOŁAJ PIEKARSKI[1], WERONIKA LEMIECH[1], IRENA OSZCZAPOWICZ[3]
and ANNA JELIŃSKA[1]

[1]Department of Pharmaceutical Chemistry, Faculty of Pharmacy, Poznań University of Medical Sciences,
6 Grunwaldzka St., 60-780 Poznań, Poland
[2]Department of Oncological Surgery II, Great Poland Cancer Centre,
15 Garbary St., 61-688 Poznań, Poland.
[3]Department of Modified Antibiotics, Institute of Biotechnology and Antibiotics,
5 Starościńska St., 02-515 Warszawa, Poland

Abstract: The influence of temperature and relative air humidity on the stability of two novel derivatives of daunorubicin: [(*N*-piperidine)methylene]daunorubicin hydrochloride and [(*N*-pyrrolidine)methylene]daunorubicin hydrochloride was investigated. The process of degradation was studied by using high-performance liquid chromatography with ultraviolet (UV) detection. The kinetic and thermodynamic parameters of degradation were calculated.

Keywords: [(*N*-piperidine)methylene]daunorubicin hydrochloride, [(*N*-pyrrolidine)methylene]daunorubicin hydrochloride, stability in solid state, kinetic and thermodynamic parameters

Anthracycline antibiotics are compounds of a glycoside structure, containing sugar and aglycone moieties (Fig. 1). The sugar is usually daunozamine, an aminosugar of the hexoses group. The aglycone moiety consists of four six-carbon rings, where rings B and D are aromatic and ring C is quinone. Ring A contains a small substituent with the carbonyl group. Anthracyclines are a group of anticancer drugs with an established position in the treatment of malignant neoplasms. The mechanism of action of these antibiotics involves:

- direct intercalation of DNA, resulting in the biosynthesis of macromolecular stoppage,
- induction of oxidative stress inside cells by generating free radicals,
- combining with DNA and its alkylation,
- cross-linking of DNA strands,
- interrupting the DNA-helicase activity,
- direct impact on cell membranes and interruption of their activity,
- induction of DNA damage and apoptosis with topoisomerase II activity stoppage.

Each of these processes is closely connected with the structure of anthracyclines. The compact inner arrangement of the aglycone rings is reflected by their flat spatial structure. That is especially typical of rings B, C and D. This is crucially important for the intercalation of DNA by anthracyclines. The flat structure of the rings allows them to penetrate between the two DNA strands and react with the bases. Anthracyclines mainly react with cytosine and guanine. The remaining parts of the anthracycline molecule, the sugar and the cyclohexane ring A, do not penetrate the DNA strands but stay on the outside of the double helix. Their role is to stabilize the newly created DNA-anthracycline complex. That happens thanks to the electrostatic interaction between the antibiotic molecule and the outside parts of the nucleotides or through cross-linking between the sugar moiety and the nucleotides. According to the latest research, it is the part of the anthracycline molecule, which does not penetrate DNA, that has the most significant role in DNA intercalation.

* Corresponding author: e-mail: pzalewski@ump.edu.pl

The main disadvantage of anthracyclines is their general toxicity, especially cardiotoxicity. Therefore, while looking for new derivatives, it is important to maintain the antitumor activity of the base drug and to ensure lower general toxicity. The complex structure of anthracyclines allows many modifications, such as the introduction of a new substituent, the modification of the existing ones or the development of selective stereoisomers of given compounds. Notably, chemical modifications can include both the aglycone and the sugar moiety. Many novel anthracycline derivatives modified in the sugar moiety have been synthesized. It was proven that a group of 3'-formamide-substituted daunorubicin derivatives show a much lower tendency to produce free radicals. Consequently, their similar antitumor activity to that of daunorubicin is combined with lower toxicity to the healthy cells of the body (1–3).

[(*N*-piperidine)methylene]daunorubicin hydrochloride (PIP) and [(*N*-pyrrolidine)-methylene]daunorubicin hydrochloride (PYR) were obtained by the replacement of the primary amino group at C-3' of the daunosamine moiety in daunorubicin hydrochloride by an amidine substituent containing a piperidine ring or a pyrrolidine ring, respectively (Fig. 1) (3).

Previous studies proved that daunorubicin hydrochloride and its new derivatives are vulnerable to degradation in the solid state (4, 5) in aqueous (6–9) and in intravenous (10) solutions.

In the solid state, the degradation of daunorubicin hydrochloride (DAU) and its amidine derivative [(N-morpholine)metylene]daunorubicin hydrochloride (MOR) (Fig. 1) at an increased temperature and relative air humidity (RH > 50%) was a first-order autocatalytic reaction relative to DAU or MOR concentration (4, 5).

In aqueous solutions, in the pH range 0.45–13.08, the degradation of daunorubicin hydrochloride and its derivatives is a pseudo-first order reaction (6–9). For the daunorubicin hydrochloride amidine derivatives the reactions of protonated molecules catalyzed by hydrogen ions occurred at a similar rate but significant differences in the degradation rate were observed in spontaneous hydrolysis under the influence of water. In the pH range from 0.5 to 13.1, daunorubicin hydrochloride was more stable than its amidine derivatives and demonstrated the greatest stability in the pH range from 4 to 6. Its amidine derivatives are the most stable at pH ≈ 3. At pH < 4 DAU degraded to aglycone daunorubicinone and amino sugar daunosamine. Under more stressful conditions and in an alkali environment aglycone is degraded to more simple structures (11).

The photodegradation of the daunorubicin hydrochloride derivatives and epirubicin in solution is a pseudo-first-order reaction, which depends on substrate concentration (9, 12). The products of photodegradation at a wavelength of 365 nm were red and colorless at 510 nm.

All of the previous studies demonstrated that the differences in the chemical structures of the daunorubicin hydrochloride derivatives did not influence their stability or the kinetic mechanism of their degradation.

The aim of this study was to determine the effect of temperature at RH ≈ 76.4% on [(*N*-piperidine)methylene]daunorubicin hydrochloride (PIP) and [(*N*-pyrrolidine)methylene]-daunorubicin hydrochloride (PYR) and to evaluate their stability at 373 K in dry air (0% RH).

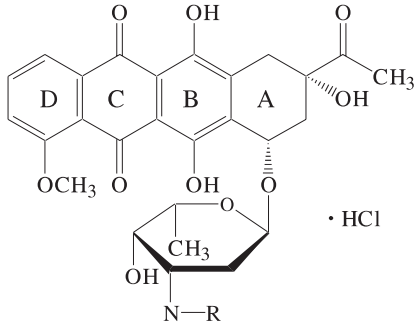

Derivative	R
DAU	H_2
PYR	=CH–N
PIP	=CH–N
MOR	=CH–N O

Figure 1. The chemical structure of daunorubicin hydrochloride (DAU), [(*N*-pyrrolidine)methylene]daunorubicin hydrochloride (PYR), [(*N*-piperidine)methylene]daunorubicin hydrochloride (PIP) and [(*N*-morpholine)methylene]daunorubicin hydrochloride (MOR)

EXPERIMENTAL

Chemicals, reagents and solutions

[(*N*-piperidine)methylene]daunorubicin hydrochloride (PIP) and [(*N*-pyrrolidine)methylene]daunorubicin hydrochloride (PYR) were obtained from the Institute of Biotechnology and Antibiotics in Warszawa. Quinidine hydrochloride was used as an internal standard. All other chemical substances and solvents were the products of Sigma and were of analytical or high-performance liquid chromatographic grade. High-quality pure water was prepared by using a Millipore purification system (Exil SA 67120, Millipore, Molsheim, France).

Instrumentation

The chromatographic apparatus consisted of an LC-61 isocratic pump, an SPD-6AV UV-Vis detector set at 254 nm (Shimadzu) and Rheodyne Berkeley 7120 injector with a 25 µL loop. Separations were performed on a LiChrospher 100-RP 18 column (250 × 4 mm; 5 µm particle size; Merck).

Chromatographic conditions

Chromatographic separations and quantitative analysis were performed by using an HPLC method (13, 14).

The mobile phase consisted of a mixture of acetonitrile and water (50 : 50, v/v) with the addition of 2.88 g/L sodium lauryl sulfate and 1.4 mL/L phosphoric acid (V) (1.42 g/mL). The flow rate was 1.5 mL/min. The internal standard was a solution of quinidine hydrochloride (0.100 g/mL). All chromatographic procedures were conducted at ambient temperature.

Conditions of kinetic studies

For the experiments, 0.005 g samples of PIP and PYR were weighed into 5 mL vials. The samples of the substances tested for the influence of temperature in a humid environment were inserted in desiccators containing saturated solutions of sodium chloride (≈ 76.4% RH). These samples were placed in heat chambers set to the desired temperatures: 343, 353, 363 and 373 K.

To evaluate the stability of PIP and PYR in dry air, the vials containing 0.005 g of these substances were immersed in sand bath placed in the heat chambers at 373 K.

Each batch to be studied comprised 10–15 samples. At specific time intervals, determined by the rate of degradation, the vials were removed, cooled to room temperature and the contents dissolved in a mixture of acetonitrile and water (1 : 1 v/v). The resultant solutions were quantitatively transferred into volumetric flasks and completed to a total volume of 10.0 mL with the same mixture of solvents. To 1.0 mL of the resultant solution (after filtration) 1.0 mL of the internal standard solution was added. Samples (25 µL) were injected onto the column.

Calculations

The rates constant of a first-order reaction were calculated from:

$$\ln c = \ln c_0 - k_{obs} \times t \qquad \text{(equation 1)}$$

where c_0 and c are concentrations at time t = 0 and t, respectively, and k_{obs} is the observed rate constant of degradation, while the rates constant of a first-order autocatalytic reaction relative to the substrate concentration were calculated from:

$$\ln c_t/(c_0 - c_t) = -k_{obs} \times t + g \qquad \text{(equation 2)}$$

where c_0 and c_t are substrate concentrations at t_0 and t; $c_0 - c_t$ are product concentrations at time t; g is a constant related to the induction time and k_{obs} is the observed rate constant of degradation (15).

Thermodynamic parameters (E_a, activation energy; $\Delta H^{\neq}$, enthalpy; $\Delta S^{\neq}$, entropy) were calculated from:

$$E_a = -a \times R \qquad \text{(equation 3)}$$

$$\Delta H^{\neq} = E_a - T \times R \qquad \text{(equation 4)}$$

$$\Delta S^{\neq} = R \times (\ln A - \ln (k_B \times T/h)) \qquad \text{(equation 5)}$$

where: k_B = Boltzmann's constant (1.3807×10^{-23} J × K^{-1}); h = Planck's constant (6.626×10^{-34} J × s); R = universal gas constant (8.314 $K^{-1} \times mol^{-1}$), T = temperature [K]; a = slope of the Arrhenius relationship; A = frequency coefficient where: (ln A = b) (15).

Statistical parameters of the respective equations were calculated using Microsoft Excel 2010.

RESULTS AND DISCUSSION

Kinetics of degradation of PIP and PYR

The degradation of PIP at an increased temperature and ≈ 76% RH was a first-order reaction relative to the substrate concentration (Fig. 2) and the rate constants were calculated from equation 1.

The degradation of PYR in the same environment was a first-order autocatalytic reaction relative to the substrate concentration (Fig. 3) and the rate constants of this reaction were calculated from equation 2.

The semilogarithmic plots $c_t/(c_0 - c_t) = f(t)$ were straight lines and their slopes corresponded to the rate constants of the reaction ($-k_{obs}$).

The degradation of PIP at an increased temperature and 0% RH was a first-order autocatalytic

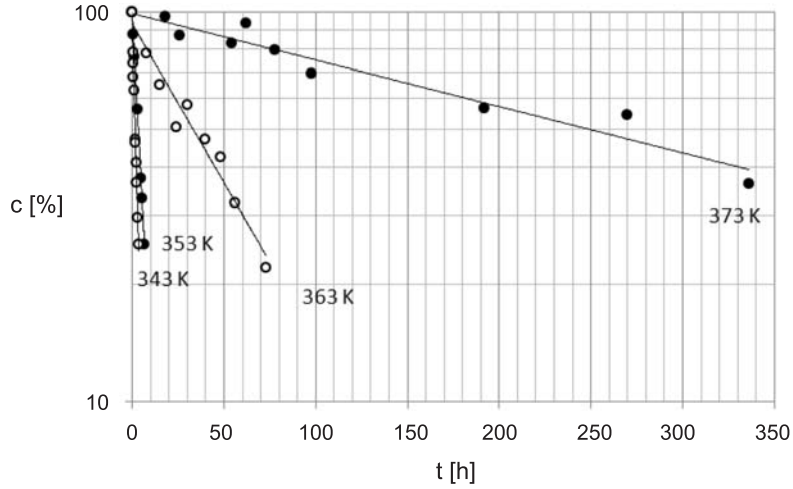

Figure 2. Semilogarithmic plots of ln c[%] = f(t) for the degradation of [(*N*-piperidine)methylene]daunorubicin hydrochloride (PIP) at RH ≈76.4%

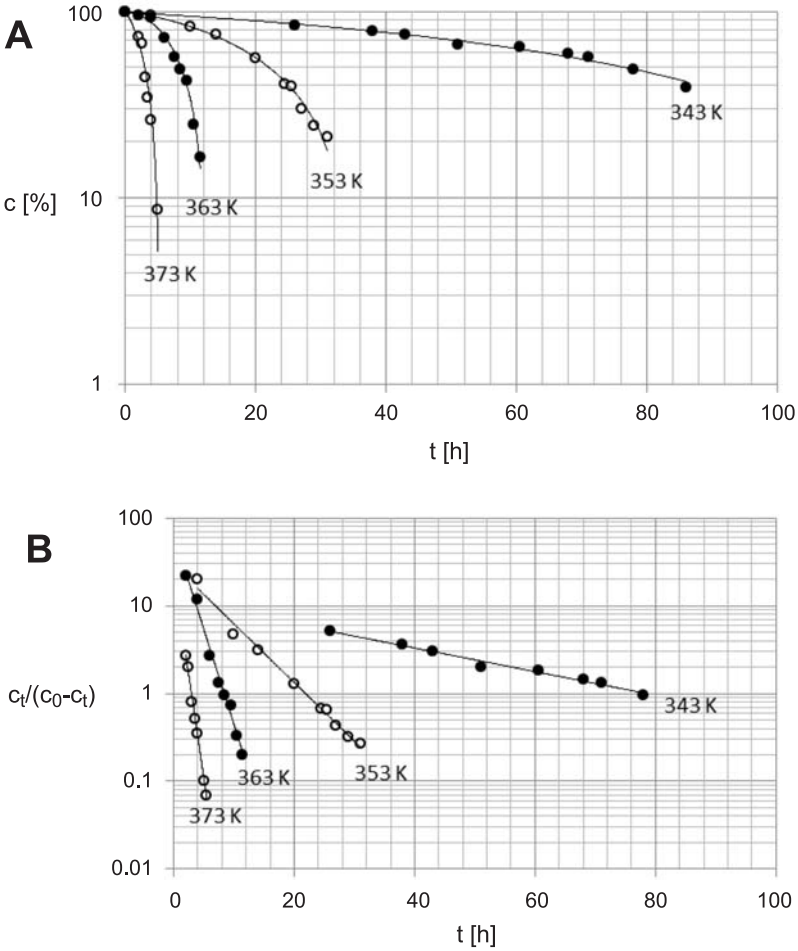

Figure 3. Semilogarithmic plots of ln c[%] = f(t) (**A**) and ln $c_t/(c_0 - c_t)$ = f(t) (**B**) for the degradation of [(*N*-pyrrolidine)methylene]daunorubicin hydrochloride (PYR) at RH ≈76.4%

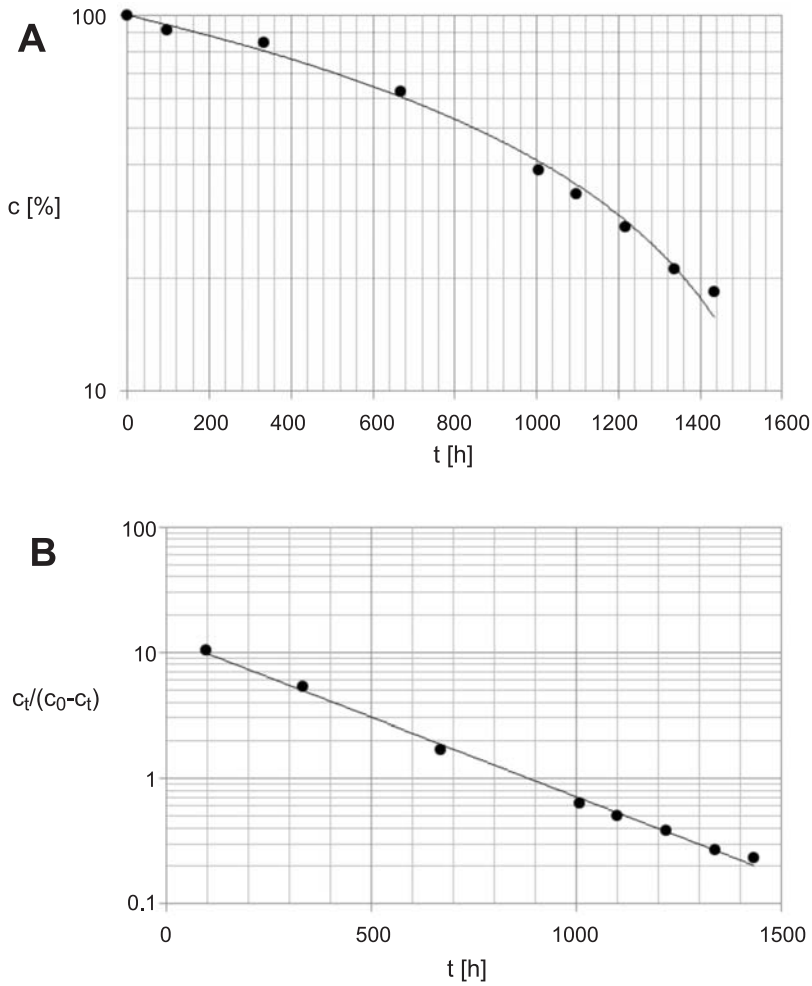

Figure 4. Semilogarithmic plots of ln c[%] = f(t) (**A**) and ln $c_t/(c_0 - c_t)$ = f(t) (**B**) for the degradation of [(*N*-piperidine)methylene]daunorubicin hydrochloride (PIP) at 373 K and RH = 0%

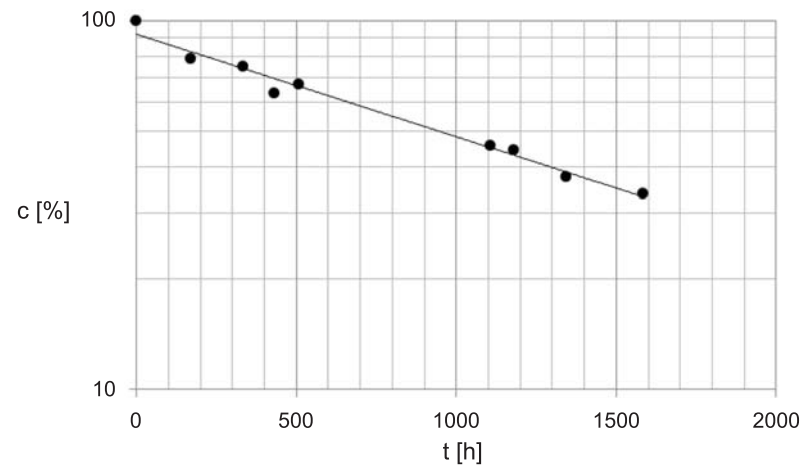

Figure 5. Semilogarithmic plot of ln c[%] = f(t) for the degradation of [(*N*-pyrrolidine)methylene]daunorubicin hydrochloride (PYR) at 373 K and RH = 0%

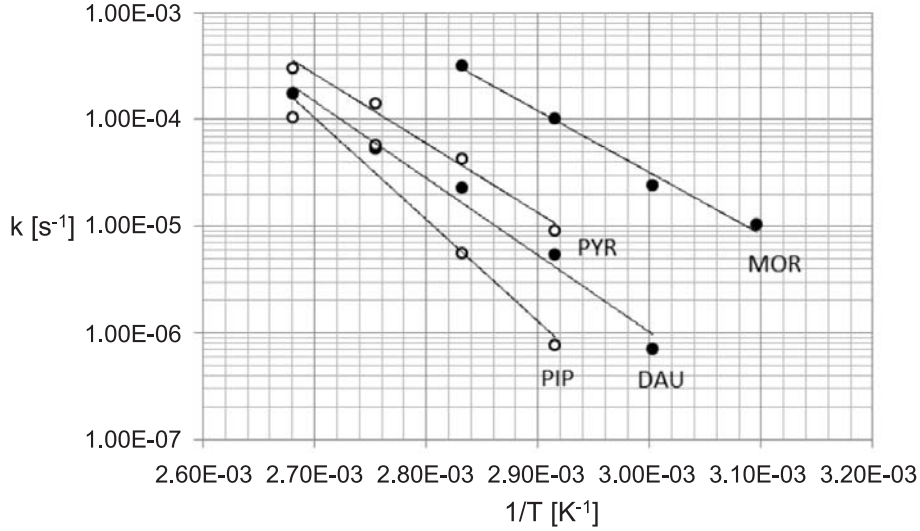

Figure 6. Semilogarithmic plot of ln k[s^{-1}] = f(1/T) [K^{-1}] for the degradation of daunorubicin hydrochloride (DAU) and its amidine derivatives [(*N*-pyrrolidine)methylene]daunorubicin hydrochloride (PYR) [(N-piperidine)methylene]daunorubicin hydrochloride (PIP) and [(N-morpholine)methylene]daunorubicin hydrochloride (MOR) at RH ≈ 76.4%

Table 1. Kinetic and thermodynamic parameters of the degradation of daunorubicin hydrochloride (DAU) and its amidine derivatives [(*N*-pyrrolidine)methylene]daunorubicin hydrochloride (PYR) [(N-piperidine)methylene]daunorubicin hydrochloride (PIP) and [(N-morpholine)methylene]daunorubicin hydrochloride (MOR) in solid state at constant relative air humidity (RH = 76.4%).

T [K]	$(k_i \pm \Delta k) \times 10^5$ (s^{-1})	Statistical evaluation of ln $k_i = f(T^{-1})$	Thermodynamic parameters
[(*N*-piperidine)methylene]daunorubicin hydrochloride (PIP)			
343	0.0762 ± 0.015	a = -21950 ± 13232 S_a = 3075 b = 50.1 ± 37.0 S_b = 8.60 r = - 0.981	E_a = 182.5 ± 110.0 [kJ mol^{-1}] $\Delta H^{\neq}$ = 180.0 ± 110.0 [kJ mol^{-1}]* $\Delta S^{\neq}$ = 171.5 ± 62.8 [JK^{-1} mol^{-1}]*
353	0.564 ± 0.062		
363	5.68 ± 0.51		
373	10.4 ± 0.9		
[(*N*-pyrrolidine)methylene]daunorubicin hydrochloride (PYR)			
343	0.910 ± 0.113	a = -14647 ± 4145 S_a = 963.5 b = 31.3 ± 11.6 S_b = 2.69 r = - 0.996	E_a = 121.8 ± 34.5 [kJ mol^{-1}] $\Delta H^{\neq}$ = 119.3 ± 34.5 [kJ mol^{-1}]* $\Delta S^{\neq}$ = 15.3 ± 148.5 [JK^{-1} mol^{-1})]*
353	4.27 ± 0.39		
363	13.9 ± 1.5		
373	29.9 ± 3.1		
[(*N*-morpholine)methylene]daunorubicin hydrochloride (MOR) (10)			
323	1.03 ± 0.23	*a* = -13316 ± 4639 S_a = 1078 *b* = 29.6 ± 13.7 S_b = 3.19 r = 0.9935	E_a = 110 ± 39 [kJ mol^{-1}] $\Delta H^{\neq}$ = 108 ± 39 [kJ mol^{-1}]* $\Delta S^{\neq}$ = 1 ± 130 [JK^{-1} mol^{-1}]*
333	2.37 ± 0.25		
343	10.1 ± 0.7		
363	31.6 ± 0.9		
Daunorubicin hydrochloride (DAU) (4)			
333	0.071 ± 0.008	*a* = -16581 ± 3972 S_a = 1248 *b* = 35.94 ± 11.3 S_b = 3.5 r = 0.9916	E_a = 138 ± 33 [kJ mol^{-1}] $\Delta H^{\neq}$ = 135 ± 33 [kJ mol^{-1}]* $\Delta S^{\neq}$ = -149 ± 203 [JK^{-1} mol^{-1}]*
343	0.53 ± 0.07		
353	2.26 ± 0.38		
363	5.25 ± 1.95		
373	17.5 ± 0.2		

E_a = activation energy; $\Delta H^{\neq}$ = enthalpy; $\Delta S^{\neq}$ = entropy were calculated from equations 3, 4 and 5, respectively. * calculated for 298 K.

reaction relative to the substrate concentration (Fig. 4), whereas the degradation of PYR in dry air was a first-order reaction relative to the substrate concentration (Fig. 5).

For the interpretation of the straight line plots $\ln c_t/(c_0 - c_t) = f(t)$ and $\ln c_t = f(t)$ such statistical parameters as slope (a), error range of slope (Δa) , intercept (b), error range of intercept (Δb), standard deviations s_a, s_b, s_y and the coefficient of linear correlation (r) were calculated by using the least squares method. The values of Δa and Δb were obtained for f = n – 2 degrees of freedom, with $\alpha = 0.05$. Statistical parameters of the respective equations were calculated using Microsoft Excel 2010.

The values of reaction rate constants k_{obs} were used to calculate the Arrhenius relationship in order to interpret the influence of the temperature on the reaction rate at ≈ 76.4% RH. The energy, enthalpy and entropy of activation for 298 K were calculated based on the parameters of the slope $\ln k_i = f(T^{-1})$ (Table 1). The influence of temperature on the stability of PIP and PYR was described as:

$$\ln k_{PIP} = (2.19 \pm 1.32)10^4 T^{-1} - (50.12 \pm 37.03)$$

$$\ln k_{PYR} = (1.47 \pm 0.41)10^4 T^{-1} - (31.32 \pm 11.63)$$

The slope *a* expresses the effect of temperature on the stability of PIP and PYR in the solid state (Table 1). After comparing the plots $\ln k = f(1/T)$ a parallelism test proved that the influence of temperature on the rates degradation of PIP, PIR, MOR (5) and DAU (4) did not show any statistically significant differences. Because the kinetic mechanisms of degradation of DAU and its derivatives differed, the values $t_{0.5}$ were used to compare their stability, which could be ordered as follows: DAU > PIP > PIR > MOR.

Although the energy of activation of PIP, PYR, DAU and MOR obtained at an increased temperature did not show statistically significant differences, the stability of daunorubicin hydrochloride and its three derivatives were compared as follows: PIP > DAU > PYR > MOR.

The rate constants of PIP and PYR degradation at 373 K and 76.4% RH were $(1.04 \pm 0.09)10^{-4}$ s^{-1} and $(2.99 \pm 0.31)10^{-4}$ s^{-1}, respectively, while at 373 K and 0% RH they were $(8.08 \pm 0.48)10^{-7}$ s^{-1} and $(1.78 \pm 0.21)10^{-7}$ s^{-1}, respectively, which demonstrated that increased relative air humidity determined their degradation.

CONCLUSIONS

The degradation of PIP was a first-order reaction relative to the substrate concentration at an increased temperature and relative air humidity, whereas at an increased temperature and 0% RH it was a first-order autocatalytic reaction relative to the substrate concentration. The degradation of PYR, DAU and MOR was a first-order autocatalytic reaction relative to the substrate concentration at increased temperature and ≈76.4% RH and it was a first-order reaction relative to the substrate concentration in dry air.

The study demonstrated that the kinetic mechanism of the degradation of the derivatives of daunorubicin hydrochloride depends on storage conditions. The influence of relative air humidity on the stability of the studied substances indicated that relative air humidity determines the rate and mechanism of their degradation. The stability of daunorubicin hydrochloride and its amidine derivatives is similar in the solid state. It is otherwise known that the amidine derivatives of DAU have superior pharmacological properties, especially by demonstrating lower cardiotoxicity compared to their parent compound. Of the derivatives studied in this work, the greatest antiproliferative activity was shown by MOR; however, this derivative exhibits the lowest stability in solid state (5) and in aqueous solutions (8).

Acknowledgment

This study was supported by a grant from the State Committee for Scientific Research, Poland (No. N N405 179535).

REFERENCES

1. Wasowska M., Wietrzyk J., Opolski A., Oszczapowicz J., Oszczapowicz I.: Anticancer Res. 26, 2009 (2006).
2. Wasowska M., Oszczapowicz I., Wietrzyk J., Opolski A., Madej J., Dzimira S.: Anticancer Res. 25, 2043 (2005).
3. Ciesielska E., Studzian K., Wasowska M., Oszczapowicz I., Szmigiero L.: Cell. Biol. Toxicol. 21, 139 (2005).
4. Cielecka-Piontek J., Jelińska A., Zając M., Sobczak M., Bartold A., Oszczapowicz I.: J Pharm. Biomed. Anal. 50, 576 (2009).
5. Zalewski P., Jelińska A., Prusinowska P., Cielecka-Piontek J., Krause A., Oszczapowicz I.: Acta. Pol. Pharm. Drug Res. 68, 759 (2011).
6. Jelińska A., Uszak J., Cielecka-Piontek J., Zając M., Lamberti A., Oszczapowicz I., Wąsowska M.: React. Kinet. Catal. Lett. 98, 69 (2009).
7. Zalewski P., Zając M., Jelińska A., Cielecka-Piontek J., Oszczapowicz I.: Asian J. Chem. 23, 835 (2011).

8. Krause A., Jelińska A., Cielecka-Piontek J., Klawitter M., Zalewski P., Oszczapowicz I., Wąsowska M.: Drug. Dev. Ind. Pharm. 38, 1024 (2012).
9. Zalewski P., Jelińska A., Zając M., Cielecka-Piontek J., Piekarski M., Mielcarek J., Krause A. et al.: J. Pharm. Res. 3, 1700 (2010).
10. Cielecka-Piontek J., Jelińska A., Dołhań A., Zalewski P., Burek D., Piekarski M., Krause A. et al.: Asian. J. Chem. 24, 769 (2012).
11. Beijnen J.H., Potman R.P., van Doijen R.D., Driebergen R.J., Voskuilen M.C., Renema J., Underberg W.J.M.: Int. J. Pharm. 32, 123 (1986).
12. Zalewski P., Firlej A., Medenecka B., Jankowska J., Mielcarek J., Oszczapowicz I.: Ann. UMCS Sect. DDD 22(4), 43 (2009).
13. Łukawska M., Oszczapowicz I., Jelińska A., Cielecka-Piontek J., Zając M., Dobrowolski L., Ziółkowska G. et al.: Chem. Anal. (Warsaw) 54, 907 (2009).
14. Jelińska A., Zając M., Cielecka-Piontek J., Głąb K., Tomaszewicz B., Krause A., Oszczapowicz I., Wąsowska M.: Chromatographia 67, 107 (2008).
15. Yoshioka S., Stella V.J.: Stability of Drugs and Dosage Forms. Kluwer Academic Publishers, New York 2002.

Received: 3. 04. 2013

Acta Poloniae Pharmaceutica – Drug Research, Vol. 71 No. 3 pp. 439–449, 2014 ISSN 0001-6837
Polish Pharmaceutical Society

THE EFFECT OF EXCIPIENTS ON THE RELEASE KINETICS OF DICLOFENAC SODIUM AND PAPAVERINE HYDROCHLORIDE FROM COMPOSED TABLETS

REGINA KASPEREK[1]*, HANNA TRĘBACZ[2], ŁUKASZ ZIMMER[1] and EWA POLESZAK[1]

[1]Chair and Department of Applied Pharmacy, Medical University of Lublin,
Chodźki 1, 20-093 Lublin, Poland
[2]Chair and Department of Biophysics, Medical University of Lublin,
Jaczewskiego 4, 20-090 Lublin, Poland

Abstract: For increased analgesic effect, new composed tablets containing diclofenac sodium (DIC) with an addition of papaverine hydrochloride (PAP) were prepared to investigate the mechanism of release of the active substances from tablets with different excipients in eight different formulations. To detect the possible interactions between active substances and excipients differential scanning calorimetry (DSC) was used. A shift of the melting point and enthalpy values of the physical mixtures of tablets components suggested a kind of interaction between components in certain formulations, however, the tabletting process was not disturbed in any of them. Kinetics of drug release from formulations was estimated by zero order, first order and Higuchi and Korsmeyer–Peppas models using results of dissolution of DIC and PAP from tablets. The study revealed that the mechanism of release of active substances was dependent on the excipients contained in tablets and the best fitted kinetics models were obtained for formulations with potentially prolonged release of DIC and PAP.

Keywords: diclofenac sodium, papaverine hydrochloride, tablets excipients, dissolution kinetics, differential scanning calorimetry

Diclofenac sodium {sodium 2-[(2,6-dichlorophenyl)amino]phenylacetate, DIC} is a non-steroidal anti-inflammatory drug (NSAID) with analgesic and antipyretic properties. It is taken to reduce inflammation and as an analgesic reducing pain in the long-term treatment of degenerative diseases such as rheumatoid arthritis and osteoarthritis (1, 2). In order to increase the therapeutic effect or decrease the adverse effects of diclofenac sodium, the composed pharmaceutical dosage forms were obtained (3–5). Papaverine hydrochloride (PAP) was assessed as a spasmolytic agent, for the treatment of renal colic as a single and in combination with sodium diclofenac (6). For increased analgesic effect, composed tablets containing diclofenac sodium with addition of papaverine hydrochloride were prepared and patented (7).

The successful formulation of a stable and effective solid dosage form depends on the selection of the excipients. Because the drug has intimate contact with the excipients, assessment of possible interactions between the active substance and different excipients is an important part of the development of dosage forms (8). Physical analysis, such as differential scanning calorimetry (DSC) was used to detect possible drug : carrier interactions (9). Incompatibilities of components can be deduced from appearance, shift or disappearance of peaks and/or variations in the corresponding enthalpy values obtained from DSC traces (10). It is of importance to detect any possible interactions, since it has been shown that certain interactions can change the bioavailability or stability of the product (11).

Thermodynamic behavior, including the solubility of a solid in a liquid, plays an important role in drug design as well as in the design and optimization of production processes (12). However, solubilities of diclofenac sodium and papaverine hydrochloride are different and depend on pH of the dissolution medium. Diclofenac sodium is almost insoluble in acidic pH of the stomach and soluble in phosphate buffer at pH 6.8 (13, 14). Solubility of papaverine

* Corresponding author: e-mail: reginakasperek@umlub.pl

hydrochloride increases proportionally to the decrease of pH of the medium (15, 16).

In vitro dissolution is one of the most important elements of the drug development process. The quantity of the active substance dissolved in a specified time is expressed as a percentage of the content stated on the label. Several models may be used to describe dissolution profiles where f (t) is a function of t time (t) that is related to the amount of drug dissolved from a dosage form. The quantitative interpretation of the values generated in dissolution studies is facilitated by the use of generic equations. The equations translate dissolution curves mathematically as a function of certain parameters related to the dosage forms under investigation. In some cases, the equations can be deduced by a theoretical analysis of the processes to which the dosage form is subjected. A water-soluble drug incorporated into a hydrophilic matrix is released mainly by a diffusion-controlled process, whereas for a poorly water-soluble compound, the principal mechanism of release is a function of erosion of the matrix that carries the drug (17).

The use of mathematical modeling turns out to be very useful as this approach enables to predict the release kinetics before the release systems are realized. More often, it allows the measurement of some important physical parameters, such as the drug diffusion coefficient and resorting to model fitting on experimental release data. Thus, mathematical modeling, whose development requires the comprehension of all the phenomena affecting drug release kinetics, has a very important value in the process optimization of such formulation (18, 19).

The aim of the study was to investigate the mechanism of release of diclofenac sodium and papaverine hydrochloride from tablets with different excipients using different formulations. To detect the possible interactions drug : drug or drugs : excipients the differential scanning calorimetry (DSC) was used.

EXPRIMENTAL

Materials and reagents

Diclofenac sodium (DIC) was produced by Caesar and Loretz, GmbH, Hilden, Germany, papaverine hydrochloride (PAP) was purchased from Galfarm PPH, Cefarm Lublin, Poland, polyvinylpyrrolidone K 22 (PVP 22), mannitol (M), potato starch (PS), microcrystalline cellulose (MC) were the products of Merck, Germany, polyvinylpyrrolidone K 10 (PVP 10) and β-lactose (lactose) were purchased from Sigma Aldrich, hydroxypropylmethylcellulose (HPMC) was purchased from Fluka. Pregelatinized starch (GPharmGel) produced by Cargill, Benelux, microcrystalline cellulose (Avicel PH102, Avicel) and croscarmellose sodium (AcDiSol) produced by FMC BioPolymer, Belgium were obtained as gifts from IMCD, Warszawa, Poland. Colloidal silicon dioxide 200 (Aerosil) produced by Evonic, Germany was obtained as a gift from Chempol, Warszawa, Poland. Magnesium stearate (StMg) was purchased from POCh, Gliwice,

Table 1. Different tablet compositions.

Name of component	Quantity (%) per tablet of 300 mg weight							
	T1	T2	T3	T4	T5	T6	T7	T8
Diclofenac sodium	16.67	16.67	16.67	16.67	16.67	16.67	16.67	16.67
Papaverine hydrochloride	6.67	6.67	6.67	6.67	6.67	6.67	6.67	6.67
PVP 10	5	5	5	5	5	5	-	-
PVP 22	-	-	-	-	-	-	23.3	23.3
Avicel PH102	20	-	33.3	-	60.2	33.3	-	-
MC	-	-	-	-	-	-	-	5
HPMC	-	-	-	-	-	-	-	10
Lactose	40.7	45.7	36.8	50.2	-	21.8	-	-
Mannitol	-	-	-	-	-	-	23.3	37.3
Potato starch	-	-	-	-	-	-	30	-
CPharmGel	-	20	-	20	-	10	-	-
Aerosil	-	-	0.5	0.5	0.5	0.5	-	-
AcDiSol	10	5	-	-	10	5	-	-
Magnesium stearate	1	1	1	1	1	1	-	1

Table 2. Physical properties of tablets prepared.

Test	Results							
	T1	T2	T3	T4	T5	T6	T7	T8
Weight (mg) SD	299.33 ± 1.21	292.83 ± 1.43	304.74 ± 3.02	302.43 ± 1.69	300.97 ± 2.64	299.71 ± 2.97	300.54 ± 2.45	298.76 ± 2.35
Thickness (mm) SD	4.28 ± 0.01	3.89 ± 0.02	3.97 ± 0.02	3.78 ± 0.01	6.11 ± 0.03	4.22 ± 0.01	4.02 ± 0.02	4.15 ± 0.03
Disintegration time (min) SD	8 ± 1.7	28 ± 2.2	31 ± 4.2	33 ± 2.7	0.6 ± 0.1	18 ± 3.5	7 ± 2.5	11 ± 3.7
Hardness (kG/mm^2), SD	0.09 ± 0.03	0.085 ± 0.02	0.105 ± 0.02	0.102 ± 0.04	0.004 ± 0.001	0.095 ± 0.02	0.105 ± 0.01	0.103 ± 0.02
Friability (%)	0.044	0.21	0.11	0.13	0.14	0.06	0.09	0.15
Drug content (%) DIC, SD	98.02 ± 2.34	99.56 ± 3.65	100.14 ± 4.12	97.24 ± 3.42	98.24 ± 2.75	97.50 ± 2.63	99.08 ± 1.17	97.68 ± 2.51
(%) PAP, SD	98.35 ± 1.64	100.15 ± 4.73	97.05 ± 2.14	92.70 ± 2.39	94.85 ± 3.05	99.95 ± 3.32	100.05 ± 1.76	93.75 ± 2.43

SD = mean standard deviation

Poland. All the reagents and chemicals used were of analytical grade.

Preparation of tablets

The composition of various formulations of tablets (T1–T8) are given in Table 1.

Tablets were obtained by direct compression of granules, which were previously prepared by using a wet granulation method.

Powders of the components were sieved through a 0.710 mm mesh screen. All of the components, except the lubrificant (magnesium stearate), were mixed manually with addition of aqueous solution of PVP (10 or 22), to obtain the desired consistency of the mass.

The wet mass was then granulated using a rotary granulator (Erweka, Germany) by passing it through a 1.0 mm mesh screen. Granules were dried in a hot air oven (Memmert INB-500) at 40°C for 1 h. The dried granules (moisture 3–5%) were passed through a 1.00 mm mesh screen. At the end, 1.0% (w/w) of the lubrificant magnesium was added, and mixed manually. From the granules, the 300 mg tablets were obtained in a press tabletting machine (Erweka, Germany) with 9 mm concave punches.

Evaluation of physical properties of formulation tablets

The tablets were tested according to standard procedures for weight variation (n = 20), thickness (n = 20), hardness (n = 6), friability (n = 20), disintegration time (n = 6) and drug content (n = 10) (Table 2).

Weight uniformity test

For each formulation twenty tablets were selected randomly and weighed together and their mean weight was calculated. Next, they were individually weighed using a weighing balance (Ohaus AV 513C, USA).

Tablet dimensions

Tablet diameter and thickness were measured using a Vernier Caliper (Digital Caliper 0–150 mm, Comparator).

Hardness test

Hardness of tablet was determined by using an Erweka tablet hardness tester (Erweka, Germany).

Friability test

An Erweka (Germany) friabilator was used for the test.

Twenty tablets were weighed and subjected to attrition at 25 rpm for 4 min and the tablets were reweighed. The percentage loss in weight equivalent to friability was calculated from the equation:

Friability (%) = (loss in weight/initial weight) × 100

Disintegration time

Disintegration time was measured by using the pharmacopoeia method (USP) by using a USP Apparatus (Erweka, Germany).

Each of six tablets was put into a basket-rack in a vessel and it was covered with a disk. After the apparatus was turned on, the disintegration time of the tablets was observed.

Drug content analysis

Drug content of DIC and PAP were analyzed by measuring the absorbance of standard and samples at 238 nm for PAP and 278 nm for DIC, using UV/visible spectrophotometer (model Helios Omega UV-VIS, Spectro-Lab, Thermo Scientific, England) with 10 mm matched quartz cell.

Ten tablets from each series were selected at random, weighed together and the mean weight was determined. The tablets were crushed together and exactly 300 mg in powder form (n = 6) was weighed, dissolved in methanol in a 50 mL volumetric flask, filtered by using the Whatman filter and appropriately diluted with methanol. The obtained solution was mixed with phosphate buffer at pH 6.8 in 1 : 1 proportion. The absorbance of the diluted solutions were read in a UV/visible spectrophotometer. The drugs content for each series of tablets was calculated based on simultaneous equation method reported earlier (20). This method obeys Beer's Law in the employed concentration ranges of 2.5–25 µg/mL for two active substances. The limit of quantification (LOQ) was determined to be 1.5 µg/mL for DIC and 1.8 µg/mL for PAP. The limit of detection (LOD) was calculated as 0.5 µg/mL and 0.6 µg/mL for DIC and PAP, respectively. The calibration curves of DIC, at 238 nm $y = 0.0231x + 0.0074$, $R^2 = 0.9993$, at 278 nm $y = 0.0309x + 0.0147$, $R^2 = 0.9997$; for PAP, at 238 nm $y = 0.134x – 0.047$, $R^2 = 0.9998$, at 278 nm $0.0105x + 0.0449$, $R^2 = 0.9992$, were determined.

Differential scanning calorimetry

Samples (about 5 mg) of DIC, PAP and physical mixtures of DIC with PAP, and DIC, PAP and excipients in eight different formulations were hermetically sealed in aluminum pans. DSC analyses

Table 3. Dissolution kinetics of DIC.

Formulation	Zero order		First order		Higuchi		Korsmeyer–Peppas	
	k	r^2	k	r^2	k	r^2	n	r^2
T1	0.3958	0.3139	0.00115	0.2511	4.6855	0.482	0.1807	0.7055
T2	1.6266	0.9634	0.05136	0.9438	15.192	0.9938	0.8231	0.9927
T3	0.6597	0.9806	0.00942	0.9858	6.3131	0.984	0.5573	0.9946
T4	1.5208	0.8983	0.04606	0.9762	15.073	0.9668	0.7925	0.9757
T5	0.0392	0.2305	0.00115	0.2224	0.2944	0.1422	0.0035	0.0438
T6	0.9772	0.7533	0.04145	0.9063	10.135	0.8878	0.3556	0.9546
T7	1.0152	0.6727	0.02602	0.7608	10.776	0.8303	0.5579	0.8972
T8	0.9947	0.7969	0.01958	0.8456	10.178	0.9141	0.6075	0.9582

Table 4. Dissolution kinetics of PAP.

Formulation	Zero order		First order		Higuchi		Korsmeyer–Peppas	
	k	r^2	k	r^2	k	r^2	n	r^2
T1	0.4361	0.4615	0.01405	0.5168	4.8724	0.6312	0.1745	0.8024
T2	1.5865	0.9866	0.0456	0.8769	14.834	0.9861	0.8974	0.9956
T3	0.1824	0.8524	0.0009	0.8384	1.6234	0.7399	0.4501	0.7389
T4	1.2032	0.914	0.02188	0.9643	11.87	0.9746	0.9433	0.9719
T5	0.1566	0.6711	0.00253	0.7	1.6257	0.7929	0.0883	0.8822
T6	0.6795	0.7069	0.01267	0.7471	7.1349	0.8541	0.3895	0.9386
T7	1.0061	0.6808	0.02695	0.7805	10.664	0.8381	0.5271	0.9033
T8	0.9911	0.8055	0.01958	0.8582	10.13	0.9219	0.6018	0.9584

were carried out using DSC Q200 Thermal Analyzer (TA Instruments, USA). Indium standard was used to calibrate the temperature and enthalpy scale. The samples were heated at a constant rate of 10°C/min, over a temperature range from 40°C to 310°C in nitrogen atmosphere at the flow rate of 50 mL/min. As a reference an empty pan was used.

***In vitro* dissolution study of the tablets**

The dissolution of DIC and PAP from prepared tablets was carried out by Erweka (Germany) dissolution tester using USP apparatus 2 (paddle method). One tablet was set in each of six vessels and rotated at 100 rpm for 60 min. As a dissolution medium, 900 mL of phosphate buffer at pH 6.8 at 37 ± 0.5°C was used. The samples (2 mL) were drawn after 2, 5, 10, 15, 20, 25, 30, 35, 40, 45, 50, 55 and 60 min. For each sample drawn, an equivalent volume of phosphate buffer at pH 6.8 (2 mL) was added to the dissolution medium. After dilution of each of the drawn samples, the solutions were analyzed spectrophotometrically at 238 nm and 278 nm. The amount of the released substances was calculated by reference to a Beer's plot by using the method reported earlier (20).

Drug release kinetics

To study the release kinetics of the drug, data obtained from *in vitro* drug release studies were plotted in various kinetic models: zero order (Eq. 1) as a cumulative percentage of drug release *vs*. time, first order (Eq. 2), as a log of the amount of drug remaining to be released *vs*. time and Higuchi's model (Eq. 3), as a cumulative percentage of drug release *vs*. square root of time.

The zero order kinetics describes the systems where the drug release is independent of its concentration.

$$Q = K_0 t \qquad \text{(Eq. 1)}$$

where Q is the amount of drug released in time t, K_0 is the zero order rate constant expressed in units of concentration (21).

The first order kinetics describes the release where release rate is concentration depended.

$$Log\ Q = Log\ Q_0 - Kt/\ 2.303 \qquad \text{(Eq. 2)}$$

where Q is the amount of drug released in time t, Q_0 is the initial concentration of drug and K is the first order rate constant (22).

Higuchi's model describes the release of drugs from insoluble matrix as a square root of time dependent process based on Fickian diffusion.

$$Q = K\ t^{1/2} \qquad \text{(Eq. 3)}$$

where Q is the amount of drug released in time t, K is the constant reflecting the design variables of the system (23).

Mechanism of drug release

To evaluate the mechanism of drug release from tablets, data of drug release were plotted according to Korsmeyer et al. (24) equation (Eq. 4), as a log of cumulative percentage of drug released *vs*. log time, and the exponent n value was calculated through the slope of the straight line.

$$M_t /M8 = Kt^{n} \qquad \text{(Eq. 4)}$$

For a cylindrical matrix tablets, if the exponent n = 0.45, then the drug release mechanism is Fickian diffusion, and if 0.45 < n < 0.89 then it is non-Fickian diffusion. An exponent value of 0.89 is indicative of case II transport or typical zero order release, n > 0.89 is super case-II transport (25).

Statistical and kinetic analyses were made using a Statistica 8.0 software.

RESULTS AND DISCUSSION

Physical properties

The physical properties of prepared tablets and the drugs content are shown in Table 2. Average weight, thickness, hardness, friability and the drugs content of all prepared tablets were within pharmacopoeial specification (26).

The DSC analyses

DSC thermograms of the active substances (DIC and PAP), physical mixture of active substances (DIC + PAP) and mixtures of components of tablets T1–T8 are shown in Figure 1.

The DSC trace for DIC showed that DIC melted at temperatures in the range from 285 to 292°C with enthalpy of about 110 J/g. The melting endotherm was followed by decomposition of the substance. Bucci et al. (27) reported that the thermal decomposition of DIC is a two-step process: one of this is endothermic melting peak 285°C, and second partially overlapped the exothermic peak at 294°C. The studies conducted by Palomo et al. (28) showed that DIC melted in the range from 280.45 to 349.96°C, but Szűts at al. (29) reported that it was in the range from 280 to 294°C.

Thermal activity of PAP was found in the range from 226 to 230°C with enthalpy 220 J/g. This is in agreement with studies conducted by Ventura et al. (30) and Marciniec et al. (31). Their studies showed that PAP had a single melting endotherm with a peak at 230°C.

The DSC thermogram for the mixture (DIC + PAP) was different from those of the individual substances. Thermal activity of the mixture started at 135°C with a process resembling a glass transition. A wide and complex melting endotherm with a peak

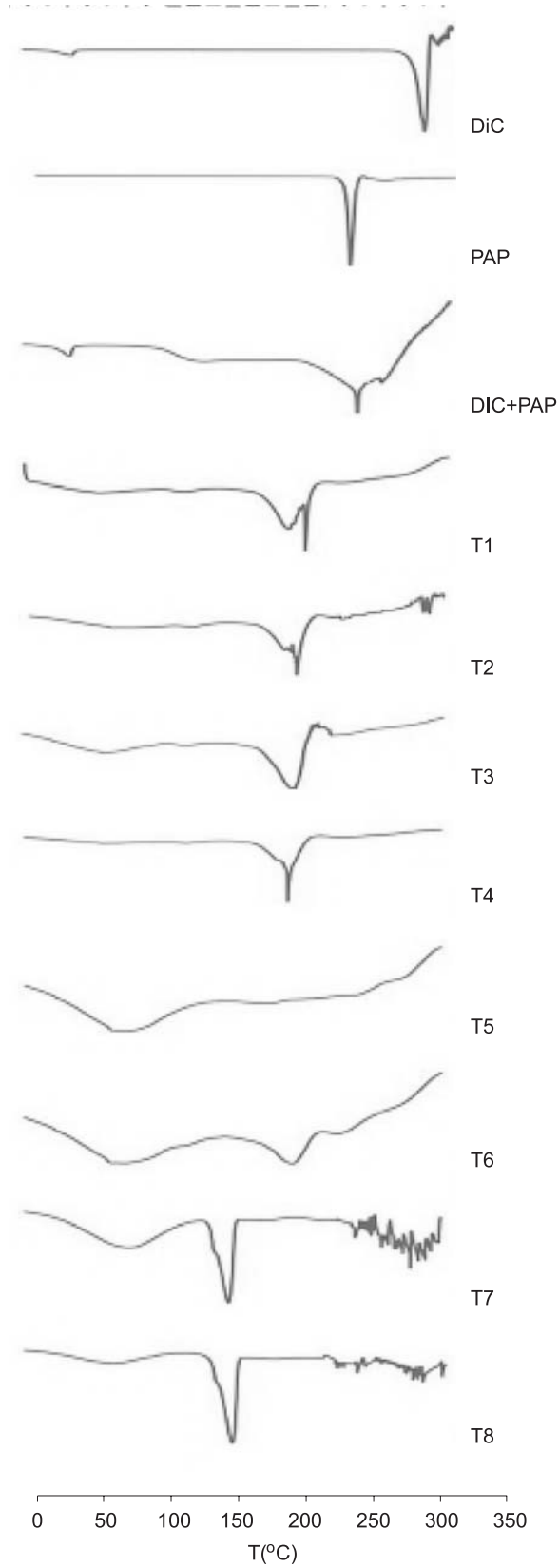

Figure 1. DSC in nitrogen of DIC, PAP, mixture of powders DIC and PAP (DIC + PAP) and tablets T1–T8

at 245°C and enthalpy change 80 – 85 J/g was followed by an exothermal process. The DSC trace for (DIC + PAP) suggested a possible interaction of DIC with PAP. If the solid-solid interaction is weak or non-existent, the reduction of the melting point is usually inconsequential (10).

The DSC traces for T1, T2 and T4 were similar to each other. A glass transition at 124–132°C was followed by a wide endotherm between 180 and 220°C overlapped with a narrow and deep peak at 200–210°C. The enthalpy of the endotherm (DH) for T1, T2 and T4 was equal to 70 J/g, 70 J/g and 100 J/g, respectively. The shape of DSC traces for T1, T2 and T4 was similar to the trace for (DIC + PAP). One can conclude that an addition of Avicel, AcDiSol in T1 or CPharmGel, AcDiSol in T2 and CPharmGel, Aerosil in T4 together with lactose did not change thermal properties of (DIC + PAP) and that excipients, which are contented in these tablets, should not cause interactions between components. In the DSC thermograms of T3 and T6 one can observed a wide endothermic peak in the range from 80 to 90°C and a larger one with the melting point at 204°C and enthalpy about 50 J/g for T3 and 25 J/g

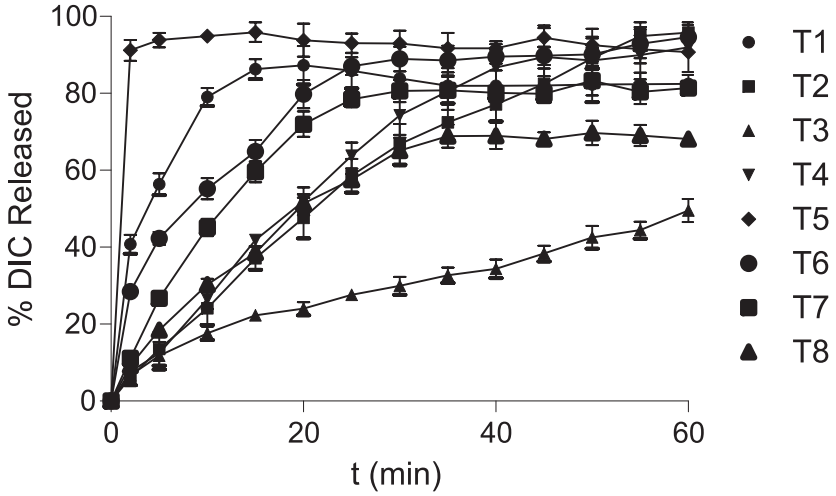

Figure 2. Mean dissolution profiles of DIC from composed tablets (mean values, n = 6)

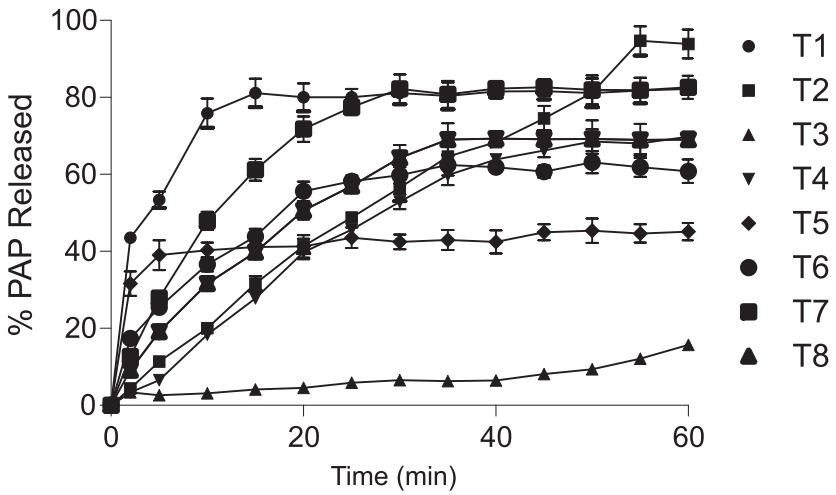

Figure 3. Mean dissolution profiles of PAP from composed tablets (mean values, n = 6)

for T6. The mixtures of T3 i T6 contained the same quantity of Avicel (33.3%) and Aerosil (0.5%), but they were different by the amount of lactose T3 (36.8%), T6 (21.8%) and an addition of CPharmGel (10%) and AcDiSol (5%) in T6. In the DSC thermogram of T5 there was only a wide endothermic process in the range from 85 to 102°C with the maximum at 94°C and enthalpy 65 J/g and no thermal activity at higher temperatures. T5 was different from other formulations by a large contents of Avicel (60.2%) and a lack of sugars.

The putative interactions between components in formulations T3, T5 and T6 indicated a risk of a strong solid-solid interaction that might occurr while compressing powders or granules in a press tabletting machine (32). However, the tabletting process in our study was not disturbed for any formulation.

The DSC traces for T7 and T8 showed lowering of melting temperature as compared to the endotherm of the mixture of active substances (DIC + PAP) but the enthalpy values were not changed that indicated that the interaction or incompatibility should not occurr.

The DSC trace for T7 showed a melting point at 162°C with ΔH = 110 J/g, following glass transition at 96°C and for T8, melting point at 153°C with ΔH = 111 J/g and glass transition at 87°C.

The release study

The dissolution profiles of DIC and PAP for each formulation (T1–T8) are presented in Figures 2 and 3.

From T1, 86.5% DIC and 81.15% PAP were released within 15 min and from T2, above 80% of active substances were released within 50 min (80.04% DIC and 81.2% PAP). The difference in release time for about 80% of both active substances from T1 and T2 was about 35 min and difference in disintegrating time of tablets was 20 min (8 min T1 and 28 min T2). These formulations are similar in quantities of lactose (40.7% T1 and 45.7% T2) and different in additions of Avicel (20%) and AcDiSol (10%) in T1 or CPharmGel (20%) and AcDiSol (5%) in T2. This indicated that an addition of CPharmGel instead the Avicel may result in prolonged release time, but on that time may affect also 5% more of AcDiSol in T1.

In T6, there are both Avicel (33.3%) and CPharmGel (10%) and lactose (21.8%), AcDiSol (5%), Aerosil (0.5%). The release study showed that above 80% DIC (87.08%) was released within 25 min (94.66% after 60 min), but PAP 60.8% within 60 min. The disintegrating time of this tablets is 18 min. Comparing T6 to T1 and T2 it can be observed that DIC was released slower about 10 min from T6 than from T1 and 25 min faster from T6 than from T2. PAP was not released in 80% from T6. The quantity of released PAP from T6 in comparison with T1 and T2 shows that inhibition of the release process of PAP can be caused higher of quantity of Avicel in T6 about 13% (in comparison with T1) and less of the quantity of CPharmGel on 10% in T6 (in comparison with T2) at simultaneously decreased the quantity of AcDiSol on 5% in T6 (comparing to T1).

Tablets T3 and T4 comprised lactose at different quantities (36.8% T3 and 50.2% T4) and Aerosil at the same quantities (0.5%), but they are different in an addition of Avicel (33.3%) in T3 and CPharmGel (20%) in T4. Within 60 min, only 49.52% DIC and 15.7% PAP from T3 were released, but within 35 min 80.58% DIC (91.98% within 60 min) and within 60 min 69.75% PAP from T4 were released, although the disintegration times of both of tablets are similar (31 min T3 and 33 min T4). Both formulations do not contain AcDiSol as a disintegrator. From this it follows that the release process is highly affected by other excipients such as Avicel, CPharmGel and lactose.

When comparing T3 and T4 it can be noticed that addition of CPharmGel in a quantity of 20% in T4 increased the quantity of released DIC and PAP, but Avicel, in an addition of 33.3% in T3, without AcDiSol, caused inhibition of the release process of the active substances.

Avicel in a quantity of 60.2%, with the addition of 10% AcDiSol and 0.5% Aerosil in T5, caused a fast disintegrated process of a tablet (0.6 min), but there occurs the difference of the release process. Within 2 min, 91.18% DIC and within 60 min 45.1% PAP from T5 were released. In comparison with T1, it can be observed that the absence of lactose in T5 caused the fast release process of DIC, but inhibition of the release of PAP.

Within 30 min, 80.59% of DIC and 82.19% of PAP from T7 and within 60 min 68.14% of DIC and 69.04% of PAP from T8 were released. Tablets T7 and T8 were similar in content of mannitol at different quantities (23.3% T7 and 37.3% T8), but varied in addition of potato starch to T7 and microcrystalline cellulose and HPMC to T8. The data of the release study showed that cellulose and their derivatives, especially HPMC, in T8 caused prolonged the release of both active substances. The differences in the release process of DIC from tablets can be caused by different production process, different excipients or differences at size of particle of active substance. The effect of different excipients on the

dissolution profiles of diclofenac sodium from tablets or pellets were reported by Bertocchi et al. (2), Savaser et al. (33), Kibria et al. (34) and Mourão et al. (35).

According to pharmacopoeial requirements for uncounted tablets (26), 80% of active substances were released from T1 and T7 within 45 min. The disintegration times of these tablets were 8 and 7 min for T1 and T7, respectively. The disintegration times for tablets T2, T3, T4 and T6 exceeded 15 min as recommended by Polish Pharmacopoeia (26) and were in the range from 18 to 33 min. The release process of active substances from tablets T2, T4 and T6 run similarly; as above, 80% of DIC were released within 45 min. However, amounts of released PAP were lower and equal in the range from 60.70 to 74.52%. The disintegration time of T3 was 18 min, but only 38.36% DIC and 8.1% PAP were released within 45 min. The differences observed within the release process and disintegration times were probably caused by type of binder added to the formulation. In tablets T2 and T4, 20% of CPharmGel was added, in T6 10% CPharmGel and 33.3 % of Avicel, and in T3 only 33.3% of Avicel was added. Moreover, the release process can also be influenced by addition of a disintegrator and a lubricant. In formulas T3 and T4, only Aerosil (0.5%) was added resulting in disintegration time 31–33 min. An addition of 5% of AcDiSol to T2 caused a bit shorter time (28 min). When 5% of AcDiSol and 0.5% of Aerosil in T6 were used, the disintegration time was 18 min. Bearing in mind the above data, it can be noticed that mixing of different excipients considerably changed the release process of active substances from uncoated tablets. The positive effect of a binder on pore structure and tablet strength resulted in an increased disintegration time. Although addition of a disintegrator generally improved the disintegration time, the effect was decreased when the formulation included more deformable binders (36).

Kinetic analysis of dissolution data

The obtained drug release data were analyzed by zero order, first order, Higuchi and Korsmeyer–Peppas models, to know the mechanism of drug release from the formulations. The release rate constants were calculated from the slope of the appropriate plot and determination coefficient (r^2) were determined (Tables 3 and 4).

In this study, the *in vitro* release profiles of DIC from formulations T2 and T4 containing CPharmGel and T3 containing Avicel as base excipients were explained by Higuchi model, where the determination coefficient (r^2) is in the range from 0.9968 to 0.9938; for the first order r^2 equals from 0.9438 to 0.9858) and for the zero order r^2 equals from 0.8983 to 0.9806). The release of DIC from formulation T2 was best explained by Higuchi's equation as the plot showed the highest linearity (r^2 = 0.9938) followed by zero order (r^2 = 0.9634). This indicates that the release of drug from the matrix is a square root of time dependent process and is close to zero order release kinetics. The best linearity for formulations T3 and T4 were found in first order rate equation plot describing the drug release rate relationship with concentration of DIC, so r^2 equals 0.9858 for T3 and 0.9762 for T4, respectively.

The *in vitro* release profiles of PAP from formulation T2 showed the highest linearity with the zero order kinetics (r^2 = 0.9866), followed by Higuchi's (r^2 = 0.9861) and from T4 was best explained by Higuchi's model (r^2 = 0.9746), followed by the first order equation (r^2 = 0.9643).

The obtained data were plotted according to the Korsmeyer-Peppas equation to know the confirmed diffusion mechanism.

For DIC release, the formulations T2 and T3 showed good linearity (r^2 equals 0.9927 and 0.9946, respectively) with exponent (n) values 0.8231 (T2) and 0.5573 (T3), indicating a coupling of the diffusion and erosion mechanism so called anomalous transport (non-Fickian). For PAP release, the formulation T2 showed good linearity (r^2 = 0.9956) with release exponent 0.8947, indicating zero order release where concentration was nearly independent of drug release profile. The formulations T4 and T8 showed release exponent (n) 0.7925 (T4) and 0.6075 (T8) with r^2 0.9757 (T4) and 0.9582 (T8) for DIC release, indicating anomalous transport.

For PAP release, formulation T4 showed release exponent (n) 0.9433 with r^2 = 0.9719 characteristic for super case II transport and for T8 (n) 0.6018 with r^2 = 0.9584, indicating anomalous transport. Case II generally refers to erosion of polymeric chain and anomalous transport (non-Fickian) refers to a combination of both diffusion and erosion controlled drug release (17).

Formulation T6 slope (n) values equal 0.3556 (DIC) and 0.3895 (PAP), indicating Fickian type of diffusional release occuring by usual molecular diffusion of the drug due to chemical potential gradient.

The tablet T5 containing high amount of Avicel pH 102 with dissolution time 0.6 min represents fast dissolving tablets (FDT). The tablets formulations T1, T2 and T8 are typical uncoated tablets with disintegration time up to 15 min. The tablet for-

mulation T3 containing Avicel and T2 or T4 containing CPharmGel can be considered as matrix tablets with potentially prolonged release. Drugs release from tablet formulation T2 was found to be very close to zero order release kinetics. Formulation T6 represents uncoated tablets with diffusion type of release. The type of excipient used as a matrix of tablet induce effect on release rate and mechanism.

CONCLUSION

The shift of the melting point and the enthalpy values for the mixtures of tablets components suggested a possible interaction of the components in some mixtures but the tabletting process was not influenced in none of the formulations. The tablet formulation containing high amount of Avicel PH 102 (60.2%) and PVP 10 (5%), AcDiSol (10%), Aerosil (0.5%) with dissolution time 0.6 min. represents fast dissolving tablets. The formulations containing PVP 10 (5%) and CPharmGel (20%), lactose (45.7%), AcDiSol (5%) or PVP 10 (5%), Avicel (33.3%), lactose (36.8%), Aerosil (0.5%) or PVP 10 (5%), CPharmGel (20%), lactose (50.2%), Aerosil (0.5%) can be considered as tablets with prolonged release, because the *in vitro* release profiles of DIC and PAP from these formulations were fitted to the kinetic models describing the dissolution of drug from modified release dosage forms.

REFERENCES

1. Martindale: The Complete Drug Reference, 37th edn. p. 44, The Pharmaceutical Press, London 2011.
2. Bertocchi P., Antoniella E., Valvo L., Alimonti S., Memoli A.: J. Pharm. Biomed. Anal. 37, 679 (2005).
3. Lala L.G., D'Mello P.M., Naik S.R.: J. Ethnopharmacol. 91, 277 (2004).
4. León-Reyes M.R., Castañeda-Hernández G., Ortiz M.I.: J. Pharm. Pharm. Sci. 12, 280 (2009).
5. Mukherjee J., Das A., Chakrabarty U.S., Sahoo B., Sengupta P., Chatterjee B., Roy B., Pal T.K.: Arzneimittelforschung 60, 8, 506 (2010).
6. Snir N., Moskovitz B., Nativ O., Margel D., Sandovski U., Sulkes J., Livne P.M., Lifshitz D.A.: J. Urol. 179, 1411 (2008).
7. Kasperek R.: Polish Patent No. P 380847 (2010).
8. Fathy M., Hassan M.A., Mohamed F.A.: Pharmazie 57, 825 (2002).
9. Fini A., Fazio G., Fernández-Hervás M.J., Holgado M.A., Rabasco A.M.: Int. J. Pharm. 121, 19 (1995).
10. Kerč J., Srčič S., Urleb U., Kanalec A., Kofler B., Šmid-Korbar J.: J. Pharm. Pharmacol. 44, 515 (1992).
11. Li Wan Po A., Morso P.V.: Int. J. Pharm. 18, 287 (1984).
12. Žilnik L.F., Jazbinšek A., Hvala A., Vrečer F., Klamt A.: Fluid Phase Equilibr. 261, 140 (2007).
13. Bravo S.A., Lamas M.C., Salamón C.J.: J. Pharm. Pharm. Sci. 5, 213 (2002).
14. Kincl M., Meleh M., Veber M., Vrečer F.: Acta Chim. Slov. 51, 409 (2004).
15. Miyajima M., Koshika A., Okada J., Kusai A., Ikeda M.: J. Control. Release 56, 85 (1998).
16. Serajuddin A.T.M., Rosoff M.: J. Pharm. Sci. 73, 1203 (1984).
17. Costa P., Sousa Lobo J.M.: Eur. J. Pharm. Sci. 13, 123 (2001).
18. Grassi M., Grassi G.: Curr. Drug Deliv. 2, 97 (2005).
19. Dash S., Narashima M.P., Lilakanta N., Prasanta C.: Acta Pol. Pharm. Drug Res. 67, 217 (2010).
20. Kasperek R., Zimmer Ł., Świąder K., Belniak P., Poleszak E.: Curr. Issues Pharm. Med. Sci. 25, 182 (2012).
21. Hadjiioannou T.P., Christian G.D., Koupparis M.A.: Quantitative Calculations in Pharmaceutical Practice and Research, p. 345, VCH Publishers Inc., New York 1993.
22. Bourne D.W., Banker G.S., Rhodes C.T.: Modern Pharmaceutics, 4th edn., p. 67, Marcel Dekker Inc., New York 2002.
23. Higuchi T.: J. Pharm. Sci. 52, 1145 (1963).
24. Korsmeyer R.W., Gurny R., Doelker E., Buri P., Peppas NA.: Int. J. Pharm. 15, 25 (1983).
25. Siepmann J., Peppas N.A.: Adv. Drug Deliv. Rev. 48, 139 (2001).
26. The Polish Pharmacopoeia IX, pp. 355, 359, 837, Polish Pharmaceutical Society, Warszawa 2011.
27. Bucci R., Magrì A.D., Magrì A.L.: Fresenius J. Anal. Chem. 362, 577 (1998).
28. Palomo M.E., Ballesteros M.P., Frutos P.: J. Pharm. Biomed. Anal. 21, 83 (1999).
29. Szűts A., Sorrenti M., Catenacci L., Bettinetti G., Szabó-Révész P.: J. Therm. Anal. Calorim. 95, 885 (2009).

30. Ventura C.A., Puglisi G., Zappalà M., Mazzone G.: Int. J. Pharm. 160, 163 (1998).
31. Marciniec B., Kozak M., Naskrent M., Hofman M., Dettlaff K., Stawny M.: J. Therm. Anal. Calorim. 102, 261 (2010).
32. Hosaka S., Sadoshima T., Sato M., Hamada C., Takahashi Y., Kitamori N.: Chem. Pharm. Bull. 55, 793 (2007).
33. Savaşer A., Özkan Y., Işimer A.: Farmaco 60, 171 (2005).
34. Kibria G., Roni M.A., Absar M.S., Jalil R.: AAPS PharmSciTech. 9, 1240 (2008).
35. Mourão S.C., da Silva C., Bresolin T.M.B., Serra C.H.R., Porta V.: Int. J. Pharm. 386, 201 (2010).
36. Mattsson S., Nyström C.: Eur. J. Pharm. Sci. 10, 53 (2000).

Received: 20. 06. 2013

Acta Poloniae Pharmaceutica – Drug Research, Vol. 71 No. 3 pp. 451–462, 2014 ISSN 0001-6837
Polish Pharmaceutical Society

IMPROVED PHYSICOCHEMICAL CHARACTERISTICS OF ARTEMISININ USING SUCCINIC ACID

MUHAMMAD TAYYAB ANSARI[1], HUMAYUN PERVEZ[2], MUHAMMAD TARIQ SHEHZAD[2], SYED SAEED-UL-HASSAN[3], ZAHID MEHMOOD[1], SYED NISAR HUSSAIN SHAH[1], MUHAMMAD TAHIR RAZI[1] and GHULAM MURTAZA[4]*

[1]Department of Pharmacy, [2]Department of Chemistry, Bahauddin Zakariya University, Multan, Pakistan
[3]University College of Pharmacy, University of the Punjab, Lahore, Pakistan
[d]Department of Pharmaceutical Sciences, COMSATS Institute of Information Technology, Abbottabad, Pakistan

Abstract: Artemisinin (ARMN) is a potent antimalarial drug, which is effective against multidrug resistant strains of *Plasmodium falciparum* and produces rapid recovery even in patients with cerebral malaria. Being poorly soluble in water, artemisinin is incompletely absorbed after oral intake due to poor dissolution characteristics in the intestinal fluids. To enhance these properties, solid dispersions of artemisinin with succinic acid (SUC) were prepared using drug-carrier ratios 1 : 1, 1 : 4, 1 : 6, 1 : 8 and 1 : 10 by solvent evaporation and freeze drying methods. These solid dispersions were characterized by differential scanning calorimetery (DSC), Fourier transform infrared spectroscopy (FTIR), x-ray diffraction patterns (XRD), phase solubility and dissolution kinetics evaluated by applying zero order, first order, Higuchi, and Korsmeyer-Peppas models. Physical mixtures produced significantly higher aqueous solubility and rate of dissolution as compared to artemisinin alone. The dissolution profiles of all formulations followed Higuchi model and exhibited diffusion-controlled release of drug. Solvent evaporation method (SLVPs) exhibited improved solubility and freeze dried solid dispersions (FDSDs) produced highest solubility but stability constant was opposite. ARMN and SUC both were found completely crystalline as shown by their XRD patterns. Physical mixtures (PMs) showed reduced intensity in their XRD patterns while solid dispersions by SLVPs exhibited twice reduced intensity and much displaced angles, whereas FDSDs showed synergistic effects in some of ARMN and SUC peaks. DSC thermograms of FDSDs at drug-carrier ratios 1 : 1–1 : 4 showed lower melting temperature and enthalpy change (ΔH) values than respective SLVPs, whereas at higher ratios, a reverse was true. SLVPs showed displaced methyl stretching bands at lower drug-carrier ratios and exhibited O-H stretching characteristic bands of SUC at higher drug-carrier ratios. In addition, carbonyl group and C-O stretching vibrations characteristic of SUC (1307 cm^{-1}) appeared prominently compared to PMs, whereas C-O stretching characteristic bands of ARMN disappeared at higher ratios. FDSDs exhibited distinct nature of bonding compared to respective SLVPs and PMs.

Keywords: artemisinin, solubility, dissolution, solid dispersions, Korsmeyer-Peppas model

Artemisinin (qinghao, ARMN) is a naturally occurring stage specific compound with impressive blood schizonticidal and gametocytocidal activity (1–3), derived from aerial parts of plant *Artemisia annua*, causing a rapid arrest and effective treatment against drug-resistant *Plasmodium falciparum* strains within the nanomolar range (4) during malaria, which still is the most prevalent and most devastating disease in the tropics. Late stage ring parasites and trophozoites are more susceptible to artemisinin than schizonts or small rings. Unlike other antimicrobial agents, they do not possess nitrogen containing heterocyclic rings, instead, they have sesquiterpene trioxane lactone containing a peroxide bridge, which is responsible for killing intraerythrozoites. At present, ARMN holds importance in the current antimalarial campaign, as the continuous infestation and spread of resistance to antimalarial drugs among parasites is posing a serious threat of an increase in mortality rate. Numerous solid dispersion systems have been demonstrated in the pharmaceutical literature to improve the solubility and dissolution properties of poorly water soluble drugs (5–8).

Succinic acid (SUC) is a safe neutraceutical, which has been used to enhance the solubility of

* Corresponding author: e-mail: gmdogar356@gmail.com; mobile: +92-314-2082826; fax: +92-992-383441

various pharmaceuticals like rofecoxib (9), acetaminophen and theophylline (10, 11), nordazepam (12), ibuprofen (13) and griseofulvin (14). SUC has been used as an excipient for the enhanced colon-specific drug delivery (15). In addition, SUC provided the fastest rate of release in the colonic fluid compared to citric, tartaric or malic acid (16). Artemisinin solid dispersions have been studied with polyvinylpyrrolidone (17, 18), nicotinamide (19), Eudragit (20), hydroxypropylmethylcellulose, polyethyleneglycol 6000 (21), artemether with polyvinylpyrrolidone (22) and dihydroartemisinin with polyvinylpyrrolidone (23). To our knowledge, there is no report available about investigation of ARMN-SUC solid dispersions at the moment.

To find the release mechanism by dissolution studies, various models like zero-order, first order, Higuchi's and Korsmeyer-Peppas equations (24, 25) were applied to dissolution data. In zero order, the drug release is independent of its concentration (26). A first order drug release depends on drug concentration (27). The Higuchi model indicates Fickian drug release from a matrix (28). In Korsmeyer-Peppas model (29), the release exponent (n) was calculated from this model. The n = 1 indicates a release rate independent of time corresponding to zero order or case II transport, n = 0.5 stands for Fickian diffusion and n > 1 shows a super case II transport (30, 31).

Because of poor water-solubility and dissolution rate nature of artemisinin, the main objective of this work was to improve its solubility and release kinetics using different models *via* preparing solid dispersions by solvent evaporation and freeze drying methods.

MATERIALS AND METHODS

Materials

Artemisinin (Alchem, New Delhi, India), methanol (Sigma-Aldrich, Germany), succinic acid (Merck, Germany), sodium hydroxide (Merck, Germany), potassium bromide (FTIR grade, Fisher Chemicals, USA), acetone (Merck, Germany), starch (Rafhan Maize, Pakistan), lactose (DMV International, The Netherlands), magnesium stearate (Royal Tiger Products, Taiwan). Demineralized water was used for the dilution of various samples and also as the dissolution media.

Artemisinin assay

ARMN concentration measurements were carried out by following the method described previously (32), after appropriate dilution with demineralized water, adding 0.2% sodium hydroxide and heating at 40°C for 30 min. The concentration of ARMN was determined at 290 nm with a UV spectrophotometer (JENWAY, 6405 UV/ VIS, UK).

Preparation of physical mixtures (PMs)

Physical mixtures of ARMN and SUC were prepared at drug-carrier ratios 1 : 1, 1 : 4, 1 : 6, 1 : 8 and 1 : 10, respectively, by soft grinding to complete mixture with the glass pestle and mortar, afterwards, passed through the sieve (US 180 µm) and transferred to desiccators at 25°C under P_2O_5 till further use.

Preparation of solid dispersions by solvent evaporation method (SLVPs)

SLVPs were prepared using ARMN and SUC at 1 : 1, 1 : 4, 1 : 6, 1 : 8 and 1 : 10 weight ratios, respectively, by dissolving the drug and SUC in 100 mL of methanol. This solution was shaken on orbit shaker for 4–5 h at 150 rpm (25°C). Methanol was removed in rotary evaporator. These solid dispersions were pulverized, passed through 180 µm (US) mesh sieve and were transferred into colored glass bottles and stored in desiccators under the same set of conditions as that of physical mixtures till further analysis.

Preparation of freeze dried solid dispersions (FDSDs)

FDSDs were prepared using drug and carrier according to the same ratios as in SLVPs at 1 : 1, 1 : 4, 1 : 6, 1 : 8 and 1 : 10 weight ratios by dissolving ARMN and SUC in 100 mL of methanol. This solution was shaken on orbit shaker for 4–5 h at 150 rpm (25°C). Methanol was removed and 20 mL of demineralized water was added and shaken for 30 min. Afterwards, this solution was frozen at –70°C in electronic deep freezer and dried in lyophilizer. Freeze dried solid dispersions pulverized through 180 µm mesh sieve, were transferred in amber glass bottles and stored in desiccators containing P_2O_5 till further analysis.

X-ray diffraction (XRD) studies

X-ray powder diffraction of ARMN, SUC, their PMs, SLVPs and FDSDs were performed using a Siemens D500 apparatus. Measurement conditions included target CuK_α, voltage 40 KV and current 30 mA. The XRD system consisted of diverging, receiving, receiving and anti-scattering slits at angle of 1°, 1°, 1° and 0.15°, respectively. Jade 6.0 program (Materials Delta Inc. USA) was used for data processing. Patterns were obtained using a step width of 0.04° 2θ between 5 and 50°C.

Fourier transform infrared spectrophotometric (FTIR) analysis

Fourier-transform infrared (FTIR) spectra were obtained on a Shimadzu-8400S (Japan) apparatus, using the KBr disc method (0.5–1% of sample in 200 mg KBr disc) on cold press adjunct. The scanning was run at 450–4000 cm^{-1} with resolution range 1 cm^{-1}. Calibration of the instrument was performed periodically before taking spectra.

Differential scanning calorimetric (DSC) analysis

Differential scanning calorimetric (DSC) analyses of PMs, SLVPs and FDSDs were performed using Setaram 131 instrumentation. The samples were heated at the rate of 10°C/min from 40 to 290°C under dry nitrogen gas purge. Cell constants were calibrated with indium. All measurements were conducted in sealed non-hermetic aluminum pans. Typical sample weight was 5–10 mg.

Phase solubility studies

For phase solubility studies, excess quantity of each sample was taken in a 25 mL vial containing 10 mL of demineralized water. It was then placed in shaking incubator at 37 ± 1°C at 100 rpm for five days. Samples were centrifuged at 6000 rpm for 15 min and withdrawn with a syringe equipped with a 0.40 µm syringe filter. All samples were diluted to a proper concentration range and assayed for ARMN. A control experiment was also performed with pure ARMN to confirm any degradation in all used solvents. All samples were analyzed in triplicate. The apparent stability constants (K_s) of the solid dispersions were calculated from the slope of the phase solubility diagrams according to the following equation (24):

$$K_s = \frac{\text{Slope}}{S_o\ (1 - \text{slope})}$$

where S_o was the equilibrium solubility of ARMN at 37°C in the absence of SUC.

Dissolution studies

Drug release was measured using dissolution apparatus (Tablet dissolution tester GDT-7TV3, Galvano Scientific, Pakistan) at 37°C and 100 rpm, the paddle apparatus (consisting of six recipients) for high volume by using demineralized water as dissolution medium instead of a buffer (32). At predetermined time intervals (5, 15, 30, 60, 90, 120, and 180 min), 5 mL of sample were taken and replaced with the same volume of fresh solvent. Samples were assayed according to analytical procedure of AEMN described as above.

Release kinetic analysis

The release data were evaluated by zero-order, first-order, Higuchi, and Korsmeyer-Peppas models. The best model was selected based on the R^2 value.

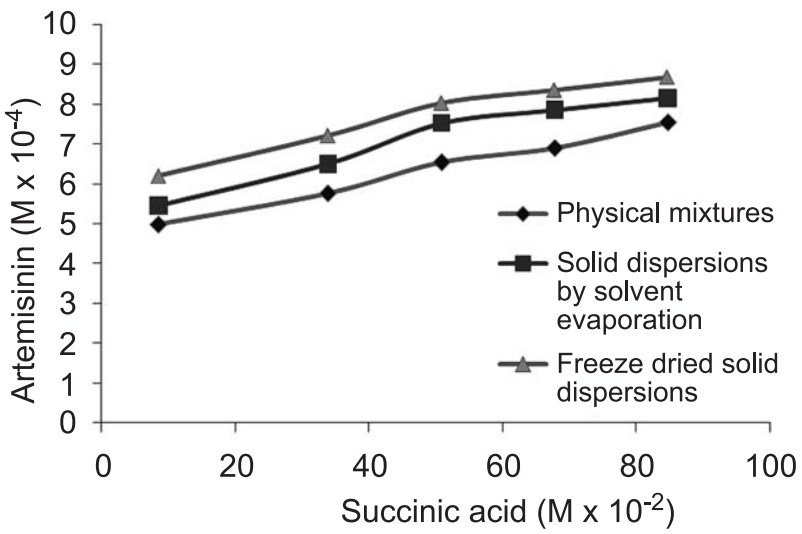

Figure 1. Phase solubility of artemisinin in physical mixtures, solvent evaporated solid dispersions (SLVPs) and freeze dried solid dispersions (FDSDs).

Table 1. Phase solubility, relative dissolution rate (RDR) and DSC results of ARMN, PMs, SLVPs and FDSDs

ARMN : SUC ratios		ΔH (J/g)	Melting onset (°C)	Peak temperature (°C)	RDR at different times (min)						Solubility ($M \times 10^{-4}$)
					5	15	30	60	90	180	
ARMN	–	44.15	149.11	151.03	–	–	–	–	–	–	0.036
PM	1 : 1	28.2	140.7	144.02	3.05	19.3	8.89	6.73	4.89	3.05	4.991
SLVP	1 : 1	19.82	139.3	142.9	3.22	20	10.1	7.4	5.78	3.54	5.435
FDSD	1 : 1	27.25	140.1	144.53	3.89	22.6	10.2	7.88	6.17	3.8	6.189
PM	1 : 4	7.414	140.4	143.24	3.39	20.9	8.99	6.78	5.09	3.24	5.766
SLVP	1 : 4	5.168	138.6	141.64	3.22	21.3	10.7	7.62	5.96	3.89	6.494
FDSD	1 : 4	3.506	139.9	142.63	4.06	23.2	11.3	8.04	6.25	3.92	7.207
PM	1 : 6	27.27	180.7	183.65	3.39	20.6	8.79	6.93	5.28	3.4	6.543
SLVP	1 : 6	41.41	182.2	184.36	4.57	24.6	11.5	7.88	6.35	4.04	7.514
FDSD	1 : 6	32.18	180.3	183.31	4.57	26	10.4	7.47	6.67	4.16	8.031
PM	1 : 8	41.18	182.2	184.74	3.89	24.6	9.79	7.31	5.42	3.48	6.895
SLVP	1 : 8	19.68	182.8	184.66	4.74	24.3	12.7	8.76	7.02	4.38	7.847
FDSD	1 : 8	28.42	182.5	184.64	4.74	30.2	12.1	8.15	6.25	4.02	8.356
PM	1 : 10	32.81	183.9	185.73	3.89	24	10.3	7.68	5.6	3.64	7.537
SLVP	1 : 10	23.19	185.3	187.16	5.08	26	11.5	8.19	6.7	4.18	8.151
FDSD	1 : 10	34.4	184.3	186.22	5.59	29	10.8	8.05	6.78	4.3	8.681

RESULTS AND DISCUSSION

Phase solubility studies

The phase solubility diagram was drawn between molar concentrations of ARMN *versus* SUC as shown in Figure 1. Solubility of ARMN was calculated as a function of SUC concentration in demineralized water. It was noted that the solubility of ARMN was enhanced with the increase in SUC concentration. Aqueous solubility of pure ARMN was found to be 0.036×10^{-6} M. Solubility of physical mixtures was found to be 7.53×10^{-4} M at 84.6×10^{-2} M of SUC concentration, whereas solubility enhancement in case of SLVPs was found to be 8.15×10^{-4} M. FDSDs exhibited more solubility than either PMs or SLVPs. Phase solubility of FDSDs at SUC concentration (84.6×10^{-2} M) was 8.68×10^{-4} M. Calculations of stability constant values for PMs, SLVPs and FDSDs yielded 12.1×10^{-2} M, 9.5×10^{-2} M and 9.3×10^{-2} M, respectively (Fig. 1 and Table 1).

Solubility of the active pharmaceutical ingredient is one of the important factors taken into consideration while developing its dosage form. Class-II drugs of BCS need improvement of their solubility to optimize their bioavailability. Phase solubility of pure ARMN and its solid dispersions were measured in demineralized water at 37°C (Table 1). SUC acid is known as a neutraceutical agent and as an excipient (9, 10–15). Keeping in mind this ability of SUC, it was applied for artemisinin. Physical mixtures produced substantial increase in the phase solubility compared to pure ARMN. They exhibited a linear increase in phase solubility of ARMN with increased SUC content. SLVPs produced further increase in solubility, i.e., 1.47–2.21 folds compared to respective PMs, that is due to interaction among drug and carrier as well as the solubilizing effect of SUC. This increase in solubility is comparable to itraconazole (33). FDSDs showed the highest solubility compared to corresponding SLVPs and PMs, respectively, while stability constant values were opposite in order. This is in accordance with respective dissolution profile discussed in previous section. Freeze drying method was found most effective for enhancing drug solubility perhaps due to an increase in surface area and the surface free energy (34–36). The slopes were lower than one in all PMs, SLVPs and FDSDs that indicate phase solubility profile was typical A_L type, which signifies that ARMN and SUC combined in 1 : 1 molar ratio similarly to diazepam (37). Our results are different from fluoxetine HCl in which SUC combined in 2 : 1 ratio, which resulted in double equilibrium solubility (38) and also different from solid dispersions of ARMN with nicotinamide, in which solubility and stability constant were the highest in FDSDs followed by SLVPs and PMs, respectively (19). Lower stability in FDSDs compared to SLVPs may be due different type of bonding reflected by our FTIR results. The high aqueous solubility of solid dispersions is attributed to high solubilizing effect of SUC similar to parabens (39). These data are consistent

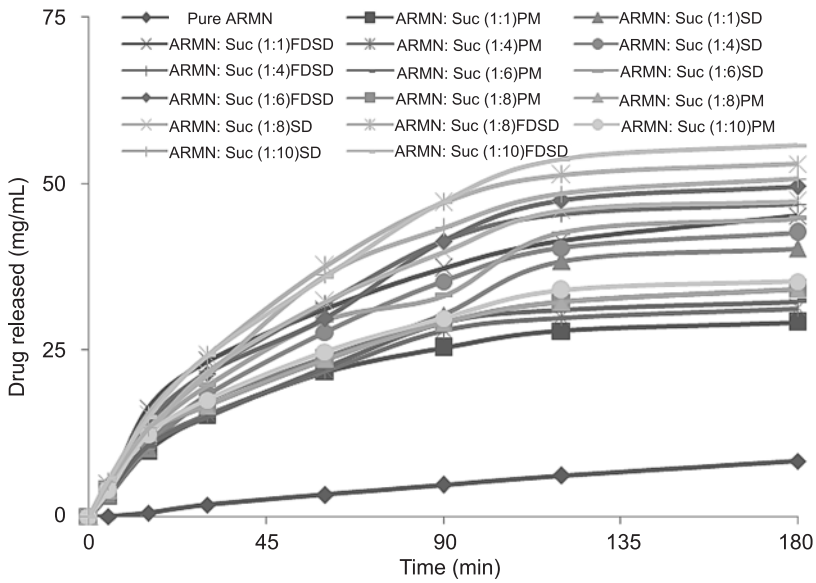

Figure 2. Dissolution curves for various formulations (ARMN – artemisinin, Suc – succinic acid)

with our XRD data, where degree of crystallinity in ARMN was reduced with enhanced SUC contents.

Dissolution profile

Physical mixtures exhibited 3.51–4.25 times higher dissolution rate than ARMN alone in demineralized water (Fig. 2.). Dissolution rate of physical mixtures increased with the rise of SUC content. SLVPs exhibited higher rate of dissolution (37.82–40.71%) than respective PMs. They exhibited 4.84 (1 : 1), 5.13 (1 : 4), 5.38 (1 : 6), 5.70 (1 :8) and 5.99 (1 : 10) times higher dissolution rate than ARMN alone, respectively. They also showed maximum dissolution rate at 1 : 10 ratio similar to corresponding PMs (Fig. 2). FDSDs exhibited the highest release rate at all ratios compared to corresponding PMs (52%) and SLVPs (12%). They showed gradual increase in dissolution rate with rise in SUC amount from 1 : 1–1 : 10 ratios, i.e., 5.44, 5.65, 5.97, 6.47, 6.60 times higher dissolution rate than ARMN alone, respectively (Fig. 2.). Relative dissolution rate (RDR) determined artemisinin solubility at different time periods in the dissolution media. The values of RDR were the highest at 15 min but it decreased with time and nearly reached to unchangeable rate after 180 min.

Dissolution rate of ARMN was increased as a function of SUC content in physical mixtures similarly to griseofulvin, where physical mixtures of 10% griseofulvin with 90% SUC showed increased dissolution rate compared to pure compound (14). This effect was attributed to increased microenvironmental solubilizing effect of SUC similar to urea (40). However, this effect was only of partial importance, because SLVPs and FDSDs showed enhanced dissolution rate than our PMs and revealed extremely fine crystals of ARMN. This was shown in XRD patterns of dispersed system, where intensity of peaks were reduced but identical crystalline structures of ARMN and SUC were observed.

The Higuchi model showed the lowest fitting values for all of the formulations. Pure ARMN followed the first order release signifying that dissolution rate is directly proportional to drug concentration in formulation. All the samples of physical mixtures fitted best in the Korsmeyer-Peppas model reflecting Fickian diffusion of drug from matrices. A release of ARMN from SLVPs was concentration dependent at 1 : 1–1 : 6 ratios, whereas at higher ratios the erosion of drug was proportional to the surface area and diameter of drug unit. FDSDs showed variable release depending upon drug-carri-

Table 2. Kinetic analysis of dissolution data.

Formulations	Zero order			First order	Higuchi	Korsmeyer-Peppas
	K_o	$T_{25\%}$ (min)	R^2	R^2	R^2	*n*
Pure ARMN	0.049	513.664	0.9898	0.9922	0.9865	0.900
ARMN : SUC (1: 1) PM	0.214	116.644	0.6308	0.7354	0.9608	0.444
ARMN : SUC (1 : 1) SD	0.279	89.455	0.8062	0.8988	0.9771	0.544
ARMN : SUC (1 : 1) FDSD	0.323	77.442	0.6515	0.8066	0.9684	0.448
ARMN : SUC (1 : 4) PM	0.229	109.154	0.6569	0.7653	0.9654	0.455
ARMN : SUC (1 : 4) SD	0.303	82.575	0.7742	0.8881	0.9723	0.526
ARMN : SUC (1 : 4) FDSD	0.342	73.040	0.7101	0.8628	0.9662	0.487
ARMN : SUC (1 : 6) PM	0.237	105.672	0.6836	0.7909	0.9656	0.471
ARMN : SUC (1 : 6) SD	0.313	79.783	0.7619	0.8809	0.9804	0.509
ARMN : SUC (1 : 6) FDSD	0.352	71.086	0.7774	0.9084	0.9739	0.526
ARMN : SUC (1 : 8) PM	0.247	101.175	0.6502	0.7681	0.9712	0.447
ARMN : SUC (1 : 8) SD	0.342	73.146	0.7363	0.8803	0.9708	0.501
ARMN : SUC (1 : 8) FDSD	0.388	64.393	0.7056	0.8839	0.9627	0.487
ARMN : SUC (1 : 10) PM	0.257	97.336	0.6602	0.7817	0.9705	0.453
ARMN : SUC (1 : 10) SD	0.366	68.225	0.7368	0.8922	0.9664	0.505
ARMN : SUC (1 : 10) FDSD	0.400	62.537	0.7582	0.9189	0.9729	0.514

er ratios, i.e., drug release was concentration dependent at 1 : 1 ratio, it transport was anomalous at 1 : 4 ratio whereas the erosion of drug was related to surface area and diameter of drug unit at 1 : 8 and 1 : 10 ratios.

Release kinetics analysis

The percent release data were fitted to several release models including zero-order, first-order, Higuchi, and Korsmeyer-Peppas models. On the basis of the highest coefficient of determination (R^2), kinetic analysis elaborates that the best fit model for dissolution data of all formulations is Higuchi's, showing the diffusion dependent release of drug from these formulations (Table 2). The role of diffusion in the release of drug from these formulations is further supported by the value of *n* obtained from the curve of Korsmeyer-Peppas model. The *n*-values are in the range of 0.444–0.544 indicating the involvement of Fickian diffusion in the release of drug from all formulations. Moreover, the value of drug release rate constant (K_0) obtained from zero order model shows that there is accelerated release of drug from formulations with the increase in concentration of SUC irrespective of technique employed for solubility enhancement, that's why ARMN : SUC (1 : 10) showed the highest rate of drug release and the rate of drug release was the slowest from ARMN : SUC (1 : 1). Dissolution curves for various formulations are shown in Figure 1, which shows that the most accelerated release of drug occurred from formulation ARMN : SUC (1 : 10) FDSD. Additionally, formulations prepared through FDSD exhibited the fastest release of drug followed by SD and then PM, thus, the methods used for formulation development can be organized (on the basis of drug release enhancing effect) as follows: FDSD > SD > PM. These results are further supported by the values of $T_{25\%}$.

Fourier transform infrared spectral studies (FTIR)

FTIR spectra of pure ARMN showed Fermi resonance of the symmetric CH_3 stretching with overtones of the methyl bending modes at 2963 cm^{-1}, C=O stretching at 1736 cm^{-1}, C-O-O-C bending (endoperoxide group) at 1123 cm^{-1}, C-O stretching at 1011 cm^{-1}, while SUC specifically produced O-H stretching at 2986 cm^{-1}, C=O stretching at 1701 cm^{-1} and C-O stretching at 1307 cm^{-1}, respectively.

FTIR spectra of physical mixtures showed shifting in O-H stretching vibrations of SUC i.e., 2961–2974 cm^{-1}, displaced carbonyl (C=O) stretching (1705–1728 cm^{-1}), slight displacement in endoperoxide bridge (C-O-O-C) stretching at 1118–1124 cm^{-1}. Stretching vibrations of C-O group representative of SUC at 1307 cm^{-1} showed slightly displaced peaks at 1310–1314 cm^{-1} while peak of C-O stretching representative of ARMN appeared only in 1 : 1 ratio at 1001 cm^{-1} and disappeared in all corresponding higher physical mixtures.

SLVPs produced O-H stretching vibrations closer to SUC (2963–2978 cm^{-1}), displaced C=O stretching (1703–1720 cm^{-1}), slight shifting in endoperoxide bridge (C-O-O-C) stretching (1116–1124 cm^{-1}) modes. Stretching vibrations of C-O group representative of SUC at 1307 cm^{-1} showed displaced peaks at 1306–1315 cm^{-1}, whereas peak of C-O stretching representing ARMN appeared only in 1 : 1 and 1 : 4 ratios at 1005 cm^{-1} and at 1008 cm^{-1}, respectively, while it disappeared in remaining ratios at higher SLVP mixtures.

FDSDs showed O-H stretching vibrations closer to SUC (2964–2982 cm^{-1}), more displaced C=O stretching (1697–1700 cm^{-1}) and slight shifting in endoperoxide bridge (C-O-O-C) stretching (1116–1126 cm^{-1}) modes. Stretching vibrations of C-O group, representative of SUC at 1307 cm^{-1}, showed displaced peaks at 1300–1311 cm^{-1} while peak of C-O stretching representative of ARMN appeared only in 1 : 1 and 1 : 4 ratios at 997 cm^{-1} and at 1002 cm^{-1}, respectively, while it disappeared in rest of the samples (Figs. not shown).

Physical mixtures revealed blue shifting in carbonyl stretching vibrations and C-O stretching peak characteristic of SUC (1307 cm^{-1}) appeared with slight red shifting and blue to red shifting in CH_3 stretching, indicating weak bonding interactions. SLVPs showed more displaced CH_3 stretching at lower ratios and exhibited O-H stretching characteristic of SUC at higher drug-carrier ratios. In addition, by increasing SUC content, carbonyl stretching frequency of SLVPs moved toward SUC. Furthermore, the C-O stretching vibrations characteristic of SUC (1307 cm^{-1}) appeared more distinct compared to PMs, while C-O stretching vibrations characteristic of ARMN (1011 cm^{-1}) disappeared at higher ratios (1 : 6–1 : 10). All this indicate enhanced interactions among ARMN and SUC in SLVPs. FDSDs, contrarily, showed red shifting in O-H stretching of succinic acid (not in PMs and SLVPs) and carbonyl group showed different kind of bonding by producing peak at lower frequency than both ARMN and SUC. In addition, they produced blue shifting in C-O stretching vibrations representative of SUC. Furthermore, C-O stretching vibrations representing ARMN showed higher blue shifting at lower ratios and disappeared at higher

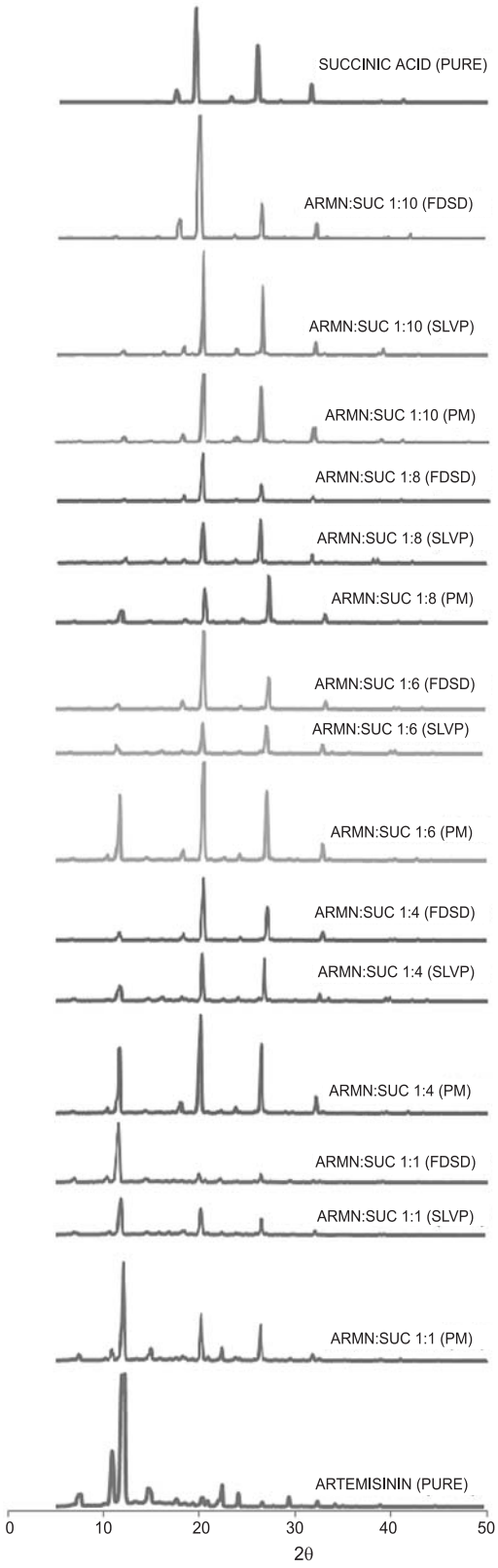

Figure 3. XRD spectra of artemisinin ARMN), succinic acid (SUC) and various preparations of artemisinin and succinic acid at drug-carrier ratios 1 : 1, 1 : 4, 1 : 6, 1 : 8 and 1 : 10

ratios (1 : 6–1 : 10). All this indicate that bonding interactions between carbonyl group of ARMN and hydroxyl group of SUC in FDSDs were of different nature compared to SLVPs and PMs, respectively. In our SLVPs and FDSDs, carbonyl group fitted stereochemically, because it finds its best position between 1720–1680 cm^{-1} (41). Furthermore, a disappearance of carbonyl stretching peak characteristic of ARMN and an appearance of carbonyl stretching peak representative of SUC at higher drug-carrier ratios also verified interaction between ARMN and SUC. Our samples at higher drug-carrier ratios showed a weak band of O-H group, which is part of the carboxyl group of SUC, similarly as reported previously (41). Displacement of stretching vibrations of C-O group (1011 cm^{-1}) representing ARMN was in the order: FDSDs > SLVPs > PMs, respectively. This peak disappeared at higher ratios correspondingly, which indicates that this group has strongly interacted with SUC, similarly to the hydrogen bonding imparted by nicotinamide with indomethacin (42) due to increased wetting ability of ARMN and solubilizing effect of the SUC. In addition, peak broadening in FTIR spectra were observed with an increase inSUC content for all PMs, SLVPs and FDSD, analogous to the carbamazepine (43). Band shifting at various functional groups, disappearance of C-O band and peak broadening are strong manifestations of interactions among ARMN and SUC. All preparations showed non-significant displacement in O-O stretching vibrations as well as stretching vibrations of endoperoxide bridge (C-O-O-C) that confirms the presence of antimalarial activity.

X-ray diffraction analysis

ARMN was observed as complete crystalline compound and XRD patterns produced strong diffraction peaks at 2θ of 10.96°, 12.20°, 14.76°, 20.44°, 22.40° and 24.12°. SUC also produced strong crystalline peaks in its XRD patterns at 2θ angle 20.12°, 26.24° and 31.68°, respectively (Fig. 3).

In physical mixtures of ARMN-SUC, a peak characteristic of ARMN at angle 2θ of 10.92° was displaced to 11.04° and showed decreased intensity with rise of SUC content. Similar behavior was exhibited by another peak of ARMN at angle 2θ of 12.20°. Characteristic peaks of SUC at angle 2θ of 20.12° was displaced from 20.08 to 20.24° and intensity at this angle increased with enhanced SUC concentration. Similarly, another characteristic peak of SUC at 2θ of 31.68° showed a displaced angle from 31.64 to 31.72° and gradual decrease in inten-

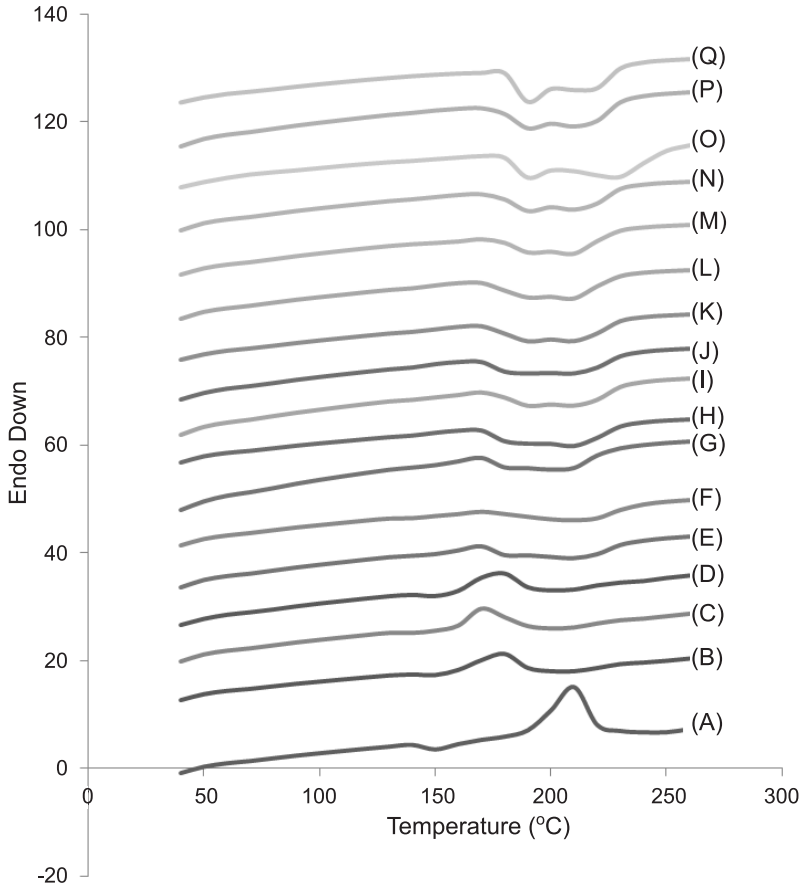

Figure 4. DSC thermograms of artemisinin (A), PMs of ARMN-SUC at 1 : 1 ratio (B), SLVPs at 1 : 1 ratio (C), FDSDs at 1 : 1 ratio (D), PMs at 1 : 4 ratio (E), SLVPs at 1 : 4 ratio (F), FDSDs at 1 : 4 ratio (G), PMs at 1 : 6 ratio (H) , SLVPs at 1 : 6 ratio (I), FDSDs at 1 : 6 ratio (J), PMs at 1 : 8 ratio (K), SLVPs at 1 : 8 ratio (L), FDSDs at 1 : 8 ratio (M), PMs at 1 : 10 ratio (N), SLVPs at 1 : 10 ratio (O), FDSDs at 1 : 10 ratio (P), succinic acid (Q)

sity with an increase in SUC content, as shown in Figure 3.

In SLVPs, a peak characteristic of pure ARMN at angle 2θ of 10.92° disappeared at all concentrations. Another characteristic peak at angle of 12.12° produced less than a half intensity compared to respective physical mixtures. Peaks at 14.76° were displaced to 15.28° having very low intensity at 1 : 4–1 : 6 ratios, while they disappeared at 1 : 6–1 : 10 ratios. Characteristic peaks of SUC at 2θ of 20.40° and at 2θ of 26.24° revealed intensity less than a half at 1 : 1–1 : 8 ratios but at 1 : 10 ratio this was almost doubled in relation to corresponding PMs. In addition, 2θ of 31.68° showed more displaced angle 2θ of 31.68–31.96° and about a half intensity than respective PMs.

FDSDs also produced no peak at 2θ of 10.92°. A peak at 12.16° exhibited more intensity than corresponding SLVPs at 1 : 1–1 : 8 ratios but showed lower intensity at 1 : 10 ratio. Another peak at 2θ of 14.88° was present only at 1 : 1 ratio, while it was absent at higher ratios. Peculiar feature of FDSDs was that a peak at 2θ of 18.32° appeared with lower intensity at 1 : 1–1 : 8 ratios than both its ingredients but at 1 : 10 ratio its intensity was more than both ARMN and SUC. Similar behavior was noted at 2θ of 20.28° but ratio was 1 : 8 and 1 : 10. Furthermore, angle 2θ of 31.68° produced a shifted angle from 31.68 to 31.88° with the lowest intensity compared to respective SLVPs and PMs.

ARMS as well as SUC was found to be completely crystalline in its XRD patterns. X-ray diffraction studies of various preparations showed altered patterns, which signify bonding interactions among ARMN and SUC depending upon extent of alterations. Physical mixed samples showed dis-

placed angles and decreased intensities that indicate bonding interactions, which agrees with solubility, dissolution and FTIR findings. Peak characteristic of ARMN at 10.92° disappeared in all SLVPs and FDSDs compared to the presence in PMs, indicating comparatively stronger interactions. Another characteristic peak at 12.12° in SLVPs showed less than half intensity and peak at 15.28° disappeared at higher drug-carrier ratio verifying these interactions. SLVPs showed the lowest peak intensities compared to respective FDSDs and PMs at 12.24, 20.12, 31.68° and most displaced angles at 14.76° that indicate somewhat stronger interactions in ARMN area and weaker interactions of SUC area. The increased solubility and dissolution rate of ARMN with SUC in SLVPs was attributed to glass dispersions so as the reason in the dissolution enhancement of rofecoxib by employing citric acid (9).

FDSDs showed variable results especially at higher drug-carrier ratios, i.e., the lowest intensity in 1 : 10 ratio at 12.24° while at other ratios it was higher than PMs; similarly, it had the highest peak intensity at 31.68° even more than SUC itself, which is characteristic of synergy. Such behavior was also noted at 20.12° when FDSDs produced the highest intensity even more than ARMN and SUC at 1 : 6–1 : 10 ratios. This synergistic effect verifies different type of bonding in FDSDs compared to SLVPs and PMs at higher ratios agrees with our FTIR spectra. In addition, FDSDs showed higher intensity than corresponding SLVPs in 1 : 1–1 : 8 ratios at 31.68° indicating that SUC made stronger bonding interactions compared to SLVPs, which agrees with our solubility and dissolution profile. This behavior was similar to flurbiprofen and ARMN with nicotinamide in solid dispersions, respectively (19, 44, 45), at low drug content ratio, because at higher carrier content solid dispersion behavior turned more towards the SUC due to the possible fine dispersion of ARMN in the carrier content. Hence, rearranged angles, synergistic effect and disappearance of some crystalline peaks verify the drug-carrier interactions.

Differential scanning calorimetry

ARMN showed melting onset temperature at 149.11°C and peak temperature at 151.03°C while ΔH value was 44.15 J/g. SUC produced ΔH value of 79.84 J/g, melting onset melting temperature of 186.88°C having peak temperature at 188.30°C. Enthalpy changes (ΔH), peak temperature and melting onset melting temperatures of physical mixture, solid dispersion and freeze dried solid dispersion are given in Table 1. Physical mixtures showed two kinds of melting temperatures i.e., one near melting temperature of ARMN at drug-carrier ratio 1 : 1–1 : 4, other near melting temperature of SUC i.e., at drug-carrier ratio 1 : 6–1 : 10. Physical mixtures at 1 : 1–1 : 4 ratios showed melting onset temperature 138.6–140.7°C and peak temperature 141.64–144.53°C whereas at 1 : 6–1 : 10 ratios melting onset temperature 180.7–183.9°C and peak temperature 183.65–185.73°C. All samples showed ΔH values lower than that of ARMN.

SLVPs exhibited higher melting temperatures than respective PMs, i.e., melting onset temperatures at 182.2–185.3°C and peak temperature at 184.36–187.16°C for 1 : 6–1 : 10 ratios and ΔH values 19.68–41.41 J/g, respectively. FDSDs showed lower melting temperatures than corresponding SLVPs, i.e., melting onset temperatures 180.31–184.30°C, while peak temperatures 183.31–186.22°C and enthalpy change values 28.42–34.4 J/g, respectively (Fig. 4).

Differential scanning thermograms revealed decreased melting onset and peak temperatures of ARMN at 1 : 1–1 : 4 ratios, while at 1 : 6–1 : 10 ratios melting onset and peak temperatures were near those of SUC but lower than those of SUC in all preparations of PMs, SLVPs and FDSDs. SLVPs exhibited the lowest melting temperatures followed by FDSDs and PMs, respectively, at 1 : 1–1 : 4 ratios, whereas FDSDs revealed lower melting temperatures than corresponding SLVPs at 1 : 6–1 : 10 ratios. It indicates the presence of stronger bonding interactions at 1 : 6–1 : 10 ratios that coincide with XRD patterns, FTIR spectra and relative dissolution rate (RDR).

Similarly, enthalpy changes (ΔH) of all prepared samples of PMs, SLVPs and FDSDs were lower than those of ARMN and SUC. Enthalpy change (ΔH) values for all prepared samples of PMs, SLVPs and FDSDs at ratio 1 : 4 were found to be lowest than for all other samples, which indicates that thermal stability was the lowest at this ratio, while other ratios showed moderate thermal stability values but lower than those for ARMN as well as SUC. It might be due to masking effect of carrier and amorphization, as well as fine dispersion of ARMN as shown from the DSC thermograms and XRD spectra. In addition, FDSDs at 1 : 8–1 : 10 ratios exhibited higher ΔH values than corresponding SLVPs, which is in agreement with XRD spectra but opposite to stability constant, that is indicative of different nature of interactions among SUC and ARMN.

Decreased enthalpy values, shifting of melting temperatures and peak broadening in DSC thermograms confirm the interaction between drug and car-

rier that is supported by decreased peak intensities, displaced angles in XRD patterns, red and blue shifting of stretching frequencies in FTIR spectra, enhanced solubility and dissolution profile.

CONCLUSION

It can be concluded from the results that ARMN solubility and dissolution rate can be enhanced by preparing its freeze dried solid dispersions using SUC as solubility enhancer.

Acknowledgments

Authors are thankful to Higher Education Commission (HEC) of Pakistan for providing funding for research project No. 2550 due to which this work was possible and Hamaz Pharmaceutical Company, Multan, Pakistan for providing facility of some instruments.

REFERENCES

1. Dutta G.P., Mohan A., Tripathi R.: J. Parasitol. 76, 849 (1990).
2. Sher M., Hussain G., Hussain M.A., Akhtar T., Akram M.R., Paracha R.N., Murtaza G.: Afr. J. Pharm. Pharmacol. 6, 2424 (2012).
3. Murtaza G., Ahmad M., Madni M.A., Asghar M.W.: Bull. Chem. Soc. Ethiop. 23, 1 (2009).
4. Khan S.A., Ahmad M., Murtaza G., Shoaib H.M., Aamir M.N., Kousar R., Rasool F., Madni A.: Latin Am. J. Pharm. 29, 1029 (2010).
5. Khan S.A., Ahmad M., Murtaza G., Aamir M.N., Kousar R., Rasool F., Zaman S.U.: Acta Pharm. Sin. 45, 772 (2010).
6. Ahmad M., Iqbal M., Akhtar N., Murtaza G., Madni M.A.: Pak. J. Zool. 42, 395 (2010).
7. FDA guideline (1987). Guidelines on General Principles of Process Validation, p. 4, US Food and Drug Administration. Maryland, USA.
8. Rasool F., Ahmad M., Khan H.M.S., Akhtar N., Murtaza G.: Acta Pol. Pharm. Drug Res. 67, 185 (2010).
9. Ahmad M., Ahmad R., Murtaza G.: Adv. Clin. Exp. Med. 20, 599 (2011).
10. Khiljee S., Ahmad M., Murtaza G., Madni M.A., Akhtar N., Akhtar M.: Pak. J. Pharm. Sci. 24, 421 (2011).
11. Khan M.I., Murtaza G., Awan S., Iqbal M., Waqas M.K.: Afr. J. Pharm. Pharmacol. 5, 143 (2011).
12. Aamir M.F., Ahmad M., Murtaza G., Khan S.A.: Latin Am. J. Pharm. 30, 318 (2011).
13. Ahmad M., Murtaza G., Akhtar N., Siddique F., Khan S.A.: Acta Pol. Pharm. Drug Res. 68, 115 (2011).
14. Chiou W.L., Niazi S.: J. Pharm. Sci. 65, 1212 (1976).
15. Nykanen P., Krogars K., Sakkinen M.: Int. J. Pharm. 184, 51 (1999).
16. Kaur K., Kim K.: Int. J. Pharm. 366, 140 (2009).
17. Ansari M.T., Haneef M., Murtaza G.: Adv. Clin. Exp. Med. 19, 745 (2010a).
18. Nijlen V.T., Brennan K., Mooter G.V.D.: Int. J. Pharm. 254, 173 (2003).
19. Ansari M.T., Pervez H., Shehzad M.T.: Pak. J. Pharm. Sci. 25, 447 (2012).
20. Hoa N.D., Long N.V.: Tap. Chi. Duoc. Hoc. 12, 17 (1999).
21. Long N.V., Hao D.N., Duong P.T.T.: Tap. Chi. Duoc. Hoc. 8, 15 (1999).
22. Ansari M.T., Karim S., Ranjha N.M.: Arch. Pharm. Res. 33, 901 (2010b).
23. Ansari M.T., Sunderland V.B.: Arch. Pharm. Res. 31, 390 (2008).
24. Costa P., Lobo J.M.S.: Eur. J. Pharm. Sci. 13, 123 (2001).
25. Philip A.K., Pathak K.: AAPS PharmSciTech 7, E1 (2006).
26. Najib N., Suleiman M.: Drug Dev. Ind. Pharm. 11, 2169 (1985).
27. Desai S.J., Sing P., Simonelli A.P.: J. Pharm. Sci. 55, 1230 (1966).
28. Higuchi T.: J. Pharm. Sci. 52, 1145 (1963).
29. Korsmeyer R.W., Gurrny R., Doelker E.M.: Int. J. Pharm. 23, 25 (1983).
30. Ritger P.L., Peppas N.A.: J. Control. Release 5, 37 (1987).
31. Siepmann J., Peppas N.A.: Adv. Drug Deliv. Rev. 48, 139 (2001).
32. Ngo T.H., Michael A., Kinget R.: Int. J. Pharm. 138, 185 (1996).
33. Zhao S.S., Zeng M.Y.: Planta Med. 3, 233 (1985).
34. Schultheiss N., Newman A.: Cryst. Growth Des. 9, 2950 (2009).
35. Onyeji C.O., Omoruyi S.I., Oladimeji F.A.: Pharmazie 62, 858 (2007).
36. Pose-Vilarnovo B., Perdomo-Lopez I., Echezarreta-Lopez M.: Eur. J. Pharm. Sci. 13, 325 (2001).
37. Betageri G.V., Makarla K.R.: Int. J. Pharm. 126, 155 (1995).
38. Rasool A.A., Hussain A.A., Dittert L.W.: J. Pharm. Sci. 80, 387 (1991).
39. Childs S.L., Chyall L.J., Dunlap J.T.: J. Am. Chem. Soc. 126, 13335 (2004).

40. Nicoli S., Zani F., Bilzi S.: Eur. J. Pharm. Biopharm. 69, 613 (2008).
41. Goldberg H., Gibaldi M., Kanig J.L.: J. Pharm. Sci. 55, 482 (1966).
42. Mitsui K., Ukaji T.: Infrared spectra of some aqueous solutions. Research Reports of Ikutoku Technical University (1977).
43. Jain A.K.: Eur. J. Pharm. Biopharm. 68, 701 (2008).
44. Sethia S., Squillante E.: Int. J. Pharm. 272, 1 (2004).
45. Varma M.M., Pandi J.K.: Drug Dev. Ind. Pharm. 31, 417 (2005).

Received: 22. 07. 2013

Acta Poloniae Pharmaceutica – Drug Research, Vol. 71 No. 3 pp. 463–468, 2014 ISSN 0001-6837
Polish Pharmaceutical Society

STUDY OF COMPARATIVE BIOAVAILABILITY OF OMEPRAZOLE PELLETS

SABIHA KARIM[1]*, YUEN KAH HAY[2], SARINGAT H. BAIE[2], NADEEM IRFAN BUKHARI[1] and GHULAM MURTAZA[3]

[1]University College of Pharmacy, University of Punjab Lahore, Allama Iqbal Campus, Lahore-54000, Pakistan
[2]School of Pharmaceutical Sciences, Universiti Sains Malaysia, Pulau Penang-11800, Malaysia
[3]Department of Pharmacy, COMSATS Institute of Information Technology, Abbottabad 22060, Pakistan

Abstract: The objective of this study was to assess the bioequivalence between the omeprazole laboratory based formulation and the commercial formulation, Zimor® Rubio, Spain, considered as reference formulation. The experiment was carried out according to a 2-period, 2-sequence crossover design with a two week washout period. A validated high performance liquid chromatographic method was applied for *in vivo* experiments. It was observed that omeprazole contents were comparable in all formulations. To establish bioequivalence, 90% confidence intervals (CI) for the differences of total AUCs of the test and reference formulations were calculated. The 95% CI ratio of the AUC within 0.80 to 1.25 was considered as bioequivalent. The carryout effect was investigated prior to assessing the bioequivalence of the two formulations.The test formulation of omeprazole was found to be comparable with the reference formulation (Zimor®) with regard to bioavailability.

Keywords: pellets, omeprazole, HPLC method, bioequivalence, Zimor®.

In vitro and *in vivo* characterization of a prepared multiparticulate formulation in terms of size distribution, dissolution and drug release is valuable during the formulation developmental stage of pharmaceutical products (1, 2), since absorption of drug is directly affected by the size of formulation. A number of variables affecting the *in vitro* and *in vivo* performance can be investigated. These, in turn, provide the basis for formulating a product with the required drug characteristics. However, *in vitro* studies, such as dissolution, cannot directly predict the *in vivo* performance of formulated product. Therefore, it is essential for a formulation to be verified through *in vivo* testing after satisfactory *in vitro* release profile has been obtained (3).

The development of delayed release omeprazole pellets with satisfactory *in vitro* release profile has been evaluated in our previous presentation (4). On the basis of their satisfactory *in vitro* dissolution tests, this bioavailability study was aimed to evaluate the test formulation in comparison with reference capsule formulation, Zimor® 20 mg in rabbits.

EXPERIMENTAL

Chemicals, solvents and materials

Omeprazole powder was purchased from Cornileus. Chloramphenicol (internal standards for omeprazole) was obtained from Hangzhou Garden Enterprise, China. Most of the chemicals and solvents used in this study were of analytical grade. Methanol, acetonitrile, glacial acetic acid, dichloromethane, crospovidone, polyvinylpyrrolidone (PVP) K90 and K30, lactose monohydrate, sodium lauryl sulfate, Avicel PH 101 and disodium hydrogen orthophosphate were purchased from Merck (Germany).

Preparation of omeprazole pellets

The sieving-spheronization and extrusion-spheronization approaches were used to prepare pellet formulations of omeprazole (F1 to F21) (Table 1) as described previously (4). Variable concentrations of microcrystalline cellulose, lactose and polyvinylpyrrolidone were employed keeping the amount of

* Corresponding author: e-mail: sabihakarim@yahoo.com; phone: +92-334-4309300; fax: +92-992-383441

Table 1. Composition of test formulation of omeprazole (F21) pellets [microcrystalline cellulose (MCC), polyvinypyrrolidone (PVP)].

Formulation Code	Drug (omeprazole)	MCC	Lactose	PVP (K30)	Sodium lauryl sulfate	Polyethylene glycol Grade (6000)	Water	Buffer
21	20 g	24 g	97.75 g	3.75 g	0.6 g	3.90 g	1 mL	7 mL

Table 2. Recovery, intraday and inter-day precision and accuracy of omeprazole from test formulation from standard solutions.

	Amount	Recovery (n = 3)		Intraday (n = 6)		Inter-day (n = 6)	
	(ng/mL)	Mean (%)	RSD (%)	Mean (%)	RSD (%)	Mean (%)	RSD (%)
From standard solution	120	100	1.85	100	1.55	100.76	1.35
	80	101	1.15	100.63	1.80	99.32	1.65
	50	99.8	3.85	98.60	2.87	98.25	3.35
	20	100	5.85	100	5.05	100.21	4.68
From rabbit plasma	120	98.32	3.59	97.35	4.54	96.98	5.43
	80	97.61	4.58	97.39	4.39	95.25	5.56
	50	95.87	4.89	96.06	4.79	95.16	5.59
	20	95.24	6.44	95.46	5.96	95.3	6.78

drug at a fixed level i.e., 20 g of omeprazole. The granulating liquid consisted of a mixture of water and phosphate buffer pH 8. The obtained dried pellets were stored in air-tight containers for further study.

In vitro dissolution test of pellets

In vitro dissolution test on 1 g of pellets from each batch was conducted in 1000 mL of phosphate buffer with pH 6.8 stirred at a rate of 100 rpm at 37.0C ± 0.5°C involving the withdrawal of samples at 10, 20, 30 and 45 min, followed by analysis using a UV/VIS spectrophotometer (Hitachi, Japan) at a wavelength of 300 nm (4). Each experiment was repeated in triplicate. The dissolution data were evaluated by applying different kinetic models (5–10). Based on *in vitro* dissolution data, the optimum formulation (F21) was opted (Table 1) and used for bioequivalence study.

HPLC method for omeprazole analysis

Preparation of omeprazole standard solutions

Stock solution of omeprazole was prepared in methanol in a concentration of 1 mg/mL. Working standard solutions of concentrations ranging from 2.5, 5.0, 10.0, 20, 40, 80, 160, 320, and 640 ng/mL were prepared by further diluting the stock solution with the mobile phase (5).

Mobile phase

The mobile phase to validate omeprazole method was prepared by mixing 0.05 M of disodium hydrogen orthophosphate and acetonitrile in the ratio of 65 : 35 (v/v). The pH of the mobile phase was adjusted to 6.5 with glacial acetic acid. The mobile phase was filtered and degassed using the same procedure as mentioned above (5).

Chromatographic conditions

The samples of omeprazole were eluted with isocratic mobile phase comprising of 0.05 M Na_2HPO_5 and acetonitrile (65 : 35 v/v) adjusted to pH 6.5. Elution time was 10 min. Flow rate was fixed at 1 mL/min. The volume of sample injected was 15 µL and detection was carried out at 302 nm (5).

Recovery, accuracy and precision of HPLC method

Standard solution of omeprazole in a concentration of 20, 50, 80 and 120 ng/mL were used to evaluate the recovery, intraday, inter-day accuracy and precision of the method. All the samples were analyzed using chromatographic conditions mentioned above.

For recovery of omeprazole from rabbit plasma, one mL aliquot of the plasma was taken in a glass tube with teflon lined screw cap, followed by the addition of 100 µL of 0.5 M disodium hydrogen phosphate, 100 µL of the internal standard solution (3 µg/mL of chloramphenicol in methanol) and 5 mL of dichloromethane. The mixture was vortexed for 30 s before centrifuging at 2000 rpm for 10 min. The organic layer was transferred into a reaction vial and evaporated to

dryness at 35°C under a gentle stream of nitrogen gas. The residue was reconstituted with 100 µL of mobile phase and 15 µL was injected into HPLC system.

The extraction recovery values were calculated by comparing the peak height of the standard after extraction with that of its standard solution at similar respective concentration. For recovery, the samples were analyzed in triplicate, while for intraday accuracy and precision each standard was analyzed 6 times in a single day and quantified at 4 data points calibrations, while for inter-day accuracy and precision each standard was analyzed 6 times for 5 consecutive days. Accuracy was expressed as a percentage of the drug while precision was expressed as relative standard deviation (RSD) (5). The validation parameters are presented in Table 2.

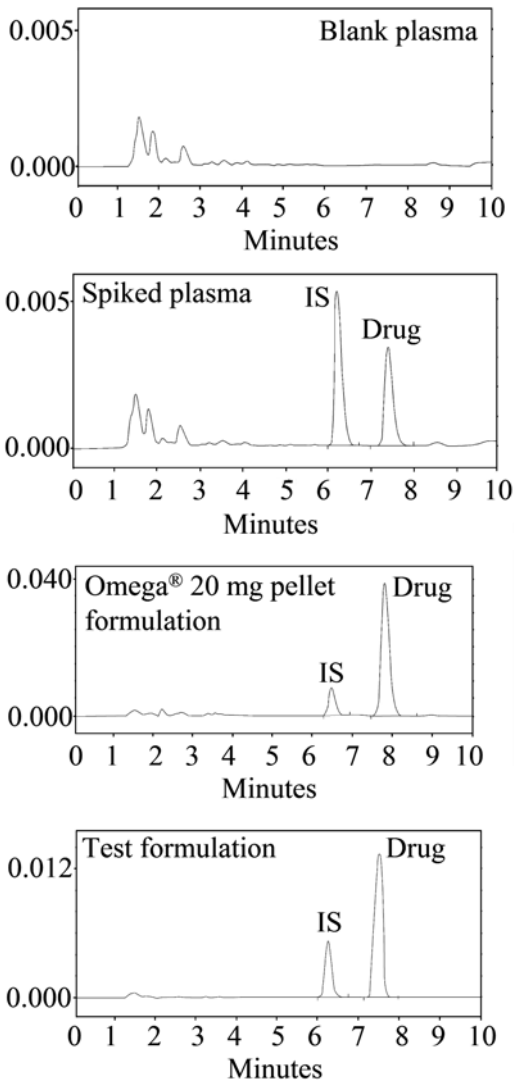

Figure 1. Chromatograms of blank plasma, spiked plasma, market formulation, and test formulation with 0.08 µg of omeprazole/mL, 3 µg internal standard (IS = chloramphenicol)

Preparation of samples of omeprazole test and market formulations for analysis

The 150 mg of omeprazole pellets (F21) equivalent to 20 mg omeprazole and a commercial formulations 150 mg granules equivalent to 20 mg omeprazole (Zimor®) were separately dissolved in 1000 mL of methanol followed immediately by further 50 times dilution with 0.01 M of disodium hydrogen orthophosphate (Na_2HPO_5) adjusted to pH 9.3. Chloramphenicol solution 20 µL of 3 µg/mL was used as an internal standard. Working samples were filtered through 0.55 µm syringe filter (Whatman, Maidstone, England) and kept in HPLC vials. The samples were analyzed in triplicate.

***In vivo* experiments**

Experimental animals

Twelve healthy white albino male rabbits weighing 3.45 ± 0.61 kg were used in the Animal House of the Universiti Sains Malaysia, Pulau Penang, Malaysia. Standard pellet diet (Gold Coin, Penang, Malaysia) and tap water were supplied *ad libitum*. The study protocol was approved by the Animal Ethics Committee, Universiti Sains Malaysia (USM/PPSF/50(014)Jld.2).

Study design

The bioavailability and pharmacokinetic studies were performed for the assessment of bioequivalence between the omeprazole laboratory based formulation, taken as test formulation (F21), and the commercial formulation, Zimor® Rubio, Spain, considered as reference formulation. The animals were randomly divided into two groups, each having six animals. The experiment was carried out according to a 2-period, 2-sequence crossover design with a two week washout period. The animals were fasted for 24 h prior to the administration of drug but had free access to water. After drug administration, no food was allowed for further 6 h but free access to water was allowed *ad libitum*.

In vivo experiments

The pellets of the laboratory formulation were filled into the hard gelatin capsules of size 4 containing 150 mg of pellets (20 mg of drug). The laboratory and the commercial preparations were administered orally to the respective animal group in each study period. The capsules were administered with the help of a 10 mL syringe. The tip of the

syringe was cut off so as to expose a hole big enough to fit a capsule. The rabbit mouth was opened with plastic probe and the syringe containing the capsule was inserted until it reached the back of the mouth. The capsule was pushed into the pharynx with the syringe plunger followed by 3 mL of water. The rabbit was observed for 20 min to ascertain that the capsule was swallowed.

Blood samples of 0.5 mL were withdrawn from the marginal ear vein into vacutainer tubes containing sodium heparin as a anticoagulant at zero min (pre dose), and at 0.5, 1.0, 2.0, 4.0, 6.0, 10.0 and 18.0 h. Blood samples were immediately centrifuged at 2500 rpm at 10°C for 10 min to separate the plasma. The plasma samples were then stored in plain vacutainer tubes at –80°C until analyzed. The drug concentrations in blood samples were determined using the validated HPLC method as reported previously (4).

The plot between drug concentration *versus* time was used to calculate the pharmacokinetic parameters, such as maximum plasma concentration (C_{max}), time to achieve C_{max} (T_{max}), area under plasma drug concentration curve (AUC) and elimination rate constant (K_e) (6).

Statistical analysis

All the samples were analyzed in triplicate and the results were presented as the mean ± SD calculated using SPSS version 13.0. The level of significance was set at 0.05.

RESULTS AND DISCUSSION

In vitro dissolution test of pellets

In this study, sieving-spheronization and extrusion-spheronization were found to be successful to formulate omeprazole pellets with high percent yield, narrow particle size distribution, and the achievement of the required release of drug i.e., greater than 80% within 45 min at pH 6.8. The dissolution profiles followed the first order equation with diffusion as prominent mode of drug release (4, 11–19).

HPLC method for omeprazole analysis

For the analysis of omeprazole, standard solutions were used to evaluate the linearity of the method. Standard curves were constructed between peak area *versus* concentration and linearity was evaluated by linear regression with correlation coefficient, $R^2 = 0.997$. The method was found linear in a range 2.5–640 ng/mL.

The chromatograms of the standard omeprazole and formulation (laboratory pellets) by using the present HPLC method are shown in Figure 1. The chromatograms show well-resolved peak without any interference. The average retention time for omeprazole was found to be 7.55 min and average retention time for internal standard (chloramphenicol) was 6.27 min. The recovery of omeprazole from excipients was 99.8–101.0% and relative standard deviation was ranged from 1.15 to 5.85%. The values for the intraday accuracy and precision were 98.60–100.63% and the relative standard deviation 1.55–5.05%. The omeprazole recovery from plasma was 95.24–98.32% with RSD of 3.59–6.44%. Interday accuracy values were 98.25–100.76% with relative standard deviation 1.35–4.68%.

The findings of the study indicated the reliability and reproducibility of the HPLC method used in this study. The recovery (n = 3), intraday and interday accuracy and precision (n = 6) were determined

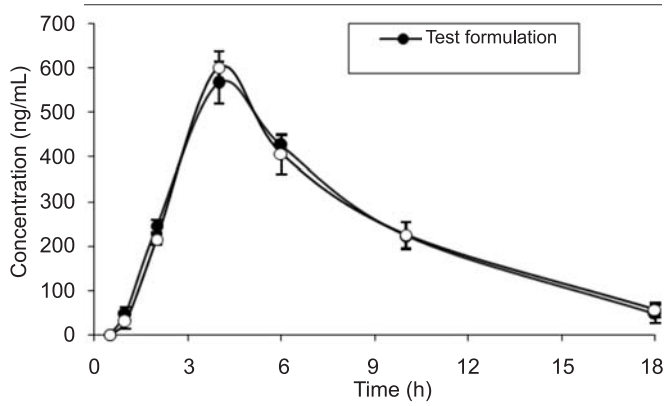

Figure 2. Plasma concentrations *versus* time profiles of test formulation of omeprazole (F21) and market formulation (Zimor®) (mean ± SD, n = 6)

using standard curves with linear regression. The recovery of extraction procedure for omeprazole and internal standard (chloramphenicol) were determined by comparing the peak heights obtained from extraction with that of aqueous drug solution of corresponding concentration without extraction. The recovery values of omeprazole from plasma were found to be 95.24–98.32%. The intraday and interday accuracy was 95.46–97.39 and 95.3–96.98%, respectively, with relative standard deviation less than 10%, hence within the acceptable limits (14, 15). The results are shown in Table 2. The results of the study indicated that the method was repeatable and accuracy was not compromised in within day and between day analyses.

Percentage contents of the developed and market formulations

A validated method was successfully applied to quantify omeprazole in different formulations. The percentage content of omeprazole was similar in the test formulation (98.87 ± 3.13) and the market products (98.21 ± 5.87). It means that the excipients and coating with Kollicoat 30DP of the pellets is suitable and produce comparable efficacy.

***In vivo* experiments**

In the present study, *in vivo* study was carried out to evaluate bioavailability and pharmacokinetics of the laboratory formulation. The laboratory formulations containing pellets of omeprazole were prepared and coated according to the optimum formulative ingredients and processing conditions. The laboratory formulation was characterized by their physicochemical properties. The laboratory formulation was found to be with appropriate characteristics and was suitable for further evaluation of *in vivo* studies. The laboratory formulation was compared for its bioequivalence to the commercial formulation, Zimor® available as granules filled in hard gelatin capsules.

Plasma drug level-time curve

The plasma concentration *versus* time profiles of test formulation and market product are shown in Figure 2. At pre-dose sampling time interval, the drug was not detectable in all the animals in both of the formulations. The concentration of the drug was undetectable at 2 h indicating a delayed release of the formulations. The rising curves for the test and reference formulation are superimposable. The declining curves were found to be similar. The products having similar pharmacokinetic profiles are called bioequivalent. The similarity in profiles of both the formations is suggestive of equivalence of the test formulation to the reference product. It means that the excipients used to prepare test formulation and method for pelletization were appropriate and could be used to prepare pelletized dosage form successfully.

Pharmacokinetic parameters

The plasma drug level-time curves of test and commercial preparations were the basis for computing the pharmacokinetic parameters of above formulations. Table 3 shows the pharmacokinetic parameters of these formulations, respectively. The extrapolated AUC was less than 15% indicating the reliable computation of $AUC_{0-\infty}$.

Bioequivalence testing

The C_{max} and $AUC_{0-\infty}$ were used to assess bioequivalence of laboratory (test) and reference formulations. Before proceeding for the bioequivalence, the carryover effect was investigated for C_{max} and $AUC_{0-\infty}$ (7). The carryover effect for both of the parameters, C_{max} and $AUC_{0-\infty}$ was not statistically significant ($p > 0.01$). The lack of carryout effect in C_{max} and $AUC_{0-\infty}$ validated the bioequivalence testing. The test formulation was bioequivalent to reference formulation as indicated by 95% CI ratios of 0.92 to 1.09 for C_{max} and 0.81 to 1.07 for AUC values of the formulations within the stipulated range

Table 3. Pharmacokinetic parameters of test and reference formulation of omeprazole (F21).

Parameter	Test formulation		Zimor®	
	Mean	SD	Mean	SD
C_{max} (ng/mL)	567.00	47.36	599.6	35.62
T_{max} (h)	4	0	4	0
AUC_{0-t} (ng.h/mL)	4345.45	212.75	4345.41	269.64
$AUC_{0-\infty}$ (ng.h/mL)	4687.015	233.77	4683.03	344.74
K_e (h^{-1})	0.189	0.036	0.168	0.03

of 0.80 to 1.25. The plasma level time curves and the pharmacokinetic parameters further support the bioequivalence of the two formulations under study.

CONCLUSION

It was observed that omeprazole contents were comparable in all formulations elaborating their similar quality. On the basis of above results, test formulation (F21) of omeprazole was found to be comparable with the reference formulation (Zimor®) regarding bioavailability.

Acknowledgments

This study was supported by the grant of School of Pharmaceutical Sciences University Sains Malaysia. Sabiha Karim is thankful to University of the Punjab, Lahore for the grant of Ph.D. study leave.

REFERENCES

1. Akhtar M., Ahmad M., Khan S.A., Murtaza G.: Afr. J. Pharm. Pharmacol. 6, 2613 (2012).
2. Mohammad S., Shah S.N.H., Nasir B., Khan Q., Aslam A., Riaz R. et al.: Afr. J. Pharm. Pharmacol. 6, 2629 (2012).
3. Murtaza G., Ahmad M., Akhtar N., Rasool F.: Pak. J. Pharm. Sci. 22, 291 (2009).
4. Karim S., Baie S.H., Hay Y.K., Bukhari N.I.: Pak. J. Pharm. Sci. 27, 425 (2014).
5. Yuen K.H., Choy W.P., Peng CY., Tan H.Y., Wong J.W., Yap, S.P.: J. Pharm. Biomed. 24, 715 (2001).
6. Shahzad M.K., Ubaid M., Murtaza G.: Tropical J. Pharm. Res. 11, 695 (2012).
7. Murtaza G., Ahmad M, Asghar M.W., Aamir M.N.: DARU J. Pharm. Sci. 17, 209 (2009).
8. D'Angelo G., Potvin D., Turgeon J.: J. Biopharm. Stat. 11, 35 (2001).
9. Sher M., Hussain G., Hussain M.A., Akhtar T., Akram M.R., Paracha R.N., Murtaza G.: Afr. J. Pharm. Pharmacol. 6, 2424 (2012).
10. Khan S.A., Ahmad M., Murtaza G., Shoaib H.M., Aamir M.N., Kousar R., Rasool F., Madni A.: Latin Am. J. Pharm. 29, 1029 (2010).
11. Murtaza G., Ahmad M., Madni M.A., Asghar M.W.: Bull. Chem. Soc. Ethiop. 23, 1 (2009).
12. Khan S.A., Ahmad M., Murtaza G., Aamir M.N., Kousar R., Rasool F., Zaman S.U.: Acta Pharm. Sin. 45, 772 (2010).
13. Ahmad M., Iqbal M., Akhtar N., Murtaza G., Madni M.A.: Pak. J. Zool. 42, 395 (2010).
14. Rasool F., Ahmad M., Khan H.M.S., Akhtar N., Murtaza G.: Acta Pol. Pharm. Drug Res. 67, 185 (2010).
15. Ahmad M., Ahmad R., Murtaza G.: Adv. Clin. Exp. Med. 20, 599 (2011).
16. Khiljee S., Ahmad M., Murtaza G., Madni M.A., Akhtar N., Akhtar M.: Pak. J. Pharm. Sci. 24, 421 (2011).
17. Khan M.I., Murtaza G., Awan S., Iqbal M., Waqas M.K., Rasool A., Asad M.H.H.B. et al.: Afr. J. Pharm. Pharmacol. 5, 143 (2011).
18. Aamir M.F., Ahmad M., Murtaza G., Khan S.A.: Latin Am. J. Pharm. 30, 318 (2011).
19. Ahmad M., Murtaza G., Akhtar N., Siddique F., Khan S.A.: Acta Pol. Pharm. Drug Res. 68, 115 (2011).

Received: 24. 07. 2013

Acta Poloniae Pharmaceutica – Drug Research, Vol. 71 No. 3 pp. 469–475, 2014 ISSN 0001-6837
Polish Pharmaceutical Society

IN VITRO – IN VIVO EVALUATION OF A NEW ORAL DOSAGE FORM OF TRAMADOL HYDROCHLORIDE – CONTROLLED-RELEASE CAPSULES FILLED WITH COATED PELLETS

DANUTA SZKUTNIK-FIEDLER[1]*, MONIKA BALCERKIEWICZ[1], WIESŁAW SAWICKI[2], TOMASZ GRABOWSKI[3], EDMUND GRZEŚKOWIAK[1], JAROSŁAW MAZGALSKI[4] and HANNA URJASZ[1]

[1]Department of Clinical Pharmacy and Biopharmacy, Poznan University of Medical Sciences, Św. Marii Magdaleny 14, 61-861 Poznań, Poland
[2] Department of Physical Chemistry, Medical University of Gdańsk, J. Hallera 107, 80-416 Gdańsk, Poland
[3]Polpharma Biologics, Trzy Lipy 3, 80-172 Gdańsk, Poland
[4]Polpharma S.A., Pelplińska 19, 83-200 Starogard Gdański, Poland

Abstract: The aim of this study was an *in vitro – in vivo* evaluation of a new oral dosage form of tramadol hydrochloride (TH), controlled-release capsules filled with coated pellets, 100 mg (TC), compared to the sustained release tablets, Tramal Retard®, 100 mg (TR). *In vitro* release study of both formulations showed a similar release profile of TH over 8 h (f2 was 52). *In vivo* study (single oral, 100 mg dose administration in 8 rabbits) showed that the amount of TH absorbed into the systemic circulation after TC and TR administration was also similar (90% CI for AUC_{0-t} and $AUC_{0-\infty}$ were 90–124% and 97–109%, respectively). However, a comparison of AUC_{0-t} of pharmacokinetics of TC and TR indicates significantly prolonged absorption and elimination processes of TH when the drug is given in controlled-release capsules filled with coated pellets. It was manifested by longer: mean absorption time ($p = 0.0016$), mean residence time ($p = 0.0268$), absorption half-life ($p = 0.0016$), elimination half-life ($p = 0.0493$) and lower: absorption rate constant ($p = 0.0016$), elimination rate constant ($p = 0.0148$) and total body clearance Cl/F ($p = 0.0076$). It may be concluded that the new TH formulation could be expected to have a more prolonged analgesic activity than commercial sustained release tablets.

Keywords: tramadol hydrochloride, controlled-release capsules, pellets, rabbits

Tramadol hydrochloride (TH) is a well-tolerated and effective synthetic, centrally acting analgesic used to treat moderate, severe, and chronic pain. It is a widely prescribed analgesic marketed in over 90 countries. The mean absolute bioavailability of TH after oral administration is approximately 70%, irrespectively of concomitant intake of food. TH has a linear pharmacokinetic profile within the therapeutic range (100–300 ng/mL). The short elimination half-life of 6 h necessitates administration of immediate-release (IR) TH preparations to patients every 4–6 h, which may be inconvenient for patients who require long-term treatment (1, 2). High-frequency dosage regimens can result in non-compliance and subsequent inappropriate plasma drug concentrations and inadequate analgesia (3). Pain management guidelines recommend the use of long-acting agents in patients with chronic pain as they provide sustained analgesia for 12 to 24 h (4, 5). Many oral sustained-release (SR) formulations of TH, including those with pellets, have been described (1, 2, 6–10). Compared to the traditional formulations, multiple-unit dosage forms with pellets are characterized by a relatively high surface area of drug release and a short diffusion way, which contributes to a more efficient use of the entire active ingredient. The pellets are less irritating to the mucous membrane of the digestive tract and they are more evenly distributed inside the stomach, which leads to a reduced risk of high local concentration and of adverse effects. What is important, it is the possibility of only partial destruction e.g., when crushing with teeth (11–16).

In order to improve pain therapy, our study proposes an alternative drug delivery system for TH – controlled-release capsules filled with coated pel-

* Corresponding author: e-mail address: d.szkutnik@wp.pl; phone: +48 (61) 6687853; fax: +48 (61) 6687855

lets (TC). The aim of our study was an *in vitro – in vivo* evaluation of this new oral dosage form of TH, developed at the Department of Pharmaceutical Technology, Medical University of Gdańsk, Poland, compared to the 100 mg SR tablets – Tramal Retard® (TR).

MATERIALS AND METHODS

Capsules filled with coated pellets

Pellet cores were prepared by wet granulation of powder mixture followed by spheronization of the extruded mass. On the basis of the initial experiments, the composition of pellet cores was determined as follows: TH 60.0%, microcrystalline cellulose**,** PH101 35.0% and glyceryl behenate 5.0%. A detailed process of preparing coated pellets with TH was described in our previous work (15).

Eighty pellets of 0.6–1.0 mm grain size with ethylcellulose film were enclosed in white hard gelatine capsules no. 2. Average mass of single capsule was 225 mg ± 1.7% and the contents of TH was 101.2 mg ± 1.3%.

In vitro release study

In vitro release study was performed using an automated Hansson Research Sr8+ basket apparatus dissolution tester (Hansson Research, Chatsworth, CA, USA) with an on-line UV/VIS spectrophotometer (Agilent 8453, Wilmington, USA; the wavelength – 272 nm, medium – 1000 mL of water at 37 ± 0.5°C, the concentrations of TH in the samples analyzed at 1, 2, 3, 4, 5, 6, 7 and 8 h; reference product SR tablets (Tramal Retard®, 100 mg) No. AN043 (Grünenthal, Aachen, Germany), all dissolution profiles – the mean of 12 dissolution tests performed under sink conditions.

Similarity of dissolution profile of the formulations was compared using model-independent method by linear regression at specified time points, and calculating a similarity factor f_2:

$$f_2 = 50\times\log\{[1 + (1/n)\sum_{t=1}^{n}(R_t - T_t)^2] - 0.5\times100\}$$

where: f_2 = the similarity factor, n = the number of time points, R_t = the mean percent drug dissolved of e.g., a reference product, and T_t = the mean percent drug dissolved of e.g., a test product (17). An f_2 value between 50 and 100 suggests that two dissolution profiles are similar.

In vivo study

Animals

The study was performed using a rabbit model: eight adult healthy New Zealand white rabbits (mean weight ± SD, 3.3 ± 0.2 kg). Animals fasted for 12 h prior to drug administration. During this time, free access to fresh water was provided. Twelve hours after drug administration, the animals were allowed access to the feed. The study was performed according to a protocol approved by the Local Ethical Committee at the University of Life Sciences in Poznan (agreement No. 71/2008), and was in accordance with the rules and guidelines concerning the care and the use for laboratory animal experiments (18).

Experimental design

Controlled-release capsules filled with coated pellets, 100 mg (TC) prepared in the Department of Pharmaceutical Technology, Medical University of Gdańsk, Gdańsk, Poland, and SR tablets Tramal Retard®, 100 mg (TR), (batch No. 292L01, Grünenthal, Aachen, Germany) were used for oral administration. A two-treatment, two-period, two-sequence, single-oral dose, randomized, crossover design was performed. The washout period was 14 days. All animals received *per os* one capsule or tablet (100 mg of TH, mean dose 30.32 ± 0.16 mg/kg) of each formulation. To ensure that the capsule or tablet was swallowed and entered the stomach, 20 mL of water were given to the rabbits at the same time as the capsule/tablet was administered.

To calculate absolute bioavailability (F) and mean absorption time (MAT) of TH two weeks after oral administration, all animals received TH intravenously (10 mg/kg, Poltram 100 mg/2 mL, batch no. 510804; Polpharma, Poland).

All TH formulations were administered between 8 a.m. and 9 a.m. Blood samples (1.5 mL) were obtained from the catheter remaining in the ear vein, prior to TH administration (sample 0) and 15, 30, 45, 60, 120 min and 4, 8, 24, 30 h following oral administration, or 1, 5, 10, 15, 30, 45, 60, 120 min and 4, 6, 8 h following intravenous administration. Blood samples were transferred into collection tubes containing lithium heparin, immediately centrifuged at 2880 × g for 10 min, then the plasma was frozen at –30°C until the time of analysis.

Drug analysis

Chemicals and reagents

Tramadol hydrochloride, $C_{16}H_{25}O_2N \times HCl$, CAS: 27203-92-5, phenacetin (internal standard), CAS: 62-44-2 and triethylamine (HPLC grade) were from Sigma-Aldrich (Steinheim, Germany). Acetonitrile, n-hexane, methanol, ethyl acetate (HPLC grade) were purchased from Merck (Darmstadt, Germany). Sodium hydroxide, monopotassium phosphate, anhydrous potassium hydrogen phos-

phate (analytical grade, pure for analysis) were from POCh (Gliwice, Poland).

Analytical method

The TH in rabbit plasma was determined using high-performance liquid chromatography with UV detection (HPLC Waters 2695 Separations Module with autosampler, Waters 2487 Dual l Absorbance Detector) according to methods described by Gan et al. (19) and Szkutnik-Fiedler et al. (20). The conditions were as follows: the wavelength 218 nm, LiChrosorb RP-18, 250 × 4.6 mm, 5 µm column from Waters, mobile phase: acetonitrile – 0.01 M phosphate buffer (30:70, v/v) with an addition of 0.05% triethylamine (0.5 mL) to achieve pH of mobile phase = 3.0, flow rate of mobile phase 1.0 mL/min, volume of each injection 100 µL, retention time of TH and phenacetin: 5.64 and 8.19 min, respectively, total analysis time 12.0 min. Data collection and processing were carried out using Empower Pro software, v. 1154. This HPLC method was adapted to the conditions of our lab and fully validated in accordance with the published EMA guidelines (21). The lower limit of quantification (LLOQ) and limit of detection (LOD) of TH were 10 ng/mL and 5 ng/mL, respectively. The calibration for TH was linear in the range of 10–1000 ng/mL. Intra- and inter-day coefficients of variation were less than 10%. TH in rabbit plasma samples was stable during the storage, freeze-thaw cycles, processing and analysis.

Pharmacokinetic and statistical analysis

Pharmacokinetic parameters of TH: the elimination rate constant (k_{el}), elimination half-life ($t_{1/2kel}$), area under the plasma curve from zero to the last measurable concentration (AUC_{0-t}), area under the plasma curve from zero to infinity ($AUC_{0-\infty}$), area under the first moment curve from zero to infinity ($AUMC_{0-\infty}$), total body clearance (Cl/F) and mean residence time (MRT) were calculated using the non-compartmental methods with validated software WinNonlin® 5.3 Professional (Pharsight, Corp., USA). The maximum drug plasma concentration (C_{max}) and the time at which C_{max} was achieved (t_{max}) were determined directly from the concentration *vs*. time curve. The absolute bioavailability (F) of TH was calculated from the AUC ratio obtained following *p.o.* and *i.v.* administration, indexed to their respective dose: $F(\%) = [AUC_{0-\infty p.o.} \times D_{i.v.}/AUC_{0-\infty i.v.} \times D_{p.o.}] \times 100$. Mean absorption time ($MAT$), absorption rate constant (k_a) and absorption half-life ($t_{1/2k_a}$) were determined according to the following equations: $MAT = MRT_{p.o.} - MRT_{i.v.}$, where MRT is the mean residence time after *p.o.* and *i.v.* administration, respectively, $k_a = 1/MAT$, $t_{1/2k_a} = 0.693 \times MAT$.

As TH was given to the rabbits in different doses (intravenous administration: 10 mg/kg; oral administration: mean dose of 30.32 ± 0.16 mg/kg) AUC and $AUMC_{0-\infty}$ values were dose normalized.

The statistical calculations were performed using Statistica PL 10 software (StatSoft, Inc.).

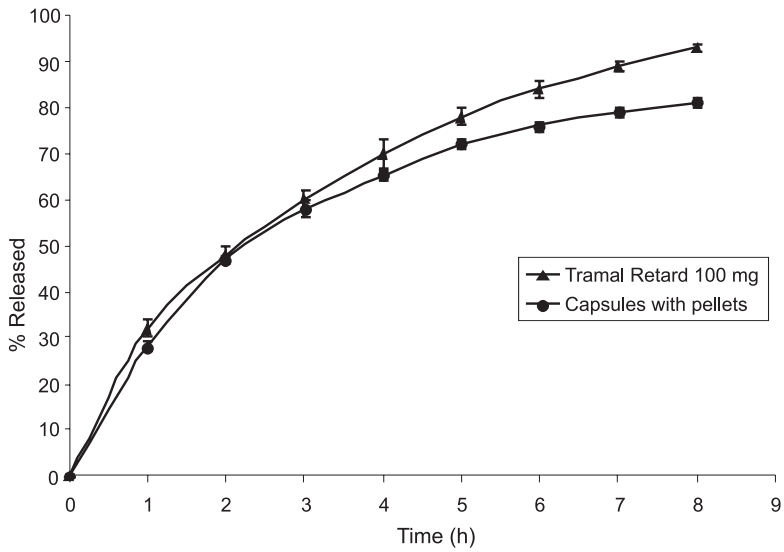

Figure 1. *In vitro* tramadol hydrochloride release (the mean ± RSD) from capsules filled with coated pellets compared to Tramal Retard® tablets (n = 12)

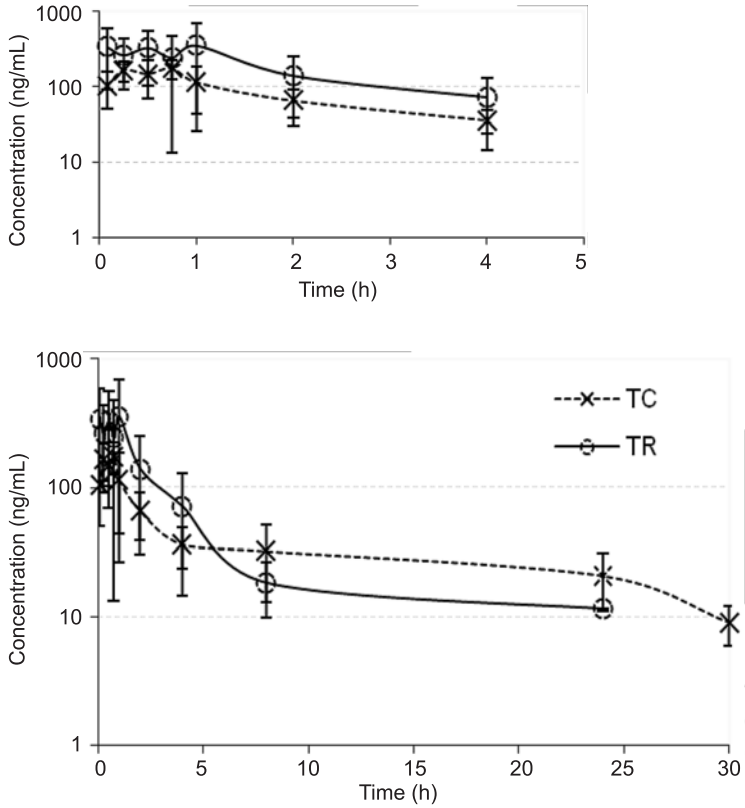

Figure 2. Plasma concentration-time profiles (the mean ± SD) of tramadol hydrochloride after oral administration of capsules filled with coated pellets (TC) and Tramal Retard® tablets (TR) in rabbits (n = 8). Significant differences (paired *t*-test) were observed for the following time points: 0.08 h (p = 0.0089), 0.25 h (p = 0.0185), 0.5 h (p = 0.0029), 1 h (p = 0.0002), and 2 h (p = 0.0147)

Paired *t*-test or Wilcoxon test (data with non-normal distribution) were used to compare plasma concentrations and pharmacokinetic parameters of TH. The results were presented as the mean ± SD (standard deviation) or median (range) (t_{max} and t_{last}). Differences resulting in a p value of less than 0.05 were considered statistically significant. Statistical analysis of variance (ANOVA) was used to compare the bioequivalence of these two formulations. The standard 90% confidence intervals (90% CIs) of the geometric mean ratios TC/TR with logarithm (ln)-transformed $AUC_{0-t,}$ $AUC_{0-\infty}$ and C_{max} were calculated. The bioequivalence acceptance criteria required that the 90% CI be within the range of 80–125%.

RESULTS

In vitro release study

Similarity factor f_2 for the TH release profiles between TC and TR formulations was 52 which suggests that the two dissolution profiles are similar (Fig. 1).

In vivo study – pharmacokinetic analysis

No adverse effects were observed after oral (100 mg, mean dose 30.3 ± 0.16 mg/kg) and intravenous (10 mg/kg) TH administration in rabbits. Mean plasma concentration-time profiles of TH after oral administration of TC and TR are shown in Figure 2. The statistical evaluation of plasma TH concentrations after TC and TR administration showed significant differences for the following time points: 0.08 h (p = 0.0089), 0.25 h (p = 0.0185), 0.5 h (p = 0.0029), 1 h (p = 0.0002), and 2 h (p = 0.0147) after administration. After 4 h, plasma concentrations of TH were similar (Fig. 2). The pharmacokinetic parameters of TH and their statistical evaluation are summarized in Tables 1 and 2. The profile of plasma TH concentration *vs*. time showed that the elimination of TH from TC formulation is longer than from TR tablets after single dose administration in rabbits. The time for the last observed concentrations (t_{last}) (median (range)) was: 30 (24–30) h and 8 (4–24) h for TC and TR, respectively (Table 2). In the group of TC-receiving rab-

bits, total elimination of the drug was noted in six out of eight animals as late as after 30 h, and in the TR-receiving group elimination in two of eight animals was complete after 24 h, in five animals after 8 h and in one as soon as after 4 h. TH concentration was not determined in any of the TR group animals after 30 h. Although all of the rabbits had similar body weight (3.3 ± 0.2 kg; range from 3.0 to 3.5 kg) and fasted 12 h prior to drug administration and 12 h after administration to minimize the variability caused by food, differences in gastrointestinal transit time, disintegration of the oral dose form and absorption rate can affect C_{max} and t_{max}. Coefficients of variation (CV) for C_{max}, AUC_{0-t} and $AUC_{0-\infty}$ values were smaller after TC administration compared to the TR formulation (Table 1). Generally, TC exhibited a significantly lower C_{max} appearing at a similar time compared with SR conventional tablet Tramal Retard® (p = 0.0003, paired *t*-test).

Ninety percent CI values for C_{max} were not within the range of 80–125% of the statistical interval proposed by EMA (17) and were 42% to 72%. TC and TR, however, led to equivalent systemic exposure to the drug (90% CI for AUC_{0-t} and $AUC_{0-\infty}$ were 90–124% and 97–109%, respectively) (Table 1). Compared to TR, TC had significantly prolonged absorption and elimination of TH, as evidenced: longer: mean absorption time MAT (p = 0.0016), mean residence time MRT (p = 0.0268), absorption half-life $t_{1/2ka}$ (p = 0.0016), elimination half-life $t_{1/2kel}$ (p = 0.0493); lower: absorption rate constant k_a (p = 0.0016), elimination rate constant k_{el} (p = 0.0148) and total body clearance Cl/F (p = 0.0076) (Table 2).

DISCUSSION

In our study, a new controlled release formulation of TH capsules filled with coated pellets was evaluated. Long-acting analgesics are often proposed for chronic pain management as they provide more consistent plasma drug concentrations (7). The efficacy of slow-release TH in the treatment of chronic pain with better patient compliance during treatment has been confirmed in several studies (7–9). It is known that technological processes and differences between the oral formulations might represent the most important factor responsible for the differences in both rate and extent of absorption of the drug, reflected in the pharmacokinetic parameters, and thus an *in vitro* and *in vivo* evaluation of any new formulation is necessary (22, 23).

In vitro tests have shown that the rate and degree of TH release were similar to those of the reference formulation – Tramal Retard® tablets. In the *in vivo* study, large inter-subject differences in the pharmacokinetic parameters of TH, both after TC and TR administration, were observed. This may be related to the differences in absorption rate, metabolism or gastrointestinal transit time. Inter-animal variability, however, is very common in pharmacokinetic studies using animal model (24–30). Despite intra-individual differences, the amounts of TH absorbed into the systemic circulation after administration of TC and TR in rabbits were similar (90% CI values for AUC_{0-t} and $AUC_{0-\infty}$ were within 80–125%). Nevertheless, TC exhibited a significantly lower maximum plasma concentration and a comparison of other pharmacokinetic parameters of

Table 1. Statistical results (ANOVA) of AUC_{0-t}, $AUC_{0-\infty}$ and C_{max} for tramadol hydrochloride after oral administration of capsules filled with coated pellets, 100 mg (TC) and Tramal Retard® tablets, 100 mg (TR) in rabbits (n = 8).

Parameter (unit)	TC	TR	Geometric mean ratio TC/TR (90% CI for the lntransformed data)
AUC_{0-t} (ng h/mL) CV (%)	970.29 ± 307.16 (31.66)	960.45 ± 665.03 (69.24)	107.3 (90 – 124)
$AUC_{0-\infty}$ (ng h/mL) CV (%)	1199.92 ± 287.33 (23.94)	1092.09 ± 658.76 (60.32)	102.8 (97 – 109)
C_{max} (ng/mL) CV (%)	217.6 ± 32.7 (15.02)	459.1 ± 257.2 (56.02)	52.2 (42 – 72)

Data are presented as the mean ± SD. Statistical analysis of the data was performed using the one-way analysis of variance (ANOVA). Abbreviations: C_{max} – maximum plasma concentration, AUC_{0-t} – area under the plasma curve from zero to the last measurable concentration, $AUC_{0-\infty}$ – area under the plasma curve from zero to infinity, CV – coefficient of variation defined as the ratio of the SD to the mean.

Table 2. The pharmacokinetic parameters of tramadol hydrochloride and their statistical evaluation after oral administration of capsules filled with coated pellets, 100 mg (TC) and Tramal Retard® tablets, 100 mg (TR) in rabbits (n = 8).

Parameter (unit)	TC	TR	TC *vs*. TR
t_{max} (h)	0.75 (0.25 – 1.00)	0.50 (0.08 – 1.00)	NS
t_{last} (h)	30 (24 – 30)	8 (4 – 24)	IS p = 0.0277
$AUMC_{0-\infty}$ (ng h²/mL)	22533.11 ± 14596.89	5158.99 ± 3461.08	IS p = 0.0183
k_{el} (h^{-1})	.06 ± 0.02	0.19 ± 0.12	IS p = 0.0148
Cl/F (mL/min)	1003.99 ± 655.65	1854.62 ± 684.45	IS p = 0.0076
MRT (h)	18.32 ± 11.18	4.79 ± 2.39	IS p = 0.0268
$t_{1/2kel}$ (h)	14.96 ± 8.12	5.12 ± 2.63	IS p = 0.0493
MAT (h)	14.63 ± 11.48	1.86 ± 1.59	IS p = 0.0016
k_a (h^{-1})	0.09 ± 0.06	0.81 ± 0.47	IS p = 0.0016
$t_{1/2ka}$ (h)	10.14 ± 7.96	1.29 ± 1.10	IS p = 0.0016
F (%)	26.95 ± 8.07	24.68 ± 15.68	NS
RB (%)	109.19		

Data are presented as the mean ± SD or median (range) (t_{max} and t_{last}). Statistical analysis of the data was performed using the paired *t*-test or Wilcoxon test (t_{max} and t_{last}). Abbreviations: IS – statistically significant difference ($p < 0.05$), NS – statistically non-significant difference ($p > 0.05$), t_{max} – time to reach maximum plasma concentration, t_{last} – time of the last observed concentration, – area under the first moment curve from zero to infinity, k_{el} – elimination rate constant, Cl/F – total body clearance, MRT – mean residence time, $t_{1/2kel}$ – elimination half-life, MAT – mean absorption time, k_a – absorption rate constant, $t_{1/2ka}$ – absorption half-life, F – absolute bioavailability, RB – relative bioavailability.

TH indicates prolonged absorption and elimination processes, when the drug is given in controlled-release capsules filled with coated pellets.

The mean absolute bioavailability of TH after TC and TR administration was 26.95 ± 8.07% and 24.68 ± 15.68%, respectively. Such a small value could be caused by a higher metabolism of TH in rabbits compared to the humans. For financial reasons, the active metabolites of TH were not determined, which is a true limitation of our study. It has been confirmed that controlled release of the drug in the stomach does not always contribute to its increased bioavailability. Moreover, biological availability of TH in animals after administration of SR tablets is usually lower than after IR tablets (13). Systemic bioavailability of TH reported by Giorgi et al. (24, 25) after oral administration of SR tablets at a dose of 100 mg was only 11% in dogs (24) and 10.5% in horses (25) (SR tablet, dose of 5 mg/kg). Similar results were observed in goats (26) (F = 30%) and horses (27) (F = 3%) administered 2 mg/kg orally; meanwhile, horses treated with 5 mg/kg immediate release capsules (25) had a bioavailability of 64%. In humans, TH bioavailability is 70% after a single oral administration, which is similar to e.g., 65% in dogs (28) but is lower than 93% in cats (29). Sustained-release tablets have a bioavailability of 87–95% compared to the capsules (13). In our study, the relative bioavailability (RB, %) of controlled-release capsules filled with coated pellets with reference to TR tablets was 109.19%.

CONCLUSION

Both TR formulations have a similar *in vitro* release profile and led to an equivalent systemic exposure to the drug. However, prolonged absorption and elimination processes of TH, which have

been achieved in rabbits after administration of controlled-release capsules filled with coated pellets, might suggest that the new formulation could be expected to have a more prolonged analgesic effect in humans than the commercial sustained release tablets. It can be concluded that our new form of TH may be an alternative to the other controlled-release preparations.

Declaration of interest

The authors report no declarations of interest.

REFERENCES

1. Silva Mde F., Schramm S.G., Kano E.K., Mori Koono E.E., Porta V., dos Reis Serra C.H.: Clin. Ther. 32, 758 (2010).
2. Chaurasia D., Kaushik K., Bhardwaj P., Chaurasia H., Jain S.K., Shobhna S.: Acta Pol. Pharm. Drug Res. 68, 795 (2011).
3. Doucette W.R., Farris K.B., Youland K.M.: J. Am. Pharm. Assoc. 52, e199 (2012).
4. Practice Guidelines for Chronic Pain Management. An Updated Report by the American Society of Anesthesiologists Task Force on Chronic Pain Management and the American Society of Regional Anesthesia and Pain Medicine. Anesthesiology 112, 810 (2010).
5. Health Care Guideline: Assessment and Management of Chronic Pain. Institute for Clinical Symptoms Improvement (ISCI). 5th edn. (2011). Available on the website www.isci.org.
6. Nicholson B.: Pain Practice 9, 71 (2009).
7. Barkin R.L.: Am. J. Ther. 15, 157 (2008).
8. Naeem Aamir M., Ahmad M., Akhtar N., Murtaza G., Khan S.A., Shahig-uz-Zaman, Nokhodchi A.: Int. J. Pharm. 407, 38 (2011).
9. Beaulieu A.D., Peloso P.M., Haraoui B., Bensen W., Thomson G., Wade J., Quigley P. et al.: Pain Res. Manag. 13, 103 (2008).
10. Alamdari N.S., Azar Z.J., Varshosaz J, Ghaffari S., Ghaffari S., Kobarfard F.: AJPP 6, 2123 (2012).
11. Bialleck S., Rein H.: Eur. J. Pharm. Biopharm. 79, 440 (2011).
12. Rujivipat S., Bodmeier R.: Eur. J. Pharm. Biopharm. 81, 223 (2012).
13. Sawicki W.: Eur. J. Pharm. Biopharm. 53, 29 (2002).
14. Sawicki W., Mazgalski J., Jakubowska I.: Drug Dev. Ind. Pharm. 36, 209 (2010).
15. Sawicki W., Mazgalski J.: Drug Dev. Ind. Pharm. 35, 857 (2009).
16. Terebesi I., Bodmeier R.: Eur. J. Pharm. Biopharm. 75, 63 (2010).
17. European Medicines Agency. Guideline of the investigation of bioequivalence. The European Agency for the Evaluation of Medicinal Products CPMP/EWP/QWP/1401/98 Rev. 1/ Corr **, London, 20 January 2010.
18. Directive 2010/63/EU of the European Parliament and of the Council of 22 September 2010 on the protection of animals used for scientific purposes. Official Journal of the European Union L276/33, 20.10.2010.
19. Gan S.H., Ismail R., Wan Adnan W.A., Wan Z.: J. Chromatogr. B Analyt. Technol. Biomed. Life Sci. 772, 123 (2002).
20. Szkutnik-Fiedler D., Grześkowiak E., Madziała J.: Farmacja Współczesna 6, 1 (2013).
21. European Medicines Agency. Guideline on bioanalytical method validation. Committee for Medicinal Products for Human Use (CHMP) EMEA/CHMP/EWP/192217/2009, 21 July 2011
22. Emami J.: J. Pharm. Pharm. Sci. 9, 31 (2006).
23. Kumar P., Singh S., Mishra B.: Acta Pharm. 59, 15 (2009).
24. Giorgi M., Saccomanni G., Łebkowska-Wieruszewska B., Kowalski C.: Vet. J. 180, 253 (2009).
25. Giorgi M., Soldani G., Manera C., Ferrarini P., Sgorbini M., Saccomanni G.: J. Equine Vet. Sci. 27, 481 (2007).
26. de Sousa A.B., Santos A.C., Schramm S.G., Porta V., Górniak S.L., Florio J.C., de Souza Spinoza H.: J. Vet. Pharmacol. Ther. 31, 45 (2008).
27. Shilo Y., Britzi M., Eytan B., Lifschitz T., Soback S., Steinman A.: J. Vet. Pharmacol. Ther. 31, 60 (2008).
28. KuKanich B., Papich M.G.: J. Vet. Pharmacol. Ther. 27, 239 (2004).
29. Pypendop B.H., Ilkiw J.E.: J. Vet. Pharmacol. Ther. 31, 52 (2008).
30. Cox S., Villarino N., Doherty T.: Res. Vet. Sci. 89, 236 (2010).

Received: 30. 07. 2013

Acta Poloniae Pharmaceutica – Drug Research, Vol. 71 No. 3 pp. 477–483, 2014 ISSN 0001-6837
Polish Pharmaceutical Society

PHARMACOLOGY

LEVOFLOXACIN RESISTANCE OF *HELICOBACTER PYLORI* STRAINS ISOLATED FROM PATIENTS IN SOUTHERN POLAND, BETWEEN 2006-2012

ELŻBIETA KARCZEWSKA[1]*, KAROLINA KLESIEWICZ[1], IZABELA WOJTAS-BONIOR[1], IWONA SKIBA[1], EDWARD SITO[2], KRZYSZTOF CZAJECKI[2], MAŁGORZATA ZWOLIŃSKA-WCISŁO[3] and ALICJA BUDAK[1]

[1] Department of Pharmaceutical Microbiology of the Jagiellonian University Medical College, Medyczna 9, 30-688 Kraków, Poland
[2] Falck Medycyna Outpatient Clinic of Gastroenterology, Mazowiecka 4–6, 30-036 Kraków, Poland
[3] Chair of Gastroenterology, Hepatology and Infectious Diseases, Jagiellonian University Medical College, Śniadeckich 5, 31-531 Kraków, Poland

Abstract: An increasing resistance of *Helicobacter pylori* (*H. pylori*) to antimicrobial agents leads to the need of regional monitoring of the prevalence resistant strains (according to the Maastricht/Florence consensus report, 2012). The aim of the study was to assess the resistance to levofloxacin of *H. pylori* strains isolated from adult patients of Małopolska region in Poland. Bioptates taken from gastric mucosa during gastroscopy constituted the material for the study. Two hundred ten *H. pylori* strains were isolated from 811 patients. A majority of strains (171) came from patients before the treatment of *H. pylori* infections while the remaining 39 strains were isolated from patients after the failed therapy. Susceptibility of *H. pylori* to levofloxacin was determined by strips impregnated with antibiotic gradient (E-test, bioMerieux). The obtained minimum inhibitory concentration (MIC) values ranged from 0.002 mg/L to 32 mg/L. The percentage of strains resistant to levofloxacin amounted to 8.10% (17/210). Among the group of strains isolated from patients before the treatment, 5.85% (10/171) of *H. pylori* strains were resistant to levofloxacin. In the group of strains isolated from patients after the treatment 17.95% (7/39) of strains were resistant. The difference in the frequency of *H. pylori* strains resistant to levofloxacin in patients before and after the treatment of the infection due to *H. pylori* was statistically significant ($p = 0.0297$). The low percentage of *H. pylori* strains resistant to levofloxacin justify that the introduction of a triple therapy with levofloxacin is a good alternative in the treatment of *H. pylori* infections, especially in regions with high prevalence of *H. pylori* strains resistant to clarithromycin (> 20%).

Keywords: *Helicobacter pylori,* drug-resistance, levofloxacin

Helicobacter pylori (H. pylori) is one of the most common human pathogens that affected about 50% of the human population (1). *H. pylori* is a Gram-negative, microaerophilic, spiral bacterium that permanently or temporarily inhabits various parts of the gastric mucosa. *H. pylori* is the main pathogenic factor of gastroduodenal diseases: gastritis B, gastric ulcer, duodenal ulcer, gastric cancer, gastric lymphoma MALT (Mucosa Associated Lymphoid Tissue) and Ménétrier's disease. Moreover, various studies reveal a relation of *H. pylori* to the development of coronary heart disease, stomatitis, liver diseases (hepatic encephalopathy, neoplasms), skin diseases and allergy (2–12).

Eradication of *H. pylori* is recommended at every stage of the disease (3). Introduction of the effective therapy guarantees eradication of the infection, which results in the relief and often in the regression of disorder changes that otherwise might lead to gastric cancer, which develops in 2% of individuals infected with *H. pylori* (5, 13, 14).

Indications for the treatment and guidelines for clinical trials are elaborated by the European Helicobacter Study Group (EHSG) (1, 15). On the basis of these recommendations, the Working Group of the Polish Society of Gastroenterology (PTG – *pl.* Polskie Towarzystwo Gastroenterologiczne) has issued guidelines that are obligatory in Poland.

* Corresponding author: e-mail: ekarczew@wp.pl; phone: +48 126205750; fax: +48 126205758

Current obligatory recommendations in Poland were established by PTG in 2008 (5) on the basis of Maastricht Consensus 2005 by EHSG. Now, there are no new recommendations based on the newest Maastricht/Florence Consensus 2012. According to all these recommendations, the treatment of *H. pylori* infection is a combined empirical therapy including three types of drugs: gastric antisecretory drugs, cytoprotective drugs and antimicrobial agents.

Current regimens of the treatment of *H. pylori* infections in Poland (2008) are shown in Table 1 and new recommendations in Europe (2012) are shown in Table 2. The difference between these recommendations are as follows:

– variability of the treatment of *H. pylori* infections in regions with low (<20%) and high (>20%) prevalence of *H. pylori* strains resistant to clarithromycin; Maastricht/Florence IV consensus report recommended to abandon clarithromycin in treatment *H. pylori* infections or perform previous susceptibility testing to clarithromycin in regions with high prevalence of *H. pylori* strains resistant to clarithromycin.

– 2nd line treatment schemes contain levofloxacin, whereas in the older version levofloxacin was only a proposal in the 3rd line treatment;

– in Maastricht/Florence IV consensus report it is strongly recommended that the 3rd line treatment have to be based on the susceptibility testing.

According to the new Maastricht/Florence Consensus 2012, the scheme for the region with the high prevalence of *H. pylori* strains resistant to clarithromycin should be introduced in Poland. Recent studies showed that 34% of strains were resistant to clarithromycin in Southern Poland (16). According to PTG data from 2008, the resistance of *H. pylori* to antibacterial drugs used in the therapy is high in Poland and amounts to 28% to clarithromycin (primary resistance 22%, secondary resistance 54%) and 46% to metronidazole (primary resistance 41%, secondary resistance 68%) (5). *H. pylori* strains

Table 1. Treatment of *H. pylori* infections (5)

The first-line treatment (one of the following):
PPI, AC (1000 mg), MZ (500 mg) – twice a day, 10–14 days.
PPI, CH (500 mg), MZ (500 mg) – twice a day, 10–14 days.
PPI, AC (500 mg), CH(500 mg) – twice a day, 10–14 days.
The second-line treatment (one of the following):
PPI, AC(1000 mg), MZ (500 mg) – twice a day, and TC (250 mg) – three times daily; prolonged to 14 days.
PPI, AC (1000 mg), MZ (500 mg) – twice a day, and bismuth salts (120 mg) – four times daily; prolonged to 14 days.
The third-line treatment:
Evaluation of the susceptibility of the strains to the currently used antimicrobial agents.
Possible introduction of levofloxacin.
Adding a probiotic.

PPI – proton pomp inhibitor; CH – clarithromycin; AC – amoxicillin; MZ – metronidazole, TC – tetracycline

Table 2. Schemes of the treatment of *H. pylori* infections according to the new guidelines – Maastricht/Florence Consensus 2012.

	Prevalence of *H. pylori* strains resistant to clarithromycin	
	Low (< 20%)	High (> 20%)
1st line treatment	PPI + CH + AC/MZ or Quadruple bismuth therapy	Quadruple bismuth therapy or – if not available sequential or concomitant non-bismuth therapy
2nd line treatment	Quadruple bismuth therapy or PPI + LE + AC	PPI + LE + AC
3rd line treatment	Based on susceptibility testing only	

PPI – proton pomp inhibitor; CH – clarithromycin; AC – amoxicillin; MZ – metronidazole, LE – levofloxacin

resistant to amoxicillin have not been found in Poland (5, 17). As a result of the frequent administration of clarithromycin and metronidazole in the treatment of infections due to *H. pylori*, bacterial strains simultaneously resistant to both drugs can be found (17–19). An increasing resistance of *H. pylori* bacteria as well as their multi-drug resistance to routinely used antimicrobial agents is a serious therapeutic problem.

Current recommendation of PTG is to consider the introduction of the scheme: levofloxacin + amoxicillin with PPI as a 3rd line empirical treatment, whereas EHSG recommended this scheme as a 2nd line treatment.

Levofloxacin (S-enantiomer of ofloxacin) is a chemotherapeutic agent of the 3rd generation fluoroquinolones with a broad-spectrum activity. The development of the resistance of *H. pylori* strains to fluoroquinolones is a result of point mutations occurring mainly at positions 87 and 91 of *gyrA* gene that encodes gyrase, a binding site for quinolones in Gram-negative bacteria (20).

The introduction of levofloxacin to the treatment schemes raises many hopes. Many studies have shown the high efficiacy of treatment schemes with levofloxacin (21–24).

The lack of data on the susceptibility of *H. pylori* strains isolated in Poland to levofloxacin constituted a base for performing the research to assess the level of the susceptibility to levofloxacin of *H. pylori* strains isolated from dyspeptic patients between the years 2006–2012.

MATERIALS AND METHODS

Patients and clinical material

In total, 811 dyspeptic patients (429 women, 382 men), with indications to gastroscopy, were enrolled to the study between 2006–2012. Medium age of patients was 45 years (16–87 years). Patients underwent gastroscopy in selected Gastroenterology Clinic in Kraków, Southern Poland. According to the clinical diagnosis, there were two main groups of patients: First group covered individuals with peptic ulcer disease (PUD), means patients with gastric or duodenal ulceration, and second group covered individuals with non-ulcer dyspepsia (NUD) means patients with diseases of upper gastrointestinal tract other than peptic ulcer disease, e.g., gastritis, duodenitis, esophagitis.

Two bioptates were taken from each patient during gastroscopy from the antrum and the body of the stomach. In total, 210 *H. pylori* strains were isolated from bioptates. These *H. pylori* strains were obtained from 210 patients (115 women, 95 men), including 51 patients with PUD and 159 patients with NUD. Eighty one percent of these *H. pylori* strains (171/210) were isolated from patients before the treatment of *H. pylori* infections, while 19% (39/210) strains were derived from patients after the failed therapy.

The plan of the study was approved by the Bioethical Commission of the Jagiellonian University and each patient signed the informed consent for participation in the trial.

H. pylori culture and susceptibility testing

Bacterial culture. Bioptates were homogenized in glass sterile mortars and inoculated onto the solid medium – Schaedler agar with 5% sheep blood (bioMérieux, France) and medium, Schaedler agar with 5% sheep blood with selective supplement DENT (Oxoid, UK). The culture was carried out for 72 h under microaerophilic conditions at 37°C. The presence of *H. pylori* in the examined material was confirmed by the macroscopic appearance of colonies on the medium, the Gram-stained preparation from the culture (Gram-negative, s-shaped bacteria) and positive tests for urease, catalase and oxidase. Each *H. pylori* strain was frozen and stored at –80°C for further analysis.

Susceptibility testing. *H. pylori* drug-susceptibility to levofloxacin was quantitatively tested by strips impregnated with antibiotic gradient (E-test, bioMérieux, France), which enables the determination of the minimum inhibitory concentration (MIC). The testing was carried out as follows: the suspension of bacteria in 0.85% NaCl sterile solution was prepared from the culture of *H. pylori*. The density of the suspension amounted to 3.0 McFarland. The suspension was inoculated onto the Schaedler agar with 5% sheep blood. After that, strips impregnated with levofloxacin gradient (E-test) were affixed according to the manual. The plates were incubated under microaerophilic conditions at 37°C for 72 h. The strains in which the MIC value exceeded 1 μg/mL were considered resistant, according to the EUCAST recommendations (25, 26). The determination was carried out against the reference *H. pylori* ATCC 43504 strain to ensure the quality of tests.

Susceptibility testing to levofloxacin for *H. pylori* strains collected between 2006–2010 was carried out after defrosting and performing the culture of the strains, due to the unavailability of E-test with levofloxacin since 2010, whereas susceptibility testing to levofloxacin for *H. pylori* strains, which were collected between 2010–2012, was carried out

immediately, together with a determination of susceptibility to other antibiotics.

Susceptibility of *H. pylori* strains to other antibiotics/chemotherapeutics was tested according to described procedures.

Interpretations of MIC values for all described strains to all tested antimicrobial agents were made according to EUCAST Clinical Breakpoint Table for *H. pylori* (26).

Statistical analysis

The following statistical parameters were calculated: mean values, probability, χ^2 test at the 0.05 significance level (the results in which $p \leq 0.05$ were considered statistically significant). In cases where the expected values were less than 5, the Yates correction was used.

RESULTS

In total, 811 patients with dyspeptic symptoms were enrolled in the study. The presence of *H. pylori* infection was confirmed in 210 cases: 115 women and 95 men, which shows that both ganders were equally represented. The average age of patients was 45 years.

Two hundred ten strains from 210 dyspeptic patients were included in the study. In total, 81% (171/210) strains were derived from patients before the treatment of *H. pylori* infection and 19% (39/210) were derived from patients after the unsuccessful treatment of *H. pylori* infections.

The susceptibility of *H. pylori* strains to levofloxacin was quantitatively determined by the E-test. The obtained MIC values ranged from 0.002 mg/L to 32 mg/L. The mean MIC values amounted to 1.01 mg/L (Figure 1).

In total, the ratio of *H. pylori* strains resistant to levofloxacin amounted to 8.10% (17/210), whereas the percentage of strains susceptible to levofloxacin amounted to 91.90% (193/210). The probability of the incidence of resistance to levofloxacin among *H. pylori* strains isolated from patients who were included into the trial was low and amounted to P(A) = 0.081.

In the group of 17 resistant to levofloxacin *H. pylori* strains, there were more strains isolated from women than from men (11 and 6; respectively).

Among the group of *H. pylori* strains isolated from patients before the treatment, 5.85% (10/171) of *H. pylori* strains were resistant to levofloxacin,

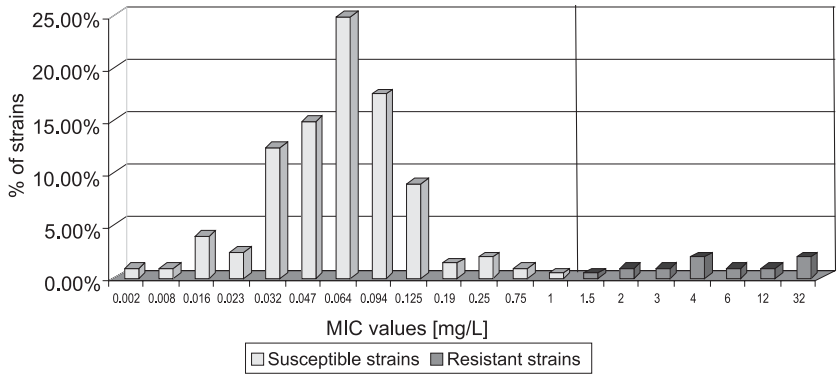

Figure 1. Activity of levofloxacin against *H. pylori* strains expressed by MIC values; MIC > 1 mg/L for resistant strains

Table 3. Comparison of *H. pylori* resistant strains isolated from patients before treatment and after failed therapy to levofloxacin (LE) out of 210 clinical *H. pylori* isolates.

Antimicrobial agent	**No. (%) of resistant strains**			
	All strains n = 210	Strains from patients before treatment n = 171	Strains from patients after failed therapy n = 39	p*
LE	17 (8.10%)	10 (5.85%)	7 (17.95%)	**0.0297****

* p (test χ^2 with Yates correction; the value p = 0.05 was deemed statistically significant;
** significant differences between *H. pylori* strains resistant to levofloxacin from patients before and after treatment

Table 4. Co-existence of *H. pylori* strains resistant to levofloxacin and other antibiotics.

H. pylori resistant to:	No. of resistant *H. pylori* strains
LE	6
LE + CH	1
LE + MZ	2
LE + CH + MZ	8
All	17

LE – levofloxacin, CH – clarithromycin, MZ – metronidazole

whereas in the group of strains isolated from patients after the treatment 17.95% (7/39) of strains were resistant to this quinolone. The statistical analysis was performed in order to check if differences between percentages of *H. pylori* strains resistant to levofloxacin from patients before and after the treatment were significant and this was the case ($p = 0.0297$) (Table 3).

Moreover, the analysis of the coexistence of resistance to levofloxacin and other antibiotics was conducted. Six from 17 strains were only resistant to levofloxacin and no other antibiotics. Eleven strains were resistant to more than one antibiotic (Table 4).

DISCUSSION

An increasing resistance of *H. pylori* strains to currently used antibiotics and chemotherapeutics is a serious therapeutic problem. A properly selected treatment model is very important as it enables *H. pylori* eradication, decreases the risk of drug-resistant strains occurrence and increases the probability of the successful therapy. Considering the high resistance of *H. pylori* strains to clarithromycin in Poland, according to Maastricht/Florence Consensus, levofloxacin should be introduced into the basic therapeutic schemes, as most of *H. pylori* strains are susceptible to this fluoroquinolone (1). An introduction of levofloxacin to the treatment regimens provides new possibilities to achieve effective *H. pylori* eradication.

The results of the study confirmed that substantial majority (91.90%) of isolated *H. pylori* strains are *in vitro* susceptible to levofloxacin. Furthermore, the low probability of incidence of *H. pylori* resistance to levofloxacin ($P(A) = 0.081$) was demonstrated. The results revealed that in the Małopolska region (Southern Poland) the resistance of *H. pylori* to levofloxacin is low and rather rare (8.10%). Therefore, an introduction of this fluoroquinolone to the therapy of *H. pylori* infections may raise the rate of *H. pylori* eradication. Nevertheless, it is worth seeing that in the group of patients after the failed therapy, the percentage of resistant strains is statistically higher than in the group of patients before the treatment (17.95% *vs.* 5.85%; $p = 0.0297$), however, it is still lower than the resistance to clarithromycin and metronidazole. In this respect, an introduction of levofloxacin to the 2nd line therapy seems to be a good solution. Moreover, it has been demonstrated that most *H. pylori* strains resistant to clarithromycin and metronidazole retain their susceptibility to levofloxacin (27, 28). Nonetheless, as shown Table 4, our study revealed the occurrence of *H. pylori* strains resistant to levofloxacin and clarithromycin or metronidazole or both these drugs. Therefore, it should be stressed the necessity of monitoring the resistance of *H. pylori* strains.

It should be underlined that the percentage of strains resistant to fluoroquinolones differs depending on the geographic region. It ranges from 5.3% in Iran (29), 14.3% in Japan, 16.8% in Belgium (25), 17.0% in Brazil to 22.1% in Germany (30).

The study performed by Zullo et al., in Italy in 2007 on 246 *H. pylori* strains isolated from dyspeptic patients showed that 19.1% of strains were resistant to levofloxacin (30). The study demonstrated an increase of the resistance to levofloxacin in that region, as Gatta et al., had reported the ratio of 14% of *H. pylori* strains resistant to levofloxacin earlier (in 2005) (24). The resistance increases also in other countries, e.g., in France it rose from 3.3% in 1999 to 17.5% in 2003 (25). The problem of an increasing resistance of *H. pylori* to quinolines is an effect of their frequent use in the treatment of many diseases, for instance those affecting airways or the urinary tract (31–33).

Results of many clinical trials have confirmed the effectiveness of levofloxacin in the therapy (27, 28, 34–36). Levofloxacin may constitute a good alternative in the case of double resistance of *H.*

pylori strains to clarithromycin and metronidazole as these strains retain susceptibility to levofloxacin (23, 27, 37).

Gatta et al. showed that the administration of levofloxacin with amoxicillin and PPI for 10 days as a third-line therapy affects the curability in over 80% (24). Gispert et al. obtained *H. pylori* eradication in 60–66% using the same therapeutic scheme, whereas Zullo reported eradication of 83% (38, 39).

In Spain, side effects and the effectiveness of the treatment of *H. pylori* infections were examined by using levofloxacin combined with amoxicillin and PPI as the first-line therapy. The study was carried out in comparison to the control group where PPI, clarithromycin and amoxicillin were administered. It was shown that the tolerance to levofloxacin was good. However, in the trial group, *H. pylori* eradication was lower as compared to the control group (71.8 and 75.5%, respectively) (40).

Nista et al. compared the effectiveness of *H. pylori* treatment between the following regimens:

– group 1: PPI, clarithromycin (500 mg), amoxicillin (1 mg),

– group 2: PPI, clarithromycin (500 mg), metronidazole (500 mg),

– group 3: PPI, clarithromycin (500 mg), levofloxacin (500 mg).

The rate of *H. pylori* eradication in these groups amounted to 75, 72 and 87%, respectively. Thus, the use of levofloxacin combined with PPI and clarithromycin gave better results than typical first-line therapeutic schemes (21).

The use of levofloxacin provides new treatment opportunities as the drug shows good tolerance and gives good therapeutic effects. Levofloxacin can be used as an alternative to amoxicillin in individuals sensitive to penicillins (34). Moreover, levofloxacin gives a higher curability rate in comparison to other therapeutic schemes, such as the standard 2nd line therapy – the quadruple therapy containing bismuth salts (41). The administration of a levofloxacin-based triple therapy for 10 days is more effective than the quadruple therapy containing bismuth salts used for 7 days (32).

CONCLUSION

The introduction of the 2nd line levofloxacin-based triple therapy is a good alternative in the treatment of *H. pylori* infections, especially in regions with high prevalence of *H. pylori* strains resistant to clarithromycin, like Poland. Nevertheless, a need for the local national resistance monitoring of *H. pylori* resistant strains should be stressed, because of the possibility of acquiring fast resistance to levofloxacin.

Moreover, it should be considered if triple therapy with levofloxacin will be better solution of 1st line treatment in region with high prevalence of *H. pylori* strains resistant to clarithromycin and unavailability of bismuth, instead of quadruple non-bismuth therapy that consists clarithromycin.

Acknowledgment

Scientific work partially was founded by the Polish Government as a research grant in the years 2011 - 2013 (NN404547640).

REFERENCES

1. Malfertheiner P., Megraud F., O'Morain C.A. Atherton J., Axon A.T. et al.: Gut 61, 646 (2012).
2. Ando T., Goto Y., Maeda O., Watanabe O., Ishiguro K., Goto H.: World J. Gastroenterol. 93, 2097 (2006).
3. Asaka M., Kato M., Takahashi S., Fukuda Y., Sugiyama T. et al.: Helicobacter 15, 1 (2009).
4. Cianci R., Montalto M., Pandol F., Gasbarrini G.B., Cammarota G.: World J. Gastroenterol. 12, 2313 (2006).
5. Dzieniszewski J., Jarosz M.: Gastroenterologia Polska 15, 323 (2008).
6. Figura N., Franceschi F., Santucci A., Bernardini G., Gasbarrini G., Gasbarrini A.: Helicobacter 15 (Suppl. 1), 60 (2010).
7. Grande R., Di Giulio M., Di Campli E., Di Bartolomeo S., Cellini L.: New Microbiol. 33, 343 (2010).
8. Karczewska E., Konturek J.E., Konturek P.C., Cześnikiewicz M., Sito E. et al.: Dig. Dis. Sci. 47, 978 (2002).
9. Kowalski M., Konturek P.C., Pieniazek P., Karczewska E., Kluczka A. et al.: Dig. Liver Dis. 33, 222 (2001).
10. Kowalski M., Pawlik M., Konturek S.J.: Med. Dypl. 13, 56 (2006).
11. Owens SR, Smith LB.: Pathолog. Res. Int. 2011, 193149.
12. Pieniazek P., Karczewska E., Duda A., Tracz W., Pasowicz M., Konturek S.J.: J. Physiol. Pharmacol. 50, 743 (1999).
13. Dzieniszewski J., Jarosz M., Grupa Robocza PTG: Gastroenterologia Polska 11, 41 (2004).
14. Życińska K., Wardyn K.A., Życiński Z.: Nowa Klin. 9, 956 (2002).

15. Malfertheiner P., Megraud F., O'Morain C. et al.: Gut 56, 772 (2007).
16. Karczewska E., Wojtas-Bonior I., Sito E., Zwolińska-Wcisło M., Budak A.: Pharmacol. Rep. 63, 799 (2011).
17. Dzierżanowska-Fangrat K., Rożynek E, Celińska-Cedro D., Jarosz M., Pawłowska J. et al.: Int. J. Antimicrob. Agents 26, 230 (2005).
18. Glupczynski Y.: Acta Gastroenterol. Belg. 61, 357 (1998).
19. Megraud F.: Gut 53, 1374 (2004).
20. Megraud F., Lehours P.: Clin. Microbiol. Rev. 20, 280 (2007).
21. Nista E., Candelli M., Zocco M., Cremonini F., Ojetti V. et al.: Am. J. Gastroenterol. 101, 1985 (2006).
22. Gisbert J.P., Morena F.: Aliment. Pharmacol. Ther. 23, 35 (2006).
23. Gisbert J.P.: The role of levofloxacin in first-line and "rescue" *Helicobacter pylori* treatment regimens. 2008, Available from: http:// 21113325116/only/artsrv2009_4pdf. (acessed 29 April 2011).
24. Gatta L., Zullo A., Perna F., Ricci C., De Francesco V. et al.: Aliment. Pharmacol. Ther. 22, 45 (2005).
25. Bogaerts P., Berhin C., Nizet H., Glupczynski Y.: Helicobacter 11, 441 (2006).
26. EUCAST clinical breakpoints for Helicobacter pylori; April 2011; Avaiable from: http://www.eucast.org/fileadmin/src/media/PDFs/EUCAST_files/Consultation/EUCAST_clinical_breakpoints_for_Helicobacter_pylori.pdf
27. Antos D., Schneider-Brachert W., Bästlein E., Hänel C., Haferland C. et al.: Helicobacter 11, 39 (2006).
28. Watanabe Y., Aoyama N., Shirasaka D., Maekawa S., Kuroda K. et al.: Dig. Liver Dis. 35, 711 (2003).
29. Talebi Bezmin Abadi A., Ghasemzadeh A., Taghvaei T., Mobarez A.M.: Intern. Emerg. Med. 7, 447 (2011).
30. Zullo A., Perna F., Hassan C., Ricci C., Saracino I. et al.: Aliment. Pharmacol. Ther. 25, 1429 (2007).
31. Hung K.H., Sheu B.S., Chang W.L., Wu H.M., Liu C.C., Wu J.J.: Helicobacter 14, 61 (2009).
32. Jaw-Town Lin: Successful treatment of *Helicobacter pylori* infections with levofloxacin: a case report from Taiwan and a review of the literature. 2008; Available from: http://21113325116/only/artsrv2008_4pdf. (accessed May 1, 2011).
33. Megraud F., Coenen S., Versporten A., Kist M., Lopez-Brea M. et al.: Gut 62, 32 (2013).
34. Gisbert J.P., Pérez-Aisa A., Castro-Fernández M., Barrio J., Rodrigo L. et al.: Dig. Liver Dis. 42, 287 (2010).
35. Gisbert J.P.: Therap. Adv. Gastroenterol. 2, 331 (2009).
36. Nista E.C., Candelli M., Cremonini F., Cazzato I.A., Di Caro S. et al.: Aliment. Pharmacol. Ther. 18, 627 (2003).
37. Branca G , Spanu T , Cammarota G., Schito A.M., Gasbarrini A. et al.: Int. J. Antimicrob. Agents 24, 433 (2004).
38. Gisbert J.P., Castro-Fernández M., Bermejo F., Pérez-Aisa A., Ducons J. et al.: Am. J. Gastroenterol. 101, 243 (2006).
39. Zullo A., De Francesco V., Hassan C.: Gut 5, 1353 2007).
40. Castro-Fernández M., Lamas E., Pérez-Pastor A., Pabón M., Aparcero R. et al.: Rev. Esp. Enferm. Dig. 101, 395 (2009).
41. Di Caro S, Fini L, Daud Y, Gasbarrini A.: Investigation of levofloxacin regimens as second-line therapy for *Helicobacter pylori*. 2010; Available from: http://www.infectweb.com/only/artsrv2010_2.pdf

Received: 16. 07. 2013

Acta Poloniae Pharmaceutica – Drug Research, Vol. 71 No. 3 pp. 485–495, 2014 ISSN 0001-6837
Polish Pharmaceutical Society

EXERCISE PREVENTED THE LANSOPRAZOLE-INDUCED REDUCTION OF ANTI-OSTEOPOROTIC EFFICACY OF ALENDRONATE IN ANDROGEN DEFICIENCY RATS

URSZULA CEGIEŁA*, MARIA PYTLIK, JOANNA FOLWARCZNA, RAFAŁ MIOZGA, SZYMON PISKORZ and DOROTA NOWAK

Department of Pharmacology, Medical University of Silesia, Katowice, Jagiellońska 4, 41-200 Sosnowiec, Poland

Abstract: Clinical studies indicate that proton pump inhibitors (PPIs), used long-term in elderly patients, increase the risk of osteoporotic fractures, and decrease the anti-fracture efficacy of alendronate. The aim of the present study was to examine the effect of physical exercise on the anti-osteoporotic efficacy of alendronate administered concurrently with lansoprazole, a PPI, in male rats with androgen deficiency induced by orchidectomy. Male Wistar rats at 3 months of age were divided into: sham-operated control rats, orchidectomized (ORX) control rats, ORX rats receiving alendronate, ORX rats receiving alendronate and lansoprazole, ORX rats receiving alendronate and subjected to exercise, and ORX rats receiving alendronate and lansoprazole and subjected to exercise. The orchidectomy or sham-operation was performed 7–8 days before the start of drug administration. The rats were subjected to the exercise on the treadmill 1 hour/day for 7 weeks (6 days a week). Alendronate sodium (3 mg/kg *p.o.*) and lansoprazole (4 mg/kg *p.o.*) were administered once daily for 7 weeks (6 days a week). Mechanical properties of the tibial metaphysis and femoral neck were assessed. Bone turnover markers, histomorphometric parameters, bone mass and mass of bone mineral were also studied. Lansoprazole weakened the anti-osteoporotic efficacy of alendronate. The exercise increased the alendronate effect. Similar changes were observed in the rats treated with lansoprazole and alendronate, subjected to exercise; no deleterious effects of lansoprazole were observed.
In conclusion, the exercise prevented the lansoprazole-induced reduction the anti-osteoporotic efficacy of alendronate in orchidectomized rats.

Keywords: bone mechanical properties, exercise, alendronate, lansoprazole, orchidectomized rats

Osteoporosis in elderely men is an important although neglected health problem (1–3). It occurs less frequently than in women, and some 5–10 years later, too (4). However, at present, it is considered one of the main causes of morbidity and mortality in elderly men (2, 5). It is assumed that among the total incidence of fractures of the spine, hip, and forearm, some 42, 30, and 20%, respectively, occur in men, while the mortality connected with such fractures is definitely higher than in women (3, 6–8). Moreover, the number of osteoporotic fractures in men increases quickly, which is connected with increasing life expectancy (1, 3). Despite that, presently, less information is available about the efficacy of anti-fracture therapy for men, in comparison with women (1, 5), and all the data hitherto provided are based upon the results of bone mineral density (BMD) examinations (9).

In the anti-fracture therapy for men, the first-line drugs are bisphosphonates. Standard therapy is based upon oral administration of alendronate or risedronate (9–13). Bisphosphonates are strong anti-resorptive drugs. They prevent the loss of BMD and reduce the risk of fracture, by direct inhibition of osteoclast activity (11, 14). The optimum treatment time with bisphosphonates in men has not been studied, though. However, from the studies performed on women it can be gathered that in most cases bisphosphonates should be administered to men for a minimum of 5 years, and – in case no substantial improvement of BMD occurs – for 2 more years (10). Long term application of bisphosphonates increases the risk of undesired effects, including osteonecrosis of the jaw, hypocalcemia, atrial fibrillation, musculoskeletal pain, as well as atypical fractures of the femur. Long term therapy with the use

* Corresponding author: e-mail: ucegiela@o2.pl, phone/fax: 48 32 3641540

of bisphosphonates also aggravates alimentary tract disorders, including gastroesophageal reflux and esophagitis, which may lead to the development of esophageal squamous cell carcinoma (10, 14).

Alimentary tract disorders occurring during therapy with bisphosphonates require simultaneous application of drugs that reduce the hydrochloric acid production, e.g., proton pump inhibitors (PPIs). PPIs are commonly used in case of elderly patients, in the treatment of esophagus reflux. There are data indicating that PPIs applied for a long time in postmenopausal women increase the risk of osteoporotic fractures (15, 16), and increased risk of fracture during PPI therapy may be greater in women than in men (17). Also, results of studies have been published, which indicate that PPIs administered to patients with osteoporosis reduce the anti-resorptive efficacy of alendronate and increase the risk of hip fractures (18, 19). Moreover, our earlier studies demonstrated that PPIs reduced the anti-resorptive activity and anti-osteoporotic efficacy of alendronate also in experimental studies conducted on rats with estrogen deficiency (model of postmenopausal osteoporosis) (20, 21).

On the basis of data provided above we assumed that lansoprazole, being a strong inhibitor of PPI (22), may reduce the anti-osteoporotic efficacy of alendronate also in male rats with experimental osteoporosis induced by orchidectomy. On the basis of reports indicating that exercise reduced the risk of fractures in women after menopause (23–25) as well as in elderly men [26], we examined whether physical exercise is capable of counteracting possible reduction of anti-osteoporotic efficacy of alendronate, induced by lansoprazole, in orchidectomized rats.

EXPERIMENTAL

Male Wistar rats at 3 months age (Center of Experimental Medicine, Medical University of Silesia, Katowice) were used in these studies. The initial rat body mass was 260–280 g. The rats were fed a standard laboratory diet (Labofeed B) *ad libitum* and were allowed free access to water. All procedures of the experiments on animals were approved by the Ethical Commission, Katowice, Poland.

Orchidectomy and sham-operation were performed in general anesthesia induced by intraperitoneal injections of ketamine – Bioketan (Vetoquinol Biowet) and xylazine – Xylapan (Vetoquinol Biowet). After 7–8 days, the rats were divided into six groups (n = 8): sham-operated (Sham) control rats, orchidectomized (ORX) control rats, ORX rats receiving alendronate, ORX rats receiving alendronate and lansoprazole, ORX rats receiving alendronate and subjected to exercise, ORX rats receiving alendronate and lansoprazole and subjected to exercise. The animals were weighed every second day. Lansoprazole (Lanzul, Inter Pharma) and alendronate sodium, substance (Polpharma S.A.) were used in the study. Alendronate (3 mg/kg) and lansoprazole (4 mg/kg) were administered by a gastric tube (*p.o.*) once daily, for 7 weeks (6 days a week), at a volume of 2 mL/kg *p.o*. Alendronate was administered in the morning hours, lansoprazole 2 h after the administration of alendronate. The control rats were administered the vehicle (distilled water) in the same volume of 2 mL/kg *p.o.* daily. Moreover, all rats were given intraperitoneal injection of 20 mg/kg of tetracycline hydrochloride (Sigma-Aldrich), to mark the calcification front (27), one day before the start of drug or exercise or vehicle administration and one day before sacrifice, in order to determine the periosteal and endosteal transverse growth.

On the day following the last administration of drugs, after 24-h fasting, the animals were killed by cardiac exsanguination, under full ketamine and xylazine anesthesia. The adrenal gland and bones: the left and right tibia and right femur were isolated from the sacrificed animals. Immediately after isolation, the left tibia and adrenal gland were weighed (with the accuracy of 0.1 mg). The left tibia and right femur were wrapped in gauze soaked in 0.9% NaCl solution and kept in the temperature of –20^{o}C until the mechanical tests were performed on thawed bones.

Exercise training

The exercise training was performed on a tape treadmill for rats (model BTP-10, Porfex, Białystok, Poland). The apparatus consisted of a 10-lane animal exerciser. The dimensions of each exercise lane are 37 × 13 × 8 cm. The animals were placed on a belt facing away from the electrified grid (2 mA intensity). Exercise sessions were always performed between 9 and 11 a.m., started in 7–8 days after the orchidectomy or sham-operation performed. The exercise consisted of a 7-week running, 6 days per week for 60 min. The time was gradually increased in the four first days (by 15 min daily) until 60 min a day was reached, and kept until the end of the training. The velocity was 25 m/min. The treadmill inclination was kept at 7^{o}C uphill during the entire training.

Studies of bone mechanical properties

Mechanical properties of the left tibial metaphysis and the neck of the right femur were assessed using the Instron 3342 500N apparatus with Bluehill 2 software, version 2.14. Mechanical properties of the left tibial metaphysis were studied using bending tests with three-point loading, as previously described (28–30). The load was applied perpendicularly to the proximal tibial metaphysis. The displacement rate was 0.01 mm/s. The load displacement curves, representing the relationships between load applied to the bone and displacement in response to the load, were analyzed. Maximum load and displacement, energy, and stress for the maximum load, as well as fracture load and displacement, energy, and stress for the fracture load were all assessed. Young's modulus was also determined. The moment of inertia in the cross-section, necessary for the calculations of the intrinsic bone mechanical parameters, was also determined, as previously described (31). Mechanical properties of the femoral neck were studied using a compression test. The maximum load (load causing the fracture of the femoral neck) was determined, as previously described (30, 31).

Bone histomorphometric studies

Bone histomorphometric parameters were assessed on histological specimens, prepared as previously described (32, 33). Histomorphometric measurements were made using an Optiphot-2 microscope (Nikon), connected through an RGB camera (Cohu) to a computer, using Lucia G 4.51 software (Laboratory Imaging), with final magnifications of 200 and 500 times, or using Osteomeasure software (magnification 70 times). The width of trabeculae in the distal epiphysis and metaphysis was measured in the longitudinal preparation from the femur. The area of the transverse cross-section of the cortical bone and the area of the transverse cross-section of the marrow cavity were determined in transverse cross-sections made from the tibial diaphysis. The periosteal and endosteal transverse growth of the tibia was also measured.

Bone mineralization studies

The mass of bone mineral (ash) was determined after mineralization. The bones were mineralized at the temperature of 640^{o}C for 48 h in the muffle furnace, and subsequently weighed. The ratio of the mass of bone mineral to the bone mass was also determined as a substitute for bone mineral density measurements.

Biochemical studies

Serum osteocalcin levels were determined using an enzyme immunoassay (Rat-MID Osteocalcin EIA, Immunodiagnostic Systems Ltd.). Serum levels of type I collagen fragments released from bone during bone resorption were determined by an enzyme immunoassay (RatLaps EIA, Immunodiagnostic Systems Ltd.). Moreover, serum total cholesterol was assayed colorimetrically, using a Pointe Scientific reagent set.

Statistical analysis

The results are presented as the arithmetical means ± SEM. Statistical estimation was carried out on the basis of the analysis of variance. After confirmation of statistically significant differences in one-way ANOVA ($p < 0.05$), further analysis was carried out by means of Duncan's *post hoc* test. In case of a lack of normality (Shapiro-Wilk's test) or of homogeneity of variance (Levene's test), nonparametric tests were used: Kruskal-Wallis ANOVA and Mann-Whitney U test. The results obtained in each experimental group were compared with those of the sham-operated control rats and orchidectomized control rats. The results obtained in rats treated with alendronate and lansoprazole, treated with alendronate and subjected to exercise, as well as treated with alendronate and lansoprazole and subjected to physical exercise were compared with those of the animals treated with alendronate. Moreover, the results obtained in rats treated with alendronate and lansoprazole and subjected to physical exercise were compared with those of the rats treated with alendronate and lansoprazole.

RESULTS

Body mass, adrenal mass and serum total cholesterol level

Androgen deficiency, in the ORX control rats, caused significant increases in the adrenal mass (by 47.4%) and in the adrenal mass expressed as the ratio to the body mass (by 39.5%), and insignificant increases in the serum total cholesterol level (by 30.1%), in comparison with the sham-operated rats. There was no effect of androgen deficiency on the body mass (Table 1). Alendronate did not affect the adrenal mass or serum cholesterol level, in comparison with the ORX control rats. Concurrent treatment with lansoprazole and alendronate led to a significant decrease in the adrenal mass in comparison with the ORX control rats. Exercise significantly increased the ratio of adrenal mass to body

Table 1. Body mass, adrenal mass and serum total cholesterol level in orchidectomized rats.

Parameters	Sham-operated rats	Orchidectomized (ORX) rats			
		Control	Alendronate	Alendronate and lansoprazole	Alendronate and exercise	Alendronate and lansoprazole and exercise
Body mass at the start of exercise and drug treatment [g]	267.3 ± 1.4	266.0 ± 3.2	267.3 ± 3.0	269.6 ± 1.6	265.0 ± 2.4	270.1 ± 3.7
Body mass after 7 weeks [g]	327.9 ± 4.0	343.8 ± 6.1	328.6 ± 7.7	331.1 ± 7.5	318.5 ± 8.2	327.5 ± 5.8
Adrenal mass [mg]	28.17 ± 1.62	41.54 ± 1.93***	36.49 ± 1.93 **	34.99 ± 1.88$^{\bullet}$ **	46.18 ± 1.45^{aaa} ***	47.33 ± 1.78$^{\bullet\ aaa}$ ***
Adrenal mass/body mass ratio [mg/100 g of body mass]	8.67 ± 0.54	12.09 ± 0.57***	11.11 ± 0.55**	10.58 ± 0.37*	14.52 ± 0.40$^{\bullet\bullet\ aaa}$ ***	14.46 ± 0.50$^{\bullet\bullet\ aaa}$ ***
Serum total cholesterol [mg/dL]	38.65 ± 2.37	50.27 ± 3.08	49.83 ± 3.07	49.03 ± 2.65	45.12 ± 5.03	45.35 ± 2.65

Results are presented as the mean ± SEM (n = 8). One-way ANOVA followed by Duncan's test or, when appropriate, Kruskal-Wallis ANOVA followed by Mann-Whitney U test was used for evaluation of the significance of the results. * – Significantly different from sham-operated rats; * – $p < 0.05$, ** – $p < 0.01$, *** – $p < 0.001$. $^{\bullet}$ – Significantly different from ORX control rats; $^{\bullet}$ – $p < 0.05$, $^{\bullet\bullet}$ – $p < 0.01$, ^{a} – Significantly different from the rats treated with alendronate; ^{aaa} – $p < 0.001$.

mass in rats treated with alendronate or alendronate and lansoprazole in relation to all other groups (Table 1).

Mass and mineral mass of the tibia

Androgen deficiency in the ORX control rats significantly reduced (by 6.7%) the mass of the tibia expressed as the ratio to the body mass, in comparison with the sham-operated rats. There was no significant effect of androgen deficiency on the bone mineral mass (Table 2). Alendronate caused significant increases in the mass of the tibia, mineral mass of the tibia and the ratio of the mineral mass of the tibia to the bone mass, in comparison with the ORX control rats. Those effects of alendronate were weakened by lansoprazole. In rats treated with lansoprazole and alendronate concurrently, the ratio of the mineral mass to the bone mass was increased, in comparison with the ORX control rats. Exercise did not affect the alendronate effect, and counteracted the weakening of the alendronate effect by lansoprazole. Significant increases in the bone mass expressed as the ratio to the body mass and bone mineral mass in the tibia were observed, in comparison with the rats treated with alendronate and lansoprazole (Table 2).

Bone histomorphometric parameters

In ORX control rats, the transverse cross-section areas of the cortical bone, of the whole diaphysis and of the marrow cavity, were not significantly affected, in comparison with the sham-operated rats, but there was a significant increase in the ratio of the transverse cross-section area of the marrow cavity to the area of the whole diaphysis (by 6.3%), and a significant decrease in the periosteal (by 8.3%) and endosteal (by 12.2%) transverse growth. In the ORX control rats, in comparison with the sham-operated rats, the width of trabeculae in the femoral epiphysis and metaphysis were significantly decreased, by 8.6 and 5.3%, respectively (Table 3). Alendronate counteracted the effect of androgen deficiency, causing significant decreases in the ratio of the transverse cross-section area of the marrow cavity to the area of the whole diaphysis, and increases in the endosteal transverse growth and in the width of trabeculae in the femoral epiphysis and metaphysis, in comparison with the ORX control rats. Lansoprazole weakened the effect of alendronate on all histomorphometric parameters studied. Exercise did not affect the alendronate effect, but counteracted the weakening of the alendronate effect by lansoprazole (Table 3).

Table 2. Mass and mineral mass of the tibia in orchidectomized rats.

Parameters	Sham-operated rats	Orchidectomized (ORX) rats				
		Control	Alendronate	Alendronate and lansoprazole	Alendronate and exercise	Alendronate and lansoprazole and exercise
Bone mass [mg]	627.83 ± 9.13	613.91 ± 10.61	637.23 ± 10.00	610.80 ± 9.18	636.30 ± 8.34	648.86 ± 13.51
Bone mass/body mass ratio [mg/100 g of body mass]	191.54 ± 2.31	178.67 ± 1.81*	193.98 ± 3.08$^{\bullet\bullet}$	184.95 ± 4.56	200.40 ± 3.98$^{\bullet\bullet\bullet}$	198.29 ± 3.76$^{\bullet\bullet\bullet}$ $^{\#}$
Mineral mass [mg]	272.36 ± 4.56	261.02 ± 4.13	279.38 ± 4.83$^{\bullet}$	269.24 ± 3.58	280.96 ± 4.37$^{\bullet\bullet}$	290.38 ± 5.81$^{\bullet\bullet\bullet}$ * $^{\#\#}$
Mineral mass/bone mass ratio [mg/100 mg of bone mass]	43.38 ± 0.30	42.53 ± 0.24	43.86 ± 0.50$^{\bullet}$	44.10 ± 0.37$^{\bullet}$	44.15 ± 0.26$^{\bullet\bullet}$	44.43 ± 0.87$^{\bullet}$ *

Results are presented as the mean ± SEM (n = 8). One-way ANOVA followed by Duncan's test or, when appropriate, Kruskal-Wallis ANOVA followed by Mann-Whitney U test was used for evaluation of the significance of the results. * – Significantly different from sham-operated rats; * – $p < 0.05$. $^{\bullet}$ – Significantly different from ORX control rats; $^{\bullet}$ – $p < 0.05$, $^{\bullet\bullet}$ – $p < 0.01$, $^{\bullet\bullet\bullet}$ – $p < 0.001$. $^{\#}$ – Significantly different from rats treated with alendronate and lansoprazole; $^{\#}$ – $p < 0.05$, $^{\#\#}$ – $p < 0.01$.

Table 3. Bone histomorphometric parameters in orchidectomized rats.

		Orchidectomized (ORX) rats					
		Sham-operated rats	Control	Alendronate	Alendronate and lansoprazole	Alendronate and exercise	Alendronate and lansoprazole and exercise
Transverse cross-section area [mm^2]	Cortical bone	3.78 ± 0.06	3.63 ± 0.07	3.64 ± 0.03	3.64 ± 0.06	3.73 ± 0.06	3.79 ± 0.07
	Marrow cavity	1.09 ± 0.02	1.13 ± 0.02	1.06 ± 0.02	1.09 ± 0.01	1.05 ± 0.04	1.08 ± 0.02
	Whole diaphysis	4.88 ± 0.07	4.77 ± 0.08	4.70 ± 0.04	4.73 ± 0.07	4.77 ± 0.09	4.87 ± 0.08
Transverse cross-section marrow cavity/diaphysis area ratio		0.224 ± 0.003	0.238 ± 0.004*	0.226 ± 0.004$^{\bullet}$	0.231 ± 0.002	0.219 ± 0.005$^{\bullet\bullet}$	0.223 ± 0.003$^{\bullet}$
Transverse growth [μm]	Periosteal	94.77 ± 1.61	86.86 ± 2.18*	94.28 ± 5.99	93.14 ± 1.71	106.06 ± 6.14$^{\bullet}$	105.30 ± 4.93$^{\bullet\bullet}$
	Endosteal	38.62 ± 1.27	33.92 ± 0.88*	39.15 ± 1.26$^{\bullet}$	38.02 ± 2.57	38.48 ± 0.71$^{\bullet\bullet}$	38.77 ± 1.28$^{\bullet}$
Width of trabeculae [μm]	Epiphysis	72.13 ± 0.68	66.95 ± 1.22**	72.73 ± 1.26$^{\bullet\bullet\bullet}$	70.03 ± 0.73$^{\bullet}$	71.45 ± 1.00$^{\bullet\bullet}$	71.49 ± 0.93$^{\bullet\bullet}$
	Metaphysis	36.71 ± 0.50	34.79 ± 0.41*	36.64 ± 0.42$^{\bullet}$	36.09 ± 0.48	37.07 ± 0.51$^{\bullet\bullet}$	37.42 ± 0.67$^{\bullet\bullet}$

Results are presented as the mean ± SEM (n = 8). One-way ANOVA followed by Duncan's test or, when appropriate, Kruskal-Wallis ANOVA followed by Mann-Whitney U test was used for evaluation of the significance of the results. * – Significantly different from sham-operated rats; * – $p < 0.05$, ** – $p < 0.001$. $^{\bullet}$ – Significantly different from ORX control rats; $^{\bullet}$ – $p < 0.05$, $^{\bullet\bullet}$ – $p < 0.01$, $^{\bullet\bullet\bullet}$ – $p < 0.001$.

Table 4. Mechanical properties of the tibial metaphysis (parameters for the fracture point and Young's modulus) in orchidectomized rats.

Parameters	Sham-operated rats	Orchidectomized (ORX) rats				
		Control	Alendronate	Alendronate and lansoprazole	Alendronate and exercise	Alendronate and lansoprazole and exercise
Fracture load [N]	85.19 ± 5.67	68.13 ± 2.25*	93.40 ± 5.04$^{\bullet\bullet\bullet}$	74.04 ± 2.50^{aa}	112.09 ± 5.92$^{\bullet\bullet\bullet\ aa}$ ***	104.98 ± 4.24$^{\bullet\bullet\bullet}$ ### **
Displacement for fracture load [mm]	1.22 ± 0.05	1.23 ± 0.06	1.19 ± 0.07	1.12 ± 0.04	1.03 ± 0.05	1.20 ± 0.07
Energy for fracture load [mJ]	73.25 ± 4.39	58.13 ± 3.23*	79.50 ± 6.79$^{\bullet\bullet}$	59.43 ± 4.01^{aa}	72.00 ± 3.27$^{\bullet}$	87.00 ± 5.52$^{\bullet\bullet\bullet}$ ###
Stress for fracture load [MPa]	75.15 ± 8.19	65.02 ± 3.82	92.14 ± 5.77$^{\bullet\bullet}$	70.36 ± 3.81^{aa}	108.12 ± 7.64$^{\bullet\bullet}$ *	97.14 ± 4.89$^{\bullet\bullet\bullet}$ ##
Young's modulus [MPa]	3616 ± 293	3077 ± 251	4655 ± 297$^{\bullet}$	3780 ± 299	4955 ± 562$^{\bullet\bullet}$	5080 ± 652$^{\bullet\bullet}$ *

Results are presented as the mean ± SEM (n = 8). One-way ANOVA followed by Duncan's test or, when appropriate, Kruskal-Wallis ANOVA followed by Mann-Whitney U test was used for evaluation of the significance of the results. * – Significantly different from sham-operated rats; * – $p < 0.05$, ** – $p < 0.01$, *** – $p < 0.001$. $^{\bullet}$ – Significantly different from ORX control rats; $^{\bullet}$ – $p < 0.05$, $^{\bullet\bullet}$ – $p < 0.01$, $^{\bullet\bullet\bullet}$ – $p < 0.001$. ^{a} – Significantly different from the rats treated with alendronate; ^{aa} – $p < 0.01$. # – Significantly different from rats treated with alendronate and lansoprazole; ## – $p < 0.01$, ### – $p < 0.001$.

Mechanical properties of the tibial metaphysis

Androgen deficiency in the ORX control rats significantly reduced, in comparison with the sham-operated rats, the maximum load (by 22.6%). Energy for the maximum load and the intrinsic mechanical parameters (maximum stress and Young's modulus) were insignificantly reduced (Figure 1, Table 4). The mechanical parameters for the fracture point were also decreased (fracture load and energy for the fracture load – significantly), in comparison with the sham-operated rats (Table 4). Alendronate significantly improved the mechanical parameters for the maximum load and the fracture point, as well Young's modulus. Lansoprazole weakened the alendronate effect on the mechanical properties of tibial metaphysis, significantly decreasing the maximum load, energy accumulated for the maximum load and maximum stress, as well as load, energy and stress for the fracture point, in relation to the rats treated with alendronate alone. Exercise intensified the alendronate effect on the mechanical properties of tibial metaphysis, significantly increasing the maximum load (Figure 1) and fracture load (Table 4) in relation to the rats treated with alendronate alone. Moreover, implementation of exercise significantly counteracted weakening of the alendronate effect by lansoprazole (Figure 1, Table 4).

Mechanical properties of the femoral neck

Androgen deficiency did not significantly affect the strength of the femoral neck in the ORX control rats, in relation to the sham-operated control rats (Figure 2). Alendronate insignificantly increased the maximum load sustained by the femoral neck of the orchidectomized rats. Lansoprazole weakened the alendronate effect on the maximum load sustained by the femoral neck. The exercising rats (both treated with alendronate, and treated with alendronate and lansoprazole) revealed increased strength of the femoral neck, in comparison with the ORX control rats (Figure 2).

Serum biochemical bone turnover markers

Androgen deficiency insignificantly increased the serum level of the biochemical marker of bone resorption (RatLaps, by 44.4%) and significantly increased the marker of bone formation (osteocalcin, by 24.0%), in comparison with the sham-operated controls (Figure 3). Alendronate significantly decreased the biochemical bone turnover markers, in comparison with the ORX control rats. Lansoprazole weakened the alendronate effect on the biochemical bone turnover markers, significant-

ly increasing the osteocalcin level in relation to the rats treated with alendronate alone. The levels of RatLaps and osteocalcin in exercising rats treated with alendronate and lansoprazole were similar to those in rats treated with alendronate alone. The level of osteocalcin in exercising rats treated with alendronate and lansoprazole was significantly increased, in relation to the rats treated with alendronate alone (Figure 3).

DISCUSSION

Orchidectomy in rats is a standard model used in examination of the influence of androgen deficiency upon the osseous system, reflecting the changes occurring in men with hypogonadism (34, 35). It causes a reduction of testosterone level in rat blood serum, by 80–95% (34, 36, 37). Reduction of mass and weakening of the bone microarchitecture may be observed as early as four weeks after the procedure, their intensity depends upon rat age and the duration of androgen deficiency (38, 39). Due to the bone mass dependence on age, orchidectomy is most often performed in fast growing rats, between third and twelfth month of life (34, 40–42). In the model applied in the study, orchidectomy was performed in three-month old rats, and the androgen deficiency lasted for 8 weeks.

Androgen deficiency increases the rate of bone turnover, causing loss of cancellous and cortical bone (34, 43–45). Also in the study reported here, the blood serum of orchidectomized control rats revealed increased levels of biochemical markers of bone turnover. Eight weeks after the procedure of orchidectomy, the mass and mass of bone mineral in the tibia were diminished. Those results indicate that the reduction of trabeculae width induced by androgen deficiency was connected with the increased resorption of cancellous bone. Bone loss was also observed in compact bone, which has been demonstrated through reduced transverse growth of the cortical bone in tibia diaphysis, from the periosteum and marrow cavity side. The loss of compact bone was less profound, and no significant changes of the

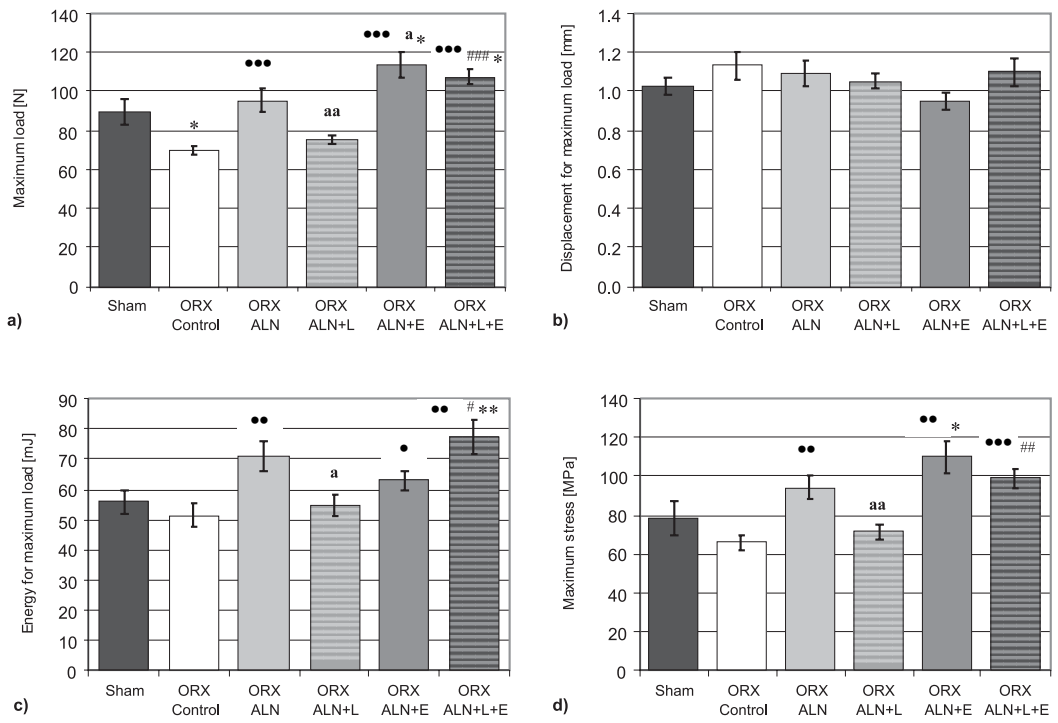

Figure 1. Mechanical properties of the tibial metaphysis (parameters for the maximum load point) in orchidectomized (ORX) rats. Results are presented as the mean ± SEM (n = 8). Kruskal-Wallis ANOVA followed by Mann-Whitney U test was used for evaluation of the significance of the results. * – Significantly different from sham-operated rats; * – $p < 0.05$, ** – $p < 0.01$. • – Significantly different from ORX control rats; • – $p < 0.05$, •• – $p < 0.01$, ••• – $p < 0.001$. ^{a} – Significantly different from the rats treated with alendronate; ^{a} – $p < 0.05$, ^{aa} – $p < 0.01$. # – Significantly different from rats treated with alendronate and lansoprazole; # – $p < 0.05$, ## – $p < 0.01$, ### – $p < 0.001$

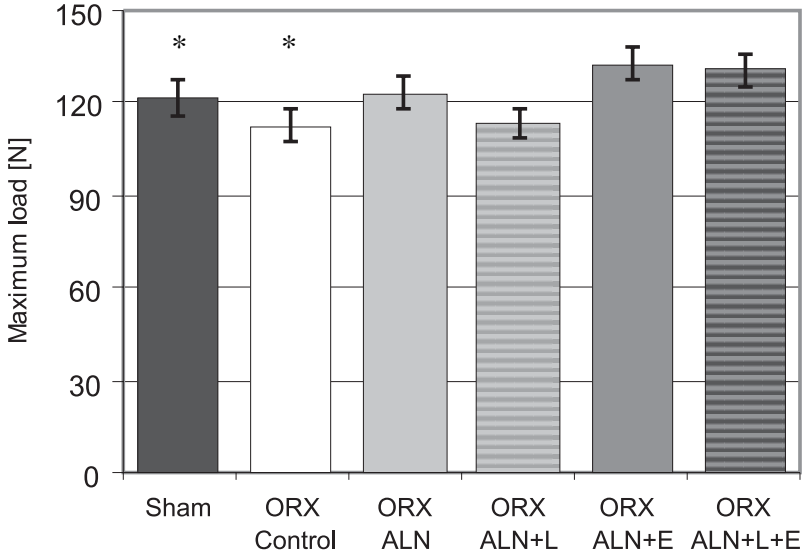

Figure 2. Mechanical properties of the femoral neck in orchidectomized (ORX) rats. Results are presented as the mean ± SEM (n = 8). Kruskal-Wallis ANOVA followed by Mann-Whitney U test was used for evaluation of the significance of the results. * – Significantly different from sham-operated rats; * – $p < 0.05$

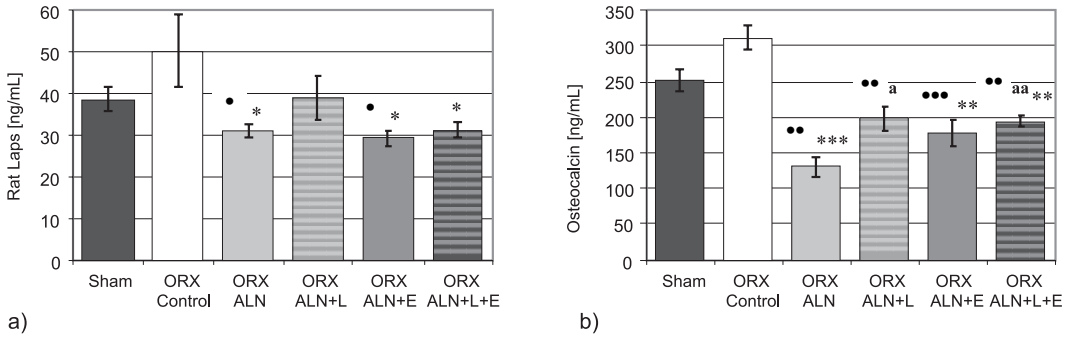

Figure 3. Serum bone turnover markers in orchidectomized (ORX) rats. Results are presented as the mean ± SEM (n = 8). Kruskal-Wallis ANOVA followed by Mann-Whitney U test was used for evaluation of the significance of the results. * – Significantly different from sham-operated rats; * – $p < 0.05$, ** – $p < 0.01$, *** – $p < 0.001$. • – Significantly different from ORX control rats; •• – $p < 0.01$, •• – $p < 0.01$, ••• – $p < 0.001$. [a] – Significantly different from the rats treated with alendronate; [a] – $p < 0.05$, [aa] – $p < 0.01$

area of cortical bone or the marrow cavity were observed. Nevertheless, the ratio of the marrow cavity the whole diaphysis area increased significantly, indicating a greater increase of resorption in the cortical bone. Those changes led to significant deterioration of mechanical properties in the spongy bone of tibia metaphysis, but not that of the femoral neck. Susceptibility to fracture of femoral neck is related mainly with the reduction of thickness of the cortical layer (46, 47). Thus, the absence of significant influence of androgen deficiency upon mechanical properties of femoral neck may be due to the lower reduction of compact bone layer. The latter has been confirmed by the study performed by Shuid et al. (34), who also failed to find a significant influence of androgen deficiency upon the mechanical properties of compact bone in femoral shaft in rats.

Preventive activity of alendronate has been examined at the dose efficient in preventing the consequences of estrogen deficiency upon the osseous system in ovariectomized rats (20, 21, 48). Alendronate is a potent antiresorptive nitrogen-containing bisphos-

phonate. It inhibits the mevalonate pathway in osteoclasts, by inhibiting farnesyl pyrophosphate synthase. This leads to a decrease of the formation of isoprenoid lipids, such as farnesyl pyrophosphate and geranylgeranyl pyrophosphate, required for the post-translational prenylation of proteins. The lack of geranylgeranyl pyrophosphate in osteoclasts is responsible for inhibiting activity and induction of osteoclast death by apoptosis (49). In the study reported here, the anti-resorptive activity of alendronate was reflected in the reduced level of a biochemical marker of bone resorption. Alendronate occurred to prevent the orchidectomy-induced, reduction of trabeculae width in cancellous bone, what is more, it also inhibited the influence of androgen deficiency upon the growth of compact bone, counteracting bone mass loss and reduction of mechanical strength of the tibia metaphysis and femoral neck in orchidectomized rats.

As we assumed, the activity of alendronate was significantly reduced by the lansoprazole, which was applied in a dose lower than the effective dose enabling protection against gastric ulcers induced by acidified ethanol and indomethacin in rats (22). Lansoprazole administered in orchidectomized rats together with alendronate weakened the preventive activity of alendronate upon the examined parameters in compact and cancellous bone, reducing its anti-osteoporotic efficacy. Lansoprazole abolished the beneficial influence of alendronate upon all the examined mechanical parameters of tibia metaphysis, and weakened its influence upon the strength of femoral neck. A similar effect has been observed after the administration of omeprazole or pantoprazole to ovariectomized rats (20, 21). The mechanism mediating the attenuation of anti-osteoporotic efficacy of alendronate by PPIs has not been recognized. Earlier reports suggested that increased risk of fracture after the application of PPIs may be connected with inhibition of calcium absorption from intestines (50), later reports – however – did not confirm the influence of PPIs upon calcium absorption (51, 52). It seems that also interaction between PPIs and alendronate at the absorption stage may be excluded, since ranitidine, another drug that reduces the secretion of hydrochloric acid, enhanced the bioavailability of alendronate (53). The latest *in vitro* studies demonstrated that omeprazole decreases the activation of osteoclasts and increases the activation of osteoblasts, which may induce a state resembling osteopetrorickets [54]. Also the studies of the skeletal phenotype in H^+/K^+-ATPase β-subunit knockout female mice revealed increased OPG/RANKL ratio and PTH, as well as reduced BMD, and inferior mechanical bone strength (55).

The exercise completely prevented the loss of anti-osteoporotic efficacy of alendronate, caused by lansoprazole. What is more, we demonstrated a positive interaction that occurred between the exercise and alendronate. The application of the exercise together with alendronate significantly increased the maximum and fracture load of tibia metaphysis, in comparison with rats treated with alendronate only. It also caused a significant increase of the force causing femoral neck fracture, in comparison with control orchidectomized rats. However, the most significant observation of the present study is that application of exercise to rats treated with alendronate and lansoprazole restored the lansoprazole-reduced anti-osteoporotic efficacy of alendronate. The exercise normalized the rate of bone turnover, promoting bone formation in compact and cancellous bone. The exercise is known to increase mechanical loading to bones, preventing apoptosis of osteocytes, that are main regulators of bone remodeling (56, 57). In response to mechanical load caused by the exercise, activation of the Wnt/β-catenine pathway also occurs, which is of key importance for differentiation and bone formation activity of osteoblasts (57, 58). Mechanical loading is a potent anabolic stimulus that strengthens bones and a major regulator of bone mass, geometry and microarchitecture (56, 57). In the study reported here, the exercise increased the width of trabeculae in cancellous bone and growth of compact bone from periosteum and marrow cavity, as well as bone mass, counteracting the lansoprazole-induced reduction of anti-osteoporotic efficacy of alendronate. Physical effort that rats treated with alendronate and lansoprazole have been exposed to significantly increased the load, energy, and stress in the points of the maximum and fracture loads in the tibia metaphysis, in reference to rats treated with alendronate and lansoprazole concurrently. It also significantly increased the load causing femoral neck fracture in comparison with orchidectomized control rats.

The data obtained so far indicate, however, that exercise is known to intensity- and duration-dependently induce the activation of the hypothalamus-pituitary-adrenocortical axis, as well as the sympatho-adrenomedullary system (59–61). Indicators that enable verification of exercise intensity in the study reported here may be the mass of adrenals and rat body mass (60, 61). Exercise causes intensity-dependent increase of the adrenal mass in mice (60) and in rats (61). We also noted an increase of adrenal mass, yet which was not statistically significant, at a level observed by Bartalucci et al. (60) in mice subjected to low-

intensity physical exercise. On the other hand, the adrenal mass to body mass ratio in our study was significantly greater than that in orchidectomized control rats, yet lesser than that observed by da Costa Lana et al. (61) in rats subjected to low-intensity exercise. Moreover, we failed to notice significant changes in rat body mass. Those results may indicate that exercise applied in the study reported here did not induce significant adaptive changes caused by the activation of the hypothalamus-pituitary-adrenals axis and the sympatho-adrenomedullary system.

In conclusion, the exercise prevented lansoprazole-induced reduction of anti-osteoporotic efficacy of alendronate in rats with androgen deficiency. Those results indicate that exercise may reduce the disadvantageous influence of PPIs upon alendronate activity and increase its anti-fracture efficacy in the treatment of osteoporosis in men.

Acknowledgment

This study was supported by Medical University of Silesia, Katowice (grant KNW-1-007/N/3/0).

REFERENCES

1. Szulc P., Kauffman J.M., Orwell E.S.: J. Osteoporos. 2012, ID675984 (2012).
2. Lambert J.K., Zaidi M., Mechanick J.I.: Curr. Osteoporos. Rep. 9, 229 (2011).
3. Rao S.S., Budhwar N., Ashfaque A.: Am. Fam. Physician 82, 503 (2010).
4. Vestergaard P., Rejnmark L., Mosekilde L.: Osteoporos. Int. 16, 134 (2005).
5. Khosla S.: J. Clin. Endocrinol. Metab. 95, 3 (2010).
6. Johnell O., Kanis J.A.: Osteoporos. Int. 17, 1726 (2006).
7. Kaufman J.M., Goemaere S.: Clin. Endocrinol. Metab. 22, 787 (2008).
8. Bliuc D., Nguyen N.D., Milch V.E., Nguyen T.V., Eisman J.A., Center J.R. et al.: JAMA 301, 513 (2009).
9. Schwarz P., Jorgensen N.R., Mosekilde L., Vestergaard P.: J. Osteoporos. 259818, (2011).
10. Adler R.A.: Ther. Adv. Musculoskelet. Dis. 3, 191 (2011).
11. Bell J.S., Blacker N., Edwards S., Frank O., Alderman C.P., Karan L., Husband A., Rowett D.: Aust. Fam. Physician 41, 110 (2012).
12. Shen L., Xie X., Su Y., Luo C., Zhang C., Zeng B.: PLoS One 6, e26267 (2011).
13. Orwoll E.S., Miller P.D., Adachi J.D., Brown J., Adler R.A., Kendler D. et al.: J. Bone Miner. Res. 25, 2239 (2010).
14. Salari P., Abdollahi M.: J. Pharm. Pharm. Sci. 15, 305 (2012).
15. Gray S.L., LaCroix A.Z., Larson J., Robbins J., Cauley J.A., Manson J.E., Chen Z.: Arch. Intern. Med. 170, 765 (2010).
16. Khalili H., Huang E.S., Jacobson B.C., Camargo C.A. Jr., Feskanich D., Chan A.T.: BMJ 344, e372 (2012).
17. Yu E.W., Blackwell T., Ensrud K.E. Hillier T.A., Lane N.E., Orwoll E., Bauer DC.: Calcif. Tissue Int. 83, 251 (2008).
18. de Vries F., Cooper A.L., Cockle S.M. van Staa TP, Cooper C.: Osteoporos. Int. 20, 1989 (2009).
19. Abrahamsen B., Eiken P., Eastell R.: Arch. Intern. Med. 171, 998 (2011).
20. Pytlik M., Cegieła U., Nowińska B., Folwarczna J., Śliwiński L., Kaczmarczyk-Sedlak I. et al.: Acta Pol. Pharm. Drug Res. 69, 113 (2012).
21. Pytlik M., Cegieła U., Folwarczna J., Nowińska B.: Pharmacol. Rep. 64, 625 (2012).
22. Chandranath S.I., Bastaki S.M., Singh J.: Clin. Exp. Pharmacol. Physiol. 29, 173 (2002).
23. Cussler E.C., Going S.B., Houtkooper L.B., Stanford V.A., Blew R.M., Flint-Wagner H.G. et al.: Osteoporos. Int. 16, 2129 (2005).
24. Bergström I., Parini P., Gustafsson S.A. Andersson G., Brinck J.: J. Bone Miner. Metab. 30, 202 (2012).
25. Howe T.E., Shea B., Dawson L.J., Downie F., Murray A., Ross C. et al.: Cochrane Database Syst. Rev. 7, ID000333 (2011).
26. Kukuljan S., Nowson C.A., Bass S.L., Sanders K., Nicholson G.C., Seibel M.J. et al.: Osteoporos. Int. 20, 1241 (2009).
27. Frost H.M.: Calcif. Tissue Res. 3, 211 (1969).
28. Turner C.H., Burr D.B.: Bone 14, 595 (1993).
29. Stürmer E.K., Seidlová-Wuttke D., Sehmisch S., Rack T., Wille J., Frosch K.H., et al.: J. Bone Miner. Res. 21, 89 (2006).
30. Folwarczna J., Nowińska B., Śliwiński L., Pytlik M., Cegieła U., Betka A.: Acta Biochim. Pol. 58, 313 (2011).
31. Cegieła U., Folwarczna J., Pytlik M., Zgórka G. et al.: Evid. Based Complement. Alternat. Med. 2012, 921684 (2012).
32. Cegieła U., Pytlik M., Janiec W.: Pol. J. Pharmacol. 52, 33 (2000).
33. Folwarczna J., Śliwiński L., Cegieła U., Pytlik M., Kaczmarczyk-Sedlak I., Nowińska B. et al.: Pharmacol. Rep. 59, 349 (2007).

34. Shuid A.N., El-arabi E., Effendy N.M., Razak H.S., Muhammad N., Mohamed N., Soelaiman I.N.: BMC Complement. Altern. Med. 12, 152 (2012).
35. Vanderschueren D., Vandenput L., Boonen S., Van Herck E., Swinnen J.V., Bouillon R.: Endocrinology 141, 1642 (2000).
36. Gill R.K., Turner R.T., Wronski T.J., Bell NH.: Endocrinology 139, 546 (1998).
37. Sosic-Jurjevic B., Filipovic B., Renko K.. Ajdzanovic V., Manojlovic-Stojanoski M., Milosevic V., Köhrle J.: J. Endocrinol. 215, 247 (2012).
38. Libouban H., Moreau M.F., Legrand E., Audran M., Baslé M.F., Chappard D.: Osteoporos. Int. 13, 422 (2002).
39. Ke H.Z., Crawford D.T., Qi H., Chidsey-Frink K.L., Simmons H.A., Li M., Jee W.S.S., Thompson D.D.: J. Musculoskelet. Neuronal. Interact. 1, 215 (2001).
40. Ramli R., Khamis M.F., Shuid A.N.: Evid. Based Complement. Alternat. Med. 2012, 501858, (2012).
41. Komrakova M., Krischek C., Wicke M., Sehmisch S., Tezval M., Rohrberg M. et al. J. Endocrinol. 209, 9 (2011).
42. Tezval M., Serferaz G., Rack T., Kolios L., Sehmisch S., Schmelz U. et al.: World J. Urol. 29, 529 (2011).
43. Iwamoto J., Matsumoto H., Takeda T., Sato Y., Xu E., Yeh J.K.: Chin. J. Physiol. 51, 331 (2008).
44. Erben R.G., Eberle J., Stahr K., Goldberg M.: J. Bone Miner. Res. 15, 1085 (2000).
45. Iwamoto J., Takeda T., Katsumata T., Tanaka T., Ichimura S., Toyama Y.: Bone 30, 360 (2002).
46. Crabtree N., Loveridge N., Parker M., Rushton N., Power J., Bell K.L. et al.: J. Bone Miner. Res. 16, 1318 (2001).
47. Mayhew P.M., Thomas C.D., Clement J.G., Loveridge N., Beck T.J., Bonfield W. et al.: Lancet 366, 129 (2005).
48. Noa M., Más R., Mendoza S., Gámez R., Mendoza N.: Drugs Exp. Clin. Res. 30, 35 (2004).
49. Roelofs A.J., Thompson K., Gordon S., Rogers M.J.: Clin. Cancer Res. 12, 6222s (2006).
50. Wright M.J., Proctor D.D., Insogna K.L., Kerstetter J.E.: Nutr. Rev. 66, 103 (2008).
51. Hansen K.E., Jones A.N., Lindstrom M.J., Davis L.A., Ziegler T.E., Penniston K.L. et al.: J. Bone Miner. Res. 25, 2786 (2010).
52. Wright M.J., Sullivan R.R., Gaffney-Stomberg E., Caseria D.M., O'Brien K.O., Proctor D.D. et al.: J. Bone Miner. Res. 25, 2205 (2010).
53. Gertz B.J., Holland S.D., Kline W.F., Matuszewski B.K., Freeman A., Quan H. et al.: Clin. Pharmacol. Ther. 58, 288 (1995).
54. Hyun J.J., Chun H.J., Keum B., Seo Y.S., Kim Y.S., Jeen Y.T. et al.: Int. J. Mol. Med. 26, 877 (2010).
55. Fossmark R., Stunes A.K., Petzold C., Waldum H.L., Rubert M., Lian A.M. et al.: J. Cell Biochem. 113, 141 (2012).
56. Bergmann P., Body J.J., Boonen S., Boutsen Y., Devogelaer J.P., Goemaere S. et al.: J. Osteoporos. 786752 (2011).
57. Gortazar A.R., Martin-Millan M., Bravo B., Plotkin L.I., Bellido T.: J. Biol. Chem. 288, 8168, (2013).
58. Galli C., Passeri G., Macaluso G.M.: J. Dent. Res. 89, 331 (2010).
59. Kawashima H., Saito T., Yoshizato H., Fujikawa T., Sato Y., McEwen B.S., Soya H.: Life Sci. 76, 763 (2004).
60. Bartalucci A., Ferrucci M., Fulceri F., Lazzeri G., Lenzi P., Toti L. et al.: Histol. Histopathol. 27, 753 (2012).
61. da Costa Lana A., Paulino C.A., Gonçalves I.D.: Rev. Bras. Med. Esporte 12, 223e (2006).

Received: 24. 07. 2013

Acta Poloniae Pharmaceutica – Drug Research, Vol. 71 No. 3 pp. 497–507, 2014 ISSN 0001-6837
Polish Pharmaceutical Society

THE INFLUENCE OF PIROXICAM, A NON-SELECTIVE CYCLOOXYGENASE INHIBITOR, ON AUTONOMIC NERVOUS SYSTEM ACTIVITY IN EXPERIMENTAL CYCLOPHOSPHAMIDE-INDUCED HEMORRHAGIC CYSTITIS AND BLADDER OUTLET OBSTRUCTION IN RATS

ŁUKASZ DOBREK*, AGNIESZKA BARANOWSKA, BEATA SKOWRON and PIOTR J. THOR

Chair of Pathophysiology, Jagiellonian University Collegium Medicum,
Czysta 18 St., 31-121 Kraków, Poland

Abstract: Signs and symptoms of secondary overactive bladder (OAB) are observed both in course of infravesical obstruction of urine outflow in patients with benign prostatic hyperplasia, and as a result of development of hemorrhagic cystitis (HC) following administration of cyclophosphamide (CP). Non-steroidal anti-inflammatory drugs (NSAIDs) alleviate symptoms of bladder overactivity reducing local synthesis of prostaglandins (PGs), but precise effects of those agents on functions of the autonomic nervous system (ANS) in course of OAB remain unknown. The purpose of this study was to evaluate the effect of piroxicam-induced prostaglandins (PGs) synthesis block on activity of the ANS in two experimental models of secondary OAB: bladder outlet obstruction (BOO) and cyclophosphamide-induced HC (CP-HC), by heart rate variability analysis (HRV). The experiment was performed on a group of rats with surgically induced 2-week BOO, and on a group of rats that were administered CP five times, with corresponding control groups. Study animals were given piroxicam (PRX) *i.p.* in two doses: 2 and 10 mg/kg b.w.
In the BOO model, PRX in both doses revealed a trend for reduction of value of all non-normalized components of HRV. The lower PRX dose caused an increased nHF value, and PRX administered in the dose of 10 mg/kg b.w. caused an increase of the nLF value. In the CP-HC model, the lower PRX dose caused a trend for an increase of values of all non-normalized components, and the higher dose – for their decrease. Both doses of PRX in that model caused increase of the nLF value. Inhibition of PGs synthesis caused changes of ANS function in both models of OAB. Both in BOO and in CP-HC, PGs seem to be ANS-activating factors, responsible for maintenance of a high parasympathetic activity. In both models, inhibition of PGs synthesis with PRX administered at the dose of 10 mg/kg b.w. lead to functional reconstruction of ANS, with marked sympathetic predominance. That may contribute to reduction of the bladder contractile action and improvement of its compliance in the filling period, which was demonstrated by other authors in urodynamic tests for NSAIDs.

Keywords: overactive bladder, cyclophosphamide, bladder outlet obstruction, prostaglandins, autonomic nervous system, heart rate variability

Abbreviations: ANS – autonomic nervous system, BOO – bladder outlet obstruction, BPH – benign prostatic hyperplasia, BWW – bladder wet weight, COX – cyclooxygenase, CP – cyclophosphamide, CP-HC – cyclophosphamide-induced hemorrhagic cystitis, HF – high frequency (HRV spectral, non-normalized component), HRV – heart rate variability, LF – low frequency (HRV spectral, non-normalized component), nHF – normalized high hrequency (HRV spectral, normalized component), nLF – normalized low frequency (HRV spectral, normalized component), NSAIDs – non steroidal antiinflammatory drugs, OAB – overactive bladder, PGs – prostaglandins, PRX – piroxicam, rMSSD – the square root of the mean squared difference of successive normal-normal (R-R) intervals, R-R – an interval between two subsequent R waves in ECG recording, SDNN – standard deviation of all normal-normal (R-R) beats, TP – total power (HRV spectral, non-normalized component), VLF – very low frequency (HRV spectral, non-normalized component)

Symptoms of the urinary bladder overactivity, with an impairment of the filling phase and its reduced compliance, are common problems of the lower urinary tract. According to the currently applied terminology, disorders suggesting some dysfunctions of the bladder filling phase (urinary urgency) and micturition (polyuria, frequent passage of small amounts of urine, urine incontinence), constitute a basis for diagnosis of the overactive bladder syndrome (OAB) (1, 2).

* Corresponding author: e-mail: lukaszd@mp.pl; phone/fax 12 632 90 56

The disease is an idiopathic disorder, or is a result of action of various etiological factors leading to detrusor overcontractility with reduced filling phase of the bladder. A general pathophysiological description of idiopathic OAB assumes, that its development is a result of complex disorders, both of myogenic (abnormal electric coupling of smooth muscle cells of the vesicular wall, contributing to contractile overreactivity) and neurogenic character. A precise pathophysiological description of idiopathic OAB exceeds the framework of this paper, and all necessary information may be found in numerous reviews in that area (3–5), also published by us (6). Bladder overactivity is also observed in course of various organic disorders of the lower urinary tract. Symptoms of OAB occur in patients treated with cytostatic alkylating drugs belonging to the group of oxazaphosphorins (e.g., cyclophosphamide), accompanying symptoms of hemorrhagic cystitis (HC; cyclophosphamide-induced HC; CP-HC). The pathogenesis of hemorrhagic cystitis is associated with development of the bladder inflammatory condition – that, according to the OAB neurogenic theory, is co-responsible for changing the activity of afferent fibres and, at the same time, the efferent control of the bladder function. The key pathogenetic factor is release of acrolein (as a result of cyclophosphamide metabolism in the bladder), as a factor initiating some complex immunological-inflammatory changes, with overproduction of NF-κB, TNF-α and overactivity of cyclooxygenases (COX) (7, 8). The pathophysiological description of that disorder has been also published in one of our earlier papers (9). It is also generally known that patients with benign prostatic hyperplasia (BPH) also present symptoms of bladder overactivity. Pathogenesis of bladder overactivity in BPH patients depends on the bladder reconstruction secondary to the existing sub-vesicular block and urine outlet obstruction (10).

The above mentioned disorders may be relatively easily studied on animal models. According to the literature, it is possible to cause a hemorrhagic cystitis by four intraperitoneal administration of 75 mg/kg b.w. cyclophosphamide to rats (the CP-HC model) (11, 12). On the other hand, BPH may be experimentally reflected by surgical creation of a partial bladder outlet obstruction (the BOO model) obtained by partial ligation of the proximal section of the urethra (13, 14).

In both above mentioned cases of secondary OAB, disturbances of the autonomic bladder control are an additional pathogenetic element. In our previous studies, we have demonstrated that in experimental CP-HC, the autonomic nervous system (ANS) activity became reduced with a proportional reduction of both sympathetic and parasympathetic tonus (15). However, evaluating function of the ANS in a 2-week BOO model in a rat, we have also found features of reduction of global autonomic activity, but with a reduced parasympathetic tonus and a relative sympathetic dominance (16). Autonomic abnormalities observed in the above mentioned experimental models may depend on altered paracrine function of the urothelium, being a result of the existing inflammatory condition (CP-HC) or excessive muscularization of the bladder due to its overpressurising. Those disorders cause release of prostaglandins (PGs) inside the bladder. PGs may be co-responsible for excessive sensitization of the bladder sensory fibres and reflexive change of tonus of efferent fibres.

It is generally known that PGs are synthesized *de novo* from arachidonic acid, in a multi-stage process with participation of cyclooxygenase (currently identified with prostaglandin H synthase, or prostaglandin endoperoxidase) and individual cellular synthases for given prostanoids. Cyclooxygenase is a molecular binding point for non-steroidal anti-inflammatory drugs (NSAIDs), that exert an analgesic and antipyretic effect by inhibition of synthesis of prostaglandins. There are several isoforms of cyclooxygenases (COX1 – constitutive, COX2 – inflammatory-induced, COX3 – central form), constituting a basis for pharmacodynamic classification of NSAIDs, depending on their – selective or non-selective – effect on individual COX isoforms (17, 18).

Studies demonstrated that PGs are synthesized locally in the bladder, both in the urothelium and the muscular coat, indicating a complex, endocrine control of the bladder function (19, 20). Intravesical PGs administration to rats caused reduction of the bladder compliance and its overreactivity (21, 22). Experimental studies demonstrated as well an increased COX expression, both in the BOO model (23) in response to the bladder overpressure and its dilation, and in the model of post-cyclophosphamide bladder injury, as a result of internal inflammation (24). Some recent studies demonstrated also that interstitial cells of Cajal, being an electric "pacemaker" of the bladder, controlling its motor function (similarly to the digestive tract) also present a high COX expression (both isoforms 1 and 2) (25).

Considering pleiotropic character of prostanoids, determination of their potential role in the bladder overactivity in course of post-cyclophosphamide, hemorrhagic cystitis and benign prostatic

hyperplasia, in context of their effect on autonomic regulation, seems important. Therefore, the purpose of this study was to determine an indirect – through a pharmacological inhibition of prostaglandin synthesis with piroxicam (PRX), a non-selective COX inhibitor – effect of prostaglandins on activity of the autonomic nervous system in experimental models of post-cyclophosphamide, hemorrhagic cystitis (the CP-HC model) and of a partial bladder outlet obstruction (the BOO model). Currently, a non-invasive evaluation of the autonomic nervous system – both for clinical and experimental purposes – is allowed by examination of the heart rate variability (HRV). The HRV analysis is based on evaluation of variability of R-R intervals in the ECG record. Those intervals fluctuate constantly due to the fact that the heart remains under constant autonomic control. That parameter is a starting point for time-domain HRV analysis, yielding some derivative parameters. It also allows determination of a HRV spectrum with its basic components (HRV spectral analysis) (26, 27). Therefore, evaluating an autonomic control of the heart, some indirect conclusions of the ANS functional status may be drawn.

EXPERIMENTAL

The study was carried out following a consent of the 1st Local Bioethics Committee in Kraków (No. 126/2010 and 28/2013).

Animals

Sixty 6-weeks-old Wistar rats obtained from the central animal house of the Pharmaceutical Faculty of the Jagiellonian University Collegium Medicum in Kraków were used for experiments. For acclimatization to new living conditions, for the first week animals were placed in five collective cages, with unlimited access to a standard laboratory feed (Labofeed, Kcynia) and water. Constant temperature of 22°C was maintained in the room. At the beginning of the experiment, rats were randomized into study groups, 10 animals in each group. During the experiment, animals in the particular group lived together in the same cage (10 animals per cage), and had unlimited access to water and feed.

General outline of the experiment

The experiment was run on animals with BOO, treated (BOO + PRX) and untreated (control) with piroxicam. Also animals with post-cyclophosphamide hemorrhagic cystitis were divided into two groups: treated with piroxicam (CP-HC + PRX) and untreated (control). Moreover, both in the BOO + PRX, and CP-HC + PRX group we have used two doses of PRX: 2 mg/kg b.w. and 10 mg/kg b.w. (choice of doses was based on previously published experimental studies using PRX (28, 29)). Therefore, finally six study groups were formed: BOO (control of the BOO model; group 1); BOO + PRX 2 mg/kg b.w (group 2); BOO + PRX 10 mg/kg b.w. (group 3); and CP-HC (control of the CP-HC model; group 4); CP-HC + PRX 2 mg/kg b.w. (group 5); CP-HC+PRX 10 mg/kg b.w. (group 6).

CP-HC model

In thirty animals, an experimental model of hemorrhagic cystitis with its overactivity was created by four (every two days – on the day one, three, five and seven) intraperitoneal administrations of cyclophosphamide – CP (Sigma Aldrich) – at the dose of 75 mg/kg b.w. The CP solution was prepared each time *ex tempore* before administration. According to the literature, dosage scheme leads to hemorrhagic cystitis following the fourth dose (11, 12). Ten animals received CP only, and formed a control group (group 4), and other 20 rats received additionally piroxicam (Feldene, Pfizer, ampoules 20 mg/mL) in two doses: 2 and 10 mg/kg b.w., as described above. PRX, the same as CP, was administered intraperitoneally four times, two hours following the administration of CP. In the group of animals receiving 10 mg/kg b.w. PRX, four animals died – therefore, only six animals were considered in the final analysis. In the CP-HC + PRX 2 mg/kg b.w. group one animal died, therefore HRV records were finally obtained from 9 animals. The controls received normal saline in volume corresponding to the volume of PRX instead of PRX. All animals in that group survived administration of the fourth dose of CP, but a majority of them were in overall poor condition. We have even observed a body weight reduction in those animals.

BOO model

Another 30 animals had the proximal section of urethra partially surgically ligated, in order to create the bladder outlet obstruction. According to the literature, a condition clinically corresponding to BPH with bladder overactivity develops within two weeks post the surgery (13, 14). The procedure was conducted under pentobarbital anesthesia (Morbital, Puławy, 40 mg/kg b.w. administered *i.p.*). Following the anesthesia, a medial cut was made in the projection over the bladder. Exposed bladder was carefully separated from the surrounding fatty tissue, and the urethra was catheterized (polyethylene catheter, diameter 0.58 mm), ligating the proxi-

mal section of the urethra around the catheter. After the catheter was removed, abdominal integument and skin were sutured in layers with standard surgical sutures (Medilen 4/0 USP; cutting needle DS2, 3/8). The surgical wound was sprayed with neomycin and the skin was sprayed with oxycort to minimize the risk of post-surgical infection. Two first days after the surgery were treated as a convalescence period. On the day three, PRX was administered *i.p.* at the dose of 2 or 10 mg/kg b.w. in both BOO + PRX subgroups (groups 2 and 3), or normal saline was administered at the volume corresponding to the volume of PRX in the control BOO group (group 1). PRX or normal saline were administered, similarly to CP-HC + PRX/CP-HC groups, four times – on the day three, seven, eleven and fifteen after the surgery. Two animals in the control BOO group did not survive the procedure. Therefore, that group consisted finally of 8 animals. Moreover, 2 animals treated with PRX at the dose of 2 mg/kg b.w. and 3 animals treated with PRX at the dose of 10 mg/kg b.w. died before reception of the final dose. Therefore, HRV records were obtained from 8 animals in the BOO + PRX 2 mg/kg b.w. group and from 7 animals in the BOO + PRX 10 mg/kg b.w. group.

Body weight and excreted urine volume measurement

On the first day of the experiment and on the last day (the day of HRV records registration) body weight of animals was measured in all study groups. Moreover, on the first day of the experiment, we measured a daily urine output in healthy animals randomized to control groups in BOO and CP-HC models (groups 1 and 4) and in animals treated with PRX (groups 2, 3, 5, 6) – after the last PRX dose and on the day preceding the HRV registration.

HRV records

In groups 1–3 HRV was recorded on the day fifteen (day after the last dose of PRX administered to animals in groups 2 and 3 and normal saline to animals in the group 1). In groups 4–6 HRV was recorded on the day eight (after the last dose of CP and PRX or normal saline). For all rats the HRV registration was performed under urethane anesthesia (Sigma Aldrich; 1200 mg/kg b.w.), considering the literature reports of the relatively lowest effect of urethane on the autonomic nervous system, compared to other anesthetics (30, 31). After an animal was anesthetized, shaved and placement of ECG gel, three disposable electrodes Ag/AgCl (E30, Sorimed, Poland) were placed in standard places. Two of them were active electrodes and one a reference, in order to obtain a single-channel, bipolar record. During the record, animals were placed under a heating lamp to prevent chilling that could negatively affect the ANS activity. ECG was registered at rest for 20 min (Polygram, ADInstruments). Following registration, records were analyzed for time- and spectral (frequency) HRV analysis, with calculation of standard parameters, according to generally accepted guidelines (26, 27). The time analysis involved: mean RR [ms] – a mean duration between subsequent R-R waves, maximum and minimum duration between subsequent R-R waves [ms], range of variability of R-R intervals [ms], mean heart rate [bpm], SDRR – standard deviation of all R-R intervals, and rMSSD – square root of mean sum of differences between R-R waves.

Evaluated in the spectral analysis were: total power (TP), powers of individual non-normalized components of the spectrum in the range of very low frequency (VLF), low frequency (LF), and high frequency (HF); all expressed in power units [ms^2], LF/HF ratio and values of normalized parameters nLF and nHF (expressed in normalized units [n.u.]). The following ranges were accepted for individual components of the spectrum: $0.18 < VLF < 0.28 < LF < 0.78 < HF < 3$.

Collection of bladders

Following HRV recording, animals were sacrificed with a lethal dose of pentobarbital (Morbital, Puławy, Poland; 100 mg/kg b.w.) for weight and histopathological analysis of their bladders. The bladder was collected from each of the study animals, following a previous separation from the surrounding fatty tissue and voiding. According to the literature data, measurement of the bladder wet weight (BWW) may be treated as an indirect evidence of the bladder reconstruction induced by inflammation (in the CP-HC model) or by outlet obstruction (in the BOO model), associated with its overactivity (32–34). Directly after collection, bladders were weighed on an analytic scale and then placed in 4% formalin solution with PBS for further histopathological evaluation. During the histopathological procedure, the urinary bladders collected during autopsy were rinsed in the saline solution. Next, they were strengthened for 24 h in the 8% formalin with phosphate buffer solution (PBS; pH 7.4). Afterwards, the samples were rinsed in the slow running water for 2 h, and then they were drained in the successive growing concentration (50–100%) of ethanol solutions. Before sinking into paraffin, the samples were moved through both pure xylene solu-

tion and mixture of xylene and paraffin (1 : 1) and incubated for 2 h with the maintenance of 37°C. Next, the individual tissue fragments were moved twice to clean paraffin and incubated again in temperature 62°C. In the end, after 2 h, the samples were sunk into blocks and after hardening were cut using the microtome. The obtained scraps were placed on the microscopic slides and dried in the thermostat at 37°C. The finally prepared microscopic sections were stained with hematoxylin eosin method (HE) to enable the histologic evaluation of the inflammatory process intensification.

Statistical analysis

Obtained results were analyzed separately for groups 1–3 and 4–6 using the Bartlett test, at $\alpha = 0.05$. Then, paired results were analyzed for groups: 1–2, 1–3 and 4–5, 4–6 using the Fischer Snedecor test at the same α value. Calculated HRV values, considering lack of their normal distribution, were converted into logarithmic values (natural logarithms) for the sake of the statistical analysis.

RESULTS

Body weight and urine volume measurements

At the beginning of the experiment, body weight of study animals was 188.30 ± 11.83 g. In the BOO population (group 1), on the day 15 of the experiment, a mean body weight of study animals was 203.20 ± 8.58 g, and in the CP-HC model (group 4), on the day 8 of the study, a day after the final dose of CP, a mean body weight was reduced to 181.67 ± 10.62 g, which was associated with poor general condition of animals in that group.

Before the experiment, healthy rats excreted a mean volume of 9.50 ± 4.37 mL of urine per day. In the BOO model (group 1), on the day 14 following induction of BOO we recorded a mean daily urine output of 6.90 ± 1.03 mL, and in the CP-HC population (group 4), on the day seven following the last dose of CP – 14.83 ± 6.43 mL. Measurements of daily urine output were intended as an additional, indirect evidence of the bladder function disorders in examined models. We did not analyze any precise changes of those parameters under influence of PRX.

Evaluation of bladder wet weight of collected bladders

In the BOO group (group 1), on the day 15 of the experiment, the bladder wet weight achieved 0.26 ± 0.24 g, and in the CP-HC population (group 4), on the day 7 following the last dose of CP – 0.17 ± 0.04 g. Similarly to the measurement of daily urine output and according to the above mentioned literature (32–34), the BWW measurement was intended as an indirect evidence of the bladder function disorders in particular studied models. The parameter wasn't also analyzed for effect of PRX. Therefore, we gave up analogous measurements in PRX-treated groups.

Conclusions of histological analysis of collected bladders

According to the pathomorphological evaluation, bladders collected from animals with experimental bladder outlet obstruction (control group of the BOO model; group 1) demonstrated signs of edema and congestion of the bladder wall, with a minimal hyperplasia of the muscular layer. In the group 4 (control group of the CP-HC model) a clear edema and signs of congestion (mostly of the cystic mucosa) were found, and also signs of focal proliferation of fibroblasts in the mucosal lamina propria, mostly around some fine, submucosal blood extravasations. Fine lymphocytic inflammatory infiltrations were visible in vicinity of vessels of the mucosal lamina propria. Epithelium of the bladder lining demonstrated focal ulceration with signs of clear proliferation of cells and of anisonuleosis focalis et papillosis. The bladder wall muscular coat was normotypic.

HRV analysis in the BOO model

Time-domain analysis

Parameters of the HRV time analysis were not significantly different in both groups treated with PRX and in the control group 1. The population treated with 2 mg/kg b.w. PRX presented the lowest value of the mean R-R interval, with the highest heart rate. Animals treated with the higher dose of PRX (group 3) demonstrated the highest SDNN value. Results of the HRV time-domain analysis of animals in the BOO model are presented in Table 1.

Spectral-domain analysis

Spectral analysis of the BOO model revealed a trend for reduction of the total power of the spectrum and its non-normalized components in both groups treated with PRX compared to the control group. Significant differences were observed for normalized spectral parameters and their mutual relations – in the group 2 (lower PRX dose) a clear dominance of nLF was observed with reduction of the nHF value; in the group 3 (higher PRX dose) that correlation was precisely reverse.

Results of the HRV spectral analysis of animals in the BOO model are presented in Table 2.

Table 1. Time-domain HRV analysis results in rats with experimental bladder outlet obstruction (BOO) model treated with piroxicam (PRX).

HRV time-domain parameter	Studied groups			Statistical analysis (for ln values)	
	group 1 BOO control	group 2 BOO + PRX 2 mg/kg b.w.	group 3 BOO + PRX 10 mg/kg b.w.	1–2	1–3
mean RR [ms]	171.80 ± 11.87	160.00 ± 8.53	172.05 ± 6.99	p = 0.01	NS
max RR [ms]	188.32 ± 1.61	178.86 ± 10.79	188.74 ± 1.25	NS	NS
min RR [ms]	149.32 ± 18.94	145.45 ± 4.22	145.75 ± 12.57	NS	NS
range [ms]	37.10 ± 15.90	33.40 ± 12.94	42.97 ± 12.47	NS	NS
average HR [bpm]	351.00 ± 25.31	375.84 ± 18.75	349.18 ± 13.99	p = 0.01	NS
SDNN	7.83 ± 3.95	5.17 ± 3.20	12.52 ± 3.94	NS	p = 0.03
rMSSD	7.87 ± 8.34	3.00 ± 4.37	13.31 ± 12.15	NS	NS

NS = not significant

Table 2. Spectral-domain HRV analysis results in rats with experimental bladder outlet obstruction (BOO) model treated with piroxicam (PRX).

HRV spectral-domain parameter	Studied groups			Statistical analysis (for ln values)	
	group 1 BOO control	group 2 BOO + PRX 2 mg/kg b.w.	group 3 BOO + PRX 10 mg/kg b.w.	1–2	1–3
TP [ms^2]	27.44 ± 33.55	11.23 ± 20.45	18.23 ± 17.84	p = 0.04	NS
VLF [ms^2]	22.30 ± 28.95	6.61 ± 15.26	17.42 ± 17.47	p = 0.01	NS
LF [ms^2]	2.20 ± 3.26	2.32 ± 3.71	0.52 ± 0.42	NS	NS
HF [ms^2]	2.94 ± 6.27	2.30 ± 2.53	0.30 ± 0.26	NS	NS
LF/HF	0.71 ± 0.58	0.75 ± 0.70	1.85 ± 0.17	NS	p = 0.01
nLF [n.u.]	44.81 ± 18.59	35.25 ± 23.27	64.75 ± 2.12	p = 0.01	p = 0.01
nHF [n.u.]	55.19 ± 18.59	64.75 ± 23.27	35.23 ± 2.12	p = 0.01	p = 0.01

NS = not significant

Table 3. Time-domain HRV analysis results in rats with experimental hemorrhagic cystitis evoked by cyclophosphamide (CP-HC) model treated with piroxicam (PRX).

HRV time-domain parameter	Studied groups			Statistical analysis (for ln values)	
	group 4 CP-HC control	group 5 CP-HC + PRX 2 mg/kg b.w.	group 6 CP-HC + PRX 10 mg/kg b.w.	4–5	4–6
mean RR [ms]	160.17 ± 11.23	168.80 ± 14.66	172.77 ± 12.77	NS	NS
max RR [ms]	184.92 ± 5.75	188.95 ± 10.08	188.94 ± 10.06	NS	NS
min RR [ms]	146.57 ± 8.62	153.63 ± 20.01	147.49 ± 16.40	NS	NS
range [ms]	38.36 ± 13.81	35.32 ± 19.97	41.47 ± 16.38	NS	NS
average HR [bpm]	376.77 ± 26.16	357.58 ± 30.70	347.90 ± 24.40	NS	p = 0.04
SDNN	6.74 ± 2.62	8.80 ± 5.57	10.46 ± 5.17	NS	NS
rMSSD	5.48 ± 4.27	14.65 ± 12.97	15.08 ± 10.44	NS	p = 0.05

NS = not significant

Table 4. Spectral-domain HRV analysis results in rats with experimental hemorrhagic cystitis evoked by cyclophosphamide (CP-HC) model treated with piroxicam (PRX).

HRV spectral-domain parameter	Studied groups			Statistical analysis (for ln values)	
	group 4 CP-HC control	group 5 CP-HC + PRX 2 mg/kg b.w.	group 6 CP-HC + PRX 10 mg/kg b.w.	4–5	4–6
TP [ms²]	15.31 ± 15.22	46.77 ± 38.50	13.94 ± 9.49	NS	NS
VLF [ms²]	10.00 ± 9.35	27.8 ± 22.01	10.43 ± 6.85	NS	NS
LF [ms²]	2.01 ± 2.33	9.37 ± 8.01	2.07 ± 1.81	p = 0.05	NS
HF [ms²]	3.29 ± 3.83	9.61 ± 9.06	1.45 ± 0.98	NS	NS
LF/HF	0.71 ± 0.58	1.74 ± 1.35	1.34 ± 0.39	NS	NS
nLF [n.u.]	34.42 ± 18.77	57.86 ± 14.86	56.34 ± 6.81	p = 0.04	p = 0.04
nHF [n.u.]	65.52 ± 18.75	42.14 ± 14.86	43.66 ± 6.81	p = 0.04	p = 0.02

NS = not significant

HRV analysis in the CP-HC model

Time-domain analysis

Just like in case of the BOO model, parameters of the HRV time analysis in animals with the CP-HC model were not significantly different in both groups treated with PRX and in the control group 2. All values were comparable in all groups, except for a mean heart rate in the group 6 – the lowest of all groups, and rMSSD – the highest.

Results of the HRV time-domain analysis in animals in the CP-HC model are presented in Table 3.

Spectral-domain analysis

Contrary to animals in the BOO model (groups 1–3), in animals in the CP-HC model treated with the lower PRX dose (group 5) a trend for increase of all non-normalized components of the spectrum was observed, compared to the corresponding control group. In the group 6 (the higher PRX dose), similarly to groups 2 and 3, TP and HF values were lower. VLF and LF powers were practically identical as in the corresponding control group. Both groups 5 and 6 were characterized by dominance of the normalized nLF parameter over nHF, and the difference was statistically significant.

Results of the HRV spectral analysis of animals in the CP-HC model are presented in Table 4.

DISCUSSION

Considering literature reports, results of daily urinary output analysis, BWW values and histological valuation of collected bladders, a conclusion could be made that study animals (groups 1 and 4) meet requirements of bladder outlet obstruction (the BOO model) and of hemorrhagic cystitis (the CP-HC model). Hence, we could treat those groups and their HRV results as control ones, taking them as a reference for BOO/CP-HC individuals treated with piroxicam.

The most important conclusions of this study are:

1. Prostaglandins seem to be factors activating the autonomic nervous system in the model of bladder outlet obstruction – inhibition of their synthesis caused a reduction of power of the HRV spectrum and of its individual non-normalized components: VLF, LF and HF. The dose of 2 mg/kg b.w. caused a particular trend for reduction of power in the VLF range, with marked increase of value of the normalized nHF parameter; the 10 mg/kg b.w. dose caused mostly a reduction of LF and HF power, but accompanied by an increase of the normalized nLF value.

2. In the CP-HC model, the dose of piroxicam of 2 mg/kg b.w. caused an increase of global activity of the autonomic nervous system and its non-normalized components. That suggests that a moderate suppression of prostaglandin synthesis was reflected by increased activity of the ANS. At the higher PRX dose the stimulating effect on the ANS functional condition disappeared, and activity of the ANS was comparable to the corresponding control group. At both PRX doses a statistically significant dominance of the normalized nLF parameter was observed.

We have chosen piroxicam, as an agent inhibiting synthesis of prostaglandins and a non-selective COX inhibitor for our experiment. Piroxicam (4-hydroxy-2-methyl-2H-1,2-benzothiazine-1-(N-(2-pyridinyl)carboxamide)-1,1-dioxide) is a precursor of the oxicam subgroup in the group of NSAIDs. The drug was discovered in 1972 and introduced to

the medical market by Pfizer in 1982 as a novel – for that time – representative of NSAIDs, recommended particularly to pharmacotherapy of rheumatic problems (35). Piroxicam is characterized by high (about 30) COX-1/COX-2 blockade ratio value. Thus, this compound, together with others commonly used in clinical practice drugs, such as ibuprofen, ketoprofen, diclofenac, naproxen, belongs to NSAIDs that inhibit both COX-1 and COX-2 with little selectivity (36). However, comparing to the other non-selective NSAIDs mentioned above, piroxicam seems to be relatively the most non-selective COX-blocking agent. Thus, the pharmacodynamic profile of piroxicam was the reason of our choice of PRX in our experiment. Moreover, early other reports of additional pharmacodynamic properties of prioxicam appeared as well and other aspects of the agents' mechanism of action have been also discovered. Already in 1983, Ando and Lombardino (37) demonstrated that PRX inhibited cellular migration in an inflammatory focus, and stabilized lisosomes of neutrophils, thus counteracting release of numerous cellular pro-inflammatory mediators (and of the lymphocytic rheumatoid factor of the IgM antibody character). Summing up, we have chosen PRX for the puropose of our study due to its non-selectivity regarding to COX and potential additional antiinflammatory effects, even despite the fact, that this agent is nowadays rarely used in clinical practice (mostly because its gross COX non-selectivity produces serious adverse effect, such as unfavorable influence on the digestive tract). Compared to other NSAIDs, this agent also exerts a relatively strong ulcerogenic effect (35, 38). That fact was an impulse for search of new derivatives of the compound, concluded with discovery of PRX analogues, including meloxicam, tenoxicam and lornoxicam, differing from their predecessor not only in scope of pharmacodynamic properties (clearly higher selectivity in relation to COX-2), but also of pharmacokinetic properties (39).

As mentioned previously in the introduction, PGs locally synthesized in the bladder intensify its overreactivity. Therefore, it is expected that NSAIDs constitute a pharmacologically attractive group of agents exerting a potentially beneficial alleviating effect on OAB symptoms. Efficacy of selected NSAIDs has been confirmed in experimental studies, and in few – so far – published clinical trials. In an experimental model of hemorrhagic cystitis induced by a single, large dose of cyclophosphamide (150 mg/kg b.w.), Takagi-Matsumoto et al. (40) demonstrated an improvement of parameters describing cystometric records in rats, in which the records were registered during an intravesical administration of a selected non-selective COX inhibitor. Those researchers evaluated an effect of aspirin (0.1–10 mg/kg b.w.), indometacin (0.01–0.3 mg/kg b.w.) and ketoprofen (0.001–0.1 mg/kg b.w.). Results obtained by them confirmed efficacy of each of the tested agents in scope of alleviation of cystometric disorders determining OAB in studied individuals (they observed a reduction of frequency of micturition episodes and a shift towards the higher value of threshold micturitional pressure during the phase of bladder filling). A significant improvement of cystometric properties of those records was accompanied by reduction of intravesical PGS level, evaluated immunoenzymatically in the vesical supernatant (40). Results of the above experiment were also confirmed by Jang et al. (41) on a similar experimental model of OAB, but with use of a selective COX-2 inhibitor (rofecoxib). Moreover, those researchers evaluated the nerve growth factor (NGF) and expression of the induced isoform of nitrogen oxide synthase (iNOS) content in vesical tissues. They demonstrated that rats with cyclophosphamide-induced chemical bladder injury receiving rofecoxib at the dose of 2 mg/kg b.w. for one hour, during the urodynamic record, were characterized by significantly lower content of both NGF and iNOS. In opinion of those authors, that results also in reduced COX-2 expression in bladders of experimental animals when considering physiological premises: NGF induces activity of COX-2 and production of PGs by vesical mastocytes, and increased enzymatic activity of iNOS and COX-2 depends on the presence of a common activator of both enzymes (nitrogen peroxide, formed in the course of NO metabolism in a focus of inflammation) (41). The theory of improvement of bladder disturbances as a result of reduced intravesical PGs synthesis by COX inhibition has been supported also by Shioyama et al. (42). Those researchers, using a different OAB model (chemical damage of the urothelium induced by intravesical administration of protamine sulfate), demonstrated that administration of loxoprofen for two weeks alleviated symptoms of bladder overreactivity.

There are also few – so far – published clinical reports on favorable effect of NSAIDs in OAB pharmacotherapy. As mentioned before in the introduction, in the BOO model, reflecting BPH, an increase of the intravesical PGs level was observed. Saito et al. (43) demonstrated a significant reduction of symptoms of bladder overactivity during night in BPH patients treated with loxoprofen (the drug caused reduction of nycturia episodes). Similarly,

Ozdemir et al. (44), evaluating BPH patients treated with the combined therapy doxazosin and tenoxicam, with use of validated questionnaire scales IPSS (International Prostate Symptom Scale) and OABSS (Overactive Bladder Symptom Scale), demonstrated improvement of their quality of life compared to the monotherapy with doxazosin.

Summing up, the review of literature confirms that inhibition of intravesical PGs synthesis with NSAIDs is associated with alleviation of overactive bladder symptoms. In our opinion, that favorable effect may be also – at least partially – associated with a change of autonomic regulation of the bladder, resulting from disappearance of the modulating role of prostaglandins. That hypothesis is supported by our HRV analysis results, particularly the spectral one (time-domain analysis revealed practically no statistically significant differences between groups).

As mentioned above, in the BOO model (corresponding to BPH), using both piroxicam doses, we found a reduction of values of non-normalized spectrum components (HF, LF) and of the total power (TP) of HRV. Additionally, the low PRX dose was associated with increased power of the normalized component nHF and a significant reduction of the VLF value, and the large one – with an increase of the normalized component nLF. On the other hand, in CP-HC animals (the model clinically corresponding to hemorrhagic, post-cyclophosphamide bladder injury), depending on the dosage, we demonstrated an increase of the spectrum total power and of its individual non-normalized components (2 mg/kg b.w. PRX), or – just like in BOO – their reduction). However, regardless the applied PRX dose, in that model we observed a statistically significant dominance of the normalized parameter nLF. According to HRV interpretation guidelines (26, 27), sympathetic activity is expressed mostly by nLF, parasympathetic – reflected by HF and nHF powers, and the TP value is associated with the global ANS tonus. There is no general consensus regarding an unequivocal interpretation of the LF component – a majority of researchers perceive that parameter as an expression of activity of both arms of the autonomic system. Even greater controversies are associated with the VLF component, which – in opinion of majority – could be an expression of various processes associated with hemodynamic regulation dependent on the sympathetic control (26, 27, 45). There is also evidence supporting the hypothesis that VLF reflects the activity of cholinergic anti-inflammatory pathway, and hence, the component is of parasympathetic origin (46, 47).

Considering the above guidelines, results obtained by us from the HRV analysis in the BOO model suggest that PGs seem to be agents stimulating global activity of the ANS, since inhibition of their synthesis causes reduction of the HRV spectrum. Evaluating non-normalized spectrum components only, it seems that the global reduction is accompanied by a proportional reduction of activity of both ANS arms. However, that thesis is negated by values of normalized parameters nLF and nHF. In our opinion, lower COX block is expressed mainly in reduced sympathetic tonus, as evidenced by reduction of nLF and VLF (accepting the hypothesis of a dominating role of the sympathetic component in generation of power of that component). COX blockage achieved with the 2 mg/kg b.w. dose and the functional sympathetic withdrawal contributed to an increased parasympathetic tonus (nHF increase), that may still fix symptoms of OAB (high parasympathetic activity stimulates contractile activity of the bladder (5)). Five times higher PRX dose (10 mg/kg b.w.; group 3), with reduction of the total vegetative reactivity, caused also reorganization of the balance within the scope of two essential components of ANS, with a sympathetic dominance described by increased nLF, that accounts for reduction of symptoms of bladder overactivity. High sympathetic activity, associated with activation of β-adrenergic receptors in the bladder, leads to a decrease of its contractile activity (5). Therefore, administration of 10 mg/kg b.w. PRX and inhibition of PGs synthesis causes changes of autonomic regulation consistent with the above cited reports regarding the alleviating effect of NSAIDs on symptoms of OAB.

Similar conclusions as those regarding group 3 may be drawn analyzing results of the spectral analysis of animals in the CP-HC model, that received PRX at the dose of 10 mg/kg b.w. (group 6). Also in that population, obtained results suggest reduction of global activity of the ANS, with a vegetative balance shifted towards the sympathetic component (reduced TP, HF, nHF values with increased nLF). However, results obtained in the group of animals with the CP-HC model but treated with a lower PRX dose (2 mg/kg b.w.; group 5) are debatable. That was the only subpopulation for which we observed a paradoxical increase of TP (increase of the ANS total activity), and of both non-normalized spectral components LF and HF (suggesting increase of both sympathetic and parasympathetic tonus). However, even in that group we observed identical relations regarding normalized parameters nLF and nHF, with a dominance of nLF, suggesting an increased sympa-

thetic tonus with COX block. We found interpretation of the fact of increased TP and all non-normalized components : VLF, LF and HF in that model and at that PRX dose, difficult. Undoubtedly, in that model, post-cyclophosphamide inflammatory changes were clearly more intense, compared to BOO. A lower PRX dose, despite its inhibitory effect on COX and PGs synthesis, probably was insufficient to reduce the activating effect of numerous other pro-inflammatory mediators on the ANS. Moreover, with increasing PRX dose, an additional, inhibitory aspect of PRX effect on activity of immunocompetent cells, as mentioned above, could appear (37). Therefore, only the higher PRX dose caused changes similar to those observed in the BOO model, with establishment of identical relations between the sympathetic and parasympathetic activity.

CONCLUSIONS

Summing up, results of our experiment support the potential efficacy of NSAIDs as PGs synthesis inhibitors in reduction of bladder overactivity in both experimental models of OAB (chemical – CP-HC and obstructive – BOO), reported in the literature. In the BOO model, PGs seem to be ANS-activating factors, and in the CP-HC model – they are undoubtedly co-activators together with other proinflammatory mediators. The dose of 10 mg/kg b.w. of piroxicam in both models caused a reconstruction of the autonomic balance, with marked sympathetic dominance, and with simultaneous reduction of total tonus of the ANS. That suggests that PGs inhibit the sympathetic activity, and directly or indirectly intensify the parasympathetic activity, contributing to contractile overactivity of the bladder. Functional rearrangement of the ANS following inhibition of PGs synthesis may cause an opposite phenomenon (reduction of contractile activity of the bladder), which undoubtedly improves bladder compliance during its filling.

Of course, we are aware of limitations of our study (no biochemical and histological studies were made, that could objectively confirm inhibition of prostaglandin synthesis and changes in ANS activity). Therefore, our results have to be treated as preliminary and requiring further clarification. Moreover, the applied high PRX dose (10 mg/kg b.w.), exceeding the usually clinical applied dose, certainly would be a causative factor of severe gastric ulceration and renal damage in humans. However, in our opinion, supporting the general concept of beneficial effect of NSAIDs on disorders associated with OAB, they are valuable, as they indicate some changes in autonomic regulation as a possible mechanism of NSAIDs action in OAB. Moreover, the additional actions of NSAIDs revealed in our study also provide new insights into pharmacodynamics aspects of these agents.

REFERENCES

1. Abrams P., Cardozo L., Fall M., Griffiths D., Rosier P., Ulmstein U., van Kerrebroeck P., Victor A., Wein A.: Neurourol. Urodyn. 21, 167 (2002).
2. Abrams P., Artibani W., Cardozo L., Dmochowski R., van Kerrebroeck P., Sand P.: Neurourol. Urodyn. 25, 293 (2006).
3. Chu F.M., Dmochowski R.: Am. J. Med. 119 (3 Suppl. 1), 3S (2006).
4. Hashim H., Abrams P.: Curr. Opin. Urol. 17, 231 (2007).
5. Clemens. J.Q.: Urol. Clin. North Am. 37, 487 (2010).
6. Dobrek Ł., Juszczak K., Wyczółkowski M., Thor P.J.: Adv. Clin. Exp. Med. 20, 119 (2011).
7. Korkmaz A., Topal T., Oter S.: Cell Biol. Toxicol. 23, 303 (2007).
8. Kiuchi H., Takao T., Yamamoto K., Nakayama J., Miyagawa Y., Tsujimura A., Nonomura N., Okuyama A.: J. Urol. 181, 2339 (2009).
9. Dobrek Ł., Thor P.J.: Post. Hig. Med. Dosw. 66, 592 (2012).
10. Briganti A., Capitanio U., Suardi N., Gallina A., Salonia A., Bianchi M. et al.: Eur. Urol. Suppl. 8, 865 (2009).
11. Dinis P., Churrua A., Avelino A., Yaqoob M., Bevan S., Nagy I., Cruz F.: J. Neurosci. 24, 11253 (2004).
12. Chopra B., Barrick S.R., Meyers S., Beckel J.M., Zeidel M.L., Ford A.P.D.W. et al.: J. Physiol. 562, 859 (2005).
13. Parsons B.A., Drake M.J.: in Handbook of experimental pharmacology, Andersson K.E., Michel M.C. Eds., p. 15, Springer-Verlag, Berlin, Heidelberg 2011.
14. Das A.K., Leggett R.E., Whitbeck C., Eagen G., Levin R.M.: Neurol. Urodyn. 21, 160 (2002).
15. Dobrek Ł., Thor P.: Arch. Med. Sci., 9, 930 (2013).
16. Dobrek Ł., Baranowska A., Skowron B., Thor P.J.: Post. Hig. Med. Dosw. 67, 221 (2013).
17. Paccani S.R., Boncristiano M., Baldari C.T.: Cell. Mol. Life Sci. 60, 1071 (2003).
18. Burian M., Geisslinger G.: Pharmacol. Ther. 107, 139 (2005).

19. Maggi C.A.: Pharmacol. Res. 25, 13 (2002).
20. Andersson K.E.: Pharmacol. Rev. 45, 253 (1993).
21. Ishizuka O., Mattiasson A., Andersson K.E.: J. Urol. 153, 2034 (1995).
22. Takeda H., Yamazaki Y., Igawa Y., Kaidoh K., Akahane S., Miyata H. et al.: Neurourol. Urodyn. 21, 558 (2002).
23. Park J.M., Yang T., Arend L.J., Schnermann J.B., Peters C.A., Freeman M.R., Briggs J.P.: Am. J. Physiol. 276, F129 (1999).
24. Wheeler M.A., Yoon J.H., Olsson L.E., Weiss R.M.: Eur. J. Pharmacol. 417, 239 (2001)
25. Collins C., Klausner A.P., Herrick B., Koo H.P., Miner A.S., Henderson S.C., Ratz P.H.: J. Cell. Mol. Med. 13, 3236 (2009).
26. Malik M. (Ed.).: Eur. Heart J. 17, 354 (1996).
27. Acharya U.R., Joseph K.P., Kannathal N., Lim C.M., Suri J.S.: Med. Biol. Eng. Comput. 44, 1031 (2006).
28. Bugajski J., Gądek-Michalska A., Bugajski A.J.: J. Physiol. Pharmacol. 54, 99 (2003).
29. Gądek Michalska A., Bugajski J.: J. Physiol. Pharmacol. 55, 663 (2004).
30. Maggi C.A., Meli A.: Experientia 42, 109 (1986).
31. Maggi C.A., Meli A.: Experientia 42, 292 (1986).
32. Schroder A., Newgreen D., Andersson K.E.: J. Urol. 172, 1166 (2004).
33. Morais M.M., Belarmino-Filho J.N., Brito G.A.C., Ribeiro R.A.: Braz. J. Med. Biol. Res. 32, 1211 (1999).
34. Zeng J., Pan C., Jiang C., Lindstrom S.: J. Urol. 188, 1027 (2012).
35. Dahl S.L., Ward J.R.: Pharmacotherapy 2, 80 (1982).
36. Praveen Rao P.N., KnausE.E.: J. Pharm. Pharm. Sci. 11, 81s (2008).
37. Ando G.A., Lombardino J.G.: Eur. J. Rheumatol. Inflamm. 6, 3 (1983).
38. Brogden R.N., Heel R.C., Speight T.M., Avery G.S.: Drugs 28, 292 (1984).
39. Miranda A.S., Bispo-Júnior W., Silva Y.K.C., Alexandre-Moreira M.S., Paula Castro R., Sabino J.R. et al.: Molecules 17, 14126 (2012).
40. Takagi-Matsumoto H., Ng B., Tsukimi Y., Tajimi M.: J. Pharmacol. Sci. 95, 458 (2004).
41. Jang J., Park E.U., Seo S.I., Hwang T.K., Kim J.C.: BJU Int. 98, 435 (2006).
42. Shioyama R., Aoki Y., Ito H., Matsuta Y., Nagase K., Oyama N. et al.: Am. J. Physiol. Regul. Integr. Comp. Physiol. 295, R714 (2008).
43. Saito M., Kawatani M., Kinoshita Y., Satoh K., Miyagawa I.: Int. J. Urol. 12, 779 (2005).
44. Ozdemir I., Bozkurt O., Demir O., Aslan G., Esen A.A.: Urology 74, 431 (2009).
45. Ori Z., Monir G., Weiss J., Sayhouni X., Singer D.H.: Cardiol. Clin. 10, 499 (1992).
46. Taylor J.A., Carr D.L., Myers C.W., Eckberg D.L.: Circulation 98, 547 (1998).
47. Silva Soares P., da Nobrega A.C.L., Ushizima M.R., Irigoyen M.C.C.: Auton. Neurosci. 113, 24 (2004).

Received: 30. 07. 2013

Acta Poloniae Pharmaceutica – Drug Research, Vol. 71 No. 3 pp. 509–514, 2014 ISSN 0001-6837
Polish Pharmaceutical Society

GENERAL

INDIVIDUAL MEDICATION MANAGEMENT SYSTEM (IMMS) IMPLEMENTATION IN PHARMACISTS' OPINION

MAGDALENA WASZYK-NOWACZYK[1]*, SEBASTIAN LAWICKI[2], MICHAŁ MICHALAK[3] and MAREK SIMON[4]

[1] Department of Pharmaceutical Technology, [2] Student's Pharmaceutical Care Group, Department of Pharmaceutical Technology, Pharmacy Practice Division, Poznan University of Medical Sciences, Bukowska 70, 60-812 Poznań, Poland
[3] Department of Computer Science and Statistics, Poznan University of Medical Sciences, Dąbrowskiego 79, 60-529 Poznań, Poland
[4] Chair and Department of Pathophysiology, Poznan University of Medical Sciences, Święcickiego 6, 60-781 Poznań, Poland

Abstract: Many countries of the world including Poland, are taking actions for improving the role of the pharmacist as a health care professional. One of those is implementation of pharmaceutical care (PC), as a documented specialist medical service, which also includes pharmacist interventions, such as preparing Individual Medication Management System (IMMS), to enhance patient's adherence. Because of the chance to monitor the dosage and to detect and prevent drug problems occurrence, IMMS is thought to be an opportunity for individualized, effective and safe patient's pharmacotherapy. The aim of the study was to define pharmacists' attitudes toward IMMS. The study included also the evaluation of pharmacist-physician cooperation to determine whether IMMS can improve partnership among health care professionals for proper patient's care. The survey was conducted in Poznań, between June 2011 and March 2012. An anonymous questionnaire was delivered personally to pharmacists. Each questionnaire was provided with a short information brochure attached and presentation of demos how to use IMMS. The survey covered 129 pharmacists (76.7% women and 23.3% men) where 48.8% had up to 5 years length of service as a pharmacist, 24.8% – 6–10 years, 14.9% – 11-20 years and 11.5% – 21 and more years. Most of the participants did not have specialization (80.6%) and only 5.4% had Ph.D. degree. Survey confirmed that 64.8% of pharmacists ($p < 0.0001$), mainly with the shortest length of service ($p = 0.02268$) and without specialty ($p = 0.00244$) didn't cooperate with physicians, but 68.8% of respondents emphasized that the range of cooperation could increase by IMMS application ($p < 0.00001$). About 50.0% of respondents' considered that patients would be interested in IMMS usage ($p = 0.00079$) and in 71.9% opinions, it would attach the patient to specific community pharmacy ($p < 0.00001$). This statement was confirmed by respondents with the shortest length of services ($p = 0.00659$). Proposed dosing system also improved patient's care serving by family or carers in pharmacists' opinion ($p < 0.00001$). A majority of pharmacists (85.3%) indicated also that IMMS would have a positive influence on PC implementation in Poland ($p < 0.00001$) and 69.0% of them confirmed that this service should be refunded by the National Health Fund ($p < 0.00001$). According to the scale of non-compliance, implementation of IMMS as a part of PC can be a chance both for patients and their physicians to increase the safety and effectiveness of therapy and for pharmacists, who are intended to highlight their role as a part of health care system.

Keywords: Individual Medication Management System, pharmaceutical care, pharmacist, physician

In recent years there has been many changes in pharmacist profession, which had significant influence on community pharmacy functioning in Poland. Development of pharmaceutical industry brought about displacing compounded drugs in community pharmacies so that pharmacists have been focused on the services for patients. (1, 2). According to different countries, they should be directed at patients' education, prevention and health care promotion (3). So that pharmaceutical care (PC) as a new idea of pharmacists' profession should assure the safest and the most effective therapy to improve a patient's quality of life. It should progress also in the cooperation with physicians (4–7).

* Corresponding author: e-mail: mwaszyk@ump.edu.pl; phone: 61-854-72-06

Essential part of PC is proposed Individual Medication Management System (IMMS; Fig. 1.) for solid drugs with special division into compartments dedicated to specific time of the day on particular days of the week. This makes it easier to check whether each dose has been taken. In comparison with classic dispensers in Poland, the basic issue is that IMMS is prepared by qualified pharmaceutical staff like master of pharmacy or technician supervised by master of pharmacy. It decreases the risk of errors, which can occur without professional intervention (8).

Pharmacist responsible for preparing IMMS is obligated to check dosing scheme propriety and relevant doses. It should be pointed out when drugs interactions occur. It has a special meaning when the patients suffer from chronic diseases with complicated dosing schemes ordered by different physicians. In this area, a great opportunity of drug problems can occur and failure to doctor's recommendations (9–11). IMMS enables the same drug under different trade names elimination**,** gives possibility of drug doses verification and indicates adverse drug reactions. Patient using IMMS should be included in PC program, which is implementing in Poland.

IMMS preparation should take place in specific community pharmacy chosen by the patient, so that the pharmacist would have an access to patient's medical documentation and history. What is more, IMMS should be implemented as a medical service with National Health Fund refund, which is a Polish Pharmaceutical Chamber suggestion (12, 13). It could be ready to use when leading physician refers patient to pharmacist or when patient will pay for this service by private order. This process needs an appropriate documentation refilled by pharmacists and physicians (14).

The aim of the study was to determine pharmacists' attitudes toward IMMS, which could be another possibility of pharmacist–physician cooperation to get a proper patient's pharmacotherapy. Thus, the study defined whether IMMS could improve partnership among health care professionals for proper patient's care. Additional goal was to define pharmacists' opinion according to patients' interest in this service, funding source and IMMS impact on PC implementation in Poland. The data assumed analysis for gender, specialty, scientific/professional degree and length of service as a pharmacist.

MATERIAL AND METHOD

The survey was conducted in Poznań, between June 2011 and March 2012. An anonymous questionnaire was delivered personally to pharmacists working in community pharmacies. The survey covered 129 pharmacists (76.7% women and 23.3% men). The most numerous group consisted of pharmacists aged up to 30 years (46.3%) with up to five years length of service as a pharmacist (48.8%). The other age groups were: 31 – 40 years – 28.1%, 41–50 years – 14.9% and 51 years and more – 10.7%. This data confirmed also the length of service as a pharmacist, which were: 6–10 years – 24.8%, 11–20 years – 14.9%, 21 and more – 11.5%. Similar results brought about that only the length of service was analyzed in the research. Most of the participants did not have specialty (80.6%). Only 17.1% had community pharmacy and 2.3% clinical pharmacy specialty, so groups were joined together and named as pharmacists with specialization. In the study, there were only 5.4% pharmacist with Ph.D.

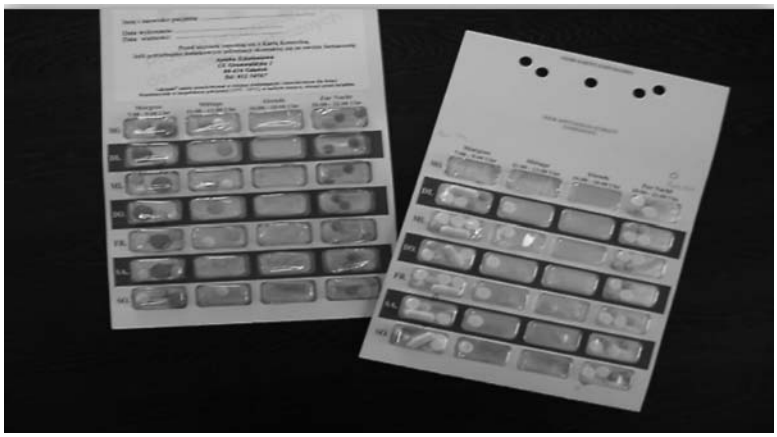

Figure 1. Individual Medication Management System (author's photo)

degree. The rest had master of pharmacy degree (94.6%).

The study included the evaluation of pharmacist–physician cooperation to determine whether IMMS could improve partnership among health care professionals for proper patient's care. The participants answered also the questions about their view of IMMS effectiveness, it funding sources and possible impact on PC implementation. Each questionnaire was provided with a short information brochure attached and presentation of demos how to use IMMS. The study received Ethical Board revision and acceptance.

The results were statistically analyzed with the use of Statistica 8.0 application (StatSoft®). In order to analyze relationships between the traits, taking into account sample size and frequency of analyzed categories of the examined traits, chi-square test of independence (χ^2) was used in case of a large sample and higher frequency of categories, and Fisher-Freeman-Halton test for low expected frequencies. For all the statistical analyses, a significance level of 0.05 was used to assess differences between groups. The effectiveness of the research was tested on the basis of questionnaire return, which was 72.9%. It leads to conclusion that research technique was relatively effective.

RESULTS

Integral element of pharmacist's profession in PC is permanent contact with physician to consult patients' pharmacotherapy. The study indicated that 64.8% of respondents did not cooperate with the

Table 1. Pharmacists' opinion concerning cooperation with physicians and pharmacists' specialty and length of service.

Pharmacists' details:	Number of cooperative physicians: 0 n (%)	1 n (%)	2 n (%)	3 n (%)	≥4 n (%)	p-value
Specialty						
Yes	9 (37.5)	4 (16.7)	2 (8.3)	3 (12.5)	6 (25.0)	0.00244*
No	74 (71.1)	8 (7.7)	10 (9.6)	1 (1.0)	11 (10.6)	
Total	83 (64.8)	12 (9.4)	12 (9.4)	4 (3.1)	17 (13.3)	
Length of service as a pharmacist						
Under 5 years	44 (74.6)	4 (6.8)	4 (6.8)	0 (0.0)	7 (11.8)	0.02268*
6–10 years	20 (66.7)	4 (13.3)	2 (6.7)	0 (0.0)	4 (13.3)	
11–20 years	10 (55.6)	1 (5.6)	2 (11.1)	4 (22.1)	1 (5.6)	
Over 20 years	6 (42.8)	2 (14.3)	2 (14.3)	0 (0.0)	4 (28.6)	
Total	80 (66.1)	11 (9.1)	10 (8.3)	4 (3.3)	16 (13.2)	

*p < 0.05. Missing values because of the lack in pharmacists' answers compared with analyzed group.

Table 2. Pharmacists' opinion concerning patients' attachment to specific community pharmacy after IMMS implementation and length of service as a pharmacist.

Length of service as a pharmacist	Yes n (%)	No n (%)	No opinion n (%)	p-value
Under 5 years	48 (81.4)	5 (8.4)	6 (10.2)	0.00659*
6–10 years	24 (80.0)	4 (13.3)	2 (6.7)	
11–20 years	13 (72.2)	2 (11.1)	3 (16.7)	
Over 20 years	5 (35.7)	2 (14.3)	7 (50.0)	
Total	90 (74.4)	13 (10.7)	18 (14.9)	

*p < 0.05. Missing values because of the lack in pharmacists' answers compared with analyzed group.

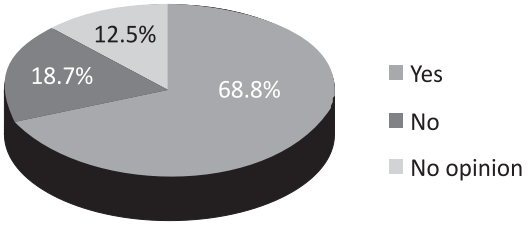

Figure 2. Pharmacists' opinion concerning partnership with physicians' expanded by IMMS application; n = 128
Missing values because of the lack in pharmacists' answers compared with analyzed group

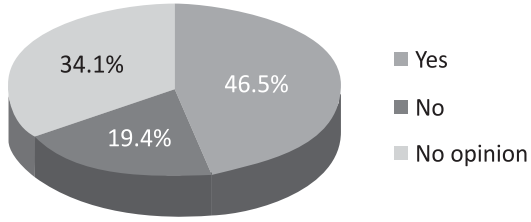

Figure 3. Pharmacists' opinion concerning patients' IMMS interest; n = 129

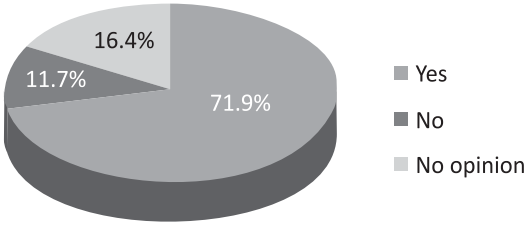

Figure 4. Pharmacists' opinion concerning patients' attachment to specific community pharmacy after IMMS implementation; n = 128
Missing values because of the lack in pharmacists' answers compared with analyzed group

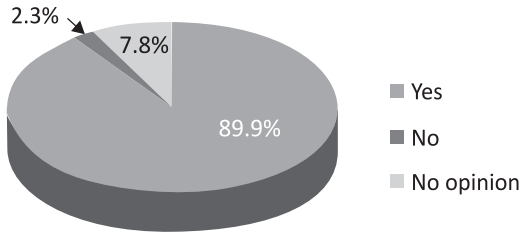

Figure 5. Pharmacists' opinion concerning simplification of patients' care serving by family or carers after IMMS implementation; n = 129

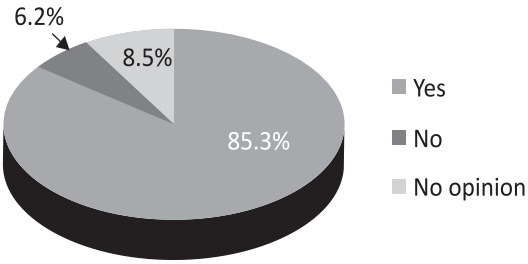

Figure 6. Pharmacists' opinion concerning positive influence of IMMS implementation on PC development; n = 129

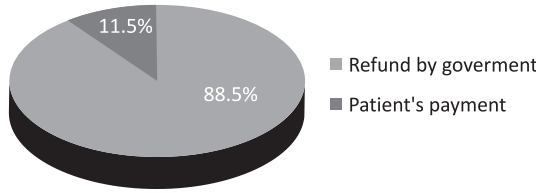

Figure 7. Pharmacists' opinion concerning the source of IMMS funding; n = 122
Missing values because of the lack in pharmacists' answers compared with analyzed group

physicians. The rest of the pharmacists collaborated with at least 1 doctor where 13.3% contacted with at least 4 of them ($p < 0.00001$; Table 1). No cooperation declared mainly respondents with the shortest length of services. It can be seen also the tendency from the data in Table 1 that the length of services determined better collaboration with doctors ($p = 0.02268$), especially when pharmacist had got a specialty ($p = 0.00244$). What's more, 68.8% questioned considered proper partnership and better effectiveness and safety of pharmacotherapy by IMMS application ($p < 0.00001$). The data are shown in Figure 2.

Forty six and a half percent of pharmacists indicated that patients' would be interested in IMMS, but 34.1% of them had no opinion according to this statement ($p = 0.00079$; Fig. 3.). Many (71.9%) believed that this service would attached the patient to chosen community pharmacy ($p < 0.00001$; Fig. 4.). As shown in Table 2, this opinion belonged mainly to respondents with the shortest length of services ($p = 0.00659$). IMMS could also

improve care of the sick serving by the family or carers ($p < 0.00001$; Fig.5.).

A majority of questioned (85.3%) considered that IMMS could have a positive impact on PC implementation in Poland ($p < 0.00001$; Fig. 6.). This service should be refunded by the National Health Fund in 88.5% pharmacists' opinion, in comparison with private patients' payment ($p < 0.00001$; Fig. 7.).

Additional gender, specialty scientific/professional degree analysis did not achieve the level of statistical significance.

DISCUSSION AND CONCLUSION

The results of the study proved that nearly 35.0% of pharmacists cooperated with physicians. These were mainly respondents with a huge professional experience, also with specialty. Similar findings were in the study from 2005, where only 25.9% of pharmacists consulted the patients' pharmacotherapy with doctors (15). This confirmed that physician and pharmacist partnership was not sufficient. The fact is that it brings a lot of outcomes especially for the patients, so it should be improved to get a better pharmacotherapy control (16–18). In this study, poor cooperation indicated mainly pharmacists with the shortest length of service. There were assumed also a tendency where the length of services determine better collaboration with doctors, especially when pharmacist had got a specialty. Probably, it is because of the huge professional experience, which gives the possibility to connect in a better way. According to the study from 2012, half of the doctors collaborated with pharmacists (14). In Ontario, physicians contacted with pharmacists five times a week to establish patients' pharmacotherapy and 28% of them – experienced ones, referred their patients directly to community pharmacies to get a drug consultation (19). The researches beyond the border of Poland confirmed also that coordinated activity of this two professional groups would bring a lot of benefits for the patient (16–18, 20–22).

This survey indicated that 68.8% pharmacists highlight necessity of enlarging the range of cooperation with physician to get effective and save pharmacotherapy by IMMS application. Iskierski and Zimmermann demonstrated that in pharmacists' opinion the patients' pharmacotherapy could be obtained by collaboration with doctors in the drug consultation but the problem was in a lack of organized forms of such cooperation (15). So IMMS could be the proposition to improve pharmacist-physician partnership.

The current study found out that pharmacists considered IMMS as a tool, which would have an influence on PC implementation. This dosing system, in definition, should indicate interactions, wrong doses and patient's nonadherence what would assure a great pharmacotherapy supervision. Szalonka in 2010 demonstrated that in 78.0% pharmacists' opinion PC should contribute to more secure drug taking. It was indicated also that the main barrier limiting PC implementation in Poland was poor communication between this two groups (23). Thus, IMMS could help in better partnership, what is also confirmed in conducted study. It was also interesting to note that in this research, respondents mainly with short experience pointed out that IMMS application would attached patients to proper community pharmacy and simplify their care serving by family or careers. Similar results were confirmed by the patients, who in 83.0% cases accepted IMMS as a significant tool to improve medical care (14). This view is supported by many studies, which reported many IMMS benefits (24–26).

Another important finding was that 46.5% of pharmacists recognized that patients would apply IMMS. This results are consistent with those of other study from 2010 but conducted on community pharmacy patients and carers – respectively, 47.2% and 56.0% (14). It generates a great possibility to make use of pharmacists as drugs experts within PC process and IMMS service. It would give a chance to achieve proper partnership with physicians and improve medical care.

Essential element of the study was financial analysis according to the source of IMMS payment. This system should be refunded by the National Health Fund not from private patients' income in pharmacists' opinion. In the study from 2012, it was highlighted that 55.4% of patients didn't accept paying for IMMS. Only 30.0% of carers presented willingness to pay for the system (14). In many countries where dosing systems are functioning, the patients are responsible for paying. In Great Britain, a customer is paying for the blister and additional charge depends on pharmacist's will (27). In Australia, the patient gives weekly rates for IMMS supplying (28).

Nowadays, the community pharmacy is exposed to many changes, especially related with application of new services such as IMMS in PC program. It gives a chance, both for patients and their physicians, to increase the safety and effectiveness of therapy and for pharmacists, who are intended to highlight their role as a part of health care system. Implementation of PC as a documented

specialist medical service, including the possibility of preparing IMMS, is expected by patients and caregivers as well as the physicians, who in collaboration with pharmacists see the opportunity of individualized and controlled patient's pharmacotherapy.

Acknowledgment

This study was supported by the funding for young scientists from Poznan University of Medical Sciences (grant no. 502-14-03314429-09415).

REFERENCES

1. Brandys J., Skowron A.: in Practical pharmacy (Polish). Jachowicz R. Ed., p. 26–27, PZWL, Warszawa 2007.
2. Tomerska-Kowalczyk E., Skowron A.: Farm. Pol. 64, 103 (2008).
3. Stasiak P., Sawicki W., Grześkowiak E.: Farm. Pol. 66, 781 (2010).
4. Vrijens B., De Geest S., Hughes D.A., Kardas P., Demonceau J., Ruppar T. et al.: Br. J. Clin. Pharmacol. 73, 691 (2012).
5. Kardas P.: in Polish patient's self-portrait – report how Polish patients obey therapeutic recommendations (Polish). Stepniewski A. Ed., p. 7–25, Polpharma, Warszawa 2010.
6. Wąsowski M.: Post. Nauk Med. 5, 446 (2011).
7. Łazowski J.: Czas. Aptek. 2, 12 (2011).
8. Skotnicki M., Skotnicka A., Opiłowski A.: Proper Locum LTD, 4 (2009).
9. Waszyk-Nowaczyk M., Simon M., Matwij K.: Acta Pol. Pharm. Drug Res. 69, 971 (2012).
10. Rajska-Neumann A., Wieczorowska-Tobis K.: Terapia 18, 24 (2010).
11. Mazzaglia G., Ambrosioni E., Alacqua M., Filippi A., Sessa E., Immordino V. et al.: Circulation 120, 1598 (2009).
12. Bąbelek T.: Czas. Aptek. 3, 12 (2007).
13. Waszyk-Nowaczyk M., Simon M.: Farm. Pol. 67, 729 (2011).
14. M. Waszyk-Nowaczyk: Patients and physicians expectations about pharmacist's role in pharmaceutical care implementation, PhD thesis, Poznan University of Medical Sciences (2012).
15. Iskierski J., Zimmermann A.: Farm. Pol. 62, 210 (2006).
16. Kucukarlsan S., Al-Bassam N., Dong Y., Kim K., Lai S.: J. Am. Pharm. Assoc. 50, 258 (2010).
17. Albsoul-Younes A., Hammad E., Yasein N., Tahaineh L.: Saudi Med. J. 32, 288 (2011).
18. McPherson T., Fontane P.: J. Am. Pharm. Assoc. 50, 37 (2010).
19. Pojskic N., Mackeigan L., Boon H., Ellison P., Breslin C.: Res. Social Admin. Pharm. 7, 39 (2011).
20. Bryant L., Coster G., Gamble G., McCormick R.: J. Pharm. Pract. 19, 94 (2011).
21. Lalonde L., Hudon E., Goudreau J., Bélanger D., Villeneuve J., Perreault S. et al.: Res. Social Admin. Pharm. 7, 233 (2010).
22. McGrath S., Snyder M., Duenas G., Pringle J., Smith R., McGivney M.: J. Am. Pharm. Assoc. 50, 67 (2010).
23. Szalonka K.: in Pharmaceutical care in Poland – conditions and chances of implementation (Polish). Szalonka K. Ed., p. 85–102, Continuo, Wrocław 2010.
24. Lakey S., Gray S.: Ann. Pharmacother. 6, 1011 (2009).
25. Schneider P.J., Murphy J.E., Pedersen C.A.: J. Am. Pharm. Assoc. 48, 58 (2008).
26. Littenberg B., MacLean Ch.D., Hurowitz L.: BMC Fam. Pract. 7, 1 (2006).
27. Oboh L. 2011: https://www.evidence.nhs.uk/ (accessed on 10.08.2013).
28. Walsh's Village Pharmacy 2013: http://www.walshspharmacy.com.au/blisterpackdispensing.html (accessed on 10. 08. 2013).

Received: 26. 08. 2013

Acta Poloniae Pharmaceutica – Drug Research, Vol. 71 No. 3 pp. 515–520, 2014 ISSN 0001-6837
Polish Pharmaceutical Society

SHORT COMMUNICATION

PRELIMINARY STUDIES EVALUATING CYTOTOXIC EFFECT OF COMBINED TREATMENT WITH METHOTREXATE AND SIMVASTATIN ON GREEN MONKEY KIDNEY CELLS

MAGDALENA IZDEBSKA*, DOROTA NATORSKA-CHOMICKA and EWA JAGIEŁŁO-WÓJTOWICZ

Department of Toxicology, Medical University of Lublin, 8 Chodźki St., 20-093, Lublin, Poland.

Abstract: Patients, affected by neoplastic disease, take usually other drugs and this may lead to a number of often rather unpredictable interactions. The statins are among the most commonly prescribed drugs in medicine but have also adverse side effects and come into interactions with other drugs. The aim of this study was to investigate the cytotoxic effect of methotrexate (5.5 or 16.5 μmol/L), simvastatin (100 or 300 μmol/L) and their combination on green monkey kidney (GMK) cells culture using cytotoxicity detection kit LDH. Besides, the effect of above drugs on the cells viability was estimated by MTT test. After 6, 12 or 24 h of simultaneous incubation of GMK cells with methotrexate (5.5 μmol/L) and simvastatin (100 μmol/L) the cytotoxicity (about 10%) of the drugs was found in LDH test. Cytotoxicity of combination: methotrexate (5.5 μmol/L) with simvastatin (300 μmol/L) after 6 or 12 h of incubation with GMK cells was similar (about 10%), but after 24 h of incubation, cytotoxicity increased to 21%. The significant increase of the cytotoxicity (about 30%) was found after 24 h incubation of GMK cells with methotrexate (16.5 μmol/L) and simvastatin (100 μmol/L). In the MTT assay, the decrease in the cells viability was found also after 12 and 24 h of GMK cells incubation with methotrexate (5.5 or 16.5 μmol/L) and simvastatin (100 or 300 μmol/L). These results suggest the adverse effect of combined application of both drugs on GMK cells especially after 24 h of incubation.

Keywords: methotrexate, simvastatin, LDH, MTT, green monkey kidney cells

A lack of knowledge about interactions of one or more drugs taken by patients can have different results, sometimes dangerous to the health. Therefore, there is a need for research on the interaction of drugs used simultaneously in the treatment of various diseases. Particular attention should be paid to drugs used in the chronic diseases of civilization (cancer, atherosclerosis or hypertension). One group of anticancer drugs are antimetabolites, which include methotrexate (MTX) – the subject of this study. MTX is a folate antagonist used for patients with acute lymphoblastic leukemia, osteosarcoma, lymphoma and other kinds of cancer. In addition, it is used at lower doses for patients with non-malignant diseases such as rheumatoid arthritis or psoriasis (1–4). Unfortunately, MTX is a highly toxic drug. MTX may cause the bone marrow depression (anemia, leucopenia, thrombocytopenia) and gastrointestinal toxicity (vomiting, diarrhea or ulcerative stomatitis and hemorrhagic enteritis). The renal dysfunction after MTX treatment is a clinically important side effect. High dose of MTX induced renal failure because drug is mainly eliminated by the kidney (5, 6). Currently, a large part of the population suffers from arteriosclerosis and hypertension. Therefore, in cancer patients, there is a risk of interaction between cytostatic and lipid-lowering drugs. Simvastatin, the drug used in this study, belongs to the statins. Statins block the synthesis of cholesterol, preventing the formation of mevalonic acid, and thus lower the level of lipids (7–9). Simvastatin is a widely used cholesterol-lowering drug in the treatment of atherosclerosis, in the prevention of cardiovascular diseases, as well as reduces stroke incidence. However, the effects of statins extend beyond their lipid-lowering actions. Recent *in vivo* studies with experimental animals and *in vitro* studies in numerous cancer cell lines have shown antitumor properties of statins. Simvastatin is attributed to inhibition of cell cycle both *in vitro* and *in vivo* (10–13). The use of simvastatin as well as other statins are associated with the

* Corresponding author: e-mail: magdalena.izdebska@umlub.pl

risk of side effects. The adverse effects of some statins are mainly on muscle, such as myopathy and rhabdomyolysis and liver (14, 15). The statins are the most commonly prescribed drugs in medicine but unfortunately can come into interactions with other drugs. The lack of the literature data about the simultaneous treatment with MTX and statins was the inspiration to undertake the research of the presented work. The aim of this pilot study was to investigate the cytotoxic effects of MTX and simvastatin on green monkey kidney (GMK) cells using LDH and MTT tests**.**

EXPERIMENTAL

Reagents

The following substances were used in the study: MTX (Metotreksat-Ebewe, Ebewe Pharma, Unterach,

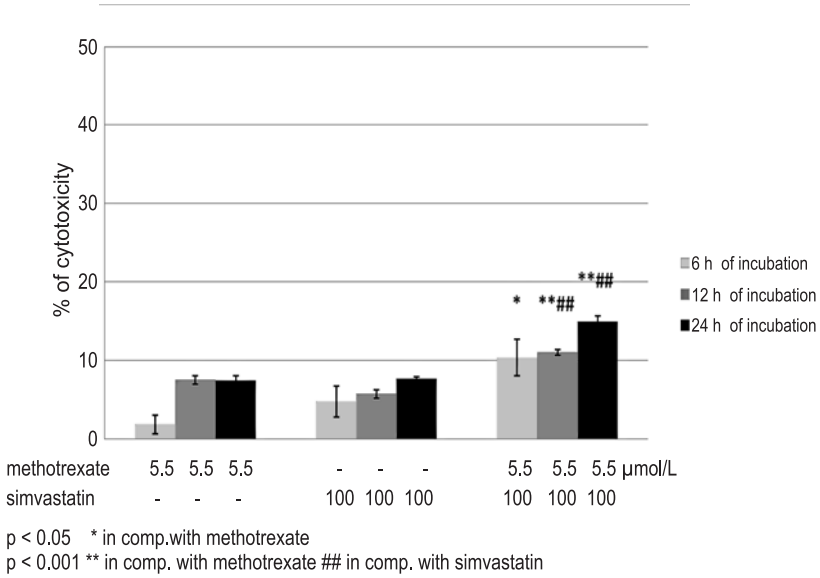

p < 0.05 * in comp.with methotrexate
p < 0.001 ** in comp. with methotrexate ## in comp. with simvastatin

Figure 1. Cytotoxicity of methotrexate (5.5 µmol/L), simvastatin (100 µmol/L) and their combination after incubation with GMK cell culture in LDH test

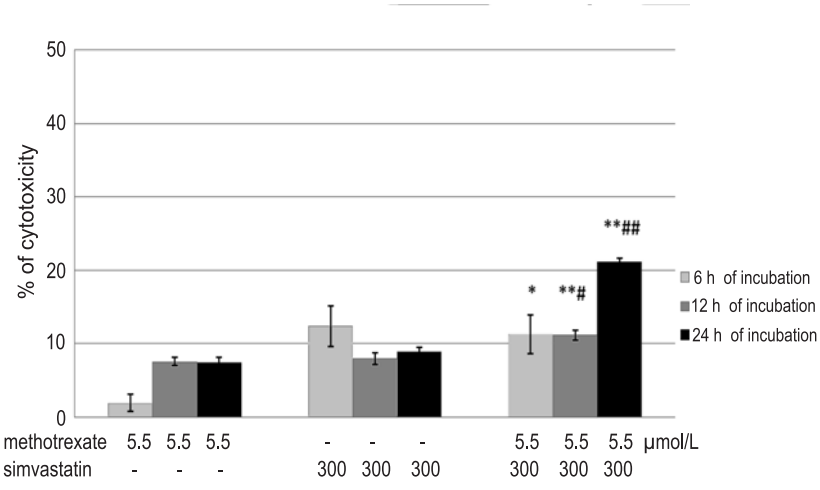

p < 0.05 * in comp.with methotrexate # in comp. with simvastatin
p < 0.001 ** in comp. with methotrexate ## in comp. with simvastatin

Figure 2. Cytotoxicity of methotrexate (5.5 µmol/L), simvastatin (300 µmol/L) and their combination after incubation with GMK cell culture in LDH test

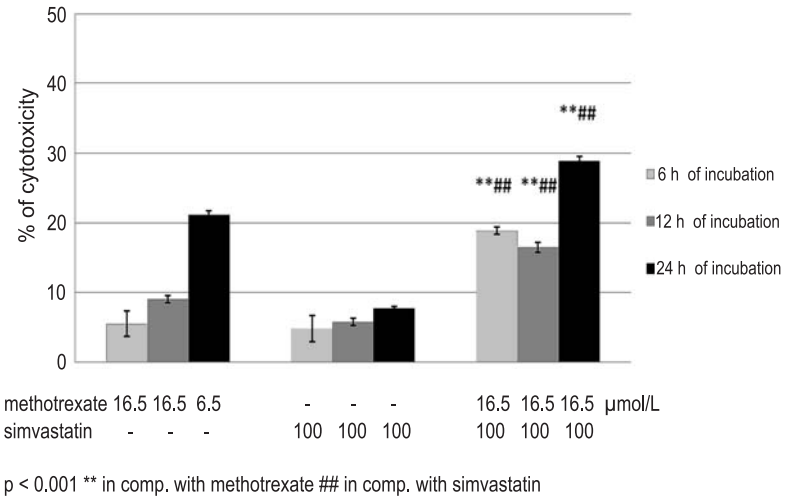

Figure 3. Cytotoxicity of methotrexate (16.5 µmol/L), simvastatin (100 µmol/L) and their combination after incubation with GMK cell culture in LDH test

Austria), simvastatin (Simvacard, Zentiva, Praga, Czech Republic), Cytotoxicity Detection Kit (LDH) (Roche Diagnostic GmbH, Mannheim, Germany), MTT (Thiazolyl blue tetrazolium bromide, Sigma-Aldrich, Steinheim, Germany). The cell culture medium RPMI-1640 (with L-glutamine and phenol red), fetal bovine serum (FBS) and antibiotics solutions: penicillin, streptomycin and amphotericin B (obtained from the PAA – The Cell Culture Company GmbH, Pasching, Austria). MTX and simvastatin were *ex tempore* prepared in RPMI-1640 medium.

Cell culture

The research was performed on green monkey kidney cells (GMK) obtained from the „Biomed" Serum and Vaccine Production Plant Ltd. in Lublin, Poland. GMK cell line was grown in RPMI-1640 medium (with L-glutamine and phenol red) supplemented with 10% fetal bovine serum heat-inactivated, 100 U/mL penicillin, 100 µg/mL streptomycin and 2.5 µg/mL amphotericin B in 25 cm^2 tissue culture flasks (EasYFlasks™Nunclon™Δ, Nunc GmbH Wiesbaden, Germany). GMK cells were cultured as monolayer in CO_2 cell incubator at 37°C in an atmosphere of 5% CO_2. Afterwards, GMK cells were counted in Neubauer hemocytometer (BlauBrand, BRAND GmbH) by means of the compact inverted microscope Olympus CKX41. The assays of cytotoxicity GMK cells were prepared at density of 2×10^6 cells/cm^3.

LDH test

The cytotoxicity detection kit (LDH) is a colorimetric assay for the quantitation of cytotoxicity/cytolysis, based on the measurement of LDH activity released from the damaged cells. To determine the cytotoxic activity of MTX, simvastatin and their combination, drugs were added to GMK cells line and incubated for 6, 12 or 24 h. Both drugs were added together in the same volume 100 µL/well at the following concentrations: (MTX – 5.5 µmol/L and simvastatin – 100 µmol/L); (MTX – 5.5 µmol/L and simvastatin – 300 µmol/L) as well as (MTX – 16.5 µmol/L and simvastatin – 100 µmol/L). Cytotoxicity of MTX, simvastatin and their simultaneous treatment was calculated from equation suggested in the instruction of the manufacturer. Cytotoxicity was expressed in %.

MTT viability assay

For assay of cell viability, MTT test based on INVITTOX protocol n°17, ECVAM – European Centre for the Validation of Alternative Methods, Database Service on Alternative Methods To Animal Experimentation was used. To determine the effects on cell viability, the combination of MTX and simvastatin were added to GMK cells line in the above concentrations and were incubated for 6, 12 or 24 h. GMK cells viability was expressed in % of control group.

Statistical analysis

Results are expressed as the mean ± SEM. Statistical significance among groups was determined using analysis of variance (ANOVA) accompanied with *post-hoc* Newman-Keuls test; p-values less than 0.05 were considered significant.

RESULTS

Cytotoxicity of drugs in LDH test

After 6 and 12 h of incubation of GMK kidney cells with the combination of. MTX (5.5 µmol/L) with simvastatin (100 µmol/L), approx. 10% cytotoxic effect was observed, while after 24 h incubation, it rose to about 15% (Fig. 1). It is worth noticing that after the same periods of GMK cell line incubation, with only MTX (5.5 µmol/L) or only simvastatin (100 µmol/L), cytotoxicity of the drugs was below 10%.

After 6, 12, and 24 h of incubation of GMK cell line with MTX (5.5 µmol/L) combined with simvastatin (300 µmol/L), their cytotoxic effect was higher as compared with the groups incubated with each of the drugs separately (Fig. 2). The highest increase (over 20%) was observed after 24 h incubation.

A significant increase in toxicity was also found when using combinations of MTX (16.5 µmol/L) with simvastatin (100 µmol/L) after the three periods of incubation with GMK cells as compared to the results of groups of GMK cells incubated with each drug separately (Fig. 3). After 24 h of incubation, cytotoxicity of the drugs combined was the highest (about 30%).

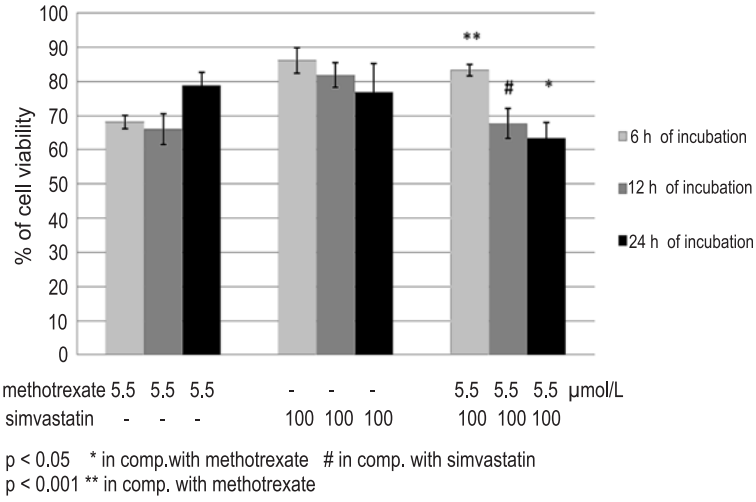

Figure 4. Effect of methotrexate (5.5 µmol/L), simvastatin (100 µmol/L) and their combination on the GMK cells viability in MTT test

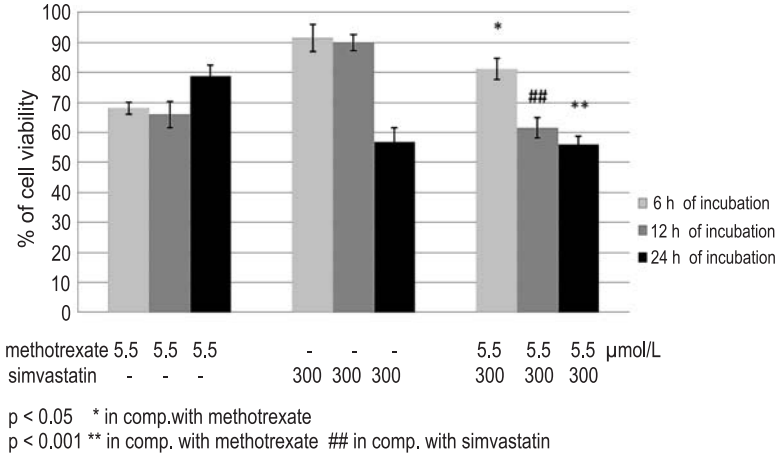

Figure 5. Effect of methotrexate (5.5 µmol/L), simvastatin (300 µmol/L) and their combination on the GMK cells viability in MTT test

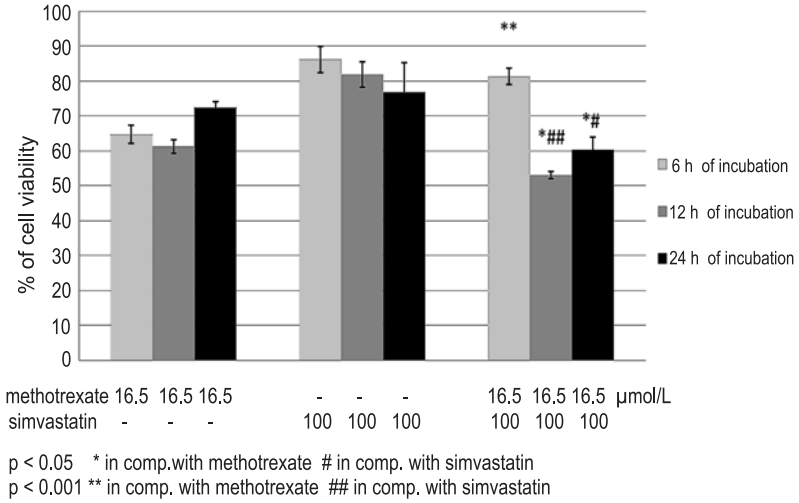

Figure 6. Effect of methotrexate (16.5 µmol/L), simvastatin (100 µmol/L) and their combination on the GMK cells viability in MTT test

The cells viability in MTT test

MTT test was used to measure the effect of administration of the drugs separately and in combination on GMK cell viability after 6, 12 and 24 h incubation. As a result of 6 h incubation of GMK cells with the combination of MTX (5.5 µmol/L) with simvastatin (100 µmol/L), viability was observed to rise when compared with the group of GMK cells incubated with MTX only. Viability of GMK cells after 12 and 24 h incubation was significantly lower as compared with MTX or simvastatin only (67.7 and 63.5%, respectively). It should be noted that after 6, 12 and 24 h incubation of GMK cell line with MTX only (5.5 µmol/L), a significant lowering of cell viability was observed (by about 30% in case of 6 and 12 h incubation and by about 20% after 24 h incubation). After 6, 12 and 24 h incubation of the cell line with simvastatin (100 µmol/l), a decrease was observed in cell viability by 13.7, 18.2 and 23.2%, respectively (Fig. 4).

When both drugs, i.e., MTX (5.5 µmol/L) and simvastatin (300 µmol/L), were applied simultaneously, cells viability was higher after 6 h of incubation, while after 12 and 24 h it decreased by 39 and 45%. It seems, however, that the lowered viability of GMK cells does not result from a point effect of the drug combination but from the effect of the two drugs used separately (Fig. 5).

After 6, 12 and 24 h incubation of GMK cells with MTX (16.5 µmol/L) and simvastatin (100 µmol/L), their viability was about 80, 55 and 60%, respectively. It is worth emphasizing that after 6 h incubation, a significant increase was noted, while after 12 and 24 h of joint incubation of GMK cells with both the drugs one could see a significant decrease in the cell viability as compared with only MTX or only simvastatin in this case points to the intensification of their cytotoxic effect (Fig. 6).

DISCUSSION AND CONCLUSION

One of important problems in modern pharmacology are drug interactions resulting from a few drugs taken simultaneously by patients. These interactions may lead to a lot of, sometimes dangerous, side effects. Cytostatics used in cancer treatment are definitely drugs with an increased risk of interactions with other drugs and affect also healthy cells (16). Drugs given in combination may produce effects that are greater than or less than the effect predicted from their individual potencies. Administration of high doses of MTX and simultaneous treatment with other drugs increased the risk of damage of kidney, liver, bone marrow, skin or mucous membranes. The kidney are the major route of MTX elimination. Long-term of MTX therapy can cause permanent impairment of kidney function, leading to the delay of drug elimination from the body and the increase of its toxicity. Acute renal failure is the result of intratubular precipitation of the drug crystals in acidic pH of urine (5, 6). There are no data, however, on simultaneous treatment with MTX and a widely used group of drugs – statins (17, 18). Simvastatin, examined in the present study, is one of them. The study evaluated cyto-

toxic effect of MTX, simvastatin and their combination on green monkey kidney cells (GMK) in LDH test, was also evaluated GMK cell viability after incubation with the two drugs in MTT test. The initial MTX concentration (5.5 μmol/L) and simvastatin (100 μmol/L) were determined in our previous research (19, 20). These concentrations were not toxic (less than the determined IC_{10} inhibitory concentration of 10%) to the GMK cells line after 24 h of incubation. The literature shows that these concentrations of both drugs used in the study are effective for various cells line (21–24). In the case of MTX, the range of cytotoxicity doses for tumor cells used in the works of different authors was quite high and it ranged from 10^{-9} – 10^{-6} mol/L (23–25).

From the research conducted in this study, one can conclude that MTX (5.5 or 16.5 μmol/L) in the combination with simvastatin (100 or 300 μmol/L) inhibited the growth of GMK cells after 12 or 24 h of incubation. The highest cytotoxicity growth, by about 30% in LDH test, was noted after applying of MTX (16.5 μmol/L) into the colony of GMK cells together with simvastatin (100 μmol/L). Similarly, the highest decrease of GMK cells viability in the MTT test also was observed after 12 and 24 h of simultaneous incubation of MTX in the combination with simvastatin. The obtained results indicate the negative influence of combined application of both drugs on the cells viability. This observations, in addition to the cognitive aspect, may have practical importance in the treatment of patients with malignant disease, suffering from lipid disorders.

REFERENCES

1. Bangert C.A., Costner M.I.: Dermatol. Ther. 20, 216 (2007).
2. Świerkot J., Szechiński J.: Pharmacol. Rep. 58, 473 (2006).
3. Shen S., O'Brien T., Yap L.M., Prince H.M., McCormack C.J.: Australas. J. Dermatol. 53, 1 (2012).
4. Tian H., Cronstein B. N.: Bull. NYU Hosp. Jt. Dis. 65, 168 (2007).
5. Chatham W.W., Morgan S.L., Alarcon G.S.: Arthritis Rheum. 43, 1185 (2000).
6. Strang A., Pulsar T.: J. R. Soc. Med. 97, 536 (2004).
7. Davignon J.: Circulation 109 III, 39 (2004).
8. Liao J.K., Laufs U.: Annu. Rev. Pharmacol. Toxicol. 45, 89 (2005).
9. Merx M.W., Weber C.: Drug Discov. Today: Dis. Mech. Cardiology 5, 325 (2008). Cheng G., Shan J., Xu G., Huang J., Ma J., Ying S., Zhu L.: Pharmacol. Res. 48, 571 (2003).
10. Duncan R.E., El-Sohemy A., Archer M.C.: Cancer Epidemiol. Biomarkers Prev. 14, 1897 (2005).
11. Graaf M.R., Richel D.J., van Noorden C.J., Guchelaar H.J.: Cancer Treat. Rev. 30, 609 (2004).
12. Hindler K., Cleeland C.S., Rivera E., Collard C.D.: Oncologist 11, 306 (2006).
13. Bellosta S., Paoletti R., Corsini A.: Circulation 109, 50 (2004).
14. Armitage J.: Lancet 370, 1781 (2007).
15. Blower P., de Wit R., Goodin S., Aapro M.: Crit. Rev. Oncol. Hematol. 55, 117 (2005).
16. Neuvonen J.P., Niemi M., Backman J.T.: Clin. Pharmacol. Ther. 80, 565 (2006).
17. Shitara Y., Sugiyama Y.: Pharmacol. Ther. 112, 71 (2006).
18. Izdebska M., Natorska-Chomicka D., Jagiełło-Wójtowicz E.: Curr. Issues Pharm. Med. Sci. 25, 18 (2012).
19. Izdebska M., Piątkowska-Chmiel I., Jagiełło-Wójtowicz E.: Bull. Vet. Inst. Pulawy 56, 57 (2012).
20. Abdoli N., Heidari R., Azarmi Y., Ali Eghbal M.: J. Biochem. Mol. Toxicol. 27, 287 (2013).
21. Yang Y.C., Huang W.F., Chuan L.M., Xiao D.W., Zeng Y.L., Zhou D.A. et al.: Chemotherapy 54, 438 (2008).
22. Decker S., Winkelmann W., Nies B., van Valen F.: J Bone Joint Surg. 81-B, 545 (1999).
23. Hattangadi D.K., DeMasters G.A., Walker T.D., Jones K.R., Di X., Newsham I.F., Gewirtz D.A.: Biochem. Pharmacol. 68, 1699 (2004).
24. Kimura E., Nishimura K., Sakata K., Oga S., Kashiwagi K., Igarashi K.: Int. J. Biochem. Cell Biol. 36, 814 (2004).

Received: 19. 08. 2013

Erratum

In the paper entitled: “Effects of 300 mT static magnetic field on IL-6 secretion in normal human colon myofibroblasts”; by Arkadiusz Gruchlik, Adam Wilczok, Ewa Chodurek, Władysław Polechoński, Daniel Wolny, Zofia Dzierżewicz; published in: Acta Poloniae Pharmaceutica – Drug Research, Vol. 69 No. 6 pp. 1320-1324 (2012) Figure 3 was erroneously printed. The correct figure is given below:

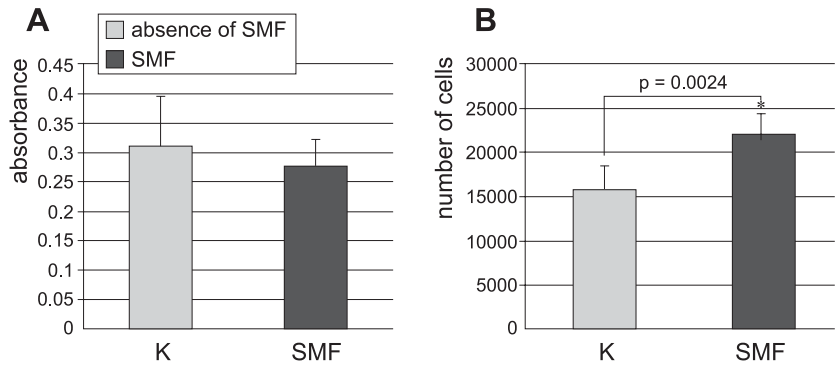

Fig. 3. Influence of the SMF with a flux density of 300 mT on the myofibroblasts viability (**A**) and proliferation (**B**). Cell viability was expressed as an absorbance and cell proliferation as a number of cells. CCD-18Co cells were cultured for 72 h in the presence and absence of SMF. The results represent the mean ± SD (n = 18 for cell viability; n = 6 for cell proliferation assay); * $p < 0.05$ compared with the control (K), (Mann–Whitney U test was used for cell viability and Student’s *t*-test for cell proliferation)

Instruction for Authors

Submission of the manuscript

All papers (in duplicate and electronic version) should be submitted directly to Editor:

Editor
Acta Poloniae Pharmaceutica –
Drug Research
16 Długa St.
00-238 Warsaw
Poland

We understand that submitted papers are original and not published elsewhere.

Authors submitting a manuscript do so on the understanding that if it is accepted for publication, copyright of the article shall be assigned exclusively to the Publisher.

Scope of the Journal

Acta Poloniae Pharmaceutica - Drug Research publishes papers in all areas of research. Submitted original articles are published in the following sections: Reviews, Analysis, Biopharmacy, Drug Biochemistry, Drug Synthesis, Natural Drugs, Pharmaceutical Technology, Pharmacology, Immunopharmacology, General. Any paper that stimulates progress in drug research is welcomed. Both, Regular Articles as well as Short Communications and Letters to the Editor are accepted.

Preparation of the manuscript

Articles should be written in English, double-spaced. Full name (first, middle initial, last) and address of authors should follow the title written in CAPITAL LETTERS. The abstract should be followed by keywords. We suggest the following structure of paper: l) introduction, 2) experimental, 3) results, 4) discussion and conclusion.

Instructions for citation of references in the e-journal:

1. In the text, sequential numbers of citations should be in order of appearance (not alphabetically) in parentheses (...) not in brackets […].
2. In the list of references, for papers the correct order is: number of reference with dot, family name and initial(s) of author(s), colon, proper abbreviation(s) for journal (Pubmed, Web of Science, no dot neither coma after one word journal name), number of volume, number of issue (if necessary) in parantheses. first page or number of the paper, year of publication (in parentheses), dot. For books: number of reference with dot, family name and initial(s) of author(s), colon, title of chapter and/or book names and initials of editors (if any), edition number, page(s) of corresponding information (if necessary), publisher name, place and year of publication.

EXAMPLES:

1. Gadzikowska M., Grynkiewicz G.: Acta Pol. Pharm. Drug Res. 59, 149 (2002).
2. Gilbert A.M., Stack G.P., Nilakantan R., Kodah J., Tran M. et al.: Bioorg. Med. Chem. Lett. 14, 515 (2004).
3. Roberts S.M.: Molecular Recognition: Chemical and Biochemical Problems, Royal Society of Chemistry, Cambridge 1989.
4. Salem I.I.: Clarithromycin, in Analytical Profiles of Drug Substances And Excipients. Brittain H.G. Ed., pp. 45-85, Academic Press, San Diego 1996.
5. Homan R.W., Rosenberg H.C.: The Treatment of Epilepsy, Principles and Practices. p. 932 , Lea & Febiger, Philadelphia 1993.
6. Balderssarini R.J.: in The Pharmacological Basis of Therapeutics, 8th edn., Goodman L., Gilman A., Rall T.W., Nies A.S., Taylor P. Eds., Vol 1, p. 383, Pergamon Press, Maxwell Macmillan Publishing Corporation, New York 1985.
7. International Conference on Harmonization Guidelines, Validation of analytical procedures, Proceeding of the International Conference on Harmonisation (ICH), Commission of the European Communities, Geneva 1996.
8. http://www.nhlbi.nih.gov/health/health-topics/topics/ms/ (accessed on 03. 10. 2012).

Chemical nomenclature should follow the rules established by the International Union of Pure and Applied Chemistry, the International Union of Biochemistry and Chemical Abstracts Service. Chemical names of drugs are preferred. If generic name is employed, its chemical name or structural formula should be given at point of first citation.

Articles should be written in the Past Tense and Impersonal style. I, we, me, us etc. are to be avoided, except in the Acknowledgment section.

Editor reserves the right to make any necessary corrections to a paper prior to publication.

Tables, illustrations

Each table, figure or scheme should be on a separate page together with the relevant legend and any explanatory notes. Tables ideally should not have more than 70, and certainly not more than 140, characters to the line (counting spaces between columns 4 characters) unless absolutely unavoidable.

Good quality line drawings using black ink on plain A4 paper or A4 tracing paper should be submitted with all lettering etc., included. Good black and white photographs are also acceptable. Captions for illustrations should be collected together and presented on a separate sheet.

All tables and illustrations should be specially referred to in the text.

Short Communications and Letters to the Editor

The same general rules apply like for regular articles, except that an abstract is not required, and the number of figures and/or tables should not be more that two in total.

The Editors reserve the right to publish (upon agreement of Author(s) as a Short Communication a paper originally submitted as a full-length research paper.

Preparation of the electronic manuscript

We encourage the use of Microsoft Word, however we will accept manuscripts prepared with other software. Compact Disc - Recordable are preferred. Write following information on the disk label: name the application software, and the version number used (e.g., Microsoft Word 2007) and specify what type of computer was used (either IBM compatible PC or Apple MacIntosh).

Fee for papers accepted for publication

Since January 2013 there is a publication fee for papers accepted for publication in Acta Poloniae Pharmaceutica Drug Research.
The fee - 1000 PLN, should be paid before publication on the bank account:
Polish Pharmaceutical Society, Długa 16, 00-238 Warszawa
Millennium S.A. account no. 29 1160 2202 0000 0000 2770 0281
with a note „publication in Acta Pol. Pharm. Drug Res., paper no. ……..

For foreign authors the payment (250 €) should be done according to the data:

1. SWIFT Address: BANK MILLENNIUM SA, 02-593 WARSZAWA, POLAND, STANISŁAWA ŻARYNA 2A St.
2. SWIFT CODE: BIGBPLPWXXX
3. Beneficiary account Number: PL 30 1160 2202 0000 0000 2777 0200
4. Bank Name: BANK MILLENNIUM SA
5. Favoring: POLSKIE TOWARZYSTWO FARMACEUTYCZNE (Polish Pharmaceutical Society), DŁUGA 16, 00-238 WARSZAWA, Poland, NIP 526-025-19-54
6. Purpose of sending money: Publication in Acta Pol. Pharm. Drug Res., paper no. …..

For payments by Western Union, the name of recipient is Katarzyna Trembulak at the address of Polish Pharmaceutical Society (see above).